Confinement Effect of Narrow Baseplates or Reaction Area on Anchor Breakout, Part 3

Final Report

Contract No. BDV28-977-09 & BED28-977-02

February 2024

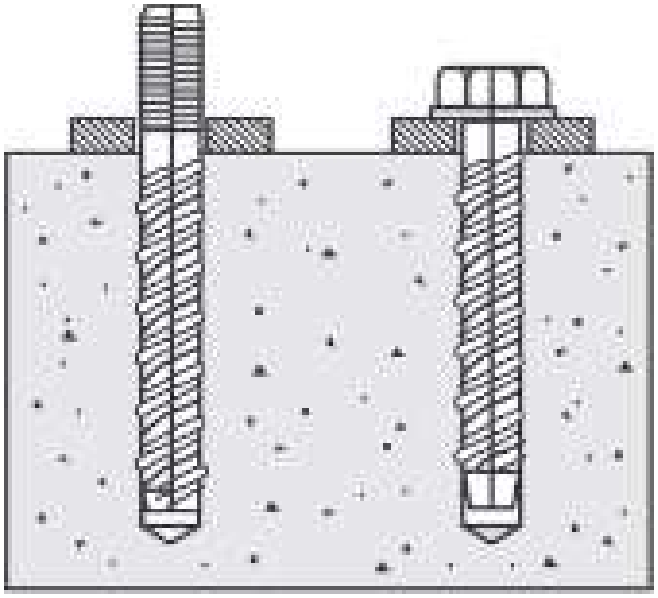

Prepared by:

Nakin Suksawang, Ph.D., P.E.
Principal Investigator
Florida Institute of Technology
150 W. University Blvd
Melbourne, FL 32901

For FDOT Project Manager:

Steven Nolan, P.E.
Senior Structures Design Engineer
State Structures Design Office
605 Suwannee Street
Tallahassee, FL 32399-0450

DISCLAIMER PAGE

The opinions, findings, and conclusions expressed in this publication are those of the authors and not necessarily those of the State of Florida Department of Transportation.

APPROXIMATE COVERSIONS TO SI UNITS

SYMBOL	WHEN YOU KNOW	MULTIPLY BY	TO FIND	SYMBOL
LENGTH				
in	inches	25.4	millimeters	mm
ft	feet	0.305	meters	m
yd	yards	0.914	meters	m
mi	miles	1.61	kilometers	km
AREA				
in^2	Square inches	645.2	square millimeters	mm^2
ft^2	Square feet	0.093	square meters	m^2
yd^2	square yard	0.836	square meters	m^2
ac	acres	0.405	hectares	ha
mi^2	square miles	2.59	square kilometers	km^2
VOLUME				
fl oz	fluid ounces	29.57	milliliters	mL
gal	gallons	3.785	liters	L
ft^3	cubic feet	0.028	cubic meters	m^3
yd^3	cubic yards	0.765	cubic meters	m^3
NOTE: volumes greater than 1000 L shall be shown in m^3				
MASS				
oz	ounces	28.35	grams	g
lb	pounds	0.454	kilograms	kg
T	short tons (2000 lb)	0.907	megagrams (or "metric ton")	Mg (or "t")

TEMPERATURE (exact degrees)				
°F	Fahrenheit	5 (F-32)/9 or (F-32)/1.8	Celsius	°C
ILLUMINATION				
fc	foot-candles	10.76	lux	lx
fl	foot-Lamberts	3.426	candela/m^2	cd/m^2
FORCE and PRESSURE or STRESS				
lbf	poundforce	4.45	newtons	N
lbf/in^2	poundforce per square inch	6.89	kilopascals	kPa

TECHNICAL REPORT DOCUMENTATION PAGE

1. Report No.	2. Government Accession No.	3. Recipient's Catalog No.

4. Title and Subtitle	5. Report Date
Confinement Effect of Narrow Baseplates or Reaction Area on Anchor Breakout, Part 3	January 2024
	6. Performing Organization Code
7. Author(s)	8. Performing Organization Report No.
Nakin Suksawang	
9. Performing Organization Name and Address	10. Work Unit No. (TRAIS)
Florida Institute of Technology 150 W. University Blvd Melbourne, FL 32901	11. Contract or Grant No. BDV28-977-09 & BED28-977-02
12. Sponsoring Agency Name and Address	13. Type of Report and Period Covered
Florida Department of Transportation 605 Suwannee Street, MS 30 Tallahassee, FL 32399	Draft Final May 2021 – Dec 2023
	14. Sponsoring Agency Code

15. Supplementary Notes

16. Abstract

The AASHTO Committee on Bridges and Structures has approved the updated ACI CODE-318, 2019 edition (ACI CODE 318-19,) into the 10th edition of the AASHTO LRFD Bridge Design Specifications. This would allow the adoption of screw anchor designs that benefit from rapid, reliable, and simplified installation procedures. However, the ACI CODE approach has been shown to be too conservative in typical FDOT applications because it does not account for the confinement effect caused by the metal baseplate's compressive force in the concrete breakout cone. Furthermore, previous studies have shown that the predominant failure mode of screw anchor is a combined failure with a much higher breakout capacity than the concrete breakout failure limited by the ACI CODE. Therefore, this research provides an experimental investigation of the failure mechanism and appropriate confinement effect of screw anchors used in typical FDOT applications. Results indicated that the screw anchors' breakout resistance consistently exceeded nominal strength predicted by ACI CODE and the required design loads. It is recommended that FDOT permit the use of screw anchors because it reduces installation cost and time because there is no additional adhesive cost or need to wait for adhesive to cure. It is also recommended that FDOT adopts a strength reduction factor of $\phi = 0.75$ for both design purposes and when evaluating future test results for screw anchors instead of the ACI CODE $\phi = 0.65$.

17. Key Word	18. Distribution Statement
Baseplates, Confinement Modification Factor, Railings, Reaction Area, Screw Anchors.	No restriction

19. Security Classif. (of this report)	20. Security Classif. (of this page)	21. No. of Pages	22. Price
Unclassified	Unclassified	191	

Form DOT F 1700.7 (8-72) Reproduction of completed page authorized

ACKNOWLEDGEMENTS

The author would like to thank the direction and support provided by the FDOT project manager, Mr. Steven Nolan. Additionally, the author would like to recognize the FDOT Structural Research Center, particularly Ms. Christina Freeman and her team, Mr. Yukai Yang, Mr. Paul Tighe, Mr. Steve Eudy, Mr. Ben Allen, Mr. Miguel Ramirez, Mr. Justin Robertson, and Mr. Michael Waters, for their assistance with the fabrication and testing of the slab with sidewalk, gravity wall, and parapet wall, test specimens. Finally, the author greatly appreciates the contribution to the experimental program by Florida Tech graduate students, namely Mr. Paul Ryan, Mr. Alex Paluzzi and Mr. Linga Pranay Sai Dyapa.

EXECUTIVE SUMMARY

The American Concrete Institute (ACI) releases a new building code ACI CODE 318, 2019 edition (ACI CODE-381-19,) that covers screw anchors in Chapter 17. This new code is part of the 2021 agenda item for the AASHTO Committee on Bridge and Structures to adopt the new ACI CODE-318-19 into Article 5.13 in the 10th edition of the AASHTO LRFD Bridge Design Specification (AASHTO BDS). This would allow the adoption of screw anchor designs that benefit from rapid, reliable, and simplified installation procedures. However, numerous studies, including the prior FDOT-funded research project BDV28-977-06, have illustrated that the ACI CODE-318-19 approach is excessively conservative. This conservatism may pose a potential hindrance to the widespread utilization of screw anchors in typical FDOT applications, notwithstanding the manifold advantages screw anchors offer over adhesive counterparts.

Employing screw anchors can further reduce the installation cost and time because there are no additional adhesive expenses and waiting period for the adhesive hardening and curing, a process that typically spans 24 – 72 hours depending on the ambient temperature. Additionally, the screw anchors remain unaffected by environmental factors, including service temperature and concrete moisture content, which can otherwise impede the bond strength of adhesive anchors, potentially causing project delay. Simultaneously, the use of screw anchors reduces variability and inspection requirements for drilled hole preparation and the type of adhesives employed, streamlining the overall construction process.

Drawing from the outcome of the prior FDOT-funded research project BDV28-977-06, the compression confinement from the baseplate significantly increases the concrete breakout resistance by at least 1.6 times the nominal concrete breakout capacity using ACI CODE-318-19 approach. This resulted in the development of an equation for the confinement modification factor to address this increase in concrete breakout resistance. Leveraging this increased strength, FDOT proceeded to adjust the adhesive anchor's embedment length, as outlined in Standard Plans Index 515-052 and 515-062, to 6 inches for sidewalk applications and 9 inches for gravity wall applications. Therefore, an investigation is warranted to determine the potential benefits of the confinement effect for an expanded use of screw anchors for typical FDOT applications.

In this research project, the investigation focused on the performance of 3/4-in and 5/8-in. diameter stainless steel and galvanized screw anchors embedded in Class NS and Class II concrete within different concrete structures, namely pavement slab, gravity wall, and parapet. The objectives encompassed reviewing and identifying the confinement effect, determining anchor group and configuration effects, understanding failure mechanisms, assessing performance under cyclic loads, and developing new FDOT Structures Design Guidelines (SDG).

To achieve the specified objectives, a series of full-scale experimental tests were conducted at the Marcus H. Ansley Structures Research Center (SRC). These tests involved subjecting 35 specimens to monotonic loads until failure, and an additional set of 10 specimens to cyclic loads. The cyclic loading consisted of pulsating tensile loads that varied sinusoidally between 150 lb and 300 lb for pipe guiderails and between 150 lb and 550 lb for picket railings, repeated for 1000 cycles. Subsequently, each specimen underwent a monotonic load test until failure. Additionally, nine specimens were retrofitted and subjected to a monotonic load test until failure.

The full-scale specimens were prepared to mimic the design standards of three different railings consisting of the following:

1. 515-052: Pedestrian/Bicycle Railing (Steel)
    a. 515-052 (Gravity Wall) with one-bolt detail
    b. 515-052 (Sidewalk) with one-bolt detail
    c. 515-052 (Parapet) with one-bolt detail
2. 515-080: Pipe Guiderail (Steel)
    a. 515-080 (Gravity Wall) with two-bolt detail
    b. 515-080 (Sidewalk) with two-bolt detail
    c. 515-080 (Parapet) with two-bolt detail
3. 515-022: Pedestrian/Bicycle Bullet Railing with two-bolt detail. It should be noted that the bullet railing was modified from standard aluminum shape to steel standard shape.

The full-scale testing program demonstrated that the screw anchors breakout resistance at least doubled the analytical nominal capacity obtained using ACI CODE-318-19. The experimental results also consistently surpassed the required design loads of the railings. Sidewalk specimens exhibited lower multipliers, attributed to guiderail/baseplate yielding, resulting in the premature termination of tests. Importantly, the performance of screw anchors remains unaffected by cyclic loading.

The recommended configurations for each railing types are as follows:

- For pedestrian (picket) rail (515-052 & -062) applications, a single 3/4 - 8.5 in. stainless steel or galvanized screw anchor is advised.
- Guiderail (515-070 & -080) installations are best served with two 3/4 - 6 in. stainless steel or galvanized screw anchors.
- Parapet (515-022) installations benefit from two 5/8 - 8 in. stainless steel or galvanized screw anchors; it's important to note that the bullet rail design may not accommodate a 3/4-in. diameter screw anchor due to space constraints.

The confinement modification factor, developed in the earlier FDOT-funded research project BDV28-977-06, is recommended for adoption within the SDG concerning post-installed anchor design for metal railings. Additionally, it is suggested that the SDG replace the current ACI CODE-318-19 load resistance factor of $\phi = 0.65$ with a more suitable $\phi = 0.75$, applicable for both design purposes and the evaluation of future test results for post-installed anchors. Furthermore, FDOT is encouraged to consider the inclusion of the proposed Section 1.6.4, outlined in Section 6.4 of this report.

In conclusion, this research project lays the foundation for improved screw anchor design standards, offering qualitative and quantitative benefits that enhance structural performance and reduce installation complexities. The proposed structural design guidelines and recommendations signify a significant step toward more efficient and reliable post-installed anchor applications for FDOT.

Table of Contents

LIST OF TABLES

LIST OF FIGURES

1. CHAPTER 1 – INTRODUCTION

1.1 INTRODUCTION

Screw anchors are a crucial advancement in the field of construction and infrastructure growth, providing a dependable and flexible approach for connecting fixtures to different surfaces. These anchors employ specialized screws to firmly engage with concrete, masonry, or other suitable materials. The ease and efficiency of screw anchors have established them as a fundamental element in countless construction projects across various sectors. Their flexibility allows for their application in various environments, ranging from securing components in constructions to providing support for vital infrastructure such as bridges, dams, and retaining walls.

The benefits of screw anchors are diverse. They have impressive load-bearing capabilities, providing great strength and stability. Moreover, their simple installation saves time and reduces labor expenses while ensuring reliability in different environmental conditions. Furthermore, their flexibility to work with different surfaces and the option to install them at various angles make them highly useful for accommodating complex design needs.

The evolution of screw anchor systems in engineering and development is ongoing, with improvements in materials and designs focusing on enhancing their performance and versatility. Therefore, it is crucial to have a thorough understanding of the mechanics, applications, and best practices associated with screw anchors to ensure their optimal utilization in construction and infrastructure projects.

1.2 PROBLEM STATEMENT

A new AASHTO LRFD Bridge Design Specification (AASHTO-BDS), Article 5.13—Concrete Anchor Design —was added to the 2016 (8th) Edition. This new section directly references the specification requirements from ACI CODE 318-14, Chapter 17, which addresses typical anchoring to concrete, including adhesive anchors such as those used for standard metal pedestrian and bicycle railings in Florida. However, the ACI CODE 318-14 approach has been shown to be too conservative in typical FDOT applications.

The ACI CODE-318-14 does not account for the confinement effect caused by the metal baseplate's compressive force in the concrete breakout cone. As a result, the existing design of post-installed anchors for standard metal pedestrian and bicycle railings would require impractical modifications to meet these design provisions if adopted by the Structures Design Guidelines (SDG). For this reason, FDOT sponsored a research project BDV28-977-06 to determine the confinement effect of a narrow baseplate on adhesive anchor breakout resistance and developed a new confinement modification factor.

Based on the research project results BDV28-977-06, the compression confinement from the baseplate significantly increases the concrete breakout resistance by at least 1.6 times the nominal concrete breakout capacity using ACI CODE-318-14 approach. The strength gain from the compression confinement allowed FDOT to modify the adhesive anchor's embedment length shown in Standard Plans Index 515-052 and 515-062 to 6 inches for a sidewalk and 9 inches for gravity wall applications. Furthermore, a new confinement modification factor has been developed to address this increase in concrete breakout resistance for similar design applications.

Since the initiation of the BDV28-977-06 project, adoption of screw anchor design provisions into the ACI CODE-318-19, Chapter 17, has been completed. Furthermore, the AASHTO Committee on Bridges and Structures has passed a ballot item in 2021 for the adoption of the updated ACI CODE-318, 2019 edition

into the AASHTO-BDS. This would allow the adoption of screw anchor designs that benefit from rapid, reliable, and simplified installation procedures.

The FDOT confinement modification factor could potentially be used for all post-installed anchors as it is applied to the concrete breakout strength. It could also be applied to other failure modes such as pullout and pry-out, but more testing would be needed to confirm its applicability. It is possible that with the proposed modification factor, screw anchor systems could be used instead of an adhesive anchor for pedestrian railing and other applications. The current design concrete breakout strength of the screw anchor is approximately 9.8 to 15 kips depending on concrete compressive strength, so if a modification factor of Ψ_M is applied, the design concrete breakout capacity could increase between 14.7 to 22.5 kips, which meets the required strength of 15.6 kips in most applications. However, the design pullout strength would have to be evaluated to determine the governed failure mode.

Using post-installed mechanical anchors can further reduce the installation cost and time, as there is no additional adhesive cost and no need to wait for the adhesive to harden and cure, which takes between 24 – 72 hours depending on the ambient temperature. Additionally, the mechanical anchor is not influenced by the surrounding environment, such as the service temperature and concrete moisture content that affect the bond strength when using adhesive anchors, which could delay the project. Therefore, there is a need to determine if the confinement effect could benefit FDOT by providing an expanded use for post-installed mechanical anchors.

1.3 SCOPE

The scope of this research project is limited to the investigation of the performance of 3/4 and 5/8 in. dia screw anchors with different anchor lengths of 8-in and 6-in. embedded in Class NS (Non-Structural) concrete and Class II concrete. The investigation included three types of concrete structures, namely concrete pavement (slab specimen), gravity wall and parapet wall. The investigation included three main railings, namely steel picket/pedestrian railing, steel guide railing and steel bullet railing that were fabricated in accordance with FDOT Design Standard, Index 515-052 and 062 for picket/pedestrian railing, 515-070 and 080 for guide railing and 515-022 for bullet railing. The investigation also included modified picket/pedestrian railings.

1.4 OBJECTIVES

The primary objectives of this research project are:

1. Review and identify the effect of confinement of narrow baseplates or reaction area on screw anchors breakout resistance.
2. Determine the effect of anchor groups and configurations on the anchor breakout resistance.
3. Determine the failure mechanism and appropriate confinement modification factor of screw anchors used in various applications.
4. Determine the screw anchors' performance under cyclic loads.
5. Develop new FDOT Structures Design Guidelines criteria for screw anchors with confinement effects.
6. Develop modified FDOT Structures Design Guidelines criteria for adhesive anchors with confinement effects if necessary.

2. CHAPTER 2 – BACKGROUND

2.1 INTRODUCTION

An overview of the behavior of anchor systems, particularly their failure mechanism and the effect of confinement effect of narrow base plate or reaction area on post-installed concrete anchors breakout resistance are presented in this section. Section 2.2 describes a review of the three main failure mechanisms of concrete anchor systems and related research. A brief explanation of ACI CODE-318-19 design criteria for different failure mechanisms are also provided in this section. Section 2.3 describes the influence of anchor brand on screw anchor capacity depending on concrete thickness. Section 2.4 discusses the relationship between tensile capacity of screw anchor and their tread profiles, also the factors influencing the determination of screw anchors ultimate tensile capacity. Section 2.5 discusses the effects of different drilling methods and their influence on the performance of screw anchors. Section 2.6 discusses the current design procedures provided in ACI CODE-318-19 for concrete anchor system and equations provided in ACI Code. Section 2.7 discusses the concept of hydrogen embrittlement and testing procedures outlined by the ACI Code to assess susceptibility to hydrogen embrittlement in anchor diameters. Finally, a summary of the literature review on anchor systems is provided in Section 2.8.

2.2 FAILURE MODES

There are three ways in which failure of screw anchors can occur. First, concrete breakout happens when the concrete mix where the anchors are placed could not withstand the applied forces, leading to significant portion of concrete to be forced out from the base material in a conical shape. Second, pullout occurs when the bond between the screw anchor and the surrounding concrete does not have sufficient strength necessary to resist the tension forces present. Third, failure of the steel anchor takes place when the anchors used exceed their ultimate strength before any other failure mode is observed. Figure 2-1 published in Advances in Structural Engineering, vol.23 (Chen et al., 2020) summarizes the effect of embedment depth of screw anchors on expected failure type.

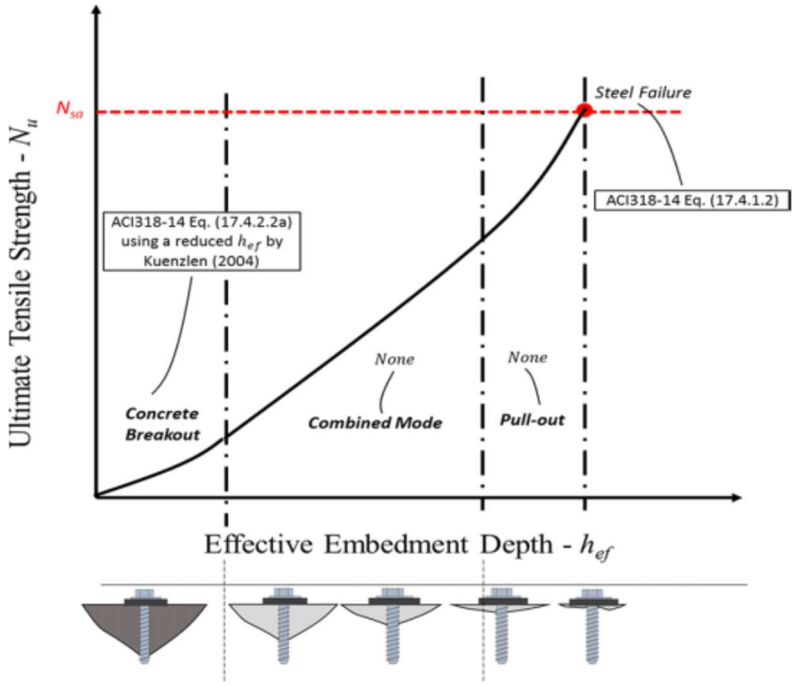

Figure 2-1: Failure mode for varying embedment depths (Chen et al., 2020)

Chen et al.'s research emphasized the significance of identifying a "combined" failure mode, which according to Chen et al., is deemed to be the most prevalent and representative type of failure among screw anchors.

According to Mohyeddin et al. (2020), the ultimate tensile capacity of anchors is significantly greater when they are embedded at greater depths. The concrete capacity design (CCD) method serves as the current designing standard for concrete screw anchors. Initially, the CCD method was introduced in the 2002 edition of ACI 318 for designing cast-in-place anchors and post-installed expansion and undercut anchors. Subsequently, it was adapted for use with adhesive anchors, as discussed in ACI 318-11 (Olsen et al., 2012). In the latest version, ACI CODE-318-19, provisions for screw anchors are now included under Chapter 17.

As per ACI CODE-318 section 17.3.1, the concrete compressive strength (fc') should not exceed 10,000 psi for cast-in anchors and 8,000 psi for post-installed anchors. This limitation is based on prior testing conducted by Primavera et al. in 1997, which revealed that the design procedures in ACI Chapter 17 become less reliable with increasing concrete strength, particularly when fc' falls within the range of 11,000 to 12,000 psi. The 8,000 psi limit for post-installed anchors is derived from testing data detailed in ACI CODE-355.2 and ACI CODE-355.4.

For screw anchors with embedment depths $5d_a \leq h_{ef} \leq 10d_a$ and $h_{ef} \geq 1.5$ in., breakout strength requirements are dictated by the design procedures of ACI CODE-318 section 17.6.2 and 17.7.2. The effective embedment depth, h_{ef}, is a reduced nominal embedment that is based on geometric characteristics of the screw. Use of h_{ef} with the CCD method accurately predicts the behavior of screw anchors in the current database.

2.3 EFFECTS OF ANCHOR BRAND

The effect of the anchor brand on screw anchor capacity is influenced by the thickness of the concrete. Through an analysis of variance (ANOVA) with a 95% confidence, it was found that in 2.1 inches thick concrete, the anchor brand has no significant effect on anchor capacity. However, in 4 inches thick concrete, the anchor brand can lead to up to a 20% variation in anchor capacity (Tarawneh et al., 2020).

In Chen et al.'s study, the ultimate strength of anchors under combined loading, N_{comb} was investigated for three manufacturers, DeWalt, Simpson Strong-Tie, and Hilti. Three diameters from each manufacturer and two effective embedment depths for each diameter were tested.

Table 1. Testing plan for screw anchors (1 in = 25.4 mm).

d (in)	hnom (in)	Manufacturer	ht (in)	hs (in)	h'_{ef} (in)	Number of repeat tests
1/2	4	SST	1/3	1/3	2.98	8
		Hilti	1/2	1/4	2.98	8
		DeWalt	3/8	3/8	2.93	8
	2 ½	SST	1/3	1/3	1.91	8
		Hilti	1/2	1/4	1.70	8
		DeWalt	3/8	3/8	1.65	8
3/8	3	SST	1/4	2/7	2.27	8
		Hilti	2/5	1/8	2.19	8
		DeWalt	1/3	2/7	2.17	8
	2	SST	1/4	2/7	1.42	8
		Hilti	2/5	1/8	1.34	8
		DeWalt	1/3	2/7	1.32	8
1/4	2 ½	SST	1/5	1/8	1.94	8
		Hilti	1/4	1/9	1.70	8
	2	DeWalt	1/5	2/5	1.28	8
	1 ½	SST	1/5	1/8	1.09	8
		Hilti	1/4	1/9	1.06	8
		DeWalt	1/5	2/5	0.85	8
Total						144

SST: Simpson Strong-Tie.

Figure 2-2: Specimen details used to produce Figure 2-1 (Chen et al., 2020)

2.4 EFFECTS OF THREAD TYPE

The tensile capacity of anchors is strongly correlated with their thread profiles. Early studies established Eq. 1, which is commonly used to calculate the ultimate tensile capacity of anchors. However, recent research suggests that using a constant reduction factor of 0.85 may not be accurate. Instead, it is recommended to determine a product-specific embedment factor through experimentation. This testing-based value would be a unique characteristic property of the anchors and would remain constant, regardless of the embedment depth or concrete compressive strength (Mohyeddin, 2020).

$$h_{ef,1} = 0.85(h_{nom} - 0.5\mathrm{h} - h_s) \qquad \text{(Eq. 1)}$$

In a study conducted by Chen et al. (2020), 144 unconfined tension tests were performed on three screw anchors with different manufacturer origins, diameters, and two effective embedment depths. Surprisingly, despite the variations in thread design among the anchors, the differences in $Ncomb$ were found to be insignificant.

2.5 EFFECTS OF DRILLING METHOD

The process of installing screw anchors involves drilling the base concrete or support at a diameter that corresponds to the anchor's size. Anchor manufacturers usually provide specific guidelines for the hole diameter to ensure that the anchors perform as intended and meet advertised standards. Ongoing research focuses on improving current drilling procedures to enhance their efficiency, which ultimately leads to time and cost savings during construction projects.

Concrete drilling can be divided into rotational, impact, and diamond drilling methods (Schwenn, M., 2021). Post-installed fasteners, are based on three different working principles;

a) Mechanical Interlock

b) Friction

c) Bond

Currently, the most common method used to drill concrete for anchor installation is hammer drilling. Reasons other drilling methods are being researched and increasingly used:

a) Worker protection (reduced dust emission compared to hammer drilling)

b) Noise and vibration reduction (diamond drilling)

c) Ability to drill through reinforcement layers

d) Less impact on the drilling base material

Hammer drilling causes undesired impact energy on the base material. The damaging forces occur in three phases (Schwenn, M., 2021). First, an elastic deformation of the concrete is observed. Second, local damage to the base material causes radial cracks to develop below the drill. Lastly, large areas break-out due to the radial cracks that run in the direction of the maximum shear stresses.

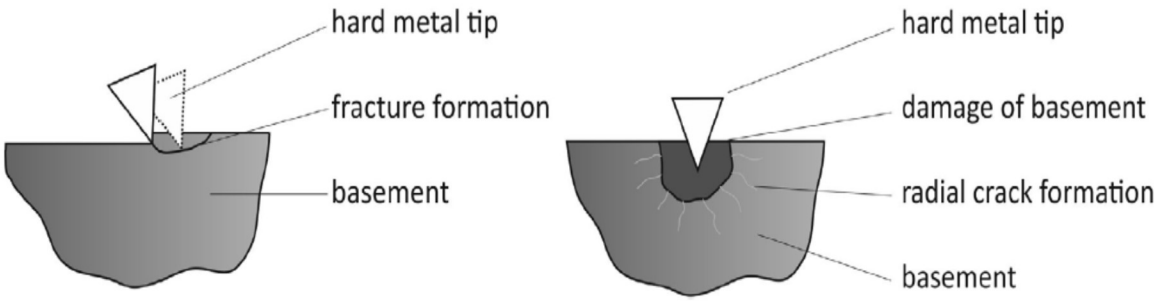

Figure 2-3: Hammer drilling schematic (Schwenn, M., 2021)

Experiments comparing anchors installed using various drilling methods reveal that the drilling technique significantly impacts the load-bearing capacity and displacement behavior of post-installed mechanical fasteners. Among the three conditions tested, anchor strength in cracked concrete, especially during cycling loads, is the most affected (see Figure 2-4). In tests conducted on non-cracked concrete, the most common failure modes are concrete breakout and steel failure. On the other hand, tests performed on cracked concrete exhibit different primary failure modes, with concrete breakout and pull-through failure being the most frequent occurrences.

Overall, among the different drilling methods, the traditional hammer drilling method with no cleaning as recommended by the manufactured provide the overall best performance. Cleaning the hole after drilling did not improve the anchor capacity nor using diamond drilling method.

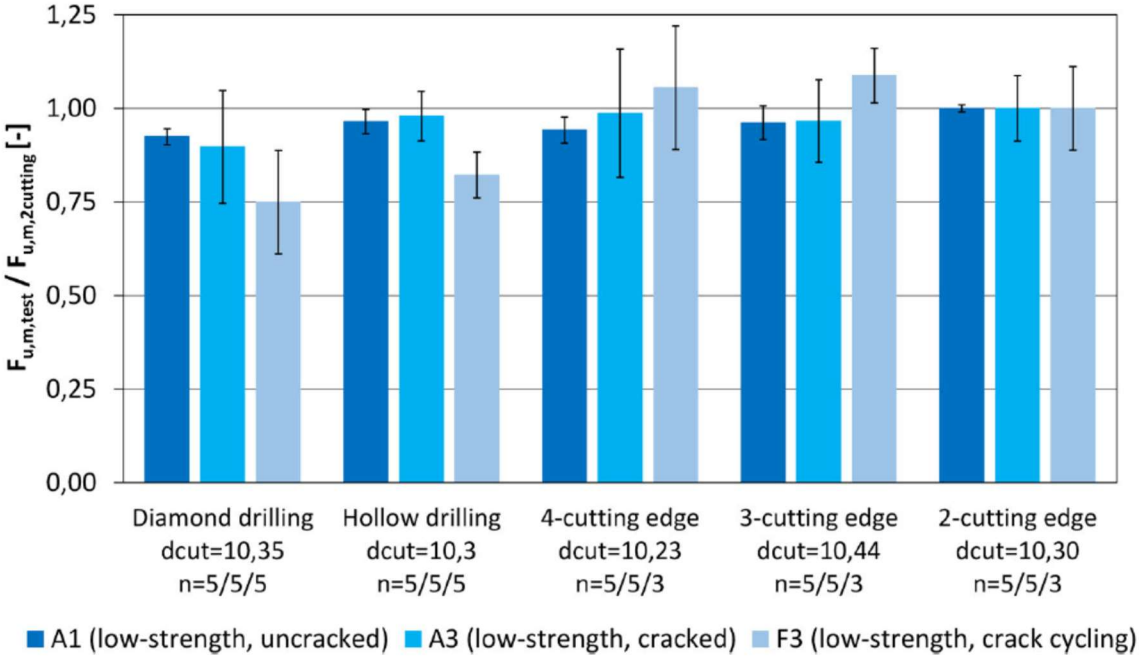

Figure 2-4: Anchor strengths after cycling (Schwenn, M. et. al, 2021)

2.6 CURRENT DESIGN PROCEDURES (ACI CODE-318-19)

The classification of concrete anchors is summarized in Figure 2-5.

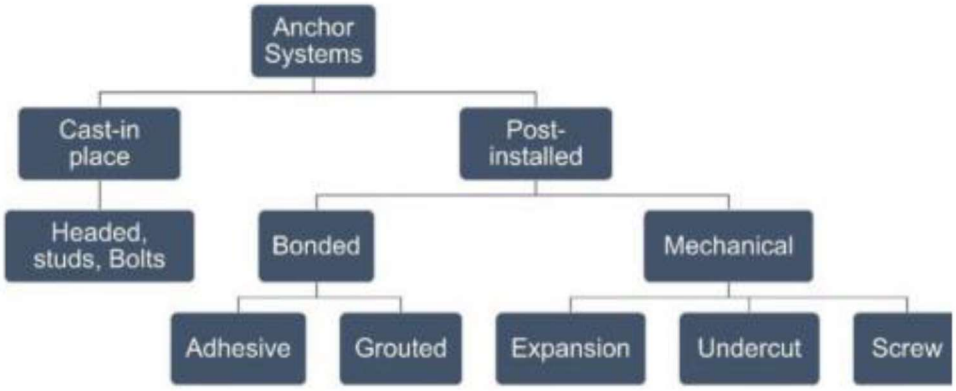

Figure 2-5: Anchor classifications (Tarawneh et al., 2020)

ACI CODE-318-19 Chapter 17 is one of the most widely accepted design standards for screw anchors currently in use. The chapter should not be used for applications where high-cycle fatigue or impact loads dominate. The design strength of anchors for all factored load combinations must adhere to the criteria summarized in ACI CODE-318 Table 17.5.2 (Table 2-1).

Table 2-1: Anchor design strength requirements (American Concrete Institute, 2019)

Failure mode	**Single anchor**	**Anchor group**	
		Individual anchor in group	**Anchors as a group**
Steel strength in tension (17.6.1)	$\phi N_{sa} \geq N_{ua}$	$\phi N_{sa} \geq N_{ua,i}$	
Concrete breakout strength in tension (17.6.2)	$\phi N_{cb} \geq N_{ua}$		$\phi N_{sag} \geq N_{ua,g}$
Pullout strength in tension (17.6.3)	$\phi N_{pn} \geq N_{ua}$	$\phi N_{pn} \geq N_{ua,i}$	
Concrete side-face blowout strength in tension (17.6.4)	$\phi N_{sb} \geq N_{ua}$		$\phi N_{sbg} \geq N_{ua,g}$
Bond strength of adhesive anchor in tension (17.6.5)	$\phi N_{a} \geq N_{ua}$		$\phi N_{g} \geq N_{ua,g}$
Steel strength in shear (17.7.1)	$\phi V_{sa} \geq V_{ua}$	$\phi V_{sa} \geq V_{ua,i}$	
Concrete breakout strength in shear (17.7.2)	$\phi V_{cb} \geq V_{ua}$		$\phi V_{cbg} \geq V_{ua,g}$
Concreate pry-out strength in shear (17.7.3)	$\phi V_{cp} \geq V_{ua}$		$\phi V_{cpg} \geq V_{ua,g}$

Notes:

- Design Strengths for steel and pullout failure modes shall be calculates for the most highly stressed anchor in the group.
- Sections referenced in parentheses are pointers to models that are permitted to be used to evaluate the nominal strengths.
- If anchor reinforcement is provided in accordance with ACI CODE-318 section 17.5.2.1, the design strength of the anchor reinforcement shall be permitted to be used instead of the concrete breakout strength

If lightweight concrete is used, the following modification factor should be used (ACI CODE-318 section 17.2.4.1) for screw anchors unless approved tests are performed

$$\lambda a = 0.8\lambda \qquad \text{(Eq. 2)}$$

Where λ is dependent upon the concrete density (ACI CODE-318 section 19.2.4)

ACI CODE-318 section 17.6.2 (Breakout Strength of Anchors in Tension)

Nominal concrete breakout strength of a single anchor in tension (ACI CODE-318 section 17.6.2.1a)

$$N_{cb} = \frac{A_{Nc}}{A_{Nco}} \Psi_{ed,N} \Psi_{c,N} \Psi_{cp,N} \mathrm{N}_b \quad \text{(Eq. 3)}$$

Nominal concrete breakout strength of a group of anchors in tension (ACI CODE-318 section 17.6.2.1b)

$$N_{cbg} = \frac{A_{Nc}}{A_{Nco}} \Psi_{ec,N} \Psi_{ed,N} \Psi_{c,N} \Psi_{cp,N} \mathrm{N}_b \quad \text{(Eq. 4)}$$

A_{Nco} and A_{Nc} are the maximum projected area for a single anchor and anchor group (respectively). If anchor group areas overlap, A_{Nc} is reduced. A_{Nc} must not exceed nA_{Nco}, where n is the number of tension resisting anchors.

$$A_{Nco} = 9h_{ef}^2 \quad \text{(Eq. 5)}$$

The critical edge distance for headed studs, headed bolts, expansion anchors, undercut anchors, and screw anchors (ACI CODE-318 section R17.6.2.1) is $1.5h_{ef}$

If anchors are $<1.5h_{ef}$ from three or more edges, the CCD method provides overly conservative results for tensile breakout strength (Lutz 1995); hence, the following value should be used to find A_{Nc}

$$h_{ef} = \max \begin{cases} c_{a,max}/1.5 \\ s/3 \end{cases} \quad \text{(Eq. 6)}$$

Where s is the maximum spacing between anchors and $c_{a,x}$ is the greatest of the influencing edge distances that do not exceed the $1.5h_{ef}$.

If a plate or washer is present, the area of the failure surface can be projected outward $1.5h_{ef}$ from the perimeter the plate or washer.

Basic concrete breakout strength of a single anchor in tension in cracked concrete (ACI CODE-318 section 17.6.2.2.1)

$$N_b = k_c \lambda_a \sqrt{f_c'} h_{ef}^{1.5} \quad \text{(Eq. 7)}$$

The above equation assumes a concrete breakout with an angle of 35 degrees. k_c values were first determined in 1955 (Fuchs et al., 1995) and, soon after, adjusted for cracked concrete (Eligehausen and Balogh, 1995; Goto, 1971). See ACI CODE-318 section R17.6.2.2 for k_c values.

The following table summarizes the modification factors used in ACI CODE-318 section 17.6.2.1a and ACI CODE-318 section 17.6.2.1b and ACI CODE-318 section 17.6.3.1 and ACI CODE-318 section 17.7.2.1a and ACI CODE-318 section 17.7.2.1b

Table 2-2: Design modification factors (American Concrete Institute, 2019)

Name	Symbol	Equation	Eq. Ref.
Breakout Eccentricity Factor	$\Psi ec,N$	$\Psi_{ec,N} = \frac{1}{1+\frac{e'_N}{1.5h_{ef}}} \leq 1.0$	ACI 17.6.2.3.1
Breakout Edge Effect Factor	$\Psi ed,N$	$\Psi_{ec,N} = 1.0 \; if \; c_{a,min} < 1.5h_{ef}$	ACI 17.6.2.4.1a
		$\Psi_{ec,N} = 0.7 + 0.3\left(\frac{c_{a,min}}{1.5h_{ef}}\right) if \; c_{a,min} < 1.5h_{ef}$	ACI 17.6.2.4.1b
Breakout Cracking Factor	$\Psi c,N$	See ACI 17.6.2.5 and R17.6.2.5	ACI 17.6.2.5 and R17.6.2.5
Breakout Splitting Factor	Ψcp,N	See ACI 17.6.2.6 and R17.6.2.6	See ACI 17.6.2.6 and R17.6.2.6
Pullout Cracking Factor	Ψc,P	Cracking at service level loads: $\Psi_{c,P} = 1.4$ No cracking at service level loads: $\Psi_{c,P} = 1.0$	ACI 17.6.3.3
Breakout Eccentricity Factor	Ψec,V	$\Psi_{ec,V} = \frac{1}{1+\frac{e'_V}{1.5c_{a1}}} \leq 1.0$	ACI 17.7.2.3.1
Breakout Edge Effect Factor	Ψed,V	$\Psi_{ed,V} = 1.0 \; if \; c_{a2} \geq 1.5c_{a1}$	ACI 17.7.2.4.1a
		$\Psi_{ed,V} = 0.7 + 0.3\left(\frac{c_{a2}}{1.5c_{a1}}\right) if \; c_{a2} < 1.5c_{a1}$	ACI 17.7.2.4.1b
Breakout Cracking Factor	Ψc,V	Cracking at service level loads: $\Psi_{c,V} = 1.4$ No cracking at service level loads: *Refer to* ACI Table 17.7.2.5.1	ACI 17.7.2.5.1
Breakout Thickness Factor	Ψh,V	$\Psi_{h,V} = \sqrt{\frac{1.5c_{a1}}{h_a}} \geq 1.0$	ACI 17.7.2.6

Notes:

- $e'N$ is eccentricity determined with respect to the center of gravity of the anchors in tension.
- Critical distance for screw anchors: $c_{ac} = 4h_{ef}$

ACI CODE-318 section 17.6.3 (Pullout Strength of Single Cast-in of Post-Installed Anchor in Tension)

Nominal pullout strength for screw anchors can be found using the following equation (ACI CODE-318 section 17.6.3.1)

$$N_{pn} = \Psi_{c,P} N_p \quad \text{(Eq. 8)}$$

For screw anchors, Np is the 5% fractile of results of tests following ACI CODE-355.2.

ACI CODE-318 section 17.7.1 (Steel Strength of Anchors in Shear)

Steel strength of post-installed anchors where sleeves do not extend through the shear plane (ACI CODE-318 section 17.7.1.2b)

$$V_{sa} = 0.6 A_{se,V} f_{uta} \quad \text{(Eq. 9)}$$

where $A_{se,V}$ is the effective cross-sectional area of an anchor in shear and

$$f_{uta} = max \begin{cases} 1.9 f_{ya} \\ 125{,}000\ psi \end{cases} \quad \text{(Eq. 10)}$$

For threaded rods (i.e. screw anchors)…

$$A_{se,V} = \frac{\pi}{4}\left(d_a - \frac{0.9743}{n_t}\right)^2 \quad \text{(Eq. 11)}$$

where n_t= # of threads per in.

For post-installed anchors where sleeves extend through the shear plane, ACI CODE-318 section 17.7.1.2b may be used, but using the 5% fractile of results of tests following ACI CODE-355.2 is preferred.

ACI CODE-318 section 17.7.2 (Concrete Breakout Strength of Anchors in Shear)

Shear perpendicular to edge on a single anchor (ACI CODE-318 section 17.7.2.1a)

$$V_{cb} = \frac{A_{Vc}}{A_{Vco}} \Psi_{ed,V} \Psi_{c,V} \Psi_{h,V} V_b \quad \text{(Eq. 12)}$$

Shear perpendicular to edge on an anchor group (ACI CODE-318 section 17.7.2.1b)

$$V_{cb} = \frac{A_{Vc}}{A_{Vco}} \Psi_{ec,V} \Psi_{ed,V} \Psi_{c,V} \Psi_{h,V} V_b \quad \text{(Eq. 13)}$$

Shear parallel to an edge (ACI CODE-318 section 17.7.2.1c)

V_{cb} or V_{cbg} equals twice the value obtained from ACI CODE-318 section 17.7.2.1a or 17.7.2.1b

Anchors at a corner (ACI CODE-318 section 17.7.2.1d)

V_{cb} or V_{cbg}= minimum of breakout strength of each edge

A_{vc} details are given in ACI CODE-318 section 17.7.2.1.1 and Fig. R17.7.2.1a and R17.7.2.1b.

When calculatingA_{vc}, if c_{a2} and h_a are <1.5c_{a1}, then ACI CODE-318 section 17.7.2.1.2 applies:

$$c_{a1} \leq max \begin{cases} c_{a2}/1.5 \\ h_a/1.5 \\ s/3 \end{cases} \quad \text{(Eq. 14)}$$

Where c_{a2} is the greatest edge distance, h_a is thickness, and s is the max. Spacing perpendicular to the direction of shear.

ACI CODE-318 section 17.7.2.1.2 exists because the CCD method is overly conservative (according to Eligehausen, 1988 and Lutz, 1995) under the section's criteria.

For a single anchor in a deep member with edge distances of at least 1.5c_{a1} in the direction perpendicular to shear (ACI CODE-318 section 17.7.2.1.3)

$$A_{Vco} = 4.5(c_{a1})^2 \quad \text{(Eq. 15)}$$

If anchors are located at varying edge distances, c_{a1} should be based on the distance from the edge to the axis of the farthest row of anchors; shear should be assumed to be resisted by this row (ACI CODE-318 section 17.7.2.1.4).

Basic breakout strength of an anchor in cracked concrete (ACI CODE-318 section 17.7.2.2.1a and 17.7.2.2.1b)

$$V_b = min\begin{cases}\left(7\left(\frac{l_e}{d_a}\right)^{0.2}\sqrt{d_a}\right)\lambda_a\sqrt{f_c'}(c_{a1})^{1.5} \\ 9\lambda_a\sqrt{f_c'}(c_{a1})^{1.5}\end{cases} \quad \text{(Eq. 16)}$$

where l_e=h_{ef} for screw anchors and $l_e \leq 8d_a$.

Basic breakout strength of an anchor in cracked concrete (ACI CODE-318 section 17.7.2.2.2)

For anchors located far from the edge, ACI CODE-318 section 17.7.2 typically does not govern.

ACI CODE-318 section 17.7.3 (Concrete Pry-out Strength of Anchors in Shear)

Single anchor (ACI CODE-318 section 17.7.3.1a)

$$V_{cp} = k_{cp}N_{cp} \quad \text{(Eq. 17)}$$

Anchor group (ACI CODE-318 section 17.7.3.1b)

$$V_{cpg} = k_{cp}N_{cpg} \quad \text{(Eq. 18)}$$

k_{cp}=1.0 for h_{ef}<2.5 in.

k_{cp}=2.0 for $h_{ef} \geq 2.5$ in.

For screw anchors, N_{cp}=N_{cb} found using ACI CODE-318 section 17.6.2.1a and N_{cpg}=N_{cbg} found using ACI CODE-318 section 17.6.2.1b.

ACI CODE-318 section 17.8 (Tension and Shear Interaction)

If tension and shear is present, the following equation must be satisfied (ACI CODE-318 section 17.8.3)

$$\frac{N_{ua}}{\phi N_n} + \frac{V_{ua}}{\phi V_n} \leq 1.2 \quad \text{(Eq. 19)}$$

Interaction between tension and shear can be ignored if the following relationship is found to be true (ACI CODE-318 section 17.8.2a and 17.8.2b)

$$\frac{N_{ua}}{\phi N_n} \leq 0.2 \; or \frac{V_{ua}}{\phi V_n} \leq 0.2 \qquad \text{(Eq. 20)}$$

ACI CODE-318 section 17.9 (Minimum Spacing and Edge Distances)

ACI CODE-318 section 17.9.2 Screw Anchors (Post-installed)

$$Minimum\ spacing = max\begin{cases} 0.6h_{ef} \\ 6d_a \end{cases} \qquad \text{(Eq. 21)}$$

$$Minimum\ edge\ distance = max\begin{cases} cover\ (ACI\ 20.5.1.3) \\ Twice\ max.aggerate\ size \\ ACI\ CODE\ 355.2\ or\ 355.4\ or \\ ACI\ CODE - 318\ Table\ 17.9.2b \end{cases} \qquad \text{(Eq. 22)}$$

Notes

- Spacing and edge distance requirements are summarized in ACI CODE-318 Table 17.9.2a
- If product-specific test information is not available, minimum edge distance for screw anchors is equal to $6da$ (ACI CODE-318 section Table 17.9.2b)
- hef for screw anchors should not exceed the greater of (23) ha and member thickness minus 4 in. (ACI CODE-318 section 17.9.4)

Critical edge distance for screw anchors (ACI CODE-318 section 17.9.5)

$$c_{ac} = 4h_{ef} \qquad \text{(Eq. 23)}$$

Results from tension tests should be used in replace of ACI CODE-318 section 17.9.5 is available.

The following equations are crucial to concrete anchor design but were omitted for lack of relation to screw anchor design:

- ACI CODE-318 section 17.6.5.1a and 17.6.5.1b: Bond Strength of adhesive anchors in tension (N_a or N_{ag})

- ACI CODE-318 section 17.7.2.2.2: Basic breakout strength of an anchor in cracked concrete that is a cast-in headed stud, headed bolt, or hooked bolt that is continuously welded to a steel attachment

- ACI CODE-318 section 17.10: Earthquake-resistant Anchor Design Requirements

- ACI CODE-318 section 17.11Attachemtns with Shear Lugs

2.7 HYDROGEN EMBRITTLEMENT

Hydrogen Embrittlement (HE) is a permanent loss of ductility in a metal or alloy caused by hydrogen in combination with externally applied or internal residual stress (Brahimi, S., 2014). Two classifications of hydrogen embrittlement exist: internal hydrogen embrittlement (IHE) and environmental hydrogen embrittlement (EHE). IHE is caused by residual hydrogen from processing. EHE is caused by hydrogen introduced into the metal from external sources while it is under stress.

Under conditions of high stress in steel (e.g., a screw anchor being tensioned), atomic hydrogen moves to the location of greatest stress, rendering otherwise ductile metal relatively brittle. The stress concentrations lead to micro-cracks, which grow as hydrogen moves to follow progressing cracks. Eventually, the steel ruptures from overload, often at a stress much lower that the ultimate strength found during a standard tensile test.

Three conditions must be met to cause hydrogen embrittlement failure:

1. Must have steel grade that is susceptible to hydrogen damage

2. Stress (e.g., tension and/or shear in the case of a screw anchor),

3. Atomic hydrogen

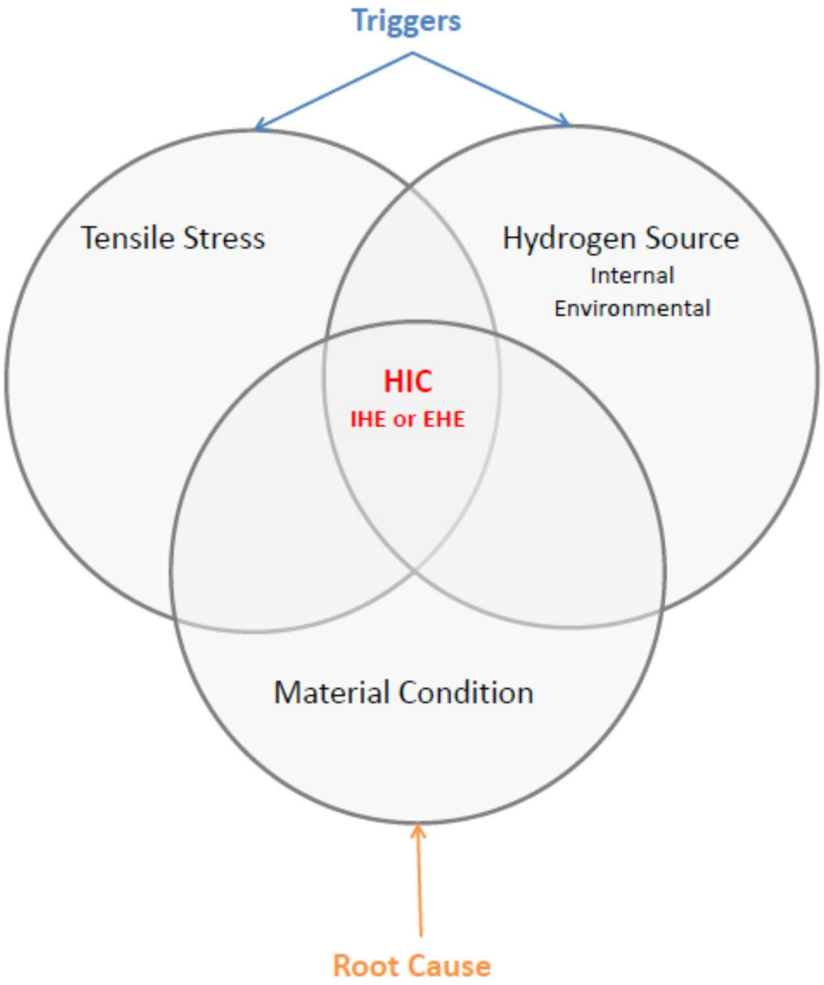

Figure 2-6: Conditions for HE (Brahimi, S., 2014)

ACI CODE-355.2 outlines procedures to test for susceptibility to hydrogen embrittlement (American Concrete Institute, 2019). Testing involves introducing hydrogen to the testing environment. According to ACI CODE-355.2 section 8.7.1.1, anchor diameters meeting the following three items over the entire length of the fastener, excluding the length *hs*, are not sensitive to brittle failure and do not have to be tested:

1. Core hardness ≤ 36 HRC

2. Case hardness ≤ 55 HRC

3. Case depth ≤ 0.02 in. (0.5 mm); case depth is defined as the depth within the cross section with hardness > 36 HRC

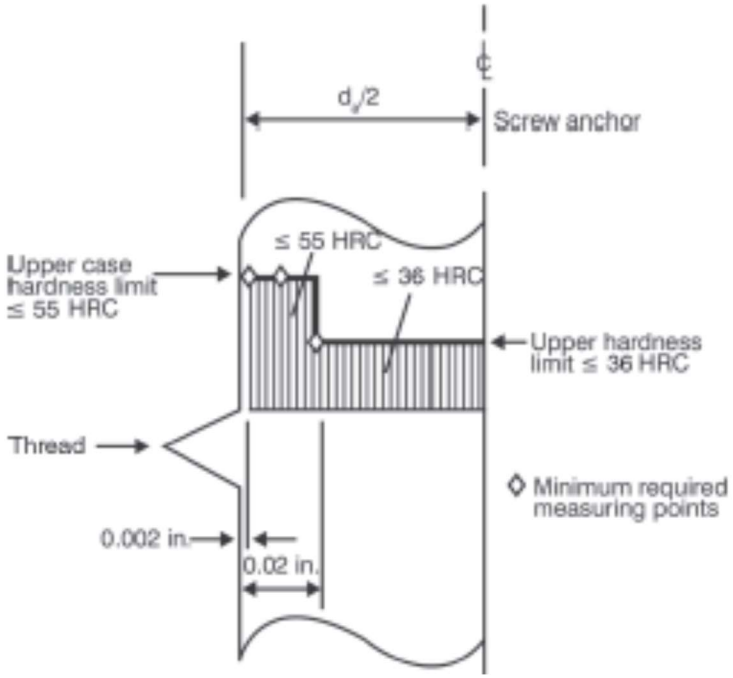

Figure 2-7: Hardness criteria-ACI CODE-355.2 (American Concrete Institute, 2019)

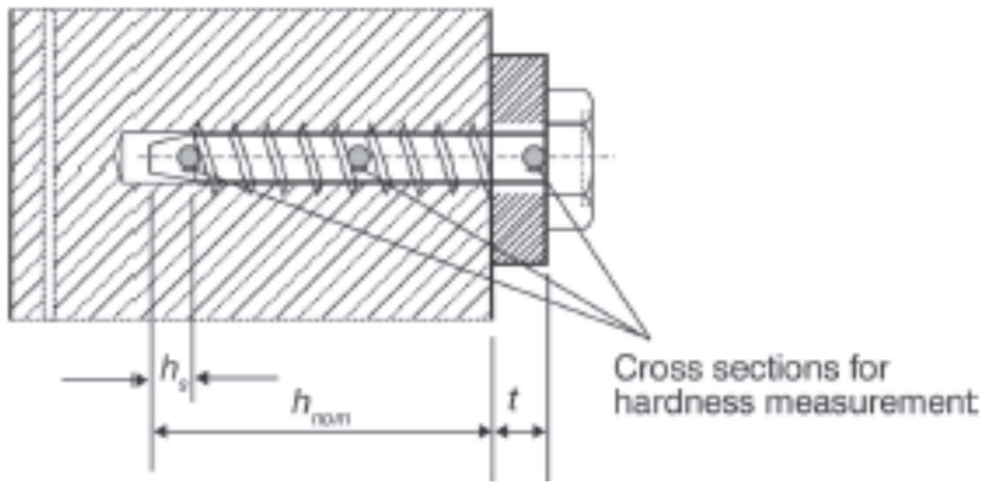

Figure 2-8: Screw anchor dim.-ACI CODE-355.2 (American Concrete Institute, 2019)

2.8 SUMMARY

There exist procedures in ACI CODE-318-19 and similar codes that are over-conservative. Such standards yield inefficient designs and should be adjusted. Through experimentation, the failure mechanism and appropriate confinement modification factor of screw anchors used in various applications should be determined. The literature review details work performed prior to and after the release of current design standards. Research published before current standards provides reasoning for modern procedures while studies developed after current practices, including ongoing studies, show recommended changes to predict both the failure mode and design strength of screw anchors more accurately.

Hydrogen embrittlement should only be considered in analyses if hardness criteria outlined in ACI CODE-355.2 are met. Additionally, anchors under low stress or located in a non-corrosive environment (i.e., indoors) will likely never experience hydrogen embrittlement. Drilling method has a significant influence over the strength of screw anchor applications when installation is performed in cracked concrete. Unlike in un-cracked concrete, the most common failure modes in cracked concrete are concrete breakout and pull-through failure. Since concrete is failing prior to the anchor steel, maximizing concrete strength is crucial; therefore, drilling method must be considered during design.

Screw Anchor Advantages

- Easy to install (compared to cast-in and adhesive anchors)
- Immediate application (no curing of adhesive or concrete is required)
- Ability to work through confinement (reinforcement) via drilling

Screw Anchor Concerns

- Not widely adopted; many codes and procedures are under development, limiting project application
- Weakening from vibration
- Strength affected by drilling method in cracked concrete
- Hydrogen embrittlement

3. CHAPTER 3 – PRELIMINARY RESEARCH

3.1 INTRODUCTION

The use of screw anchors to mount civil infrastructure to the built environment is growing in popularity due to reduced installation time (no curing time since no adhesive is required), improved cost-effectiveness (less hardware required), and reduction of resources (no bonding agent used). The design provisions provided by the American Concrete Institute (ACI CODE, 2019a) provide guidance on the various strength limit states for screw anchors subjected to different forces (tension, shear, etc.). The design strength of screw anchor systems calculated using ACI CODE-318-19 is argued to be overly conservative as the concrete breakout would typically govern the design capacity. However, for pedestrian railing, the narrow base plate would exert force onto the concrete preventing a direct concrete breakout failure. Therefore, the concrete breakout strength limit should be omitted or modified from the design calculation as was the case for the investigation of adhesive anchor under research project BDV28-977-06.

This chapter provides a preliminary analysis of the use of screw anchor in the following five Florida Department of Transportation (FDOT) design standards:

4. 515-052: Pedestrian/Bicycle Railing (Steel)
    a. 515-052 (Gravity Wall) with one and four bolt details
    b. 515-052 (Sidewalk) with one and four bolt details
5. 515-062: Pedestrian/Bicycle Railing (Aluminum)
    a. 515-062 (Gravity Wall) with one and four bolt details
    b. 515-062 (Sidewalk) with one and four bolt details
6. 515-070: Pipe Guiderail (Aluminum)
    a. 515-070 (Gravity Wall) with two and four bolt details
    b. 515-070 (Sidewalk) with two and four bolt details
7. 515-080: Pipe Guiderail (Steel)
    a. 515-080 (Gravity Wall) with two and four bolt details
    b. 515-080 (Sidewalk) with two and four bolt details
8. 515-022: Pedestrian/Bicycle Bullet Railing with two bolt detail

Each of the five structures, which will be referred to as “indexes” herein, currently utilize adhesive anchors to mount their support system(s). Many of the indexes use machined steel or aluminum plate(s) permanently fixed to the base of the structure to permit the installment of headed anchors. Given the similarities in the geometry of adhesive and screw anchors, structural modifications to existing indexes would not be needed upon the replacement of adhesive anchors with screw anchors.

The first group of FDOT Indexes of interest is 515-052 and 515-062 (Pedestrian/Bicycle Railing – Steel and Pedestrian/Bicycle Railing – Aluminum, respectively). The geometry of the indexes is identical (Figure 3-1); only material properties differ (i.e., steel vs. aluminum). Two, different base plates are used for the railing; the plate type is dependent on installation location (i.e., ramps vs. stairs). A one or four-bolt configuration is available for each plate. Additionally, the railing may be installed in a medium with significant edge distances (e.g., a sidewalk) or limited edge distances (e.g., atop a gravity wall). The design strengths for all plate and bolt variations for both installation location types were calculated, and the controlling limit state was found to be the concrete breakout strength, which is reported in Section 4.

The second set of FDOT Indexes of interest is 515-070 and 515-080 (Pipe Guiderail – Aluminum and Pipe Guiderail Railing – Steel, respectively). The geometry of the indexes is identical; only material properties differ (i.e., steel vs. aluminum). Two, different base plates are used for the railing; the plate type is dependent on installation location (i.e., ramps vs. stairs). A two or four-bolt configuration is available for each plate. Additionally, the railing may be installed in a medium with significant edge distances (e.g., a sidewalk) or limited edge distances (e.g., atop a gravity wall). The design strengths for all plate and bolt variations for both installation location types were calculated, and the controlling failure mode was found to be the concrete breakout strength as well.

The final index, 515-022 (Pedestrian/Bicycle Bullet Railing) references many other indexes regarding post spacing and application. Of all the concrete mounting structures referenced, the two-bolt mounting plate anchored atop a 27" parapet (Index No. 521-820) has the lowest capacity and was used in the analysis as illustrated in Figure 3-3. The base plates' anchor hole size and minimum embedment depth may need to be modified to accommodate manufacturer anchor geometries and a torque wrench. Instead of the 9" minimum embedment designated in index 515-022, an embedment of 6 ¼" would apply, accounting for the thickness of the base plate and bearing pad, using a 7" long screw anchor. The design strength of each screw anchor under the modified conditions was calculated and is reflected in the table provided in Section 4.

3.2 DESIGN STRENGTH

Failure among screw anchors can occur in one of three ways. First, failure of the steel anchor occurs when the ultimate strength of the anchors used is exceeded before another failure mode is observed. Second, concrete breakout occurs when the concrete surface where anchors are inserted fails to resist the applied forces, resulting in a large, often conical-shaped, section of concrete to be forced away from the base material. Third, pullout of the screw anchor occurs when the bond between the screw anchor and surrounding concrete is not of sufficient strength to resist the tension forces present. Figure 3-4, published by Chen et al. (2020), summarizes the effect of embedment depth of screw anchors on expected failure type. Based on their observation, majority of the screw anchors failed at a combined concrete breakout and pullout modes rather than the concrete breakout mode. Additionally, because most screw anchors are made with hardened steel, if not properly designed, they are vulnerable to stress-induced hydrogen embrittlement. Fortunately, all screw anchor manufacturers do evaluate their screw anchors for signs of stress-induced hydrogen embrittlement and have indicated it not to be of concern.

The American Concrete Institute's Building Code Requirements for Structural Concrete (ACI, 2019a) is the primary design guidance used to produce the calculations and commentary included herein. The Concrete Capacity Design (CCD) method has recently been adopted for screw anchors and is included in ACI CODE-318-19.

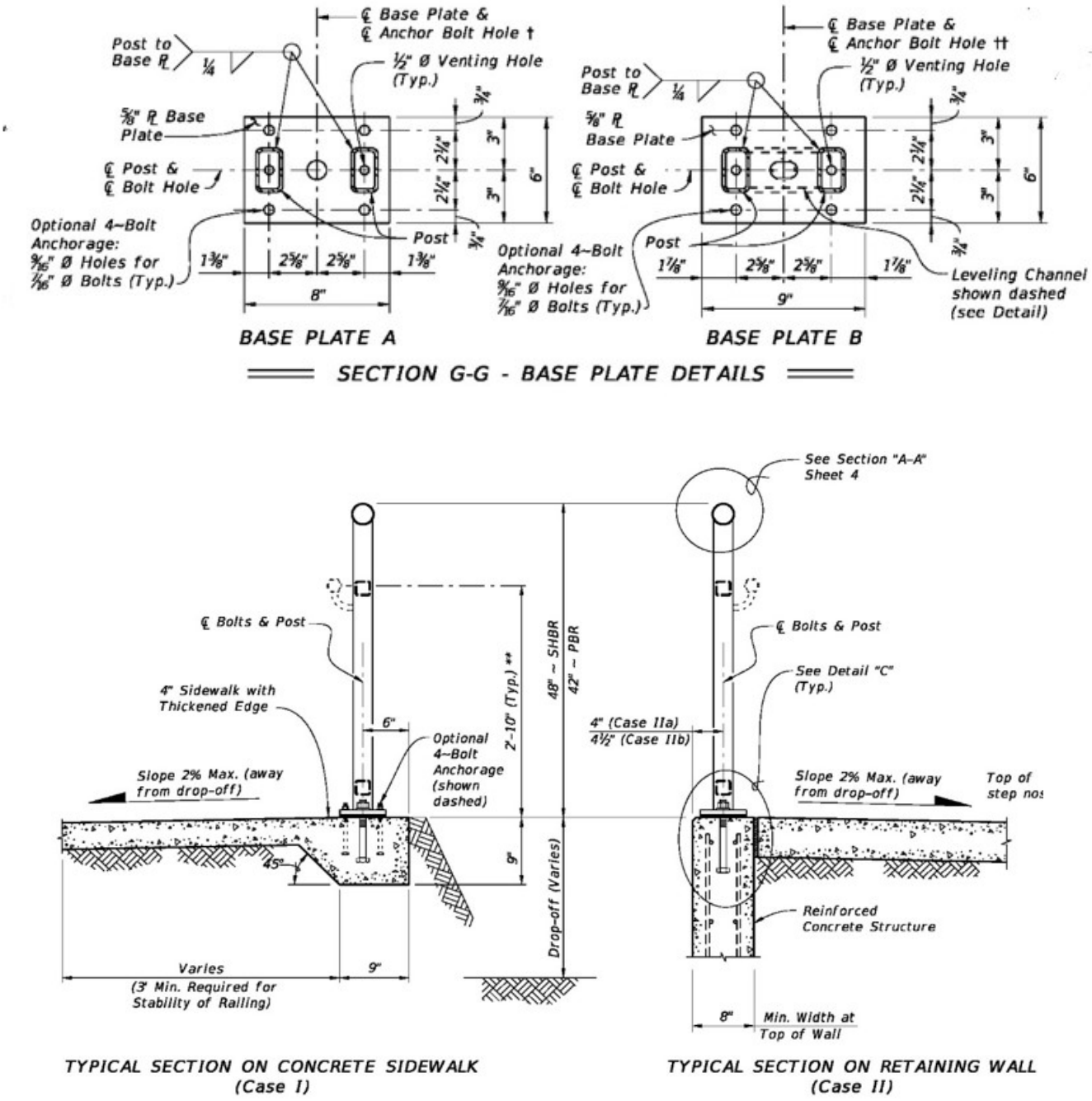

Figure 3-1: FDOT index 515-052 (Pedestrian/Bicycle Railing - Steel)

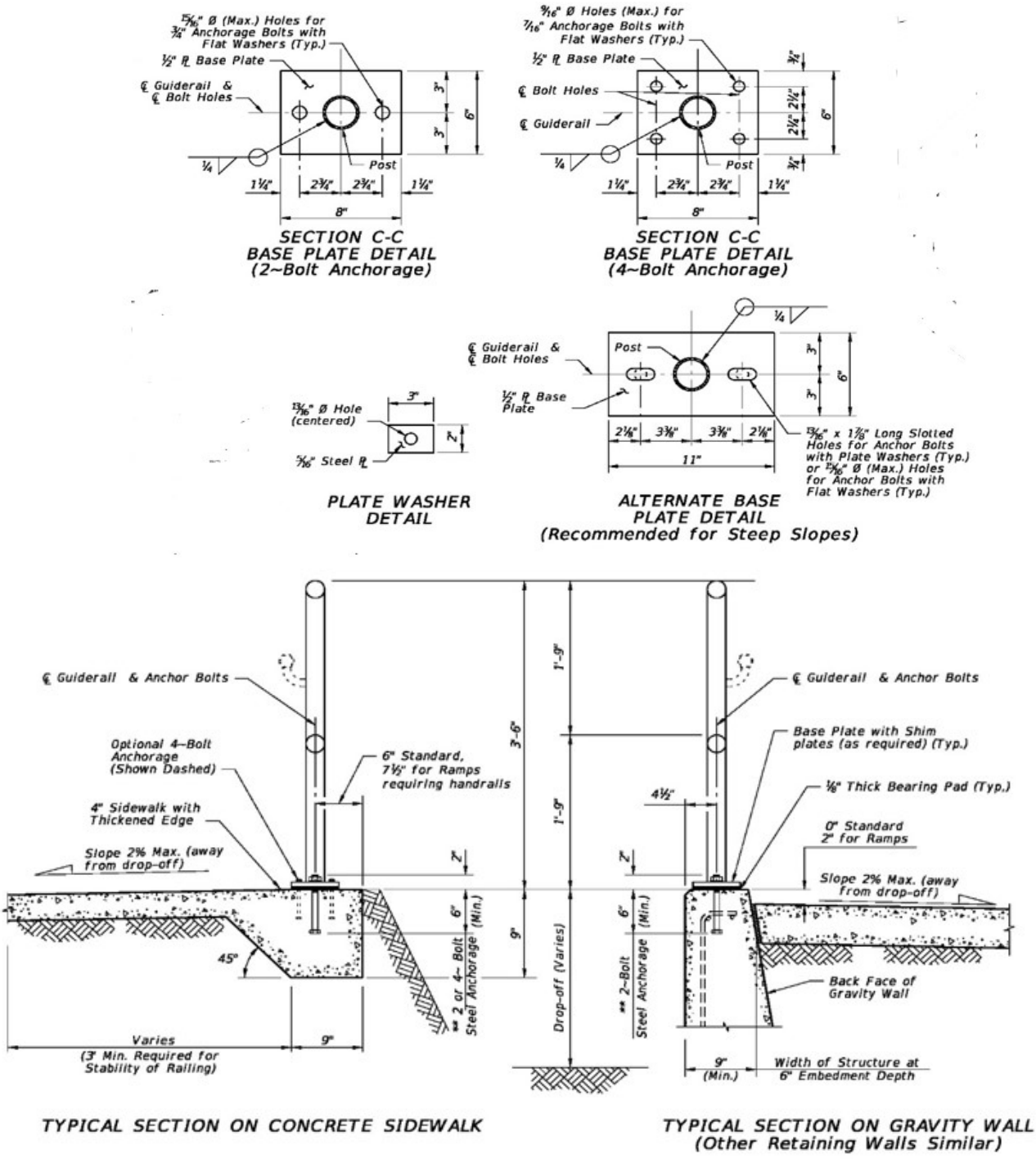

Figure 3-2: FDOT index 515-080 (Pipe Guiderail - Steel)

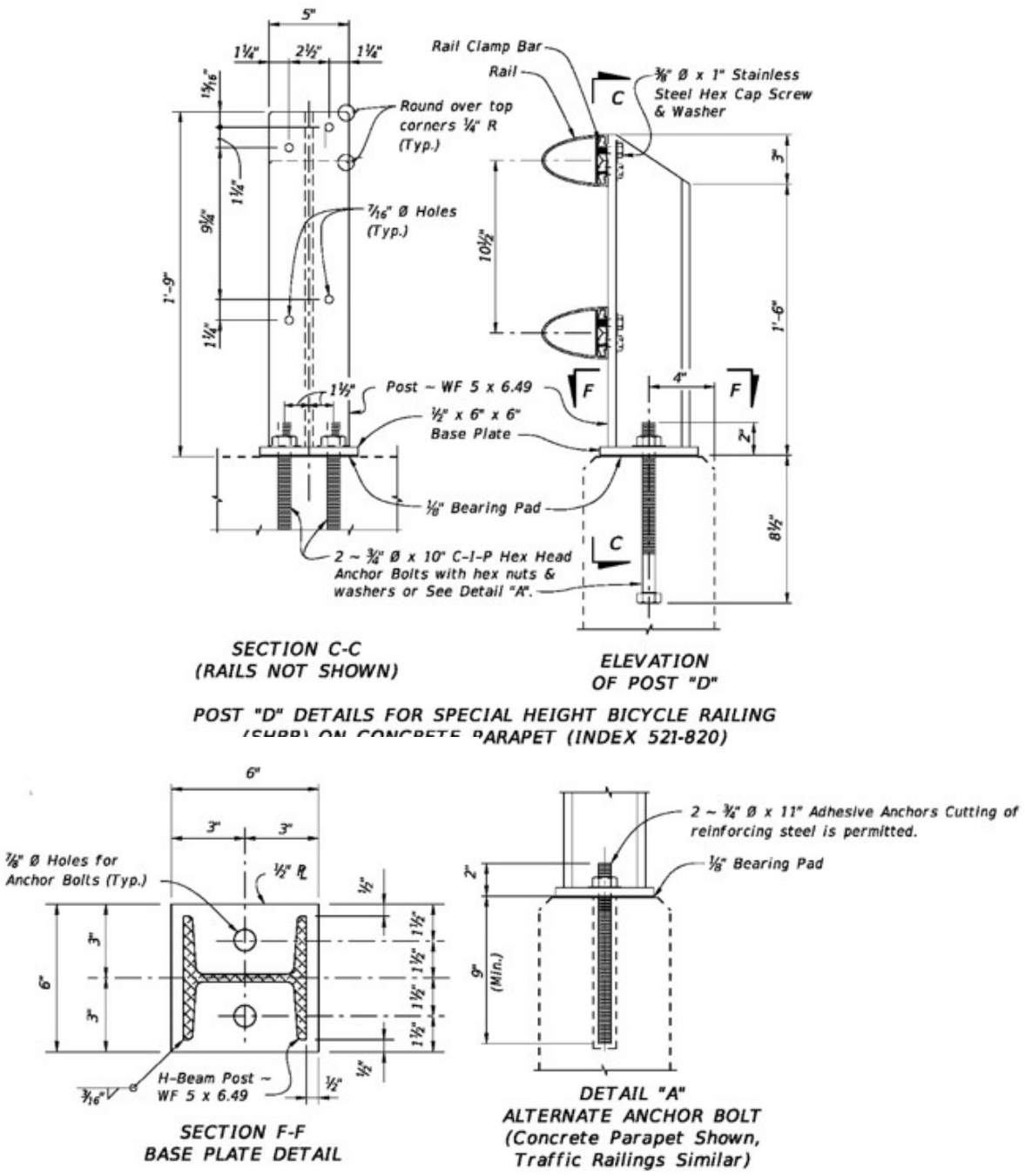

Figure 3-3: FDOT index 515-022 (Pedestrian/Bicycle Bullet Railing)

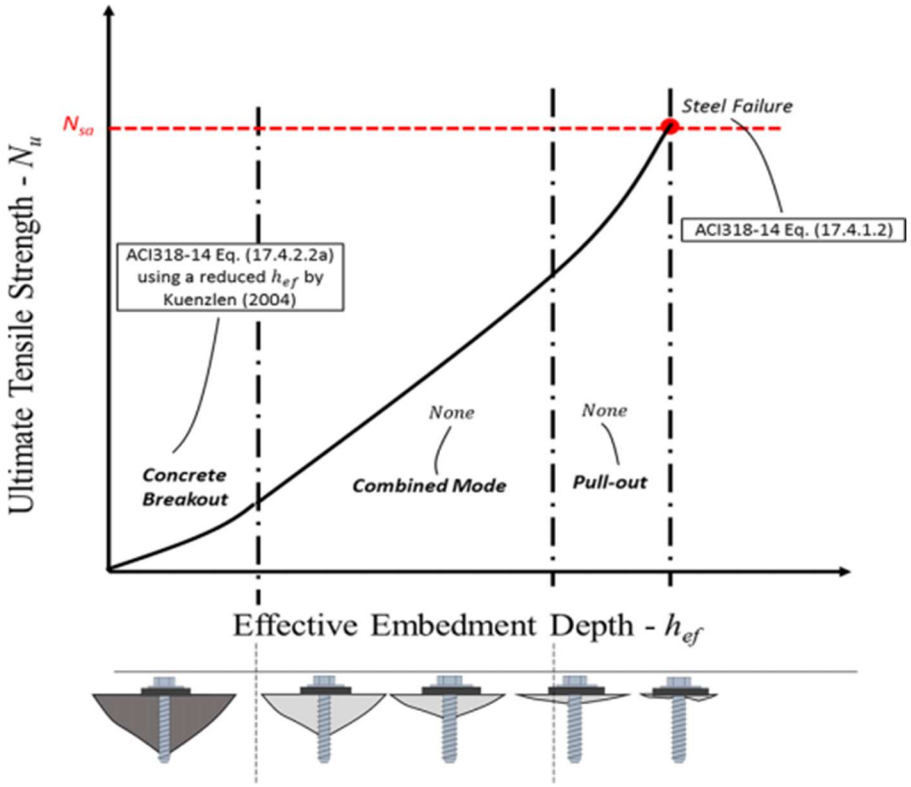

Figure 3-4: Failure mode for varying embedment depths (Chen et al., 2020)

Table 3-1 provides a summary of design strength requirements of screw anchors specified in ACI CODE-318-19, Chapter 17 for tension and shear. It should be noted that ACI CODE-318-19 does not address the applications of screw anchors where high-cycle fatigue or impact loads dominate the design. The strength reduction factors, φ, are given in Table 3-2. Anchor category 1 indicates low sensitivity to installation and high reliability; anchor category 2 indicates medium sensitivity and reliability; anchor category 3 indicates high sensitivity and lower reliability. More details are available in ACI CODE-355.2 Chapter 10. Table 3-3 provides a summary of screw anchors from various manufacturers.

If lightweight concrete is used, the following modification factor should be used (ACI 17.2.4.1) for screw anchors unless approved tests are performed

$$\lambda_a = 0.8\lambda \qquad \text{(Eq. 1)}$$

where λ is dependent upon the concrete density (ACI 19.2.4).

According to ACI 17.3.1, f_c' shall not exceed 8000 psi for post-installed anchors since prior testing (Primavera et al. 1997) indicates the design procedures in ACI Chapter 17 become unconservative with increasing concrete strength (particularly when f_c' is between 11,000 and 12,000 psi). The 8,000-psi limit is derived from testing detailed in ACI CODE-355.2 and ACI CODE-355.4.

It should also be noted that ACI Chapter 17 is only applicable for screw anchors with embedment depths $5d_a \leq h_{ef} \leq 10d_a$ and $h_{ef} \geq 1.5$ in., where d_a is the diameter of the screw anchor and h_{ef} is the effective embedment depth.

Table 3-1: Anchor design strength requirements (American Concrete Institute, 2019b)

Failure mode	Single anchor	Anchor group	
		Individual anchor in group	Anchors as a group
Design Strength in Tension			
Steel strength in tension (17.6.1)	$f N_{sa} \geq N_{ua}$	$f N_{sa} \geq N_{ua,i}$	
Concrete breakout strength in tension (17.6.2)	$f N_{cb} \geq N_{ua}$		$f N_{cbg} \geq N_{ua,g}$
Pullout strength in tension (17.6.3)	$f N_{pn} \geq N_{ua}$	$f N_{pn} \geq N_{ua,i}$	

Notes:

- Design Strengths for steel and pullout failure modes shall be calculated for the most highly stressed anchor in the group.
- Sections referenced in parentheses are pointers to equations that are permitted to be used to evaluate the nominal strengths.
- If anchor reinforcement is provided in accordance with ACI 17.5.2.1, the design strength of the anchor reinforcement shall be permitted to be used instead of the concrete breakout strength.

Table 3-2: Strength reduction factors (American Concrete Institute, 2019b)

Steel Strength		
Type of Steel Element		**Strength Reduction Factor ϕ**
		Tension
Ductile		0.75
Brittle		0.65
Concrete Breakout Strength		
Supplementary reinforcement	Anchor Category from ACI CODE-355.2	Tension (Concrete breakout, bond, or side-face blowout)
Present	Category 1	0.75
	Category 2	0.65
	Category 3	0.55
Not Present	Category 1	0.65
	Category 2	0.55
	Category 3	0.45
Concrete Pullout/Pry-out Strength		
Anchor Category from ACI CODE-355.2		Tension (Concrete pullout)
Category 1		0.65
Category 2		0.55
Category 3		0.45

Table 3-3: Anchor category

Manufacturer	Material	Nominal Anchor Diameter (in.)				
		1/4	3/8	1/2	5/8	3/4
Simpson Strong-Tie	Carbon Steel (Zinc plated or mechanically galvanized)	1				
	Stainless Steel (Type 304 or 316)	3	1			
Hilti	Carbon Steel (Zinc plated or mechanically galvanized)	1				
	Stainless Steel (Type 316)	3	1	2		
Dewalt	Carbon Steel (Zinc plated or mechanically galvanized)	1				
	Stainless Steel (Type 316)	No test data. Only ASD procedure.				

3.2.1 STEEL STRENGTH

The steel strength is based on the rupture of the screw anchor, where the ultimate load can be calculated from the stressed cross-sectional area and ultimate tensile strength of steel. The ultimate tensile strength is used by ACI CODE-318-19 rather than the yield strength used in the SDG because most of the screw anchor materials do not exhibit a well-defined yield point. The ACI CODE-318-19 steel rupture provisions are given by the following equations:

$$N_{sa} = A_{se,N} f_{uta} \quad \text{(Eq. 2)}$$

where f_{uta} is the ultimate tensile strength of the screw anchor but should not exceed either 1.9 times its yield strength or 125,000 psi. These limits were imposed on f_{uta} to ensure that under service load conditions, the stress in the screw anchor would not exceed the yield strength, especially for stainless steel. $A_{se,N}$ is the effective cross-sectional area in tension specified by the manufacturers.

3.2.2 CONCRETE BREAKOUT STRENGTH

The nominal concrete breakout strength of a single anchor in tension (ACI 17.6.2.1a) is given by

$$N_{cb} = \frac{A_{Nc}}{A_{Nco}} \Psi_{ed,N} \Psi_{c,N} \Psi_{cp,N} N_b \quad \text{(Eq. 3)}$$

For a group of anchors in tension, the nominal concrete breakout strength (ACI 17.6.2.1b) is given by

$$N_{cbg} = \frac{A_{Nc}}{A_{Nco}} \Psi_{ec,N} \Psi_{ed,N} \Psi_{c,N} \Psi_{cp,N} N_b \quad \text{(Eq. 4)}$$

where □'s are design modification factors listed in Table 3-4. A_{Nc}/A_{Nco} is a ratio of the total projected area of the anchor to the maximum projected area for a single anchor and a group of anchors as illustrated in Figure 3-5. If anchor group areas overlap, A_{Nc} is reduced. A_{Nc} must not exceed nA_{Nco}, where n is the number of tension resisting anchors. A_{Nco} is given by

$$A_{Nco} = 9h_{ef}^2 \quad \text{(Eq. 5)}$$

where h_{ef} is the effective embedment depth that is illustrated in Figure 3-6 and given by the following equation for screw anchors

$$h_{ef} = 0.85(h_{nom} - 0.5h_t - h_s) \quad \text{(Eq. 6)}$$

where h_{nom} is the distance of the embedment end of the screw anchor and the concrete surface. h_t is the tread pitch and h_s is the length of the embedded end of the screw anchor without the full height of thread.

The critical edge distance is $1.5h_{ef}$. If anchors are located $< 1.5h_{ef}$ from three or more edges (this only applies to the end post and is not considered here), the CCD method provides overly conservative results for tensile breakout strength (Lutz 1995); hence, the following value should be used to find A_{Nc}

$$h_{ef} = max\begin{cases} c_{a,max}/1.5 \\ s/3 \end{cases} \quad \text{(Eq. 7)}$$

where, s is the maximum spacing between anchors and $c_{a,max}$ is the greatest of the influencing edge distances that do not exceed the $1.5h_{ef}$.

Basic concrete breakout strength of a single anchor in tension in cracked concrete (ACI 17.6.2.2.1) is given by

$$N_b = k_c\lambda_a\sqrt{f_c'}h_{ef}^{1.5} \quad \text{(Eq. 8)}$$

The above equation assumes a concrete breakout with an angle of 35 degrees. According to ACI CODE-318-19, $k_c = 17$ for post-installed anchors; however, the code does allow manufacturers to increase this value from experimental data as specified in ACI CODE-355.2.

Table 3-4: Design modification factors (American Concrete Institute, 2019a)

Name	Symbol	Equation	Eq. Ref.
Breakout Eccentricity Factor	$\Psi_{ec,N}$	$\Psi_{ec,N} = \frac{1}{1 + \frac{e'_N}{1.5h_{ef}}} \leq 1.0$	ACI 17.6.2.3.1
Breakout Edge Effect Factor	$\Psi_{ed,N}$	$\Psi_{ed,N} = 1.0$ if $c_{a,min} \geq 1.5h_{ef}$	ACI 17.6.2.4.1a
		$\Psi_{ed,N} = 0.7 + 0.3\left(\frac{c_{a,min}}{1.5h_{ef}}\right)$ if $c_{a,min} < 1.5h_{ef}$	ACI 17.6.2.4.1b
Breakout Cracking Factor	$\Psi_{c,N}$	See ACI 17.6.2.5 and R17.6.2.5	ACI 17.6.2.5 and R17.6.2.5
Breakout Splitting Factor	$\Psi_{cp,N}$	See ACI 17.6.2.6 and R17.6.2.6	See ACI 17.6.2.6 and R17.6.2.6
Pullout Cracking Factor	$\Psi_{c,P}$	No Cracking at service level loads: $\Psi_{c,P} = 1.4$ Cracking at service level loads: $\Psi_{c,P} = 1.0$	ACI 17.6.3.3

Notes:

- e'_N is eccentricity determined with respect to the center of gravity of the anchors in tension.
- Critical distance for screw anchors: $c_{ac} = 4h_{ef}$

Indexes 515-052, 515-062, 515-070, and 515-080 reference installation in regions with significant edge clearance (e.g., sidewalks) and atop gravity walls. The different installation locations yield varying breakout strength limits; hence, a breakout strength was calculated for each installation situation for each index using a one, two, or four-bolt plate (as specified). The 4-bolt plate option allows the use of a 7/16" diameter anchor bolt on the Indexes, so a 3/8" or ½" diameter screw anchor could be evaluated, however due to minimum effective anchor depth that is available from manufacturers, a 3/4" diameter screw anchor was evaluated for the 4-bolt options.

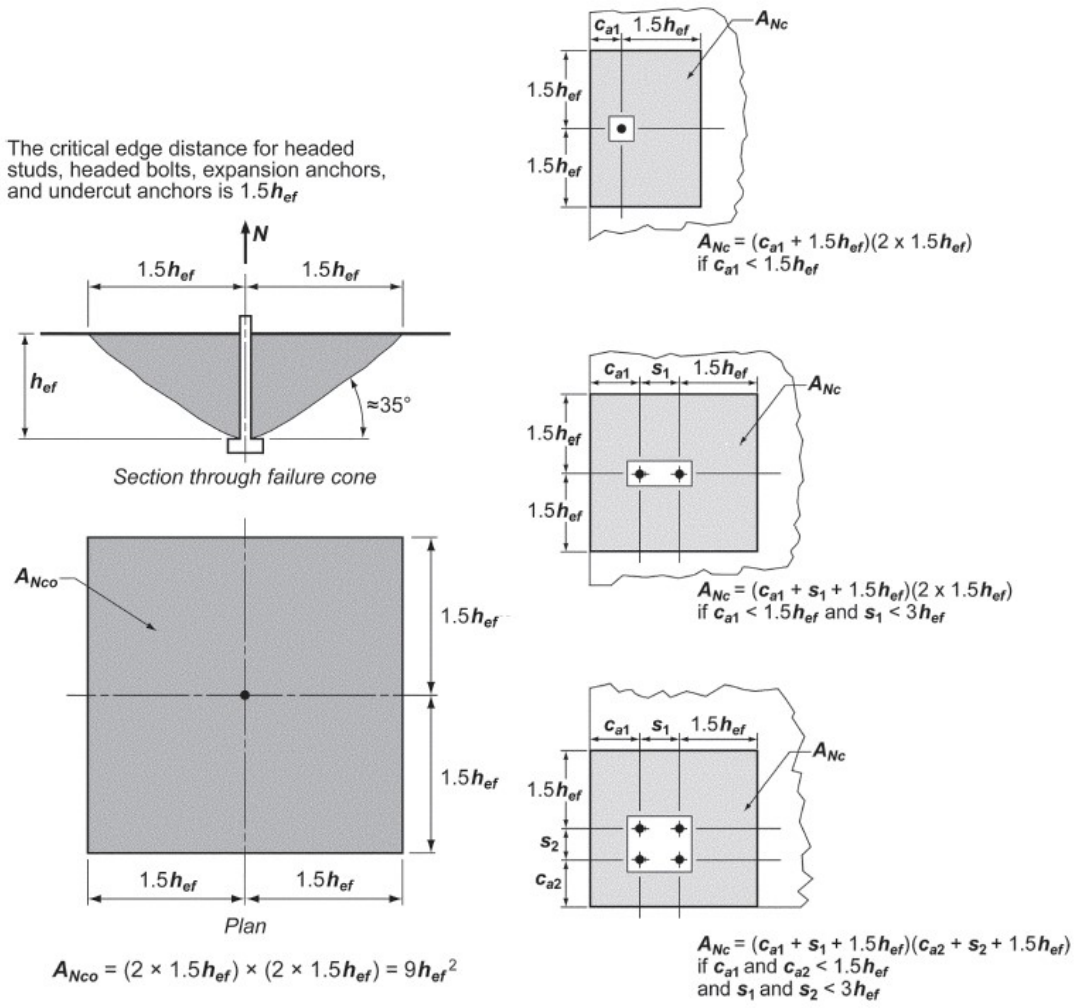

Figure 3-5: Examples of various concrete breakout failure projected area for single and group anchors (ACI CODE-318, 2019)

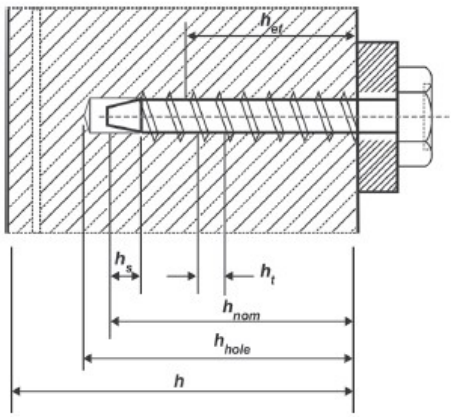

Figure 3-6: Screw anchor effective embedment depth (ACI CODE-355.2, 2019)

3.2.3 PULLOUT/PRY-OUT STRENGTH

The nominal pullout strength for screw anchors can be found using the following equation (ACI 17.6.3.1)

$$N_{pn} = \Psi_{c,P} N_p \quad \text{(Eq. 9)}$$

Where $\Psi_{c,P}$'s are design modification factors listed in Table 3-4. N_p is the 5% fractile of results of tests following ACI CODE-355.2 provided by the manufacturers. However, considering the conservative nature of the ACI concrete breakout strength equation, as illustrated in Figure 3-4, the manufacturers do not report the pullout strength for screw anchors with large diameters with longer embedment lengths. However, for FDOT railing systems, the confinement effect would increase the concrete breakout capacity. Unfortunately, we do not know if the increase would lead to pullout failure or combined failure. For this reason, experimental validation of screw anchor breakout resistance is very important.

3.2.4 ASSUMPTIONS

All manufacturer data based on available anchor lengths and size replaced the original index design demands. For example, if an index stated that a minimum embedment depth of 9-in. is required for each anchor (as seen in index 515-022), the value was replaced with the maximum possible embedment depth given manufacturer data (approximately 6 ¼-in. nominal embedment, 4-in. effective embedment). For uniformity, only Simpson Strong-Tie Company Inc. was referenced in terms of manufacturer data because they are the only manufacturer with a ¾-in. diameter stainless steel screw anchor. Simpson provides a detailed evaluation report (Simpson, 2021) that includes product geometry, design values, assumptions, limitations, and other factors as illustrated in Figure 3-7−Figure 3-9. The report is representative of manufacturer limitations and was referenced extensively during the calculation of allowable strengths. For some failure modes, the manufacturer literature does not provide design values because the modes will not control design. For example, the pullout strength of a ¾-in. screw anchor produced by Simpson Strong-Tie is not tabulated in Figure 3-8, because the value "does not govern and does not need to be considered." However, this is most likely not be the case for these railings because the confinement effect in the base plate would increase the concrete breakout capacity. Therefore, it is necessary to experimentally evaluate and determine the governed failure mode and capacity.

The evaluation report published by Simpson Strong-Tie (Figure 3-7) is the most current product data available. The publication's content was the most updated information available at the time of analysis. Regardless, the most current evaluation report, published by the International Code Council's Evaluation Service (ICC-ES, 2021) varies only slightly from the previous report (Simpson, 2021) (all controlling failure modes remain unchanged). Unless significant geometric changes are made, the design strengths of screw anchors produced by Simpson Strong-Tie are likely to continue to be controlled by the concrete breakout.

Stainless-Steel Titen HD Installation Information[1]

Characteristic	Symbol	Units	Nominal Anchor Diameter (in.)									
			¼		⅜		½		⅝		¾	
Installation Information												
Nominal Diameter	d_a	in.	¼		⅜		½		⅝		¾	
Drill Bit Diameter	d_{bit}	in.	¼		⅜		½		⅝		¾	
Minimum Baseplate Clearance Hole Diameter[2]	d_c	in.	⅜		½		⅝		¾		⅞	
Maximum Installation Torque[3]	$T_{inst,max}$	ft.-lbf.	N/A		40		70		85		150	
Maximum Impact Wrench Torque Rating	$T_{impact,max}$	ft.-lbf.	125		150		345		345		380	
Minimum Hole Depth	h_{hole}	in.	2¼	3⅛	2¾	3½	3¾	4½	4½	6	6	6¾
Nominal Embedment Depth	h_{nom}	in.	2⅛	3	2½	3¼	3¼	4	4	5½	5½	6¼
Effective Embedment Depth	h_{ef}	in.	1.27	2.01	1.40	2.04	1.86	2.50	2.31	3.59	3.49	4.13
Critical Edge Distance	c_{ac}	in.	3	3	4½	5½	6	5¾	6	6⅜	6¾	7⅜
Minimum Edge Distance	c_{min}	in.	1½	1½	1¾	1¾	1¾	2¼	1¾	1¾	1¾	1¾
Minimum Spacing	s_{min}	in.	1½	1½	3	3	4	3	3	3	3	3
Minimum Concrete Thickness	h_{min}	in.	3½	4⅜	4	5	5	6¼	6	8½	8¾	10
Anchor Data												
Yield Strength	f_{ya}	psi	88,000		98,400		91,200		83,200		92,000	
Tensile Strength	f_{uta}	psi	110,000		123,000		114,000		104,000		115,000	
Minimum Tensile and Shear Stress Area	A_{se}	in.^{2}	0.0430		0.099		0.1832		0.276		0.414	
Axial Stiffness in Service Load Range — Uncracked Concrete	β_{uncr}	lb./in.	139,300		807,700		269,085		111,040		102,035	
Axial Stiffness in Service Load Range — Cracked Concrete	β_{cr}	lb./in.	103,500		113,540		93,675		94,400		70,910	

For **SI**: 1 in. = 25.4 mm, 1 ft.-lbf. = 1.356 N-m, 1 psi = 6.89 kPa, 1 in.^{2} = 645 mm^2, 1 lb./in. = 0.175 N/mm.

1. The information presented in this table is to be used in conjunction with the design criteria of ACI 318-14 Chapter 17 or ACI 318-11 Appendix D, as applicable.
2. The minimum hole size must comply with applicable code requirements for the connected element.
3. $T_{inst,max}$ applies to installations using a calibrated torque wrench.

Figure 3-7: Simpson evaluation report (Anchor Geometry)

Stainless-Steel Titen HD Tension Strength Design Data[1,5]

Characteristic	Symbol	Units	Nominal Anchor Diameter (in.)									
			¼		⅜		½		⅝		¾	
Anchor Category	1, 2 or 3	—	3		1							
Nominal Embedment Depth	h_{nom}	in.	2⅛	3	2½	3¼	3¼	4	4	5½	5½	6¼
Steel Strength in Tension (ACI 318-14 17.4.1 or ACI 318-11 Section D.5.1)												
Tension Resistance of Steel	N_{sa}	lbf.	4,730		12,177		20,885		28,723		47,606	
Strength Reduction Factor — Steel Failure[2]	ϕ_{sa}	—	0.75									
Concrete Breakout Strength in Tension (ACI 318-14 17.4.2 or ACI 318 Section D.5.2)												
Effective Embedment Depth	h_{ef}	in.	1.27	2.01	1.40	2.04	1.86	2.50	2.31	3.59	3.49	4.13
Critical Edge Distance	c_{ac}	in.	3	3	4½	5½	6	5¾	6	6⅜	6¾	7⅜
Effectiveness Factor — Uncracked Concrete	k_{uncr}	—	24	24	27	24	27	24	24	24	27	27
Effectiveness Factor — Cracked Concrete	k_{cr}	—	17	17	21	17	17	17	17	17	17	21
Modification Factor	$\Psi_{c,N}$	—	1									
Strength Reduction Factor — Concrete Breakout Failure[3]	ϕ_{cb}	—	0.45		0.65							
Pullout Strength in Tension (ACI 318-14 17.4.3 or ACI 318-11 Section D.5.3)												
Pullout Resistance Uncracked Concrete (f'_c = 2,500 psi)	$N_{p,uncr}$	lbf.	1,725[5]	3,550[8]	N/A[4]	N/A[4]	N/A[4]	N/A[4]	3,820[5]	9,080[7]	N/A[4]	N/A[4]
Pullout Resistance Cracked Concrete (f'_c = 2,500 psi)	$N_{p,cr}$	lbf.	695[5]	1,225[5]	1,675[5]	2,415[5]	1,995[5]	N/A[4]	N/A[4]	N/A[4]	N/A[4]	N/A[4]
Strength Reduction Factor — Pullout Failure[6]	ϕ_p	—	0.45		0.65							
Tension Strength for Seismic Applications (ACI 318-14 17.2.3.3 or ACI 318-11 Section D.3.3.3)												
Nominal Pullout Strength for Seismic Loads (f'_c = 2,500 psi)	$N_{p,eq}$	lbf.	695[5]	1,225[5]	1,675[5]	2,415[5]	1,995[5]	N/A[4]	N/A[4]	N/A[4]	N/A[4]	N/A[4]
Strength Reduction Factor for Pullout Failure[6]	ϕ_{eq}	—	0.45		0.65							

For **SI**: 1 in. = 25.4 mm, 1 ft.-lbf. = 1.356 N-m, 1 psi = 6.89 kPa, 1 in.^{2} = 645 mm^2, 1 lb./in. = 0.175 N/mm.

1. The information presented in this table is to be used in conjunction with the design criteria of ACI 318-14 Chapter 17 or ACI 318-11 Appendix D, as applicable.
2. The tabulated value of ϕ_{sa} applies when the load combinations of Section 1605.2 of the IBC, ACI 318-14 Section 5.3 or ACI 318-11 Section 9.2 are used, as applicable. If the load combinations of ACI 318-11 Appendix C are used, the appropriate value of ϕ must be determined in accordance with ACI 318 D.4.4(b), as applicable.
3. The tabulated values of ϕ_{cb} applies when both the load combinations of Section 1605.2 of the IBC, ACI 318-14 Section 5.3 or ACI 318-11 Section 9.2, as applicable, are used and the requirements of ACI 318-14 17.3.3(c) or ACI 318-11 D.4.3(c) for Condition B are met. Condition B applies where supplementary reinforcement is not provided in concrete. For installations where complying reinforcement can be verified, the ϕ_{cb} factors described in ACI 318-14 17.3.3(c) or ACI 318-11 D.4.3(c), as applicable, may be used for Condition A. If the load combinations of ACI 318 Appendix C are used, the appropriate value of ϕ must be determined in accordance with ACI 318 D.4.4(c) for Condition B.
4. N/A denotes that pullout resistance does not govern and does not need to be considered.
5. The characteristic pullout resistance for greater compressive strengths may be increased by multiplying the tabular value by $(f'_c/2{,}500)^{0.5}$.
6. The tabulated values of ϕ_p or ϕ_{eq} applies when both the load combinations of ACI 318-14 Section 5.3 or ACI 318-11 Section 9.2, as applicable, are used and the requirements of ACI 318-14 17.3.3(c) or ACI 318-11 D.4.3(c) for Condition B are met. If the load combinations of ACI 318 Appendix C are used, the appropriate value of ϕ must be determined in accordance with ACI 318 D.4.4(c) for Condition B.
7. The characteristic pullout resistance for greater compressive strengths may be increased by multiplying the tabular value by $(f'_c/2{,}500)^{0.4}$.
8. The characteristic pullout resistance for greater compressive strengths may be increased by multiplying the tabular value by $(f'_c/2{,}500)^{0.3}$.

Figure 3-8: Simpson evaluation report (Anchor Strength - Tension)

Stainless-Steel Titen HD Shear Strength Design Data[1]

Characteristic	Symbol	Units	Nominal Anchor Diameter (in.)									
			¼		⅜		½		⅝		¾	
Anchor Category	1, 2 or 3	—	3		1							
Nominal Embedment Depth	h_{nom}	in.	2⅛	3	2½	3¼	3¼	4	4	5½	5½	6¼
Steel Strength in Shear (ACI 318-14 17.5.1 or ACI 318-11 Section D.6.1)												
Shear Resistance of Steel	V_{sa}	lbf.	2,285		3,790	4,780	6,024	7,633	10,422	10,649	13,710	19,161
Strength Reduction Factor — Steel Failure[2]	ϕ_{sa}	—	0.65									
Concrete Breakout Strength in Shear (ACI 318-14 17.5.2 or ACI 318-11 Section D.6.2)												
Nominal Diameter	d_a	in.	0.250		0.375		0.500		0.625		0.750	
Load Bearing Length of Anchor in Shear	l_e	in.	1.27	2.01	1.40	2.04	1.86	2.50	2.31	3.59	3.49	4.13
Strength Reduction Factor — Concrete Breakout Failure[3]	ϕ_{cb}	—	0.70									
Concrete Pryout Strength in Shear (ACI 318-14 17.5.3 or ACI 318-11 Section D.6.3)												
Coefficient for Pryout Strength	k_{cp}	—	1.0					2.0	1.0	2.0		
Strength Reduction Factor — Concrete Pryout Failure[4]	ϕ_{cp}	—	0.70									
Shear Strength for Seismic Applications (ACI 318-14 17.2.3.3 or ACI 318-11 Section D.3.3.3)												
Shear Resistance — Single Anchor for Seismic Loads (f'_C = 2,500 psi)	$V_{sa,eq}$	lbf.	1,370	1,600	3,790	4,780	5,345	6,773	9,367	9,367	10,969	10,969
Strength Reduction Factor — Steel Failure[2]	ϕ_{eq}	—	0.65									

For **SI**: 1 in. = 25.4mm, 1 lbf. = 4.45N.

1. The information presented in this table is to be used in conjunction with the design criteria of ACI 318-14 Chapter 17 or ACI 318-11 Appendix D, as applicable.
2. The tabulated value of ϕ_{sa} and ϕ_{eq} applies when the load combinations of Section 1605.2 of the IBC, ACI 318-14 Section 5.3 or ACI 318-11 Section 9.2, as applicable, are used. If the load combinations of ACI 318 Appendix C are used, the appropriate value of ϕ_{sa} and ϕ_{eq} must be determined in accordance with ACI 318 D.4.4(b).
3. The tabulated value of ϕ_{cb} applies when both the load combinations of Section 1605.2.1 of the IBC, ACI 318-14 Section 5.3 or ACI 318-11 Section 9.2 are used and the requirements of ACI 318-14 17.3.3(c) or ACI 318-11 D.4.3(c) for Condition B are met. Condition B applies where supplementary reinforcement is not provided. For installations where complying supplementary reinforcement can be verified, the ϕ_{cb} factors described in ACI 318-14 17.3.3(c) or ACI 318-11 D.4.3(c) for Condition A are allowed. If the load combinations of ACI 318-11 Appendix C are used, the appropriate value of ϕ_{cb} must be determined in accordance with ACI 318-11 D.4.4(c).
4. The tabulated value of ϕ_{cp} applies when both the load combinations of IBC Section 1605.2, ACI 318-14 5.3 or ACI 318-11 Section 9.2 are used and the requirements of ACI 318-14 17.3.3(c) or ACI 318-11 D.4.3(c) for Condition B are met. If the load combinations of ACI 318-11 Appendix C are used, appropriate value of ϕ_{cp} must be determined in accordance with ACI 318-11 Section D.4.4(c).

Figure 3-9: Simpson evaluation report (Anchor Strength - Shear)

3.3 DEMAND (APPLIED FORCE)

The variation in the application of each index (e.g., pedestrian railing versus vehicle barrier) yields vastly different applied loads. A single load case was established and applied to each index for simplicity and uniformity. The loads and load factors used herein were in accordance with AASHTO LRFD BDS.

Distributed Service Live Loads: $w_{vertical} = 50\ lb/ft.$ $w_{horizontal} = 50\ lb/ft.$

Point Service Live Load: $P_{point} = 200\ lb.$

Between most anchor plates and the corresponding mounting surface exists a 1/8" neoprene bearing pad to reduce surface imperfections and minimize corrosion potential due to ponding or trapping water beneath the baseplate. For all of the indexes analyzed, steel or aluminum base plates are used to mount the structures to roadways, sidewalks, or other unique surfaces. The surfaces are almost always constructed from granular material (i.e., concrete or asphalt). If the interaction between a baseplate and a surface is imperfect, loading may cause extreme pressures to arise. For example, suppose a sizeable rock is present under a base plate. In that case, the bearing area changes from the area of the base plate to the area of the rock, which could result in uneven load distribution and cause a concentrated moment to occur. The presence of the neoprene pad is expected to result in a more uniform but slightly larger bearing area than direct mounting to concrete. Two methods of calculating the demand (design) strength were performed, one assuming a uniform pressure area of a one-inch strip of bearing and another using a modified triangular pressure distribution:

Method 1: Contribution from a neoprene pad was considered by assuming a one-inch uniform compressive pressure strip under the extreme edge of the baseplate.

Method 2: A linearly varying compressive pressure distribution from zero at the centerline of the tension anchor bolts to a maximum at the extreme compression edge of the baseplate. Some nonlinearities in the pressure distribution provided by the Neoprene Pad contribution can be included by assuming a subjective tension reduction modification factor.

3.3.1 METHOD 1

Method 1 follows the same procedure used in the previous project, namely BDV28-977-06. The following equation was used to estimate the tension in each anchor:

$$N_n = T_{max} = (P_u)\left(\frac{L}{z}\right)$$

P_u =ultimate factored load

z = distance between the anchor centerline and the axis of the baseplate resultant reaction (assumed to be ½-inch inside the extreme compression edge of the baseplate)

L = length of moment arm of applied load above the foundation.

The applicable load factors were applied. The following sample calculation is for FDOT Index 515-052, which is identical in geometry to index 515-062:

$$P_u = \gamma_{DL} P_D + \gamma_{LL} P_L$$

γ_{DL} = dead load factor = 1.25 (vertical dead load effect is conservatively ignored)

γ_{LL} = live load factor = 1.75

$P_L = (w_{horizonta})(Post\ spacing) + P_{point}$
$= \left(50 \frac{lb}{ft}\right)(7.25\ ft.) + 200\ lb. = 562.5\ lb.$
$P_u = (1.25)(0\ lb.) + (1.75)(562.5) = 0.984\ k$

Given the geometry of the railing, the distributed and point load is assumed to induce the highest moment about the base plate when they are applied to the centerline of the top railing. Applying the loads horizontally at the top of the railing results in a moment arm length of 40.6-in. and a *z* of one-half the width of the base plate less ½-in. (2.5-in.) for the 1-bolt detail.

$$N_{n1} = T_{max} = (0.984k)\left(\frac{40.6\ in.}{2.5\ in.}\right) = 16.0\ k$$

A base plate using only one screw anchor controls as multiple anchors provide increased strength (assuming installation is in the region with adequate edge distances and the same embedment depth).

For the 4-bolt detail, only the two back anchors are in tension, *z* increases to 4.75-in.

$$N_{n4} = T_{max} = (0.984k)\left(\frac{40.6\ in.}{4.75\ in.}\right) = 8.4\ k$$

3.3.2 METHOD 2

Method 2 is assumed to be a more conservative estimation based on elastic analysis by taking a uniformly increasing bearing pressure from zero at the centerline of the tension bolt to the compression edge of the baseplate. It has been slightly modified using design requirements provided by the FDOT Project Manager. The following equation was used to estimate the tension in each anchor:

$$T_{max} = \left[\frac{M_{c,post}}{\frac{b_{plate} + 2y_b}{3}}\right](R_t) - P_v$$

P_v = Vertical ultimate factored load (conservatively assume to be zero)

$M_{c,post}$ = moment about the baseplate, = $P_u * Lb_{plate}$ = width of baseplate

y_b = lateral offset of tension bolts from baseplate centroid in the applied load location

$R_t =$ factor accounting for some nonlinear pressure distribution (recommend 0.90)

When the tension anchor bolts are located along the centerline of the post bending axis and the vertical loads are ignored, this equation reduces into a simplified form similar to Method 1:

$$T_{max} = (P_u)\left(\frac{L}{z}\right)(R_t)$$

$z = \frac{b_{plate}}{3}$ = distance between the anchor centerline and the axis of the baseplate resultant reaction (assumed here to be 2/3rds of half the baseplate width for anchor along the centerline of the baseplate)

The applicable load and strength reduction factors were applied. The following sample calculation is for FDOT Index 515-052, which is identical in geometry to index 515-062:

$P_u = (1.25)(0\ lb.) + (1.75)(562.5) = 0.984\ k \rightarrow$ From *3.1 Method 1*

Given the geometry of the railing, the distributed and point load is assumed to induce the highest moment about the base plate when they are applied to the centerline of the top railing. Applying the loads horizontally at the top of the railing results in a moment arm length *(L)* of 40.6-in.:

$M_{c,post} = (40.6\ in./12in.)(0.984\ k) = 3.33\ k-ft = 39.96\ k-in$

$$T_{max1} = \left[\frac{39.96\ k-in}{\frac{6in.+2(0\ in.)}{3}}\right](0.90) - 0\ lb. \approx 18\ k$$

Like in Method 1, a base plate using only one screw anchors controls as multiple anchors provide increased strength (assuming installation is in region with adequate edge distances and the same embedment depth).

For the 4-bolt detail only the two back anchors are in tension, and y_b increases to 2.25-in.

$$T_{max4} = \left[\frac{39.96\ k-in}{\frac{6in.+2(2.25\ in.)}{3}}\right](0.90) - 0\ lb. \approx 10.3\ k$$

Detailed load calculations for all railing types are available in Appendix A and the results are tabulated in Table 3-5.

3.3.3 ASSUMPTIONS

The following assumptions and notes apply to both methods of estimating applied loads:

- No offsetting of loads/eccentricity is present in reference to the centroid of the baseplate).
- The worst/most demanding loading scenario occurs when the moment length is maximized; hence, loads were applied at the furthest possible perpendicular distance from the anchor installation location (baseplates).
- $R_t = 0.90$ was provided by FDOT.
- Material properties were assumed to be adequate and in accordance with the limitations provided by FDOT.
- Only tension applied to each anchor was calculated as it allows for direct comparison between allowable strength and demand. A complete design would include, among combined and other unique effects, verification of flexural and shear capacities (as done in FDOT's design calculation reports.
- The base of railings is fixed (i.e., not pinned)
- All baseplates accommodate the largest screw anchor manufactured by Simpson Strong-Tie (3/4" diameter x 7" long anchor, assuming 6 ¼" nominal embedment depth).

Each index is unique in scope and geometry, requiring index-specific assumptions to be made.

The geometry of Index 515-052 and 515-062 is identical, as is the geometry of Index 515-070 and 515-080. The similarities permit the production of a single analysis for each pair of indexes.

Of all the Indexes referenced in Index 515-022, the 27" parapet (Index 521-820) is the narrowest and was used to control analysis.

3.4 RESULTS

The results of the design loads and capacity of ¾-in. stainless steel screw anchor for various FDOT indexes are summarized in Table 3-5. The applied tension represents the design loads that were computed using Method 1 and 2 described in Sections 3.3.1 and 3.3.2, respectively. Whereas the steel strength and breakout strength in tension represent the calculated capacities of the ¾-in. screw anchor when used to anchor various FDOT indexes. The nominal strengths are listed in the table represent the nominal capacities that are multiplied by various modification factors listed in Section 3.2 to obtain the factored design strengths. The significant difference in design strengths caused by the difference in modification factors can be observed in the Appendix that shows all design calculations.

It should also be mentioned that the results are based on anchors with a nominal embedded depth of 6 ¼ in. which can be achieved with a 7-in. long anchor. However, the longest anchor produced is 8.5-in. which has a longer thread length, which could potentially increase the nominal embedment depth and the breakout strength. Given no testing has been performed to justify an increased effective embedment depth, a value of h_{ef} equal to 4.13 in. was used for design and load calculations. Pullout strength was not considered in the analysis as the manufacturer literature states that pullout strength is not a controlling failure mode and does not provide strength values. Screw anchor pullout strength, according to ACI CODE-318-19, must be determined via testing according to ACI CODE-355.2-19; hence, a theoretical strength is not permitted to be calculated. Recognizing the limitations encountered due to a lack of test data, it is recommended that

strength testing should be included in the scope of the following phase of the project. Especially, testing of 6-in.-long and 8½- in.-long anchors in ¾-in. diameter should be tested.

For FDOT indexes 515-052/062, the design breakout strength using the 4-bolt detail provides approximately a 25% increase in capacity compared to the single bolt detail. However, only the design breakout strength of the 4-bolt detail installed on the sidewalk can meet the load demand if Method 1 is used for calculating the load. If Method 2 is used, the design breakout strength is approximately 7% lower than the Method 2 load calculation. It is possible that the design breakout strength of the 4-bolt detail installed on the gravity wall may meet Method 1 load if the confinement effect is considered. There are also various sizes (4, 5, 6, 7, and 8½-in.) of ¾-in. stainless steel anchors listed on the Simpson Strongtie website. However, the design capacity is limited to the test data provided in Figure 3-7, Figure 3-8 and Figure 3-9. Considering the confinement effect from the base plate, it is possible that using the ¾′−8½′ inches. stainless-steel screw anchor may result in a much larger strength to meet both Method 1 and 2 load requirements. Therefore, it is recommended that the 4-bolt detail be further experimentally evaluated. It is also possible that for the sidewalk application, shorter screw anchors could be used.

On the other hand, except for the 2-bolt detail used in the gravity wall, the design breakout strengths for FDOT indexes 515-070/080 all exceed Method 1 and 2 load requirements. The design breakout strength of the 2-bolt detail installed in the gravity wall is only 15% and 24% below Method 1 and 2 load requirements, respectively. Considering the confinement effect, it is anticipated that the ¾′−7′ inches. stainless-steel screw anchor would provide adequate design strength for FDOT indexes 515-070/080 for all applications but should be further evaluated experimentally. However, we recommend using ¾′−8½′ inches. screw anchor for the experimental program because the additional length would provide slightly higher design strength and there is not a significant effort in drilling a slightly deeper hole. This would also provide a more consistent testing program for different FDOT indexes.

For the FDOT index 515-022, installed over a 27” parapet, the design strength using the 2-bolt detail is significantly lower than the load requirement. However, the nominal breakout strength is higher than Method 1 load requirement. The limiting factor here lies in the edge distance atop of the parapet where the effective embedment depth of the anchor has less influence on the design strength. However, if the confinement effect would increase the design strength by a factor of 1.5 and using Method 1 load analysis, the ¾′−8½′ inches. screw anchor may be able to adequately provide the design strength for this index. It is recommended that an experimental program include this detail as well if the testing results of the FDOT index 515-070/080 in gravity wall show much higher design capacity.

It is important to note that the ACI breakout strength equation is very conservative. In fact, in the adhesive anchors' research project BDV28-977-06, the governed failure mode was not found to be the concrete breakout but closer to the adhesive pullout strength. According to ACI CODE-318-19 Section 17.6.3.2.1, the pullout strength of screw anchors is based on the 5% fractal results of tests performed and evaluated according to ACI CODE-355.2-19. However, because the manufacturer does not provide this data, the value will need to be obtained experimentally. According to ACI CODE-355.2, the minimum sample size for evaluating the anchor system breakout resistance is 5. Therefore, at least five samples will be evaluated in a later task.

Table 3-5: Design loads and capacity of ¾-in. stainless steel screw anchors used on various FDOT indexes

FDOT Index No. 515-	Applied Tension (kips)		Steel Strength in Tension		Breakout Strength in Tension (ACI)	
	Method 1	Method 2	Nominal Strength (kips) N_{sa}	Design Strength (kips) ϕN_{sa}	Nominal Strength (kips) N_{cbg}	Design Strength (kips) ϕN_{cbg}
052/062 (Gravity Wall) 1-Bolt Detail	15.99	17.98	47.61	35.71	7.38	4.80
052/062 (Gravity Wall) 4-Bolt Detail	8.41	10.28			9.03	5.87
052/062 (Sidewalk) 1-Bolt Detail	15.99	17.98			11.74	7.63
052/062 (Sidewalk) 4-Bolt Detail	8.41	10.28			17.14	11.14
070/080 (Gravity Wall) 2-Bolt Detail	8.53	9.59			10.66	6.93
070/080 (Gravity Wall) 4-Bolt Detail	4.49	5.48			9.16	5.95
070/080 (Sidewalk) 2-Bolt Detail	8.53	9.59			16.95	11.02
070/080 (Sidewalk) 4-Bolt Detail	4.49	5.48			17.38	11.30
022 (27-in. Parapet) 2-Bolt Detail	8.19	9.21			8.63	5.61

Note:

Design Strength > Applied Load
Nominal Strength > Applied Load
Both Nominal and Design Strength < Applied Load

Table 3-6: ACI strength reduction factors

Steel Strength in Tension	Breakout Strength in Tension	Pullout Strength in Tension
ACI Modification Factor ϕ_{ACI}	ACI Modification Factor ϕ_{ACI}	ACI Modification Factor ϕ_{ACI}
0.75	0.65	0.65

3.5 PROPOSED PHASE 1 TESTING SCHEMES

Based on the results, the Research Team proposed that the three FDOT indexes with steel pedestrian posts be tested using the details with minimal anchorage (i.e., 1- and 2-bolt). All should be anchored using the ¾ ′ 8 ½ in—type 316 stainless steel screw anchor. For FDOT Index 515-070/080, a shorter screw anchor (¾ ′ 6 in.) could also be evaluated to determine the effect of effective embedment length on the capacity and to determine at what effective length would the failure mode shift from anchor pullout failure (or combined failure) to concrete breakout failure.

The proposed testing schemes consist of installing the pedestrian railing on 1) sidewalk, 2) gravity wall, and 3) parapet. The sidewalk test specimen will have a dimension of 30 ′ 30 ′ 12 in. and be made using Class NS concrete. Two edge distances of 15 in. (i.e., no edge distance effect) and 6-in. (standard edge distance of sidewalk) will be evaluated for FDOT Index 515-052 with BOTH 1-bolt and 4-bolt details. Figure 3-10 illustrates the test setup of the sidewalk application. For the gravity wall and the parapet, the 4-bolt detail may be considered impractical due to the close edge distances and concerns for side face cracking during drilling and installation of the anchors. For this reason, a 1-bolt detail is also included in the test matrix. The gravity wall will be made of Class NS concrete as illustrated in Figure 3-11 and Figure 3-12. An edge distance of 4.5 in. will be used for the gravity wall. The parapet will be made of Class II concrete, where the railing will be installed at 4.0 in. from the edge as illustrated in Figure 3-13. A minimum of 5 specimens will be tested for each test setup.

For the sidewalk test setup with 6 in. edge distance, one concrete sidewalk can be used to evaluate two screw anchors, so only three concrete specimens are needed. Table 3-7 summarizes the proposed testing scheme for Phase 1, which consists of anchor breakout capacity testing. More details on the test program will be developed in the next task.

The concrete specimen's detail will have to be modified once the Research Team confirms the actual testing location, which will be described in Task 3.

Table 3-7: Summary of the proposed phase 1 testing schemes

Post Type	**Pedestrian/Picket Railing**					**Guiderail**					**Bullet Rail**
Index No.	**515 -052 and -062**					**515-070 and -080**					**515-022**
Foundation	**Sidewalk No Edge**	**Sidewalk w/ Edge (4-bolt)**	**Sidewalk w/ Edge (1-bolt)**	**Gravity Wall (4-bolt)**	**Gravity Wall (1-bolt)**	**Sidewalk No Edge**	**Sidewalk w/ Edge**	**Sidewalk Shorter h_{ef}**	**Gravity Wall**	**8" Parapet**	**8" Parapet**
# Anchors	4	4	1	4	1	2	2	2	2	2	2
Spacing (in.)	4.5	4.5	- n/a	4.5	- n/a	5	5	5	3	3	3
Anchor Size (in.)	0.75	0.75	0.75	0.75	0.75	0.75	0.75	0.75	0.75	0.75	0.75
Anchor Length (in.)	8.5	8.5	8.5	8.5	8.5	8.5	8.5	6	8.5	8.5	8.5
Baseplate thickness	0.625	0.625	0.625	0.625	0.625	0.5	0.5	0.5	0.5	0.5	0.5
Pad thickness and washer	0.1875	0.1875	0.1875	0.1875	0.1875	0.1875	0.1875	0.1875	0.1875	0.1875	0.1875
Nominal Embed. (in.)	7.688	7.688	7.688	7.688	7.688	7.813	7.813	5.313	7.813	7.813	7.813
Effective Embed. (in.)	5.478	5.478	5.478	5.478	5.478	5.603	5.603	3.103	5.603	5.603	5.603
Edge Distance to baseplate centerline (in.)	15.00	6.00	6.00	4.50	4.50	15.00	6.00	6.00	4.50	4.00	4.00
Number concrete test specimens	5	3	3	5	5	5	3	3	5	5	5
Concrete Class	Class NS	Class NS	Class NS	Class NS	Class NS	Class NS	Class NS	Class NS	Class NS	Class II	Class II
Concrete Strength (psi)	2500	2500	2500	2500	2500	2500	2500	2500	2500	3400	3400
Concrete Size (in.)	30 x 30 x 12	30 x 30 x 12	30 x 30 x 12	See Fig. 3-11	See Fig. 3-12	30 x 30 x 12	30 x 30 x 12	30 x 30 x 12	See Fig. 3-12	See Fig. 3-13	See Fig. 3-13
Concrete volume per specimen (cu.ft)	6.25	6.25	6.25	7.11	7.11	6.25	6.25	6.25	7.11	5.33	5.33
Total Concrete Volume (cu.yd)	1.16	0.69	0.69	1.32	1.32	1.16	0.69	0.69	1.32	0.98	0.98
Grand Total Concrete Volume (cu.yd)	11.00										

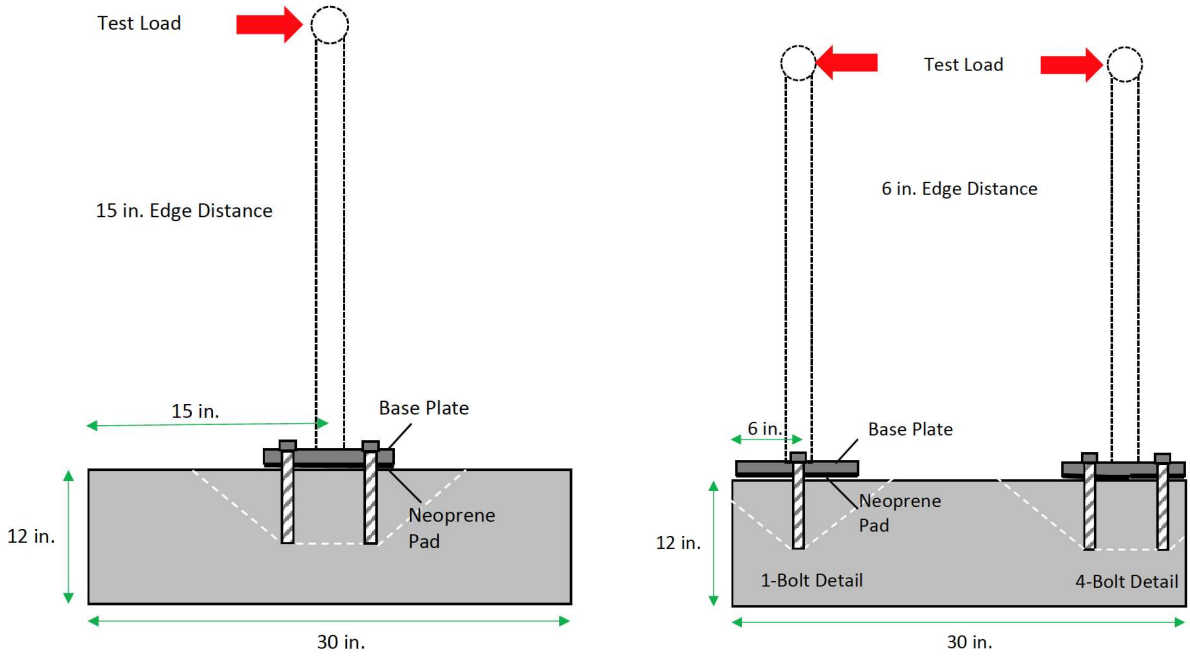

Figure 3-10: Sidewalk test setups

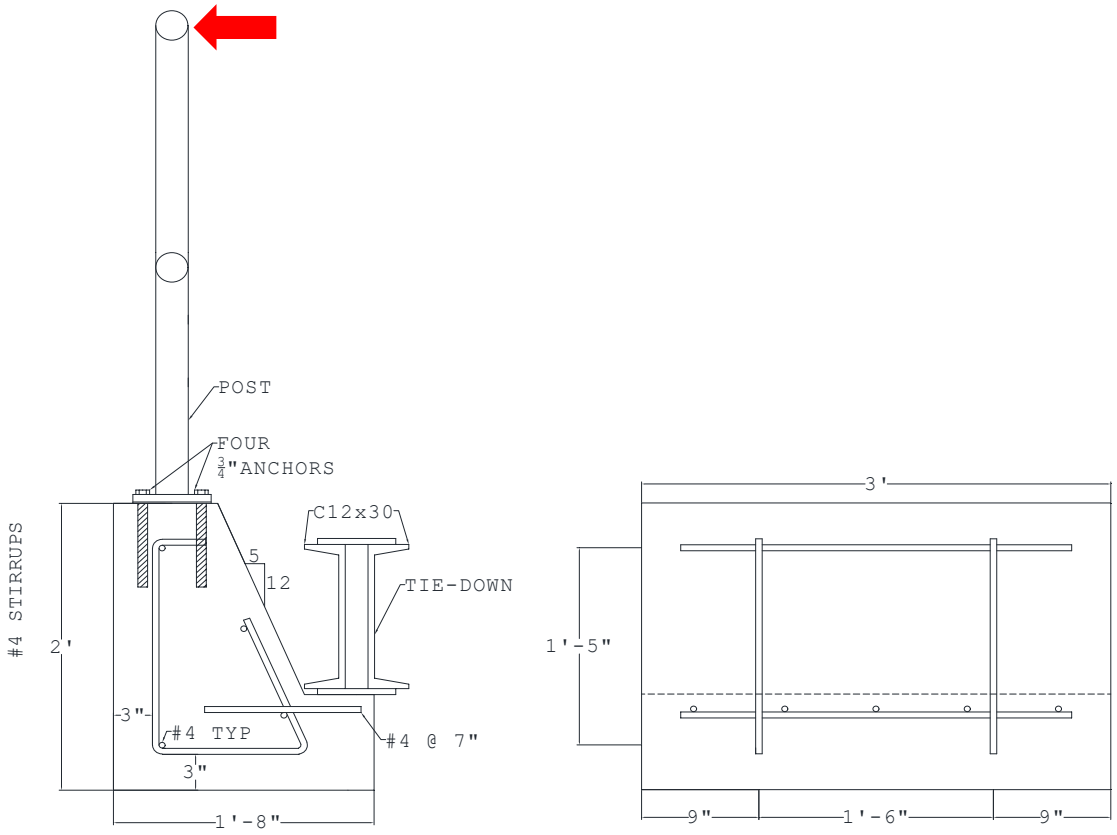

Figure 3-11: Gravity wall with four screw anchors test setup

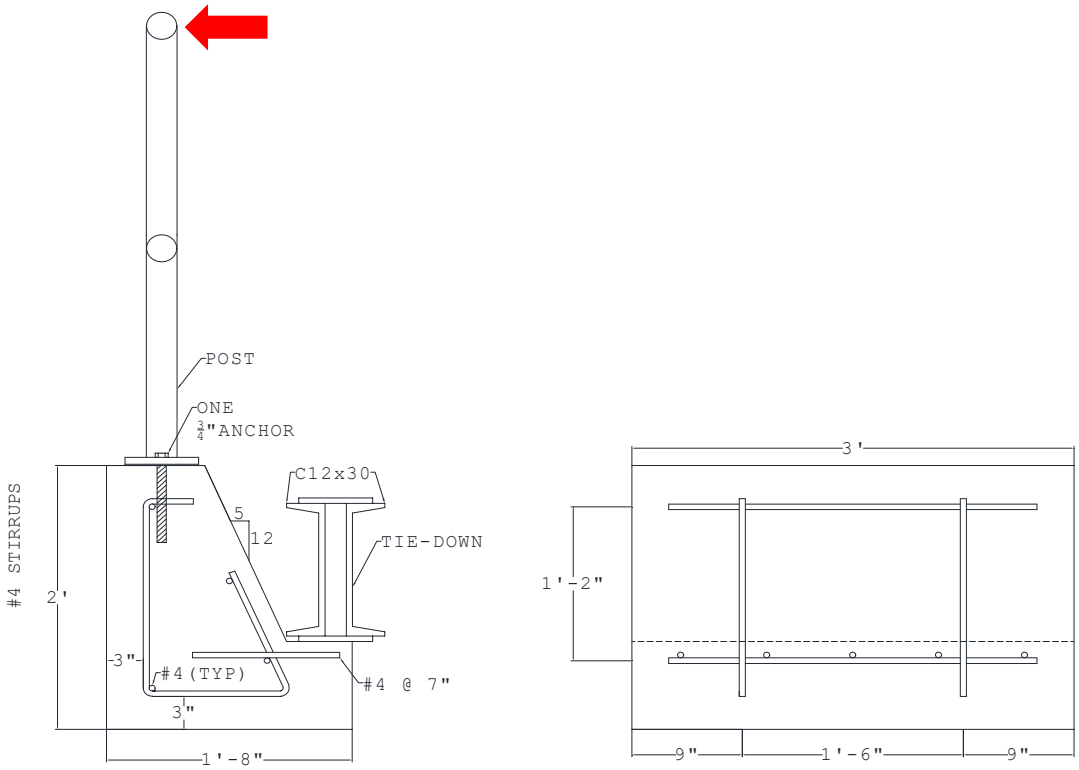

Figure 3-12: Gravity wall with one screw anchor test setup

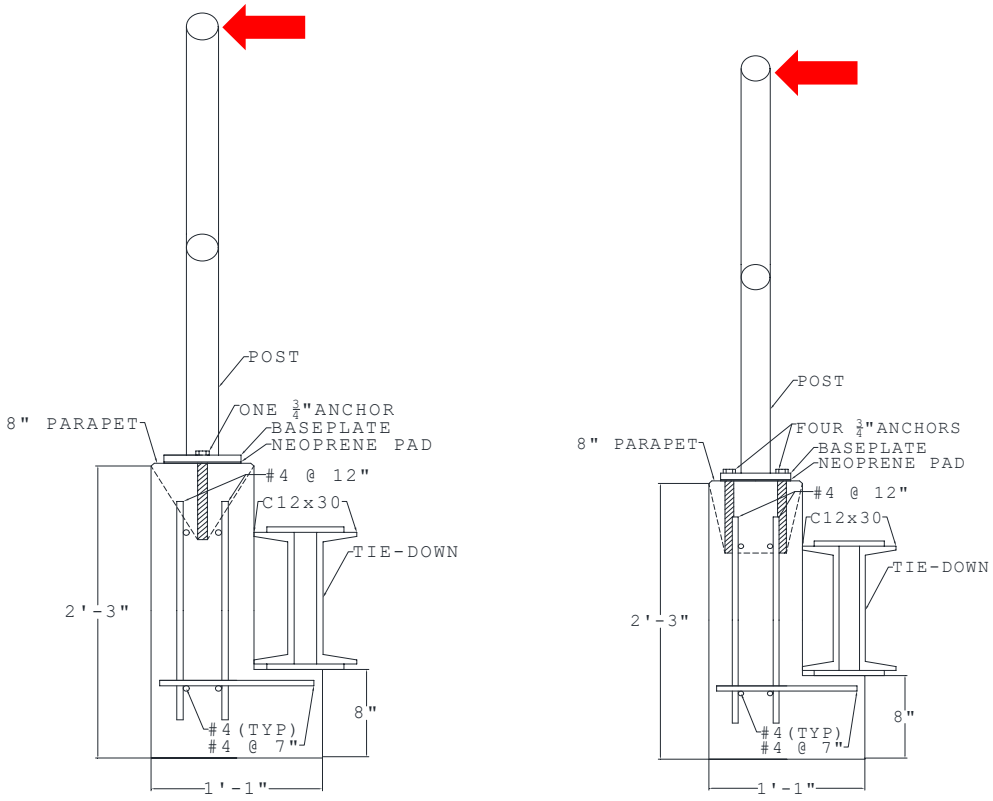

Figure 3-13: Parapet test setup

3.6 SUMMARY

The Florida Department of Transportation can significantly benefit from adopting screw anchors for use in pedestrian railings and other applications. The anchors provide rapid, reliable, and simplified installation procedures compared to adhesive anchors. Although ACI CODE-318-19 has adopted screw anchor design criteria, the provisions often yield conservative allowable strengths, predominantly when concrete breakout governs the design. As reported herein, many research studies indicated that the predominant mode of failure is a combined concrete breakout and pullout failure that exceeds the design capacity obtained using the concrete breakout alone (see Figure 3-4), meaning concrete breakout is an inadequate design limitation. Furthermore, there is no research on the effect of confinement of the base plate on the concrete breakout capacity other than the previous BDV28-977-06 project. Design guidance adjustment through experimentation needs to be performed to equip designers better to capture the actual failure mechanism and appropriate confinement modification factor of screw anchors used in various applications.

Considering that there is a potential for using screw anchor in all FDOT indexes, it is recommended that all indexes be experimentally evaluated in this study. A testing program for each index will be described in the next Task.

4. CHAPTER 4 – EXPERIMENTAL PROGRAM

4.1 INTRODUCTION

This chapter describes the test setup, procedure, and test matrices of the use of screw anchor in the following five Florida Department of Transportation (FDOT) design standards:

9. 515-052: Pedestrian/Bicycle Railing (Steel)
    a. 515-052 (Gravity Wall) with one and four bolt details
    b. 515-052 (Sidewalk) with one and four bolt details
10. 515-062: Pedestrian/Bicycle Railing (Aluminum)
    a. 515-062 (Gravity Wall) with one and four bolt details
    b. 515-062 (Sidewalk) with one and four bolt details
11. 515-070: Pipe Guiderail (Aluminum)
    a. 515-070 (Gravity Wall) with two and four bolt details
    b. 515-070 (Sidewalk) with two and four bolt details
12. 515-080: Pipe Guiderail (Steel)
    a. 515-080 (Gravity Wall) with two and four bolt details
    b. 515-080 (Sidewalk) with two and four bolt details
13. 515-022: Pedestrian/Bicycle Bullet Railing with two bolt detail

However, the test will only be performed on the steel posts to avoid premature failure and pliability of aluminum posts since the focus of this research project is on the screw anchor breakout capacity.

4.2 TEST SETUP

The test will be performed at the FDOT Marcus Ansley Structural Research Center (SRC) on the strong floor using the existing lateral test frame that was previously used for the barge impact project. A pulley system will be bolted to the top transfer beam to allow a vertical mounted 55-kips servo-controlled hydraulic actuator to apply a transverse load to the test specimens that are anchored to the strong floor as illustrated in Figure 4-1. An adaptor plate will be fabricated by the Research Team to allow the 55 kips servo-controlled hydraulic actuator to be mounted to the strong floor since the actuator shoe has a different bolt pattern than the strong floor. A steel platform consisting of a double W18´40 steel beam and a 1-inch-thick steel top plate will also be fabricated. The steel platform is needed to elevate the test specimens approximately 19-inches off the ground such that the top of the steel post aligns with the top of the pulley system so that the applied load would be exactly perpendicular to the steel post. The cantilevered end of the test specimen will be directly anchored to the strong floor using two 1.5-inches threaded rods. Detailed drawings of the test setup, pulley system, and adaptor plate are illustrated in the appendix.

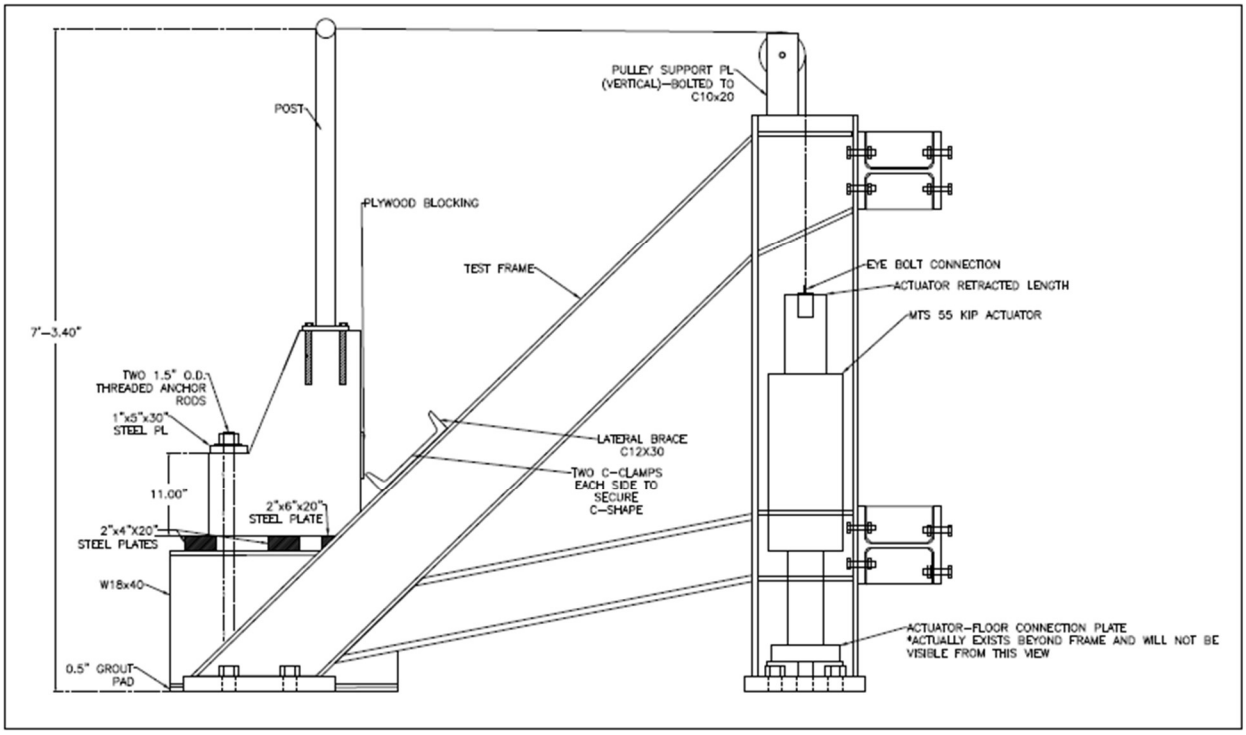

Figure 4-1: Test setup

The design of the test setup is based on the following assumptions:

Monotonic Load Test

The maximum nominal strength of the screw anchor is approximately 18 kips.

If we assume a factor of safety of 2, the maximum tensile load, T_{max}, of the screw anchor is 36 kips.

Given the geometry of the railing, the distributed and point load is assumed to induce the highest moment about the base plate when they are applied to the centerline of the top railing. Applying the loads horizontally at the top of the railing results in a moment arm length, h, of 40 in. and a z of 4.75 in for the 4-bolt detail. The maximum actuator load, P_u can be computed as follow:

$$P_u = \frac{T_{max} z}{h} = \frac{36{,}000 \times 4.75}{40} = 4{,}275 \text{ lbs} \approx 5{,}000 \text{ lbs}$$

For this reason, the test pulley system is rated as 5,000 lbs capacity. This capacity is overly conservative since it is much higher than the anticipated yield and plastic capacity of the pipe guiderail and standard pedestrian rail, which are calculated using the equations below.

Yield Load:

$$P_y = \frac{F_y S_x}{h}$$

Plastic Load:

$$P_p = \frac{F_y Z_x}{h}$$

where, F_y is the steel yield strength, S_x is the elastic section modulus, Z_x is the plastic section modulus, and h is the rail height of 40 inches. Table 4-1 provides a summary of the expected yield and plastic loads.

Table 4-1: Expected yield and plastic loads

Rail Type	**ASTM**	**F_y (ksi)**	**S_x (in3)**	**Z_x (in3)**	**P_y (lbs)**	**P_p (lbs)**
Pipe Guiderail	A53 Grade B	35	0.523	0.713	458	624
Standard Pedestrian Rail	A500 Grade B	46	2(0.705)	2(0.915)	1,622	2,105
Bullet Rail	A572 Grade 50	50	8.55	9.63	10,688	12,038

The maximum deflection can be conservatively taken as 2.5 times the elastic deflection (actual plastic analysis would yield approximately 1.8 times the elastic deflection). It should be noted that the bullet rail used in this study is significantly stronger than the standard aluminum rail. Therefore, the maximum deflection is calculated using the maximum pulley capacity of 5,000 lbs.

For pipe guiderail:

$$\Delta_{max} = 2.5\frac{Ph^3}{3EI} = 2.5 \times \frac{0.458 \times 40^3}{3 \times 29{,}000 \times 0.627} = 1.53\ in.$$

For standard pedestrian railing:

$$\Delta_{max} = 2.5\frac{Ph^3}{3EI} = 2.5 \times \frac{1.622 \times 40^3}{3 \times 29{,}000 \times 2(0.882)} = 1.74\ in.$$

For bullet railing:

$$\Delta_{max} = 2.5\frac{Ph^3}{3EI} = 2.5 \times \frac{5.00 \times 40^3}{3 \times 29{,}000 \times 21.4} = 0.43\ in.$$

These deflections should be within the range of the actuator of 6.0 inches regardless of the railing used.

Cyclic Load Test

The cyclic load test will only be performed on the pipe guiderail and standard pedestrian rail by pulsating tensile load that varies sinusoidally between a maximum and minimum load. The service load of approximately 300 lbs and 562.5 lbs for the pipe guiderail and the standard pedestrian rail, respectively. These loads will be used as the maximum load. A minimum load will need to be maintained during load to ensure stability in the system. This minimum load will be established during setup but is estimated to be 125-150 lbs. Unless premature failure occurs, the drift should not be more than 50%. Table 4-2 provides a summary of the anticipated load and deflection and additional drift due to material degradation.

Table 4-2: Anticipated loads and deflections of the cyclic load test

Rail Type	Max Cyclic Loads (lbs)	Deflection (in.)	Drift (in.)
Pipe guiderail	300	0.37	0.55
Standard Pedestrian Rail	600	0.33	0.50

Again, these loads and deflections are within the range of the actuator.

4.3 TEST PROCEDURE

The test procedures are divided into two loading regimes: 1) monotonic and 2) cyclic load tests. All tests will be performed using the 55 kips servo-controlled hydraulic actuator.

4.3.1 INSTRUMENTATION

– Load cell: Although the 55-kip actuator is equipped with a load cell, a 4-kip tension-link load cell will also be installed to potentially provide a more accurate load reading at the low load range. The tension-link load cell can be installed on the cable between the test specimen and the pulley system.

– Displacement Transducers: The top displacement is not crucial but needed for controlling the actuator. For this project, the displacement of the post will be monitored directly from the actuator displacement. The smallest LVDT will be installed on the post to measure the displacements between the post and the concrete specimen as illustrated in Figure 4-1.

– Inclinometer: An inclinometer may be installed at the steel post's base as indicated in Figure 4-1. The inclinometer will help with establishing the initiation of the concrete breakout or screw anchor pullout failures and anchor slippage.

– Crack Pattern and Width: As it is impossible to know where the crack will be initiated on the concrete, the crack initiation and pattern of the concrete specimen will be determined using a video camera and crack microscope. For the crack microscope, the research team will manually move it to the cracked position that is visible to the naked eye.

4.3.2 MATERIAL PROPERTIES

– Railing: Only steel railing will be evaluated in this study. The standard steel pedestrian railing will be made of HSS 2.5 x 1.5 x 3/16 in. using ASTM A500 Grade B structural tubing. The pipe guiderail will be made of 2" NPS Sch. 40 pipe using ASTM A53 Grade B. In lieu of the standard aluminum bullet rail, a W5x16 made with ASTM A572 or A992 Grade 50 steel will be used for the bullet rail as illustrated in the Appendix. Additionally, a 2.5" NPS Sch. 40 pipe rail will be welded to the top of the bullet rail to allow for the use of the same connection element.

– Bearing Pad: 1/8 in. plain, fabric reinforced or fabric laminated pad.

– Screw Anchor: All testing schemes will be using ¾ ′ 8 ½ in.—type 316 stainless steel screw anchor except for one monotonic and one cyclic load test series in sidewalk specimen that will be using ¾′ 6 in.—type 316 stainless steel.

– Concrete: Class NS concrete will be used for constructing the sidewalk and gravity wall. The parapet will be constructed using Class II concrete. If applicable, No. 4 Grade 60 steel reinforcement will be used.

4.3.3 SPECIMEN FABRICATION

All specimens were fabricated and constructed at the FDOT Marcus H. Ansley Structures Research Center (SRC) using the details provided in Figure 4-3, Figure 4-4 and Figure 4-5 with SRC personnel. Figure 4-2 illustrates the sidewalk specimen fabrication.

Figure 4-2: Specimen fabrication

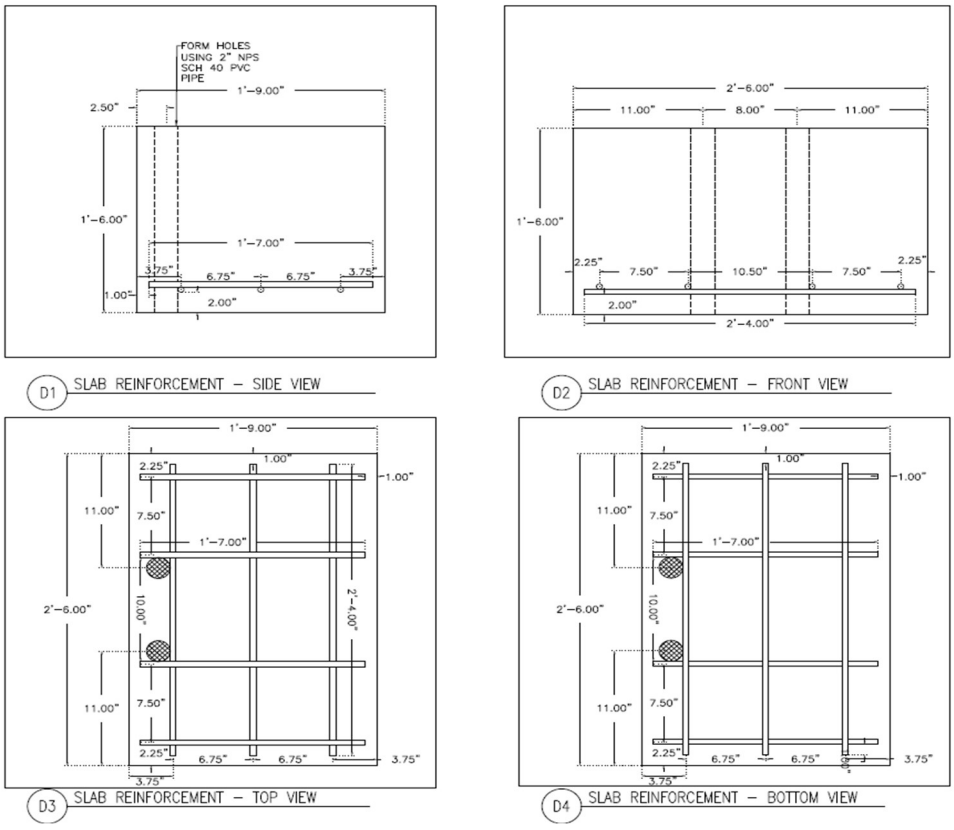

Figure 4-3: Sidewalk slab test specimen details

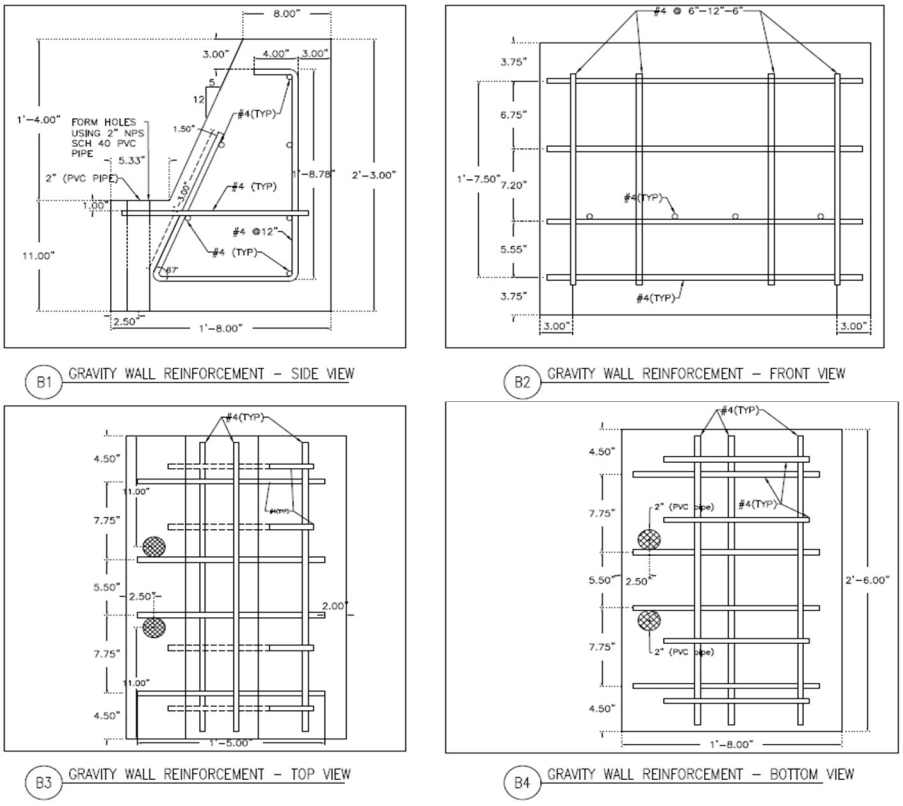

Figure 4-4: Gravity wall test specimen details

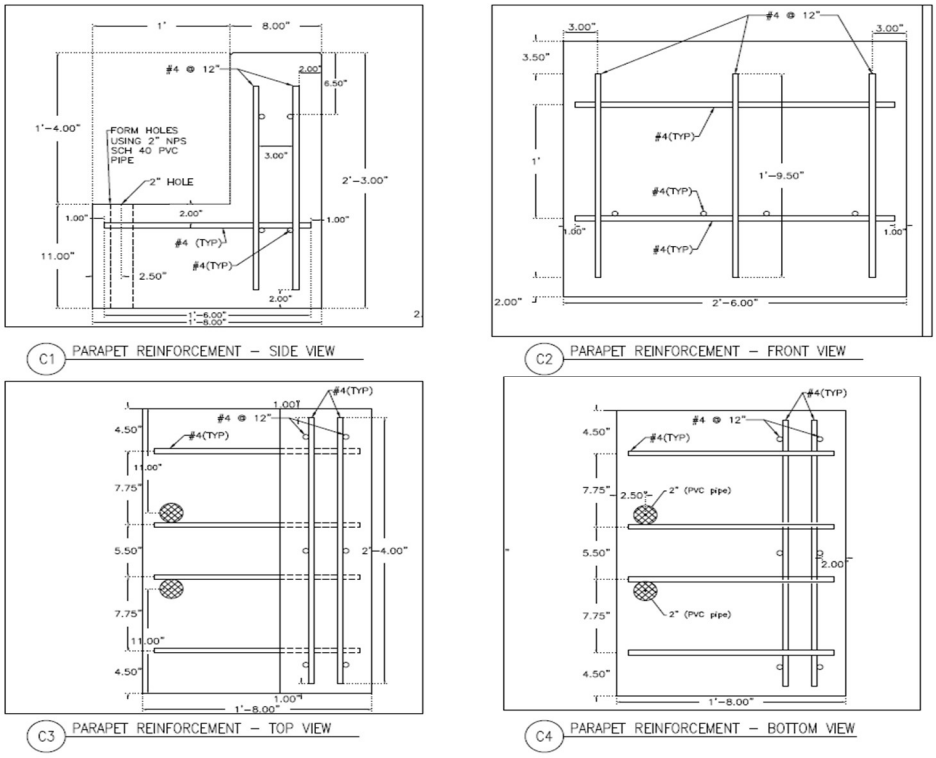

Figure 4-5: Parapet wall test specimen details

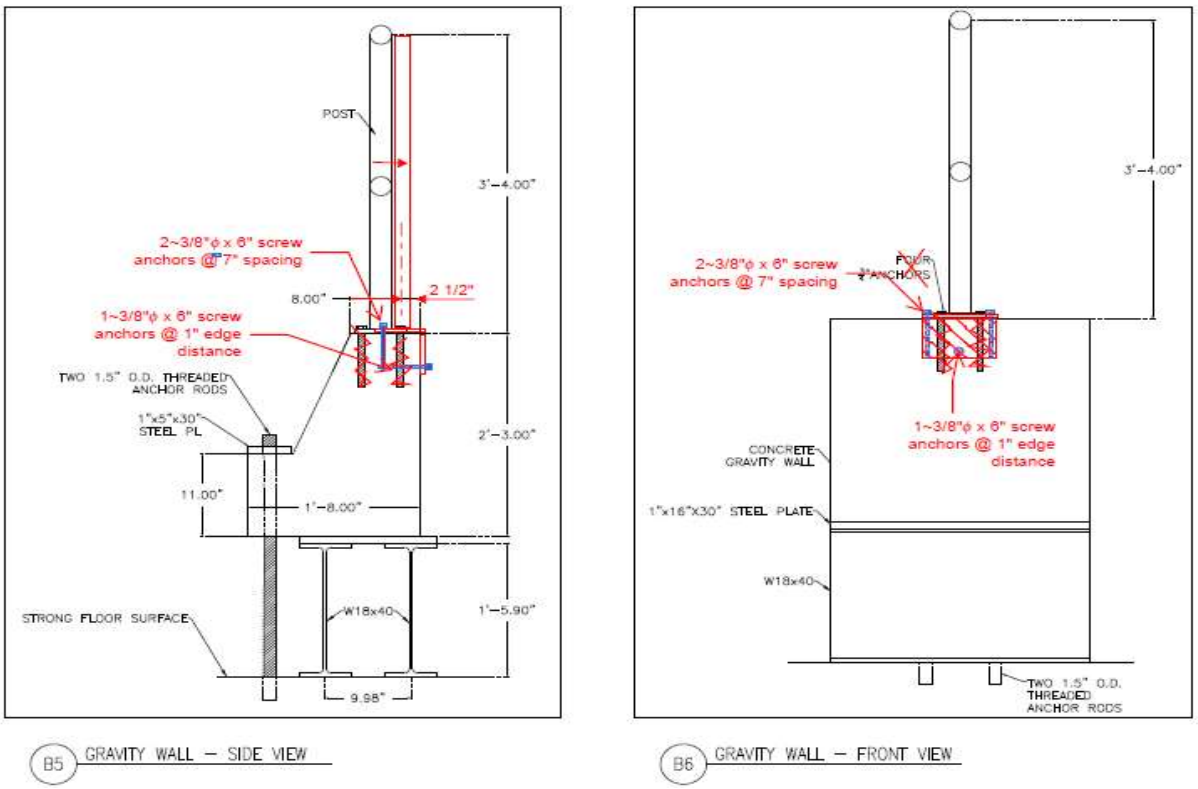

Figure 4-6: Modification of picket railing on gravity wall Specimen

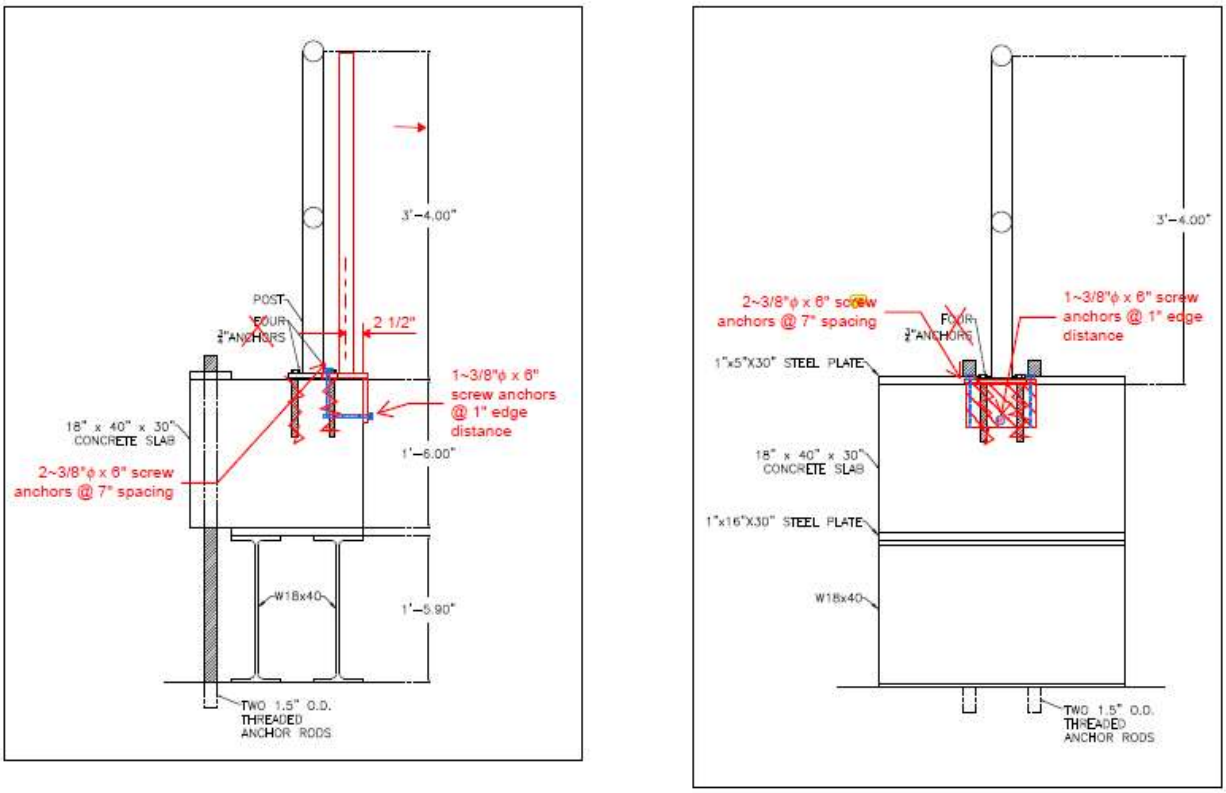

Figure 4-7: Modification of picket railing on slab specimen

4.3.4 MONOTONIC LOAD TEST

The monotonic load test will be used to evaluate the effect of confinement of the based plate on screw anchor breakout resistance. The monotonic load test protocol consists of loading, by pulling, the test specimens at a constant rate such that the ultimate load could be reached within 5 to 10 minutes. Considering that the anticipated ultimate design load is approximately 1000 lbs., the specimen should be loaded at a rate of 4 lbs./sec. Alternatively, the actuator could be programmed to be displacement controlled with a displacement rate of 0.005 in./ sec. Although the load should be continuously applied, it is possible that the load should be held to allow for the Research Team to move the crack microscope to the cracked position. Unfortunately, there is no equation or an adequate analytical method that would predict the point of holding the load. Initially, hold points should be planned at 30-second intervals. The data acquisition system should collect the load and displacement data at 2 Hz.

4.3.5 CYCLIC LOAD TEST

The cyclic load test is used to determine if the screw anchor will loosen under repeated load in un-cracked concrete. To this end, a pulsating tensile load will be applied sinusoidally between a maximum of 500-600 lbs and a minimum load of 125-150 lbs. The minimum load will need to be maintained during load to ensure stability in the system and should be exactly determined during the test setup. Should the actuator not be able to control this small load, the Research Team will determine an applicable displacement control testing sequence, which needs to be established during the test setup since additional displacement drift needs to be considered. Considering the load will be applied using the pulley system, the frequency of the load should be approximately 0.25 Hz. The test should be cycled for at least 1000 cycles or a greater number if displacements are still increasing. Continue until the increase in displacements during the cycling stabilized in the manner that failure will be unlikely to occur after an additional cycle. This could be established by evaluating the increase in deflection of each cycle does not deviate by more than 0.01 in. The data

acquisition system should collect the load and displacement data at 5 Hz during the cyclic load test (to be determined with SRC staff).

After the completion of the cyclic load test, the test specimen should be unloaded and reloaded to failure following the monotonic load test procedure. The data acquisition system should collect the load and displacement data at 2 Hz during the reloading of the test specimen.

The cyclic load test is only performed on three testing schemes as indicated in Table 4-3. These include 1) the application of pedestrian rail mounted on a sidewalk with a single screw anchor; 2) the application of guiderail mounted on a sidewalk with two screw anchors with a nominal embedment length of 7.813 in. and; 3) the application of guiderail mounted on a sidewalk with two screw anchors with a nominal embedment length of 5.313 in. A minimum of 5 specimens will be tested for each test setup.

4.4 TEST SCHEMES AND MATRICES

The experimental program is divided into four testing schemes. Table 4-3 provides a detailed summary of the parameters used in testing schemes 1, 2, and 3. The parameters used in testing scheme 4 are summarized in Table 4-4.

Scheme 1 is designated for testing FDOT Index No. 515-052 and 515-062, which comprised of testing pedestrian railings in three different applications: sidewalks, gravity walls, and parapet walls. In all applications, the pedestrian railings were secured by a single ¾ x 8.5-in. screw anchor. For the sidewalk application depicted in Figure 4-3, both monotonic and cyclic loads were applied, denoted as P-SE1 and P-SE1c, respectively. Only monotonic load was applied on the gravity and parapet walls, which are labeled as P-G1 and P-P, respectively. Figure 4-4 and Figure 4-5 illustrate the detail dimension of the gravity wall and parapet wall specimens, respectively.

Scheme 2 is designated to testing FDOT Index No. 515-070 and 515-080, which comprised of testing pipe guiderails in three different applications: sidewalks, gravity walls, and parapet walls. The pipe guiderails were secured to the concrete using ¾ x 6-in. screw anchors. Similarly, both monotonic and cyclic loads were applied to the sidewalk application, but only monotonic load was applied to the gravity and parapet wall applications. The sidewalk tests are labeled as G-SS and G-SSc for the monotonic and cyclic loads, respectively. The gravity wall tests are labeled as G-G, and the parapet wall tests are labeled as G-P.

Scheme 3 is designated to testing FDOT Index No. 515-022, which consisted of testing a bullet7 rail installed primarily with two $^{5}/_{8}$ x 6-in. screw anchors on a parapet wall. This specimen underwent monotonic load testing exclusively and is labeled as B-P. Initially, two $^{5}/_{8}$ x 8-in. screw anchors were used, but it was determined that the longer embedment was unnecessary.

Scheme 4 is incorporated into the project to assess the performance of a modified pedestrian railing, as illustrated in Figure 4-6 and Figure 4-7. This railing design was specifically developed for retrofitting purposes or situations where smaller screw anchors are preferred. The modified pedestrian railing was attached to the concrete using three $^{3}/_{8}$ x 6-in. screw anchors but with two anchors subject to tension forces and one anchor to shear forces. All applications were evaluated using existing test specimens that were not

severely damaged after being subjected to the other testing schemes. Drilled holes were grouted with Quickcrete prior to the installation of the modified railings. A total of seven sidewalk specimens were evaluated and labeled as G-S. There were only two gravity wall specimens, labeled as G-G-38 and G-G-310, and two parapet wall specimens, labeled as G-G-311 and G-G-312. All specimens within Scheme 4 underwent monotonic load testing exclusively.

Table 4-3: Detailed parameter of test schemes

Post Type	**Pedestrian/Picket Railing**			**Guiderail**			**Bullet Rail**
Index No.	**515 -052 and -062**			**515-070 and -080**			**515-022**
Load Test Specimen Code (x = 1 to 5 specimens)	**P-SE1-x P-SE1c-**	**P-G1-x**	**P-P-x**	**G-SS-x G-SSc-x**	**G-G-x G-Gc-x**	**G-P-x**	**B-P-x**
Foundation	**Sidewalk (1-bolt)**	**Gravity Wall (1-bolt)**	**Parapet**	**Sidewalk (2 bolt)**	**Gravity Wall**	**Parapet**	**Parapet**
# Anchors	1	1	1	2	2	2	2
Spacing (in.)	- n/a	- n/a	-n/a	5	5	5	3
Anchor Size (in.)	0.75	0.75	0.75	0.75	0.75	0.75	0.625
Anchor Length (in.)	8.5	8.5	8.5	6	6	6	6 and 8
Baseplate thickness	0.625	0.625	0.625	0.5	0.5	0.5	0.5
Pad thickness and washer	0.1875	0.1875	0.1875	0.1875	0.1875	0.1875	0.1875
Nominal Embed. (in.)	7.688	7.688	7.688	5.313	5.313	5.313	7.313
Effective Embed. (in.)	5.353	5.353	5.353	3.334	3.334	3.334	5.334
Edge Distance to baseplate centerline (in.)	6.00	4.50	4.00	6.00	4.50	4.00	4.00
Number concrete test specimens	5 + 5 Cyclic	5	5	5 + 5 Cyclic	5	5	5
Concrete Class	Class NS	Class NS	Class II	Class NS	Class NS	Class II	Class II
Concrete Strength (psi)	2500	2500	3400	2500	2500	3400	3400
Concrete Size (in.)	See Fig. 4-3	See Fig. 4-4	See Fig. 4-5	See Fig. 4-3	See Fig. 4-4	See Fig. 4-5	See Fig. 4-5
Concrete volume per specimen (cu.ft)	6.56	7.01	6.04	6.56	7.01	6.04	6.04
Total Concrete Volume (cu.yd)	2.43	1.30	1.12	2.43	1.30	1.12	1.12
Grand Total Concrete Volume (cu.yd)	10.82						
Estimated 7” Anchor Failure Load (kips)	0.74	0.47	0.55	0.95 (for 6” anchor)	0.68	<0.68	0.54 (for 6” anchor)
Estimated 8.5” Anchor Failure Load (kips)	0.91	0.51	0.57		0.68	<0.68	0.56 (for 8” anchor)
Estimated Railing Yield Load (kips)	1.60 – Stop test loading initially at railing yield load			0.46 – Stop test loading initially at railing yield load			10.6
Estimated Railing Ultimate Load (kips)	2.10 – Hold load to see if there is any severe bending in the rail.			0.62 – Hold load to see if there is any severe bending in the rail.			12.0

Table 4-4: Detailed parameter of modified test scheme.

Post Type	**Modified Pedestrian/Picket Railing**		
Load Test Specimen Code (x = 1 to 5 specimens)	**G-S-x**	**G-G-38 G-G-310**	**G-G-311 G-G-312**
Foundation	**Sidewalk (3-bolt)**	**Gravity Wall (3-bolt)**	**Parapet Wall (3-bolt)**
# Anchors	3	3	3
Spacing (in.)	7	7	7
Anchor Size (in.)	0.375	0.375	0.375
Anchor Length (in.)	6	6	6
Baseplate thickness	0.25	0.25	0.25
Pad thickness and washer	0.1875	0.1875	0.1875
Nominal Embed. (in.)	5.313	5.313	5.313
Effective Embed. (in.)	3.334	3.334	3.334
Edge Distance to baseplate centerline (in.)	3	3	3
Number concrete test specimens	7	2	2
Concrete Class	Class NS	Class NS	Class II
Concrete Strength (psi)	2500	2500	3400
Concrete Size (in.)	See Fig. 4-3	See Fig. 4-4	See Fig. 4-5
Estimated 6” Anchor Failure Load (kips)	0.597	0.43	0.53
Estimated Railing Yield Load (kips)	1.60 – Stop test loading initially at railing yield load		
Estimated Railing Ultimate Load (kips)	2.10 – Hold load to see if there is any severe bending in the rail		

4.5 TESTING SEQUENCES

Table 4-3 and Table 4-4 summarizes the testing sequence, which starts with testing all the sidewalk specimens under monotonic load tests. Depending on the performance of the monotonic load test, the cyclic load test would only be performed on the setup with good performance. After testing all the sidewalk specimens, the gravity wall specimens will be tested follow by the parapet specimens and finally, modified pedestrian/picket railing on sidewalk specimen, gravity wall specimen and parapet wall specimen.

5. CHAPTER 5 – EXPERIMENTAL RESULTS

*Note – detailed experimental results are provided in Appendix A.

5.1 SCHEME 1 TEST RESULTS

In Scheme 1 pedestrian/picket railing were tested using 3 specimens – Sidewalk specimen, gravity wall specimen and parapet wall specimen. Summary of the Scheme 1 test results are shown in Figure 5-1: Scheme 1 test results summary Figure 5-1. A total of 5 sidewalk specimens with pedestrian/picket railing were tested under monotonic load until failure. The ultimate capacity of specimen P-SE1-4 cannot be ascertained as the loading was terminated at 1 Kip unintentionally, therefore was not considered for calculating average values. Out of 5 sidewalk specimens only 3 specimens P-SE1-1, P-SE1-2 and P-SE1-4 had little damage and could further be subjected to cyclic load between 100 - 600 lb. for 1000 cycles followed by monotonic load until failure. A total of 5 gravity wall specimens and 4 parapet wall specimens with pedestrian/picket railing were tested only under monotonic load until failure.

*Note: - All the gravity wall specimen tests ended before their failure since the instrument reached its maximum load capacity.

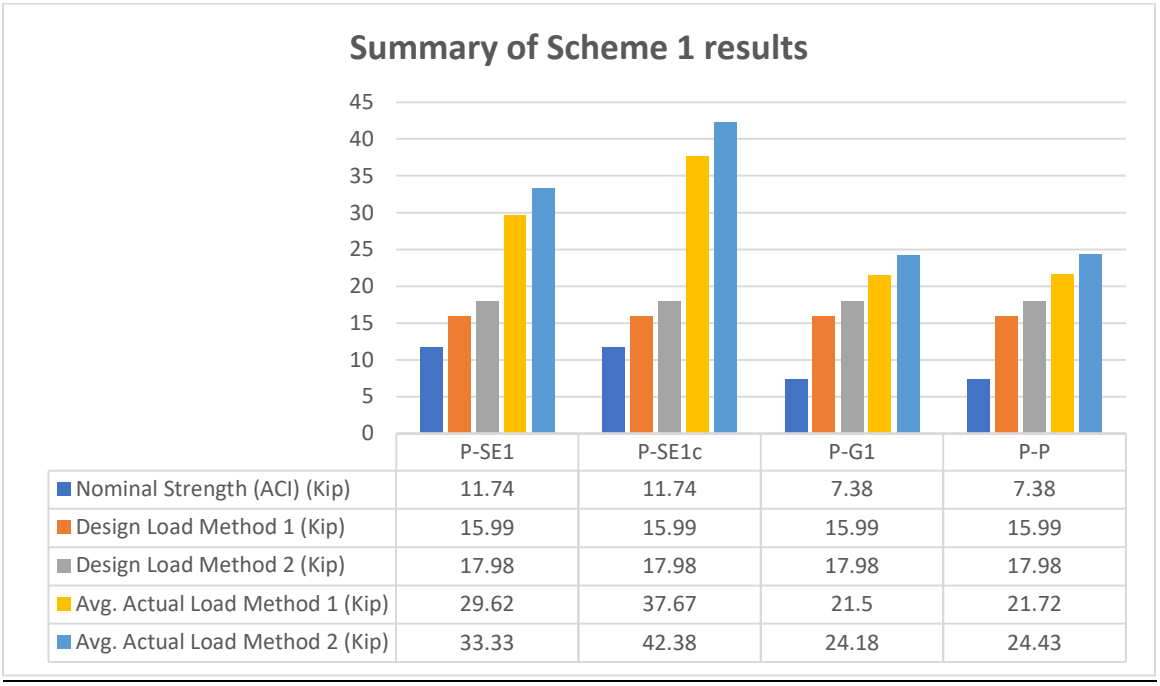

	P-SE1	P-SE1c	P-G1	P-P
Nominal Strength (ACI) (Kip)	11.74	11.74	7.38	7.38
Design Load Method 1 (Kip)	15.99	15.99	15.99	15.99
Design Load Method 2 (Kip)	17.98	17.98	17.98	17.98
Avg. Actual Load Method 1 (Kip)	29.62	37.67	21.5	21.72
Avg. Actual Load Method 2 (Kip)	33.33	42.38	24.18	24.43

Figure 5-1: Scheme 1 test results summary

5.2 SCHEME 2 TEST RESULTS

In Scheme 2 guide rails were tested using 3 specimens – Sidewalk specimen, gravity wall specimen and parapet wall specimen. Summary of the scheme 2 test results are shown in Figure 5-2. A total of 5 sidewalk specimens with guide rail was tested under monotonic load until failure. The first 4 specimens were selected to test under cyclic load followed by monotonic load until failure. A total of 6 gravity wall specimens and 3 parapet wall specimens with guide rails were tested only under monotonic load until failure.

*Note: - All the gravity wall specimen tests ended before their failure since the instrument reached its maximum load capacity.

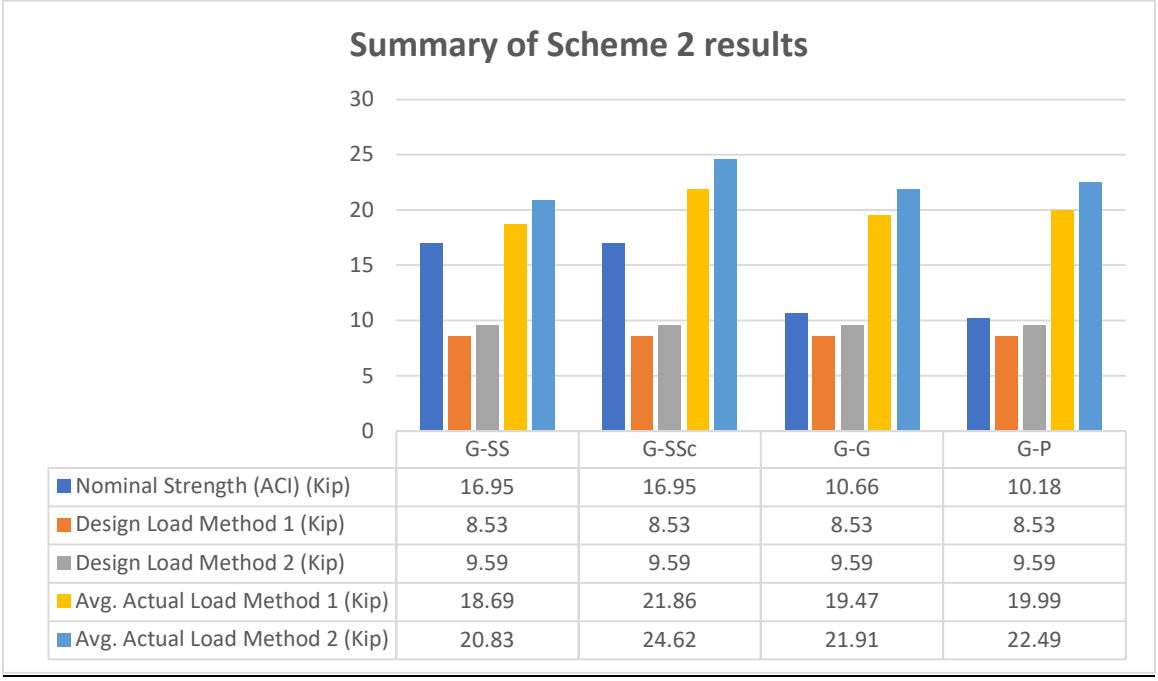

	G-SS	G-SSc	G-G	G-P
Nominal Strength (ACI) (Kip)	16.95	16.95	10.66	10.18
Design Load Method 1 (Kip)	8.53	8.53	8.53	8.53
Design Load Method 2 (Kip)	9.59	9.59	9.59	9.59
Avg. Actual Load Method 1 (Kip)	18.69	21.86	19.47	19.99
Avg. Actual Load Method 2 (Kip)	20.83	24.62	21.91	22.49

Figure 5-2: Scheme 2 test results summary

5.3 SCHEME 3 TEST RESULTS

In Scheme 3 bullet rails were tested only using parapet wall specimen. Summary of the scheme 3 test results are shown in Figure 5-3. A total of 3 parapet wall specimens with bullet rails installed using 8" anchor length bolts and 3 parapet wall specimens with bullet rails installed using 6" anchor length bolts were tested under monotonic load until failure.

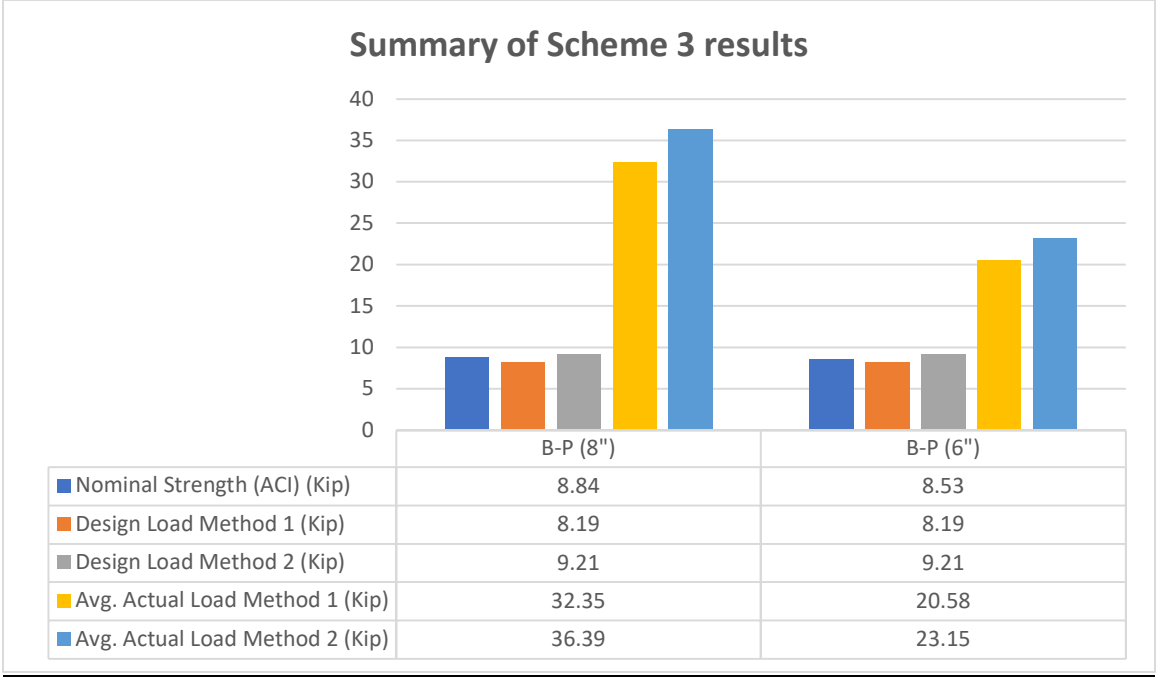

	B-P (8")	B-P (6")
Nominal Strength (ACI) (Kip)	8.84	8.53
Design Load Method 1 (Kip)	8.19	8.19
Design Load Method 2 (Kip)	9.21	9.21
Avg. Actual Load Method 1 (Kip)	32.35	20.58
Avg. Actual Load Method 2 (Kip)	36.39	23.15

Figure 5-3: Scheme 3 test results summary

5.4 SCHEME 4 TEST RESULTS

In Scheme 4 modified pedestrian/picket railing were tested using 3 specimens – sidewalk specimen, gravity wall specimen and parapet wall specimen. Summary of the scheme 4 test results are shown in Figure 5-4.

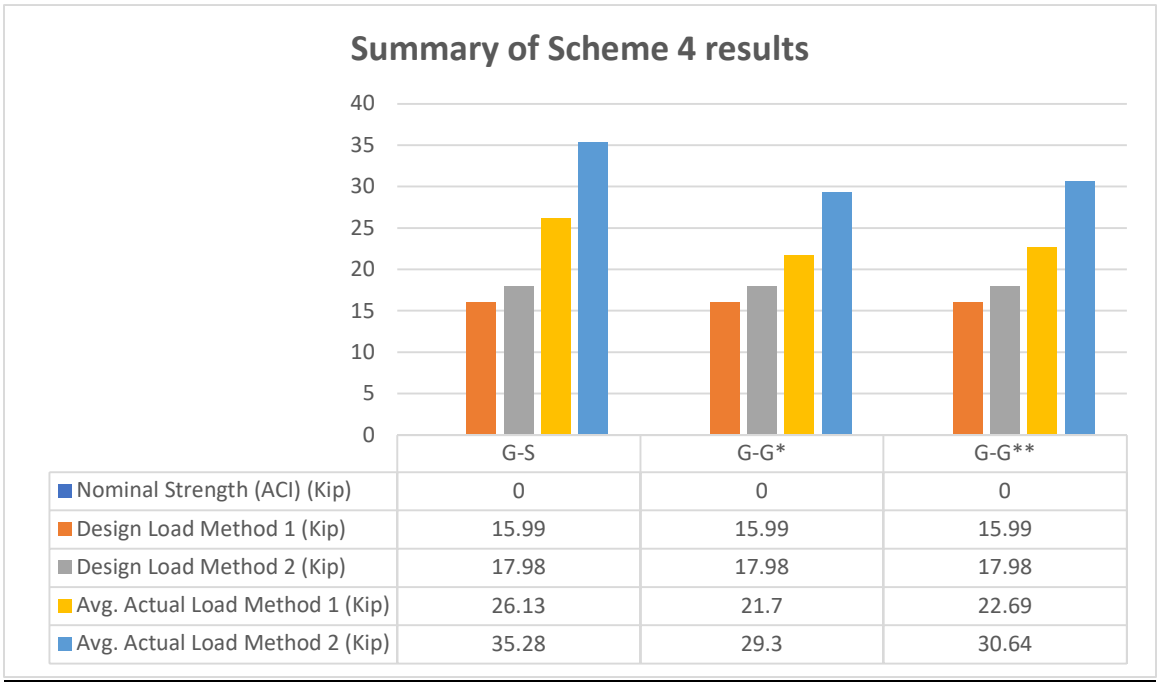

	G-S	G-G*	G-G**
Nominal Strength (ACI) (Kip)	0	0	0
Design Load Method 1 (Kip)	15.99	15.99	15.99
Design Load Method 2 (Kip)	17.98	17.98	17.98
Avg. Actual Load Method 1 (Kip)	26.13	21.7	22.69
Avg. Actual Load Method 2 (Kip)	35.28	29.3	30.64

Figure 5-4: Scheme 4 test results summary

5.5 ANALYSIS

Table 5-1summarizes the nominal screw anchor breakout resistance using ACI CODE-318-19 and the experimental results. In general, the experimental results (actual load) are an average of 2.38 and 2.68 times higher than the ACI CODE-318-19 nominal strength using Methods 1 and 2, respectively. However, the multiplier factors for test series' G-SS and G-SSc are much smaller with only 1.10 and 1.29, respectively, using Method 1 and 1.23 and 1.45, respectively, using Method 2. Similarly, the test series' G-G and G-P also have lower multiplier factors of 1.83 and 1.96, respectively using Method 1; and 2.06 and 2.21, respectively using Method 2. The lower multiplier factors for guiderail test specimens, specifically when installed on sidewalks, are due to the dominant failure mode being the yielding of the guiderail since it is designed to resist much lower applied loads. This caused the test to end prematurely when the actuator stroke reached its limit. Therefore, these results do not accurately represent the minimum breakout resistance of the screw anchor and should not be directly compared to the ACI nominal strength to avoid excessive conservatism. Nevertheless, the actual loads far exceeded the design loads for the guiderail test specimens, as shown in Table 5-1.

If the guiderail specimens are removed from the dataset, the multiplier factors are 2.93 and 3.30 using Methods 1 and 2, respectively. These numbers far exceed the confinement modification factor, Ψ_m that was proposed as part of the Project BDV 28-977-06, which recommended a multiplier of only 1.75. However, if the failure mode is concrete breakout with a prying action, as observed in guiderail installed on gravity and parapet walls (test series G-G ad G-P), the multiplier factor is closer to the proposed confinement modification factor. However, this is only the case when the embedment is relatively short. Considering the unpredictability of these results, it is recommended that load tests should be performed instead of relying on ACI CODE-318-19 that result in a much lower design capacity in the case of pedestrian railings.

Table 5-1: Comparison of ACI CODE-318-19 to experimental results

Specimen Code	Calculated Anchorage Design Load (M1)	Calculate Anchorage Design Load (M2)	Nominal Strength (ACI)	Failure Load (M1-E)	Failure Load (M2-E)	$\frac{(M1-E)}{(ACI)}$	$\frac{(M2-E)}{(ACI)}$
P-SE1 #4	15.99	17.98	11.74	29.62**	33.33**	2.52**	2.84**
P-SE1c #3			11.74	37.67**	42.38**	3.21**	3.61**
P-G1 #5			7.38	21.50	24.18	2.91	3.28
P-P #4			7.52	21.72	24.43	2.89	3.25
G-SS #5	8.53	9.59	16.95	18.69**	20.83**	1.10**	1.23**
G-SSc #4			16.95	21.86**	24.62**	1.29**	1.45**
G-G #6			10.66	19.47	21.91	1.83	2.06
G-P #3			10.18	19.99	22.49	1.96	2.21
B-P (8") #3	8.19	9.21	8.84	32.35	36.39	3.66	4.12
B-P (6") #3			8.53	20.58	23.15	2.41	2.71

*Note: All loads are in kips. M1 denotes Method 1, which assumes a one-inch uniform compressive pressure strip under the extreme edge of the baseplate. M2 denotes Method 2, which assumes a linearly varying compressive pressure distribution from zero at the centerline of the tension anchor bolts to a maximum at the extreme compression edge of the baseplate.

** Failure mode by excessive post yielding, not concrete anchorage failure.

Table 5-2: Comparison of strength reduction factors

FDOT Index No.	**Specimen Code**	**Railing Design Load (lb)**	**Avg. Actual Test Load (lb)**	**Factored Resistance based on Avg. Load (ϕ = 0.65)**	**Factored Resistance based on Avg. Load (ϕ = 0.75)**	**Description of Common Failure Modes**
515-052 and 062	P-SE1 #4	984	1828	1188	1371	No Failure**
	P-SE1c #3		2324	1511	1743	No Failure**
	P-G1 #5		1326	862	995	Screw anchor pullout and Concrete breakout
	P-P #4		1348	876	1011	Concrete breakout
515-070 and 080	G-SS #5	525	1156	751	867	No Failure, test stop due to large deflection**
	G-SSc #4		1367	888	1025	No Failure, test stop due to large deflection**
	G-G #6		1216	790	912	Concrete breakout with prying action
	G-P #3		1241	807	931	Concrete breakout with prying action
515-022	B-P (8") #3	1050	1996	1297	1497	Concrete breakout with prying action
	B-P (6") #3		1270	826	953	Concrete breakout with prying actions

Table 5-2, continued

Modified Picket railing	G-S #7	984	1620	1053	1215	Concrete breakout, Screw anchor pullout and steel plate yielding
	G-G-38,310 #2		1352	879	1014	Screw anchor Pullout and Concrete breakout
	G-G-311,312 #2		1414	919	1060	Concrete breakout

*Notes: -

- #No. represents number of specimens considered for obtaining average values.
- The specimens P-SE1, P-SE1c, G-SS and G-SSc did not fail in the concrete anchorage under the test loads, but minor cracks did form on the surface. Therefore, these specimens have an undetermined higher capacity.
- All the specimens with concrete breakout failure show similar crack patterns consisting of shear cracks on the back face and tension cracks at the front face. Few specimens only had shear cracks on the back face.

Table 5-2 presents a comparison of the actual load multiplied by different strength reduction/resistance factors (ϕ). The analysis shows that when $\phi = 0.75$the factored resistance, except for the bullet rail installed on the parapet wall with 6-inch screw anchors labeled as test series B-P (6"), would exceed the design load based on the test results. However, when a lower $\phi = 0.65$ per ACI is employed, there are several cases where the design load significantly surpasses the test results. It is important to note that the design load is based on AASHTO LRFD using higher load factors. Considering the absence of data from an actual reliability analysis, using $\phi = 0.75$ should be deemed acceptable. Mixing AASHTO load factors and ACI strength reduction factors is not recommended, even though it would yield more conservative results. Thus, it is recommended FDOT adopts $\phi = 0.75$ for design and when analyzing future test results for screw anchors.

Table 5-3: 5% fractile of test results.

Specimen Code	Design Load		Mean Load (R_n)		COV	Number of tests	K	5% Fractile ($R_{5\%}$)		$\phi R_{5\%}$	
	M1	M2	M1	M2				M1	M2	M1	M2
P-SE1 and SE1c	15.99	17.98	30.07**	37.21**	0.172**	7	2.894	15.10**	18.69**	11.33**	14.02**
P-G1			21.5**	24.18**	0.125**	5	3.400	12.39**	13.94**	9.29**	10.45**
P-P			21.72	24.43	0.109	4	3.957	12.38	13.93	9.29	10.45
G-SS and SSc	8.53	9.59	20.13**	22.43**	0.121	9	2.649	13.69**	15.26**	10.27**	11.44**
G-G			19.47	21.91	0.125	6	3.091	11.93	13.42	8.95	10.07
G-P			19.99	22.49	0.076	3	4.514	13.11	14.74	9.83	11.06
B-P (8")	8.19	9.21	32.35	36.39	0.025	3	4.514	28.65	32.23	21.49	24.17
B-P (6")			20.58	23.15	0.036	3	4.514	17.27	19.43	12.96	14.57

** Conservative values, since no concrete anchorage failure at maximum post loading for sidewalk specimens.

Table 5-3 presents a comprehensive analysis of the utilization of a 5% fractile of test results as advised by ACI CODE-355.2. Upon examination, it is evident that when this methodology is combined with a strength reduction factor of $\phi = 0.75$, the design values for the pedestrian railing are lower than the calculated design loads. However, the effectiveness of employing the 5% fractile approach alongside the load and resistance factor design remains unverified, as there is insufficient data available to ascertain the probability of failure when both methods are integrated into the design. The current policy of both the ACI CODE-318-19 code and the ACI 355 committee is to adopt a more conservative approach in light of this ambiguity. Our analysis suggests that utilizing the 5% fractile values might be excessively conservative, particularly considering that the pullout and pry-out failures did not manifest abruptly like the concrete breakout failure did. Consequently, we recommend that FDOT consider using the average test results instead, enabling the use of screw anchors in conjunction with pedestrian railings.

5.6 CONCLUSION

In conclusion, the analysis of the experimental results and their comparison with ACI CODE-318-19 nominal strengths has provided valuable insights into the performance of screw anchors in various scenarios. Table 5-1 revealed that the experimental results consistently surpassed the ACI nominal strengths. However, it is important to note that these multipliers were significantly lower for sidewalk test specimens, primarily due to the yielding of the guiderail or baseplate that prevents the test to continue.

Considering the uncertainties and unpredictability of the results, it is recommended to perform load tests instead of relying solely on ACI CODE-318-19 provisions, especially when designing pedestrian railings. The comparison in Table 5-2, using different strength reduction factors (ϕ), indicated that employing $\phi = 0.75$ would generally ensure that the factored resistance exceeds the design load, except for a specific case with shallow embedment. Using $\phi = 0.65$ per ACI resulted in several instances where the design load would not be met. It is important to recognize that the design load is based on AASHTO LRFD Live Load, which uses higher load factors (1.75 verses 1.60), so using ACI resistance factors in combination with AASHTO load factors is approximately 9% more conservative before considering the actual reliability of the test results and conservatism of the design method.

Table 5-3 examined the use of a 5% fractile of test results as recommended by ACI CODE-355.2 in conjunction with a strength reduction/resistance factor of $\phi = 0.75$ for the concrete anchorage. It was observed that this combination would not meet the targeted design load. However, due to insufficient data and the lack of reliability analysis, the applicability of using the 5% fractile approach alongside the load factors and resistance factor design remains questionable. The current conservative approach adopted by ACI CODE-318-19 and the ACI 355 committee reflects this ambiguity.

Based on our analysis, it is recommended that FDOT consider using the average test results instead of the 5% fractile values, enabling the use of screw anchors in combination with pedestrian railings. This approach is supported by the observation that the pullout and pry-out failures did not occur abruptly like the concrete breakout failure did. By incorporating these recommendations, FDOT can enhance the design and implementation of screw anchors while ensuring the safety and reliability of pedestrian railings.

6. CHAPTER 6 – RECOMMENDATION TO CURRENT DESIGN STANDARDS

6.1 INTRODUCTION

Currently, the SDG does not address screw anchors in the design provisions. The current American Concrete Institute (ACI, 2019a) Chapter 17 provides a conservative design approach that typically limits the strength of screw anchors to concrete breakout failure, as illustrated in Figure 6-1. However, based on many studies, including this one, a combined mode of failure or pullout failure mode is frequently reported. Unlike many building applications where smaller screw anchors are frequently used, transportation structures typically need to withstand higher loads that call for much larger screw anchors and longer embedment depth. Furthermore, especially for railing applications, narrow base plates exert a reaction force onto the concrete preventing a direct concrete breakout failure mode and indirectly increasing the screw anchor breakout resistance by changing the angle of the failure plane surfaces. These effects increase the screw anchor resistance to a combined or pullout failure mode. Unfortunately, there is no code equation to predict the combined and pullout failure modes. Therefore, it is recommended to either introduce modification factors or conduct testing to address this challenge. This report serves as a resource, offering guidance on potential modification factors that can be integrated with ACI CODE-318-19 for screw anchor resistance equations, along with advocating for the incorporation of new design criteria within the SDG.

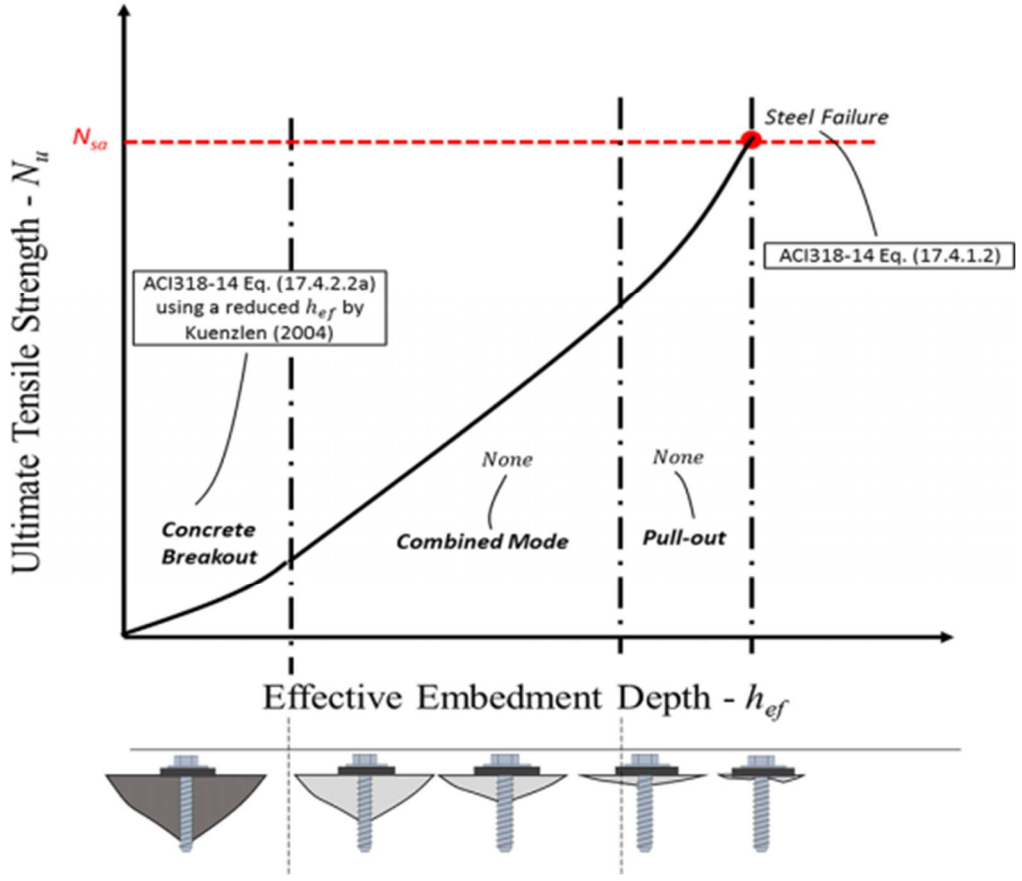

Figure 6-1: Failure mode for varying embedment depths (Chen et al., 2020)

6.2 CONFINEMENT MODIFICATION FACTOR

To develop a design procedure for supplementing the ACI CODE-318-19 specifications that accounting for the confinement effect on screw anchor breakout resistance, several modification factor equations, as summarized in Table 6-1 and Table 6-2, were evaluated with the experimental results and other results from literature. The confinement modification factor was computed from experimental results by taking the average breakout capacity divided by the nominal concrete breakout resistance obtained from the ACI CODE-318-19 procedure.

$$\Psi_m = \frac{N_{exp}}{N_{cb}} \qquad \text{(Eq. 1)}$$

Where:

N_{exp} = the average breakout capacity obtained from the experiment;

N_{cb}= the nominal concrete breakout resistance obtained from ACI 318-14 Equation 17.6.2.1a.

The experimental results, in conjunction with other data and equations, have been graphically represented in Figure 6-2. Upon examination, it becomes evident that among the six equations, the Zhao (1993) equation appears to offer the most accurate representation of the confinement effect on screw anchor breakout resistance. It is worth noting that several data points fall below this curve, potentially leading to an overestimation of the screw anchor breakout resistance, and thus, these data points should be regarded as the upper limit, however when combined with the current resistance factors (0.65-0.75) might still be considered conservative. It should also be noted that the marked data in Figure 6-2 are the results of "Guiderail on sidewalk specimens" for which the load applied to the railing posts exceeded the ultimate strength of the railing as shown in Figure 6-3 and Figure 6-4, resulting in yielding of post before reaching the maximum capacity of the screw anchor capacity or the failure of specimen. Therefore, it is recommended not to consider these data points while evaluating the performances of confinement equations.

Conversely, the Suksawang equation (developed for the adhesive anchor Project BDV28-977-06) provides a more conservative estimation, making it a suitable lower bound. The Fichtner (2011) linear equation strikes a balance between the two, presenting a middle-ground approximation.

Considering these findings, it is recommended that FDOT consider adopting either the Fichtner (2011) or Suksawang equations to provide a more conservative estimate of screw anchor breakout resistance, particularly when concrete breakout governs the design.

Table 6-1: Confinement modification factor equations

No.	Equation		References
1	$\Psi_m = \frac{1.5h_{ef}}{z}$	for $0 \leq \frac{z}{h_{ef}} \leq 1.5$	Zhao (1993)
	$\Psi_m = 1$	for $\frac{z}{h_{ef}} > 1.5$	

Table 6-1, continued

2	$\Psi_m = 2 - \frac{z}{h_{ef}}$ $\Psi_m = 1$	for $0 \leq \frac{z}{h_{ef}} \leq 1.0$ for $\frac{z}{h_{ef}} > 1.0$	Bruckner (2001)
3	$\Psi_m = \frac{2.5}{1+\frac{z}{h_{ef}}}$ $\Psi_m = 1$	for $0 \leq \frac{z}{h_{ef}} \leq 1.5$ for $\frac{z}{h_{ef}} > 1.5$	Fichtner (2011) Parabolic Equations Adopted in SDG Section 1.6

Table 6-2: Confinement modification factor equations

No.	Equation		References
4	$\Psi_m = 2 - \frac{2z}{3h_{ef}}$ $\Psi_m = 1$	for $0 \leq \frac{z}{h_{ef}} \leq 1.5$ for $\frac{z}{h_{ef}} > 1.5$	Fichtner (2011) Linear Equations
5	$\Psi_m = 2.5 - \frac{z}{h_{ef}}$ $\Psi_m = 1$	for $0 \leq \frac{z}{h_{ef}} \leq 1.5$ for $\frac{z}{h_{ef}} > 1.5$	Herzog (2015)
6	$\Psi_m = 1.75 - \frac{z}{2h_{ef}}$ $\Psi_m = 1$	for $0 \leq \frac{z}{h_{ef}} \leq 1.5$ for $\frac{z}{h_{ef}} > 1.5$	Suksawang (Project BDV 28-977-06)

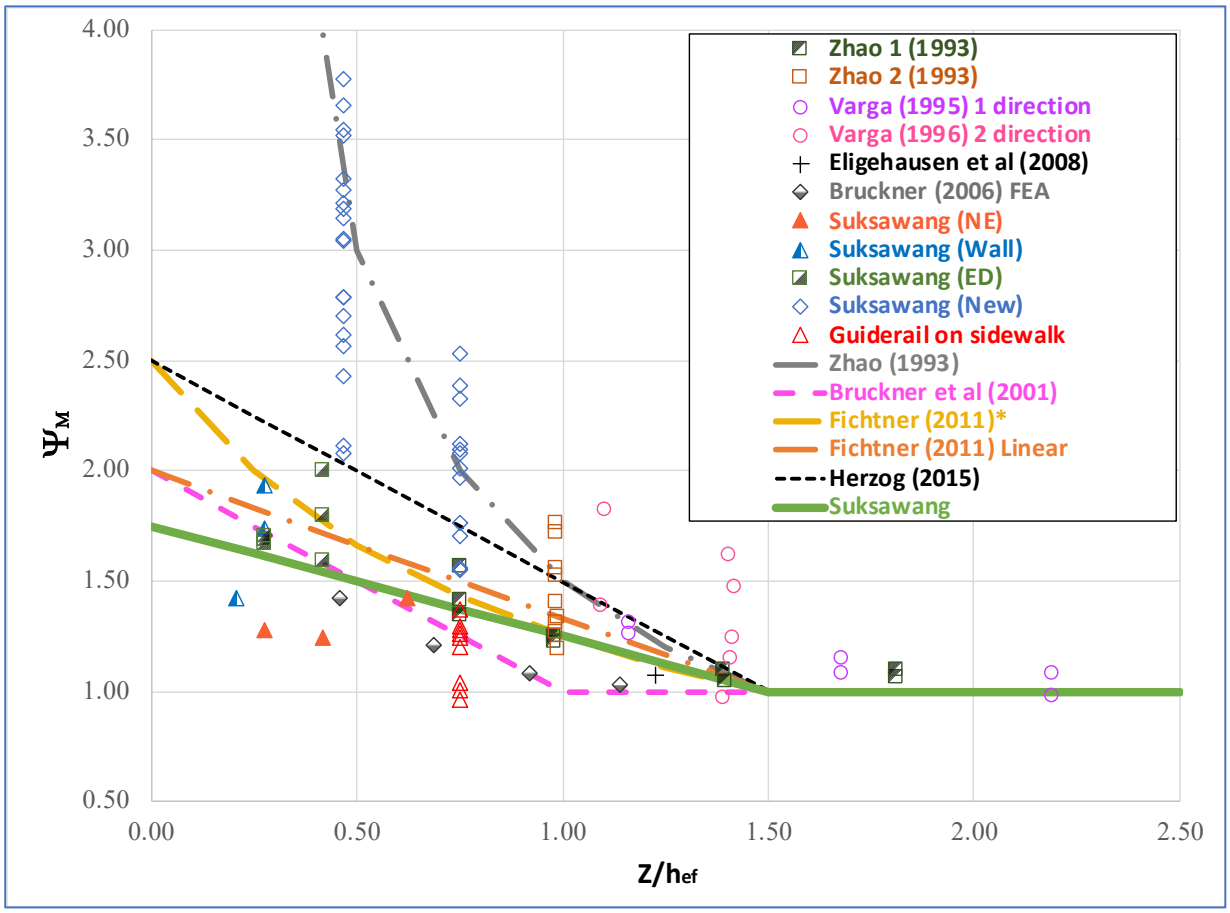

Figure 6-2: Factor Ψm as a function of z/hef ratio

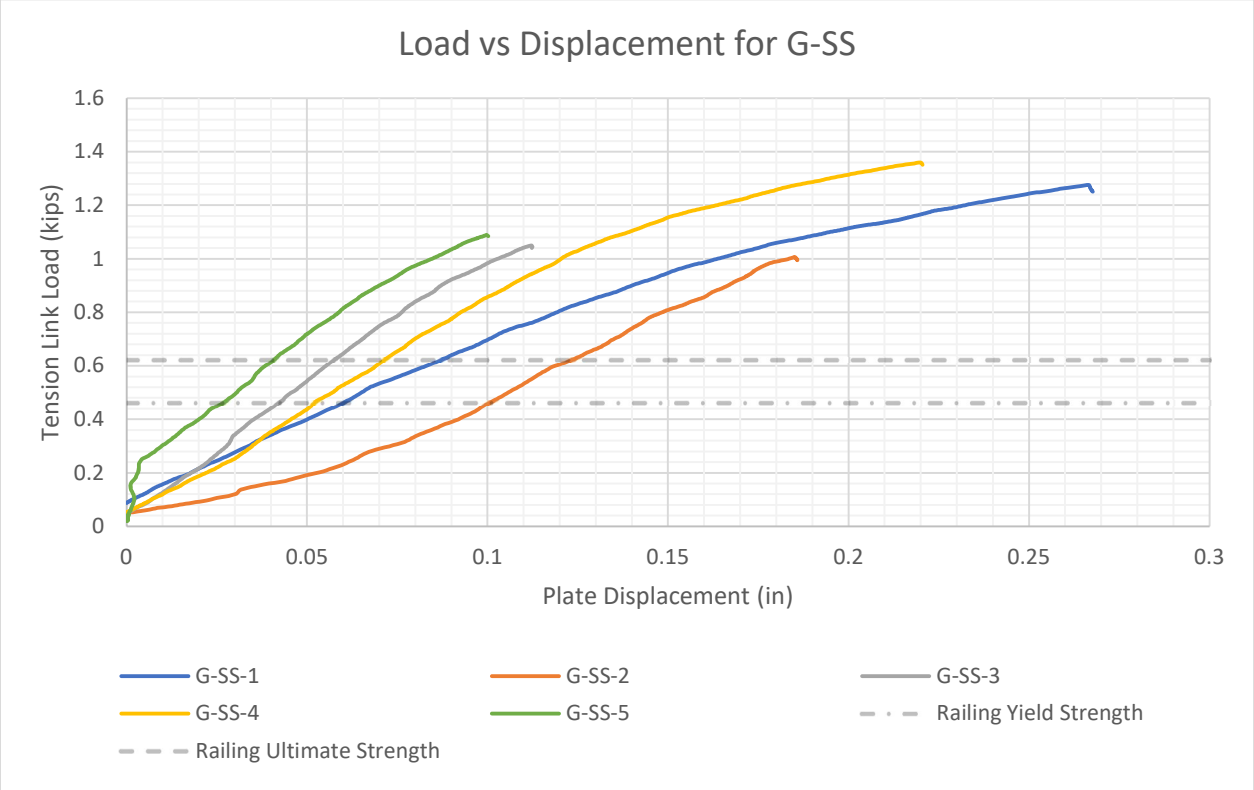

Figure 6-3: Results of guiderail on sidewalk specimen (under monotonic load)

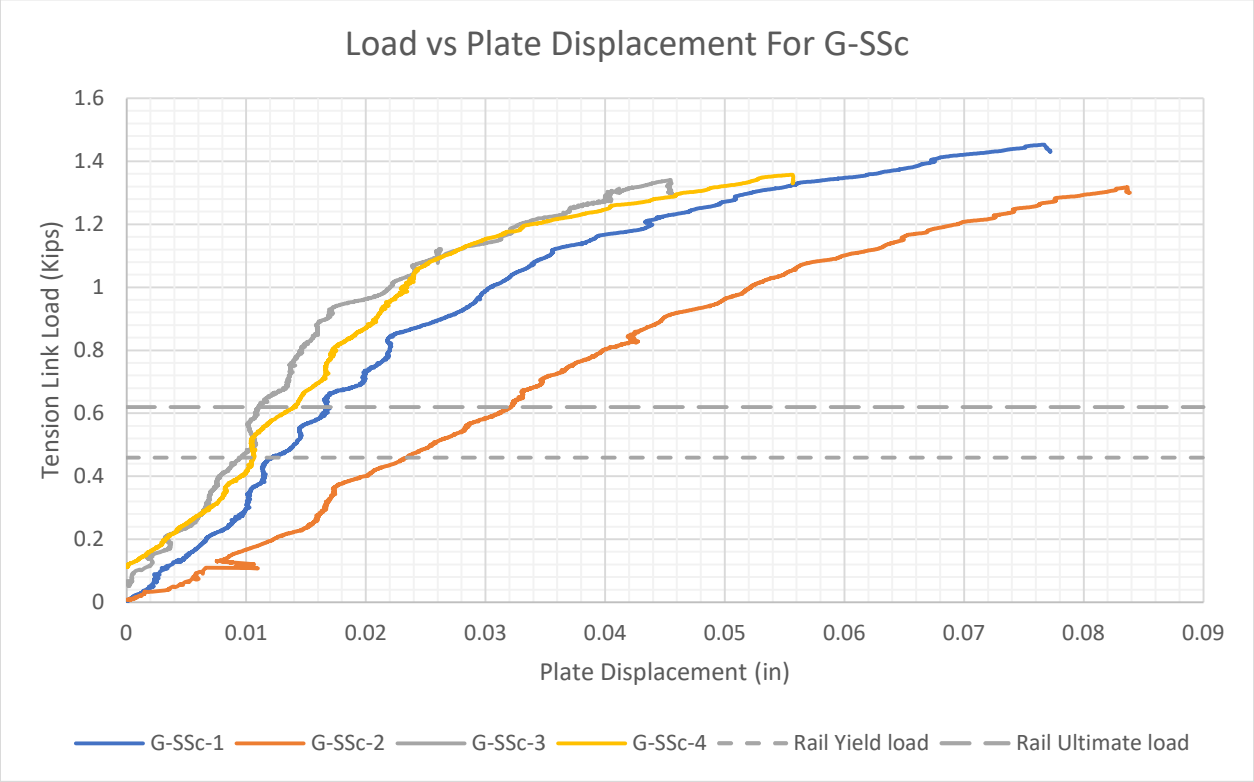

Figure 6-4: Results of guiderail on sidewalk specimen (under cyclic load and monotonic load)

6.3 RESISTANCE FACTORS

Table 6-3 offers a comprehensive comparison of the actual load values, adjusted with various strength reduction or resistance factors (ϕ). The analysis reveals that, with ϕ set at 0.75, the factored resistance generally exceeds the design load, except in the case of bullet rail installations on parapet walls using 6-inch screw anchors, designated as test series B-P (6").

Conversely, when a lower ϕ of 0.65 is applied in accordance with ACI CODE-318-19, several instances emerge where the design load significantly exceeds the test results. It's important to emphasize that the design load is calculated based on AASHTO LRFD using more conservative load factors. While there is a lack of data from an actual reliability analysis, employing ϕ = 0.75 can be considered an acceptable practice.

Mixing AASHTO load factors with ACI strength reduction factors is not recommended, despite the fact that it may yield more conservative results. Therefore, it is advisable for FDOT to adopt ϕ = 0.75 for both design purposes and when evaluating future test results for screw anchors.

Table 6-3: Comparison of strength reduction factors

FDOT Index No.	**Specimen Code**	**Railing Design Load (lb)**	**Avg. Actual Test Load (lb)**	**Factored Resistance based on Avg. Load (ϕ = 0.65)**	**Factored Resistance based on Avg. Load (ϕ = 0.75)**	**Description of Common Failure Modes**
515-052 and 062	P-SE1 #4	984	1828	1188	1371	No Failure**
	P-SE1c #3		2324	1511	1743	No Failure**
	P-G1 #5		1326	862	995	Screw anchor pullout and Concrete breakout
	P-P #4		1348	876	1011	Concrete breakout
515-070 and 080	G-SS #5	525	1156	751	867	No Failure, test stop due to large deflection**
	G-SSc #4		1367	888	1025	No Failure, test stop due to large deflection**
	G-G #6		1216	790	912	Concrete breakout with prying action
	G-P #3		1241	807	931	Concrete breakout with prying action
515-022	B-P (8") #3	1050	1996	1297	1497	Concrete breakout with prying action
	B-P (6") #3		1270	826	953	Concrete breakout with prying actions
Modified Picket railing	G-S #7	984	1620	1053	1215	Concrete breakout, Screw anchor pullout and steel plate yielding
	G-G-38,310 #2		1352	879	1014	Screw anchor Pullout and Concrete breakout

Table 6-3, continued

	G-G-311,312 #2	984	1414	919	1060	Concrete breakout

*Notes: -

- #No. represents number of specimens considered for obtaining average values.
- The specimens P-SE1, P-SE1c, G-SS and G-SSc did not fail in the concrete anchorage under the test loads, but minor cracks did form on the surface. Therefore, these specimens have an undetermined higher capacity.
- All the specimens with concrete breakout failure show similar crack patterns consisting of shear cracks on the back face and tension cracks at the front face. Few specimens only had shear cracks on the back face.

6.4 PROPOSED DESIGN CRITERIA

ACI CODE-318-19 outlines three potential failure modes for screw anchors. First, steel anchor failure occurs when the anchor's tensile strength is surpassed. Second, concrete breakout arises when the concrete surface where the anchor is inserted fractures and cannot withstand the applied forces, causing a chunk of concrete to break away. Third, pullout happens when the bond between the screw anchor and the surrounding concrete is not strong enough to withstand the tension forces, often leading to the shearing of the concrete interface around the hole's perimeter due to the thread-cut grooves.

However, it is worth noting that, according to these findings from this project, most screw anchors fail due to a combination of concrete breakout and pullout rather than pure concrete breakout. Therefore, we recommend incorporating the confinement modification factors and recommended resistance factors into the SDG design criteria. The proposed design criteria should be added in Section 1.6.4 as follows.

1.6.4 Screw Anchor Systems

A. Screw Anchors may be used for traffic railing anchorages on new construction and other applications in lieu of Adhesive Bonded Anchors where appropriate and applicable.
B. EOR's Design Criteria
    1. Use the following criteria for providing factored design load(s), bolt diameter, embedment depth and anchor configuration in the plans for each Screw Anchor location.
    2. Contact the State Structures Design Engineer for additional design guidance.
    3. Design Screw Anchors in accordance with ACI CODE-318, Chapter 17, using the product data provided by the ACI CODE-355.2 product evaluation report.
    4. Use LRFD Section 3 for determining design loads and a resistance factor of $\phi = 0.75$ when evaluating resistance using ACI CODE-318, Chapter 17.
    5. Use the effective embedment depth specified in the product datasheet or the following equation.

$$h_{ef} = 0.85(h_{nom} - 0.5h_t - h_s) \quad \text{(Eq. 1)}$$

where h_{nom} is the distance of the embedment end of the screw anchor and the concrete surface. h_t is the tread pitch and h_s is the length of the embedded end of the screw anchor without the full height of thread.

6. For end post, when the critical edge distance is $< 1.5h_{ef}$ from three or more edges, the CCD method provides overly conservative results for tensile breakout strength; hence, the following value should be used to find A_{Nc}:

$$h_{ef} = max\begin{cases} c_{a,max}/1.5 \\ s/3 \end{cases} \quad \text{(Eq. 2)}$$

where, s is the maximum spacing between anchors and $c_{a,max}$ is the greatest of the influencing edge distances that do not exceed the $1.5h_{ef}$.

7. Use the effective factor for uncracked concrete (k_c) as taken from the ACI CODE-355.2 product evaluation report.
8. When the resultant compressive reaction, approximately equivalent to the anchorage tensile force, occurs within a distance "z" from anchor(s) in tension, multiply the concrete breakout resistance, ACI CODE-318, Equations 17.6.2.1a and b by the confinement modification factor below.

$$\Psi_m = 1.75 - \frac{z}{2h_{ef}} \qquad \text{for } 0 \leq \frac{z}{h_{ef}} \leq 1.5$$

$$\Psi_m = 1 \qquad \text{for } \frac{z}{h_{ef}} > 1.5$$

9. In lieu of design calculation in accordance with ACI CODE-318, Chapter 17, the EOR can use the average proof load test to show that the screw anchors can withstand the design load in accordance with LRFD Section 3 using a resistance factor of $\phi = 0.75$.

7. CHAPTER 7 – CONCLUSION

The following conclusion can be made for this research project:

- **Experimental Analysis of Screw Anchors Performance**
    - Experimental results consistently exceeded ACI nominal strengths and design loads.
    - A single 3/4 x 8.5-in. stainless steel or galvanized screw anchor is recommended for the pedestrian (picket) rail.
    - Two 3/4 x 6-in. stainless steel or galvanized screw anchors are recommended for the guiderail.
    - Two 5/8 x 8-in. stainless steel or galvanized screw anchors are recommended for the parapet. It should be noted that due to the bullet rail design, there is insufficient room for ¾-in. diameter screw anchor.
    - Sidewalk specimens had lower multipliers due to guiderail/baseplate yielding resulting in premature termination of the test.
    - Cyclic loading performed under this project did not affect the performance of screw anchors. Cyclic load testing under ACI CODE-355.2 would still be required for seismic cyclic tension qualification.
- **Recommendation for Load Testing**
    - Uncertainties and unpredictability suggest reliance on load tests over ACI CODE-318-19 provisions.
    - The proposed test setup of cantilever loading should be used instead of a direct tension test.
    - The ACI 355.2 recommendation of using 5% fractile with the load resistance factor should not be followed.
    - Instead, the average test results should be multiplied by $\phi = 0.75$ to ensure that the factored resistance exceeds the design load.
- **Recommendation for Design Standards**
    - A new confinement modification factor should be included in the design of post-installed anchors.
    - FDOT should adopt $\phi = 0.75$ for both design purposes and when evaluating future test results for screw anchors.
    - FDOT should consider adopting the proposed Section 1.6.4 as shown in Section 6.4.
- **Project Benefit**
    - Faster installation time.
    - Lower installation cost.
    - Potential use in other application, e.g., anchoring of structural components to existing concrete structures.

8. REFERENCES

[1] American Association of State Highway And Transportation Officials. (2017). *AASHTO LRFD bridge design specifications.* Washington, Dc: American Association of State Highway And Transportation Officials.

[2] ACI Committee 318. (2014). *Building code requirements for structural concrete (ACI 318-14) : An ACI standard and commentary on building code requirements for structural concrete (ACI 318R-14)-: An ACI report*. American Concrete Institute, ACI.

[3] ACI Committee 318. (2019). *Building code requirements for structural concrete (ACI 318-19) : an ACI standard-: commentary on building code requirements for structural concrete (ACI 318R-19)*. American Concrete Institute.

[4] ACI Committee 355. (2019). *ACI 355. 2-19 Qualification of Post-Installed Mechanical Anchors in Concrete and Commentary (supersedes ACI 355. 2-07)*. American Concrete Institute.

[5] FDOT. (2021). Florida Department of Transportation Structures Manual, volume 1, Structures Design Guidelines. https://fdotwww.blob.core.windows.net/sitefinity/docs/default-source/structures/structuresmanual/currentrelease/2021/structuresmanual-jan2021.zip?sfvrsn=8dc3c599_8

[6] Brahimi, S. (2014). Hydrogen Embrittlement in Steel Fasteners. https://www.boltcouncil.org/files/HydrogenEmbrittlementInSteelFasteners-Brahimi.pdf

[7] Chen, Z., Nassiri, S., & Lamanna, A. (2020). Investigation of a combined failure mode for screw anchors under tension. *Advances in Structural Engineering*, *23*(13), 2803–2812. https://doi.org/10.1177/1369433220924795

[8] Eligehausen Rolf Rainer Mallée and J. F. Silva. (2006). *Anchorage in Concrete Construction*. Berlin: Ernst & Sohn Verlag.

[9] Lotfi Guizani, Chaallal, O., & Seyed Sina Mousavi. (2017). Local bond stress-slip model for reinforced concrete joints and anchorages with moderate confinement. *Canadian Journal of Civil Engineering*, *44*(3), 201–211. https://doi.org/10.1139/cjce-2015-0333

[10] Keseli, O., Bilčík, J., & Hollý, I. (2018). Screw Anchors Used as Post-Installed Shear Reinforcement in Flat Slabs. In Solid State Phenomena (Vol. 272, pp. 53–63). Trans Tech Publications, Ltd. https://doi.org/10.4028/www.scientific.net/ssp.272.53

[11] Lechner, J., & Feix, J. (2019). First experiences with concrete screw anchors as postinstalled shear reinforcement in concrete bridges. *Civil Engineering Design*, *1*(1), 17–27. https://doi.org/10.1002/cend.201800004

[12] Moehle, J. P. (2019). Key changes in the 2019 edition of the ACI building code (ACI 318-19). *Concrete International, 41*(8), 21-27. Retrieved from https://portal.lib.fit.edu/login?url=https://www.proquest.com/trade-journals/key-changes-2019-edition-aci-building-code-318-19/docview/2270508596/se-2

[13] International Code Council Evaluation Service (2021). Titen HD Screw Anchor for Cracked and Uncracked Concrete. *ICC-ES Evaluation Report, ESR-2713*.

[14] Mohyeddin, A., Gad, E., Aria, S., & Lee, J. (2020). Effect of thread profile on tensile performance of screw anchors in non-cracked concrete. *Construction and Building Materials*, *237*(Article number 117565). https://doi.org/10.1016/j.conbuildmat.2019.117565

[15] Mohyeddin, A., Gad, E. F., Yangdon, K., Khandu, R., & Lee, J. (2016). Tensile load capacity of screw anchors in early age concrete. *Construction and Building Materials*, *127*, 702–711. https://doi.org/10.1016/j.conbuildmat.2016.10.046

[16] Olsen, J., Pregartner, T., & Lamanna, A. J. (2012). Basis for Design of Screw Anchors in Concrete. *ACI Structural Journal*, *109*(4). https://doi.org/10.14359/51683875

[17] Simpson Strong-Tie Company Inc. (2021). Stainless Steel Titen HD Screw Anchors for Use in Cracked and Uncracked Concrete. *Evaluation Report, Number 493*.
[18] Schwenn, M., Zeman, O., Schorn, J., & Bergmeister, K. (2021). Influence of different drilling methods on the behavior of post-installed mechanical fasteners in uncracked and cracked concrete. *Structural Concrete*, *22*(3), 1600–1611. https://doi.org/10.1002/suco.202000466
[19] Stuart, G. A., Harrison, D. K., Wood, B. M., & Maclachlan, M. (2010). A proposed methodology for the design and characterisation of concrete screw anchors. *Meccanica*, *45*(5), 635–656. https://doi.org/10.1007/s11012-009-9246-7
[20] Tarawneh, A. N., Ross, B. E., & Cousins, T. E. (2020a). Shear Behavior and Design of Post-Installed Anchors in Thin Concrete Members. *ACI Structural Journal*, *117*(3). https://doi.org/10.14359/51723508
[21] Wiss, Janney, Elstner Associates, Inc. (2019). Reliability of Screw Anchors for Brittle Failure [PowerPoint slides].
[22] Sulaiman, M. F., Ma, C.-K., Apandi, N. M., Chin, S., Awang, A. Z., Mansur, S. A., & Omar, W. (2017). A Review on Bond and Anchorage of Confined High-strength Concrete. *Structures*, *11*, 97–109. https://doi.org/10.1016/j.istruc.2017.04.004
[23] Tarawneh, A. N., Ross, B. E., & Cousins, T. E. (2020b). Tensile Behavior and Design of Screw Anchors in Thin Concrete Members. *ACI Structural Journal*, *117*(1), 91. https://doi.org/10.14359/51718011
[24] ASTM Standard A53 . (2020). "Standard Specification for Pipe, Steel, Black and Hot-Dipped, Zinc-Coated, Welded and Seamless." *ASTM International, West Conshohocken, PA*. https://doi.org/10.1520/a0053_a0053m-20
[25] ASTM Standard A500 . (2021). "Standard Specification for Cold-Formed Welded and Seamless Carbon Steel Structural Tubing in Rounds and Shapes." *ASTM International, West Conshohocken, PA*. https://doi.org/10.1520/a0500_a0500m-21a
[26] ASTM Standard A992. (2020). "Standard Specification for Structural Steel Shapes." *ASTM International, West Conshohocken, PA*. https://doi.org/10.1520/a0992_a0992m-20
[27] Suksawang, N., (2019) "Confinement Effect of Metal Railing Narrow Baseplates on Adhesive Anchor Breakout Resistance" Final Report submitted to FDOT, Contract No. BDV 29-977-06, p. 44.https://fdotwww.blob.core.windows.net/sitefinity/docs/default-source/research/reports/fdot-bdv28-977-06-rpt.pdf

Appendix A: DETAILED TEST RESULTS

A1 – SCHEME 1 TEST RESULTS

A1.1 – MONOTONIC LOADING OF PEDESTRIAN RAILING ON SIDEWALK SPECIMENS

A total of 5 pedestrian railings installed on sidewalk specimens were monotonically loaded until failure and their results are summarized in Table A-1. The lateral load obtained from the tension link versus plate displacement is plotted in Figure A-1. Figure A-2 illustrates a plot of tension link versus tilt sensor. Specimen P-SE1-5 could not be graphed as a result of faulty displacement data. In the case of Specimen P-SE1-4, the loading was unintentionally halted at 1 kip. It is worth noting that Specimen P-SE1-1 was loaded beyond the yield strength of the railing, while Specimen P-SE1-2 was loaded beyond its ultimate strength. It should be noted that during the testing, pads were not utilized in the case of Specimen P-SE1-2.

The lateral load was converted to anchor breakout strength using methods 1 and 2, which are also plotted in Figure A-3 and Figure A-4, respectively. Interestingly, the bolts utilized in all specimens displayed greater breakout resistance than the nominal strength determined by the ACI code. Furthermore, the bolts in Specimens P-SE1-1, P-SE1-2, and P-SE1-3 demonstrated superior breakout resistance compared to the applied strength calculated by both methods 1 and 2.

However, the capacity of the bolt in Specimen P-SE1-4 could not be ascertained as the loading process was terminated before it could reach its maximum loading capacity.

Table A-1: Monotonic loading of pedestrian and picket railing attached to sidewalk specimens

Specimen's code	**P-SE1-1**	**P-SE1-2**	**P-SE1-3**	**P-SE1-4**	**P-SE1-5**
Max Lateral Load (kip)	1.960	2.310	1.509	0.986	1.534
Displacement (in)	0.282	0.244	0.201	0.116	-
Tilt (^{o} Deg)	3.788	3.344	2.942	1.752	2.490
Tension in bolts (method 1) Kip	31.760	37.429	24.450	15.975	24.852
Tension in bolts (method 2) Kip	35.732	42.108	27.507	17.972	27.959
Nominal Strength (ACI) Kip	11.74				
Applied Strength (Method 1) Kip	15.99				
Applied Strength (Method 2) Kip	17.98				

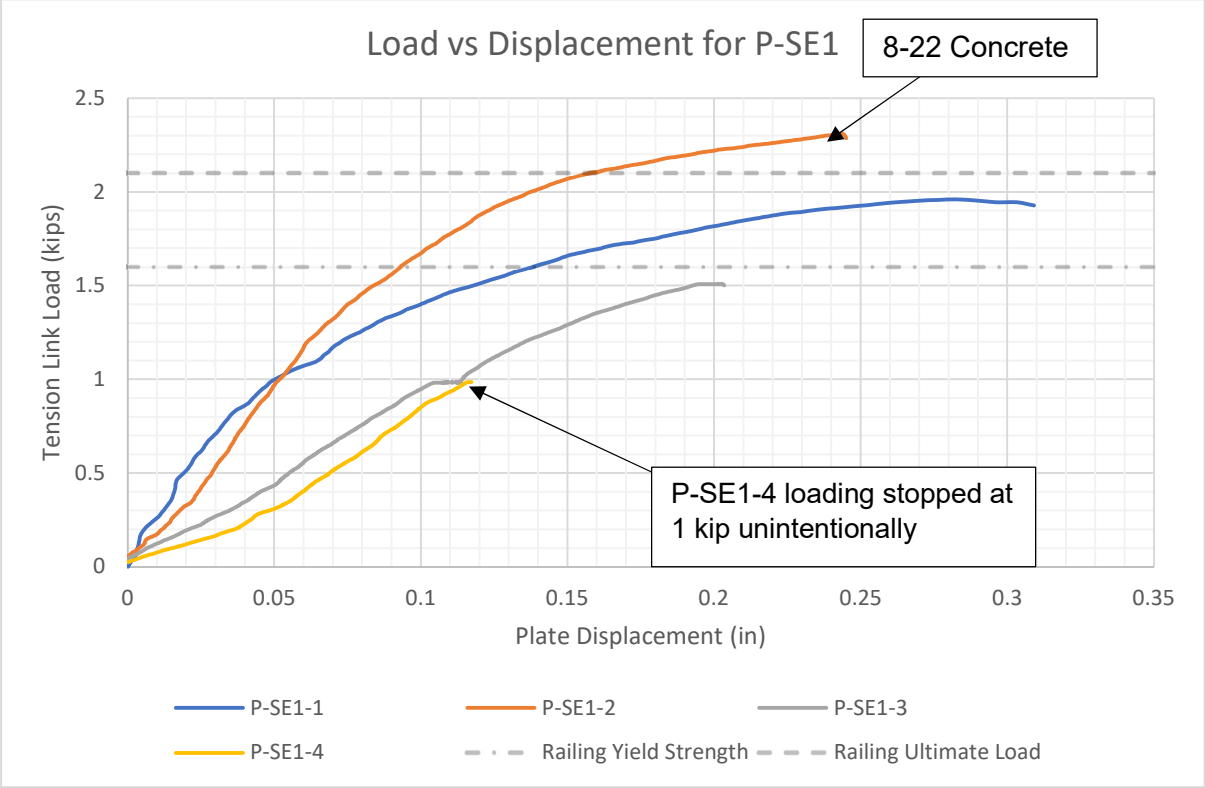

Figure A-1: Relation between load and displacement for P-SE1

"Note: - P-SE1-5 not graphed because of faulty displacement data"

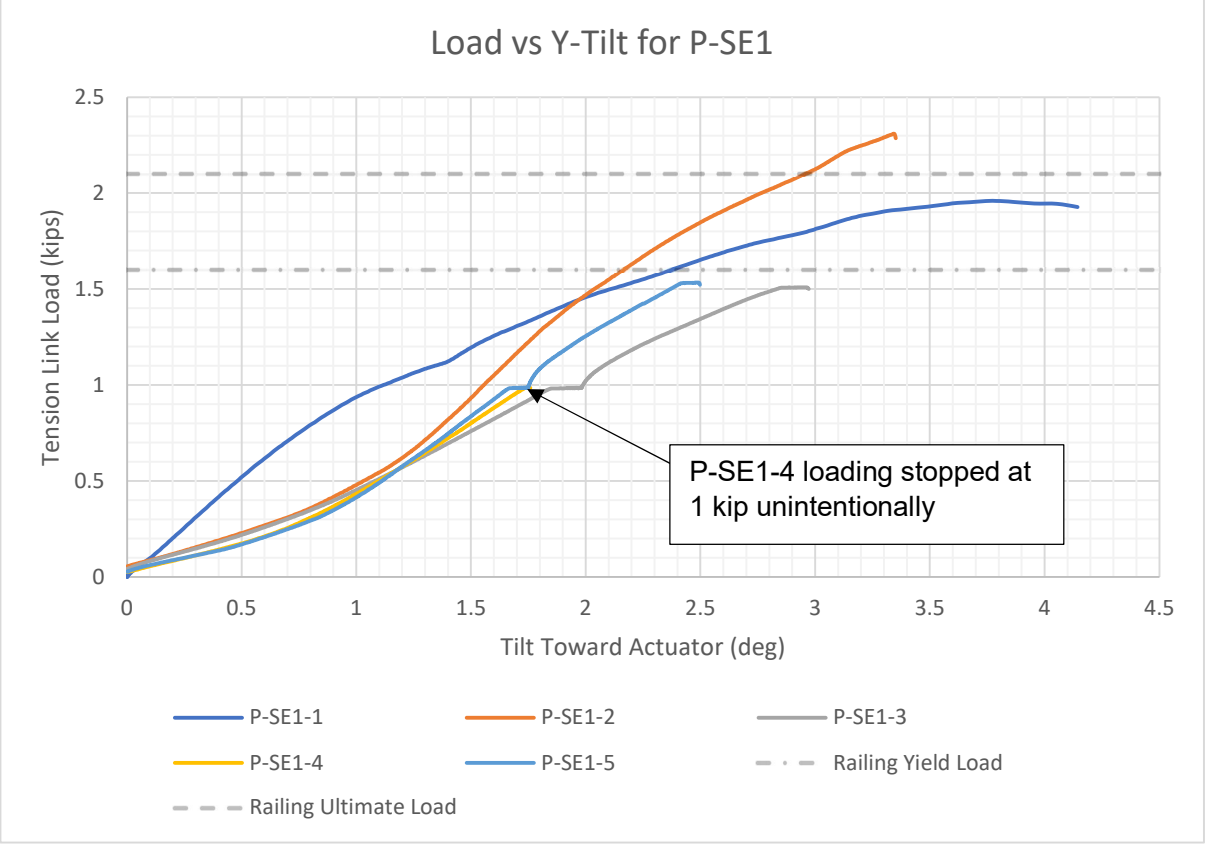

Figure A-2: Relation between load and y-axis tilt for P-SE1

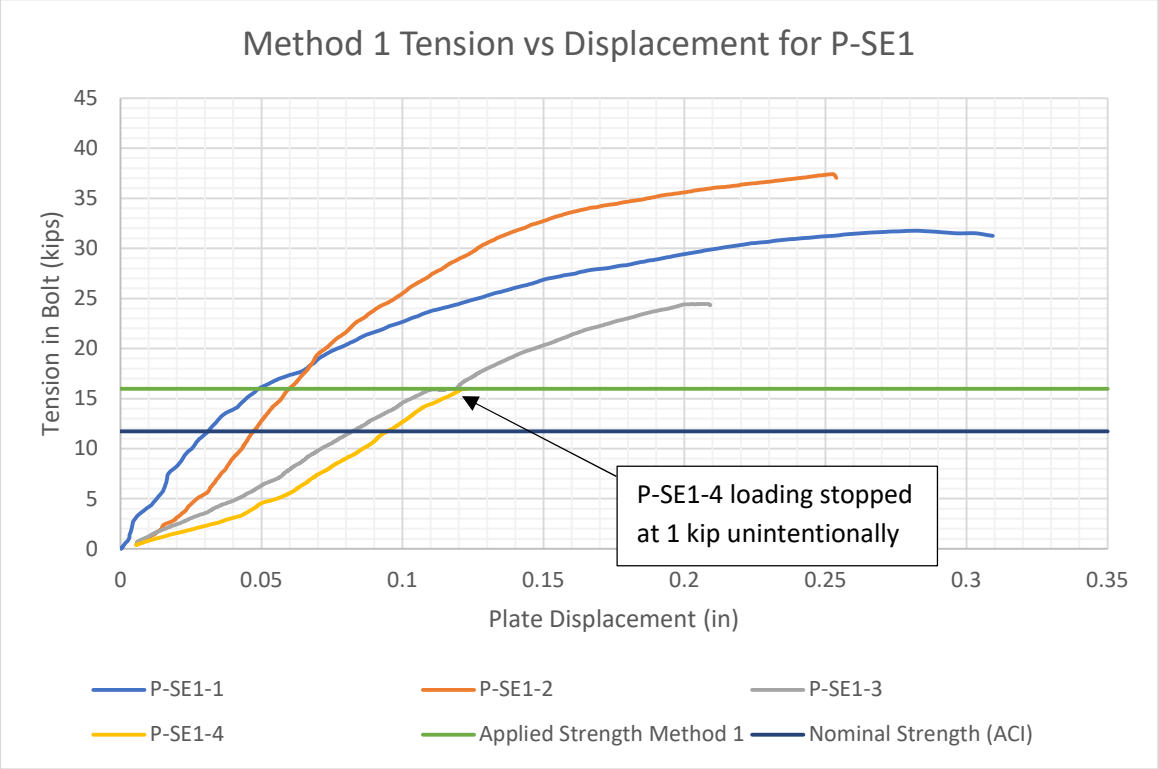

Figure A-3: Relation between tension in bolts using method 1 and displacement for P-SE1

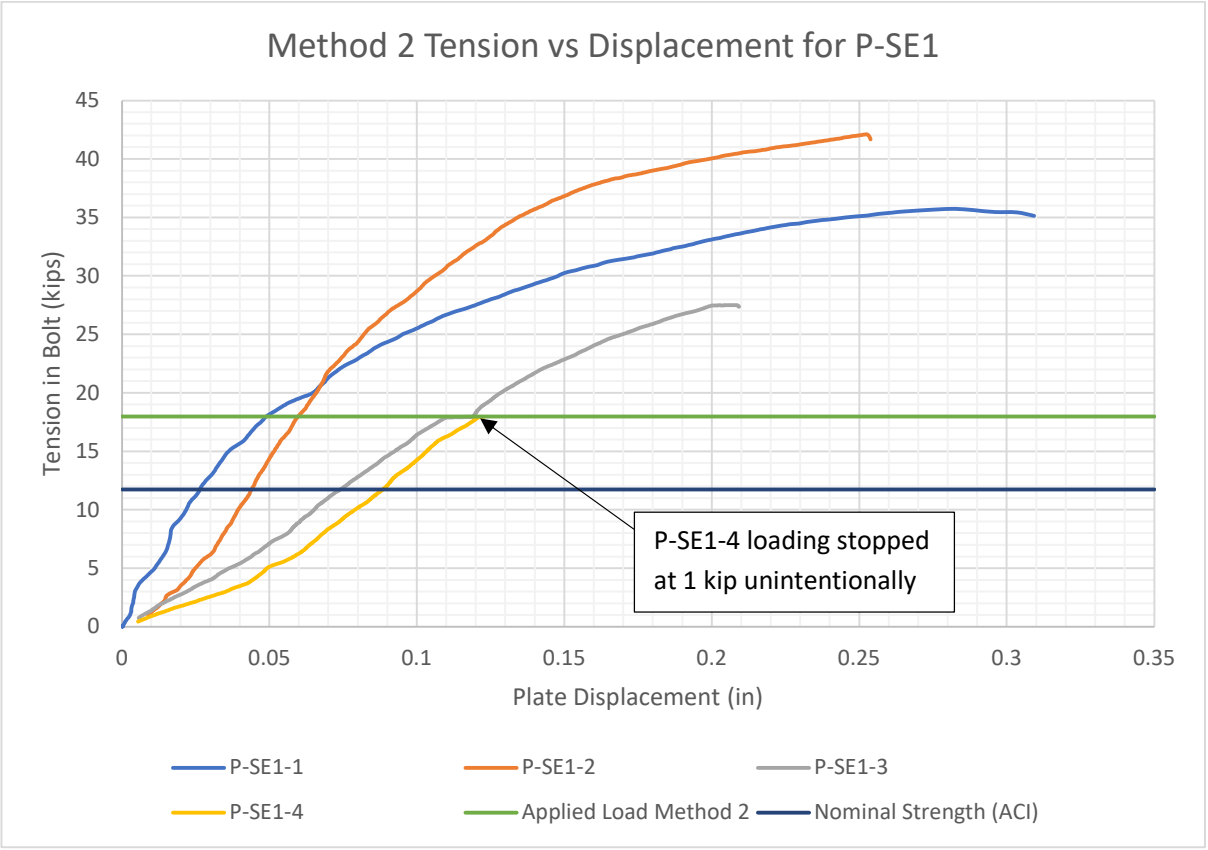

Figure A-4: Relation between tension in bolts using method 2 and displacement for P-SE1

Photographs depicting the documentation of the failure modes of each specimen are illustrated in Figure A-5 toFigure A-14. From these photographs, it is observed that bolts used in Specimens P-SE1-1 and P-SE1-2 exhibited signs of bending after being subjected to loading. The bend in these bolts was observed at the neck region. Conversely, the bolts in the remaining specimens did not display any noticeable bending.

However, it was observed that all specimen bolts had damage at the lower threads. This damage was consistent across all specimens tested and is attributed to the griding action occurred during installation.

Cracks that formed during the testing occurred within the predicted area as anticipated. Notably, a significant crack near the PVC of the P-SE1-1 specimen was already present prior to the testing phase.

Figure A-5: P-SE1-1 specimen screw after loading

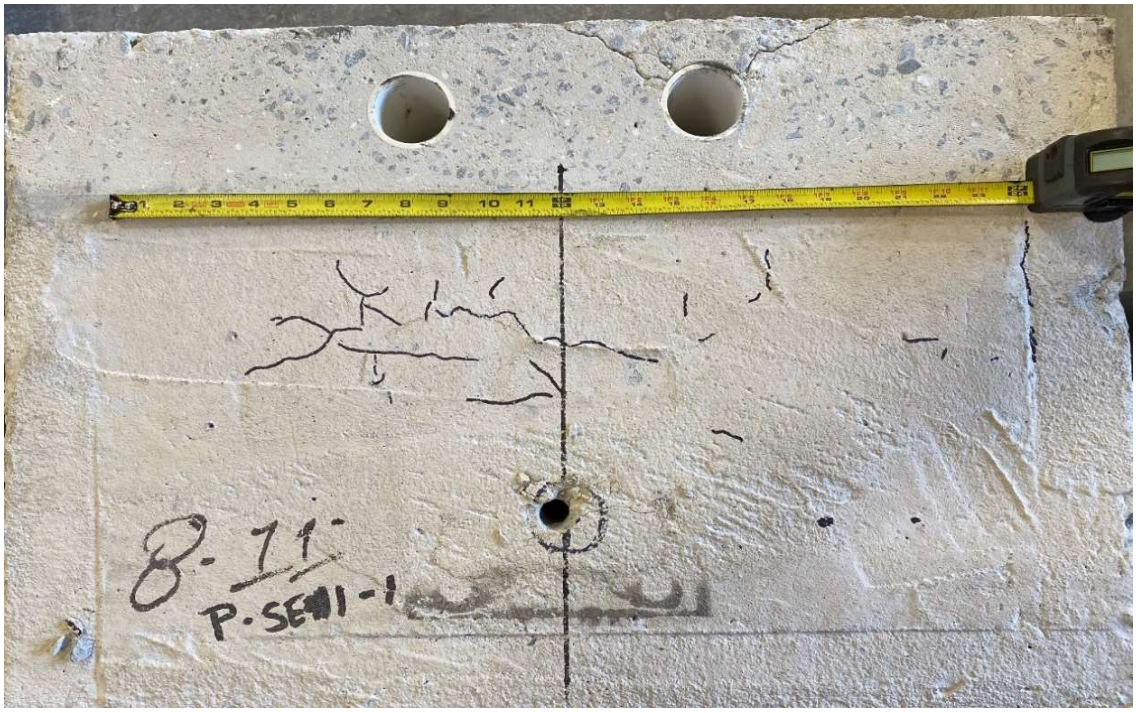

Figure A-6: P-SE1-1 specimen concrete after loading

Figure A-7: P-SE1-2 specimen screw after loading

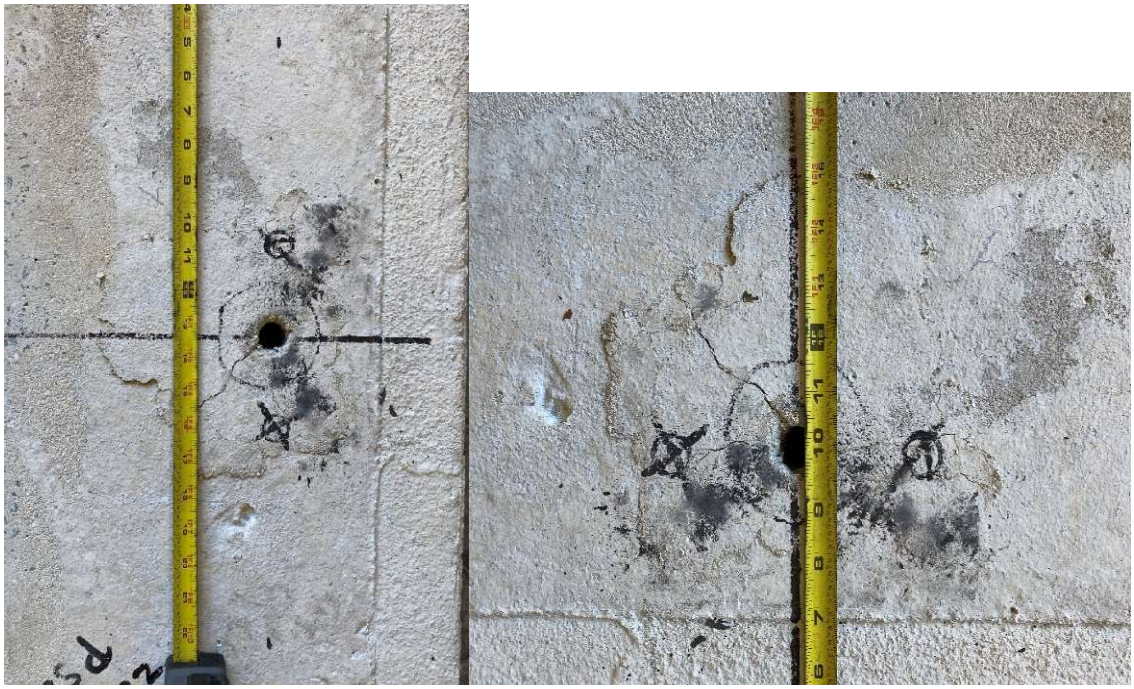

Figure A-8: P-SE1-2 specimen concrete after loading

Figure A-9: P-SE1-3 specimen screw after loading

Figure A-10: P-SE1-3 specimen concrete after loading

Figure A-11: P-SE1-4 specimen screw after loading

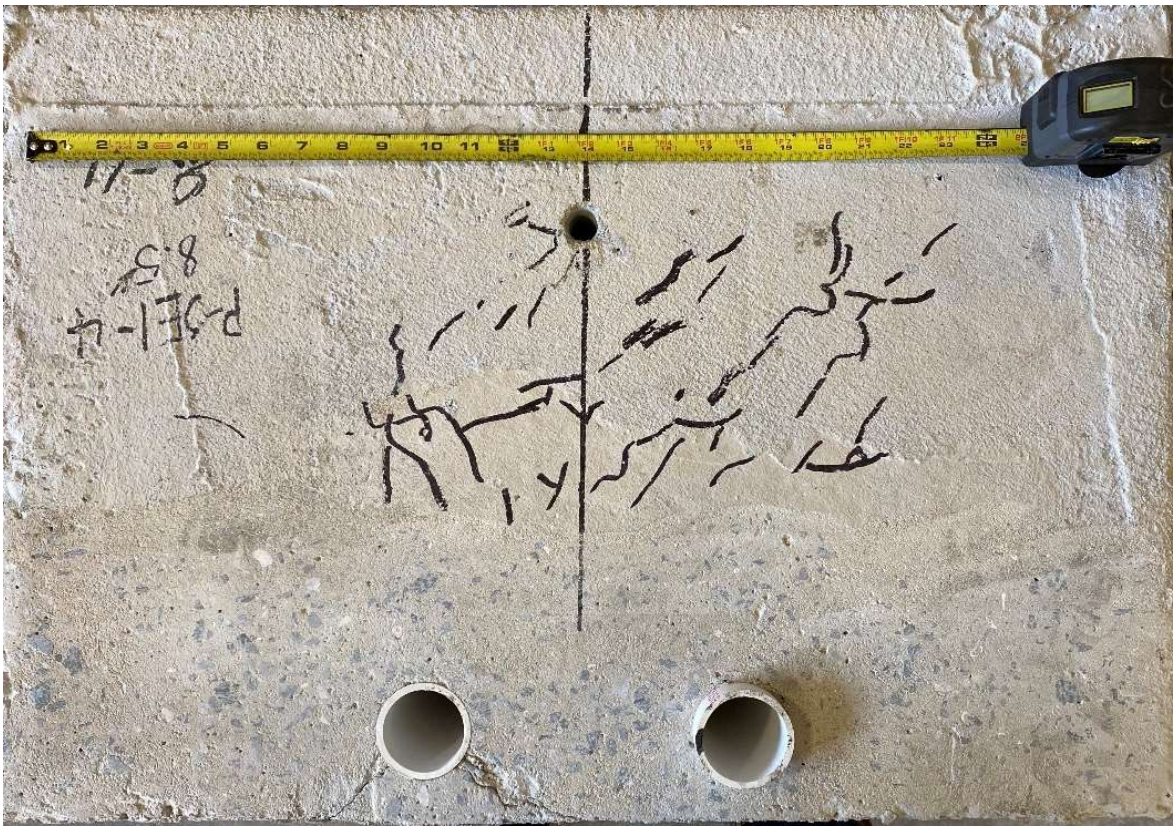
Figure A-12: P-SE1-4 specimen concrete after loading

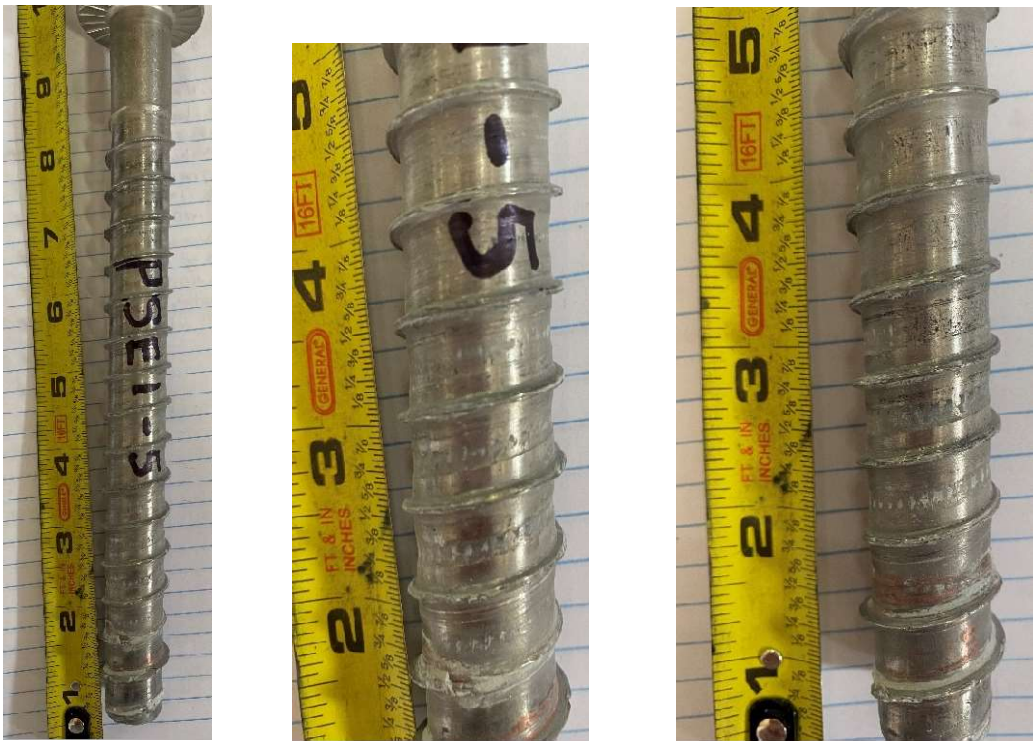

Figure A-13: P-SE1-5 specimen screw after loading

Figure A-14: P-SE1-5 specimen concrete after loading

A1.2 – CYCLIC LOADING OF PEDESTRIAN RAILING ON SIDEWALK SPECIMEN

A total of 3 pedestrian railings installed on sidewalk specimens were cyclically loaded between 100 – 600 lbs for 1000 cycles followed by monotonic loading until failure. The ultimate loads are summarized in Table A-2. It appears that the cyclic loads have no influence to the ultimate failure of the screw anchor breakout capacity. All specimens were subjected to loading conditions that surpassed both the yield strength and ultimate strength of the railings.

Impressively, the bolts employed in all specimens exhibited a remarkable capacity to withstand nearly four times the nominal strength calculated according to the ACI code.

Furthermore, the bolts across all specimens showcased a remarkable ability to endure twice the applied strength as calculated by both methods 1 and 2 as illustrated in Figure A-15 - Figure A-18.

Table A-2: Test results of pedestrian railing on sidewalk after subjected to cyclic loading.

Specimen's code	**P-SE1c-1**	**P-SE1c-2**	**P-SE1c-4**
Max Lateral Load (Kip)	2.278	2.371	2.325
Displacement (in)	0.263	0.250	0.228
Tilt (^{o}deg)	2.830	3.061	2.390
Tension in bolts (method 1) (Kip)	36.919	38.413	37.672
Tension in bolts (method 2) (Kip)	41.534	43.215	42.382
Nominal Strength (ACI) (Kip)	11.74		
Applied Strength (Method 1) (Kip)	15.99		
Applied Strength (Method 2) (Kip)	15.99		

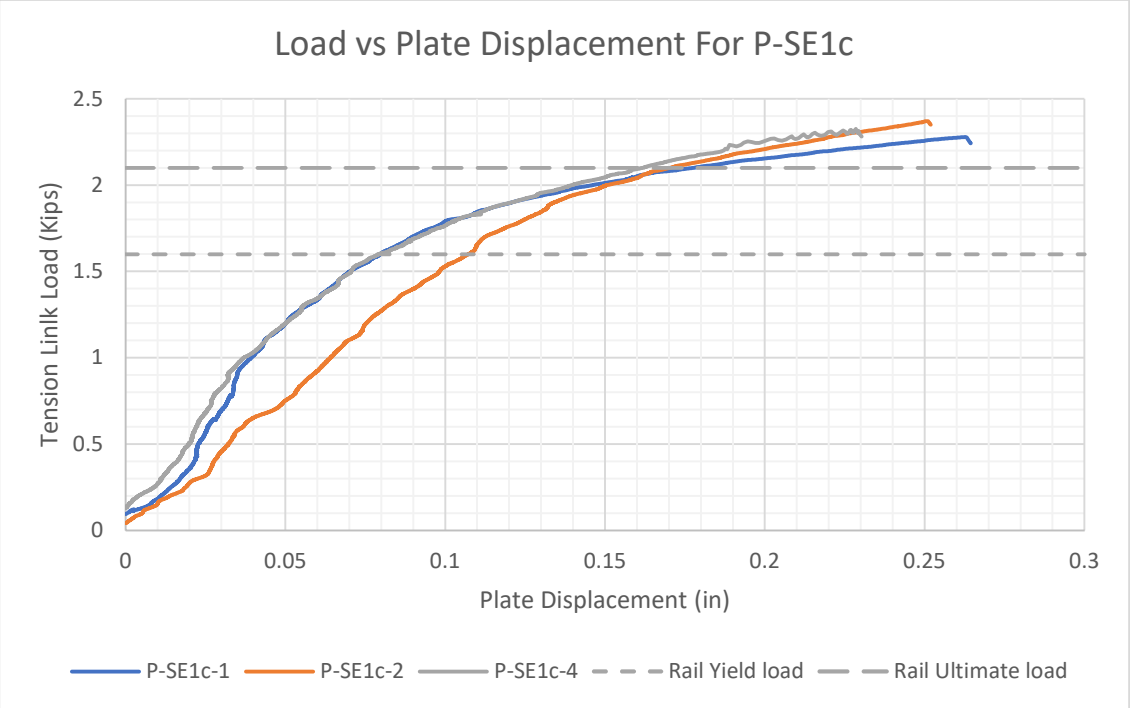

Figure A-15: Relation between load and displacement for P-SE1c

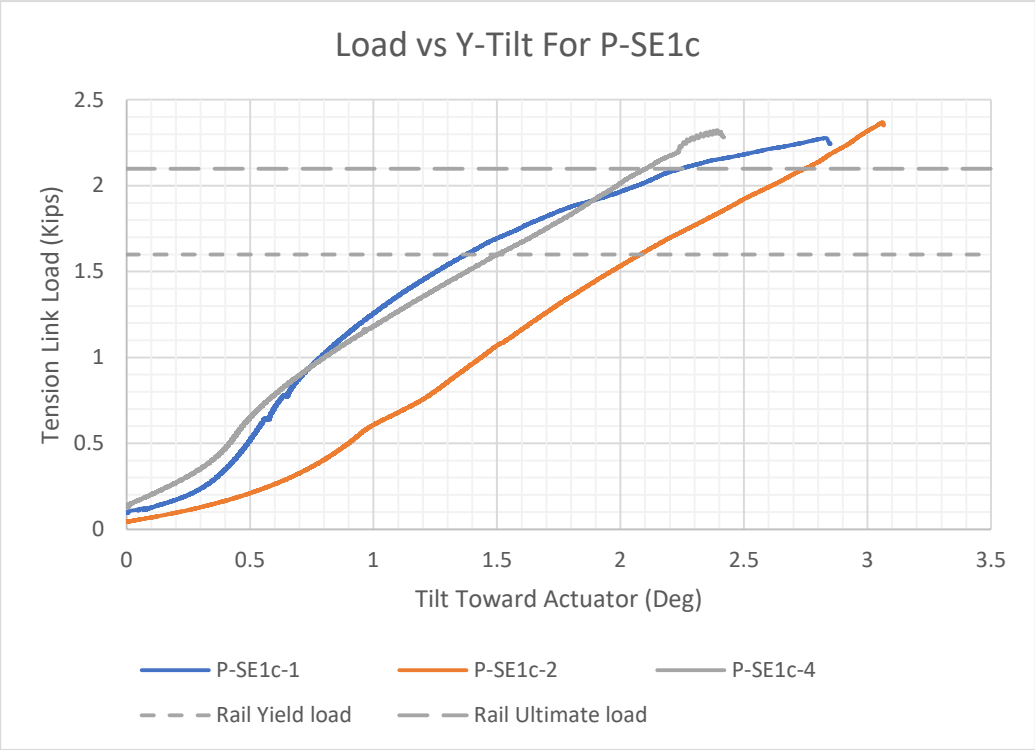

Figure A-16: Relation between load and y-axis tilt for P-SE1c

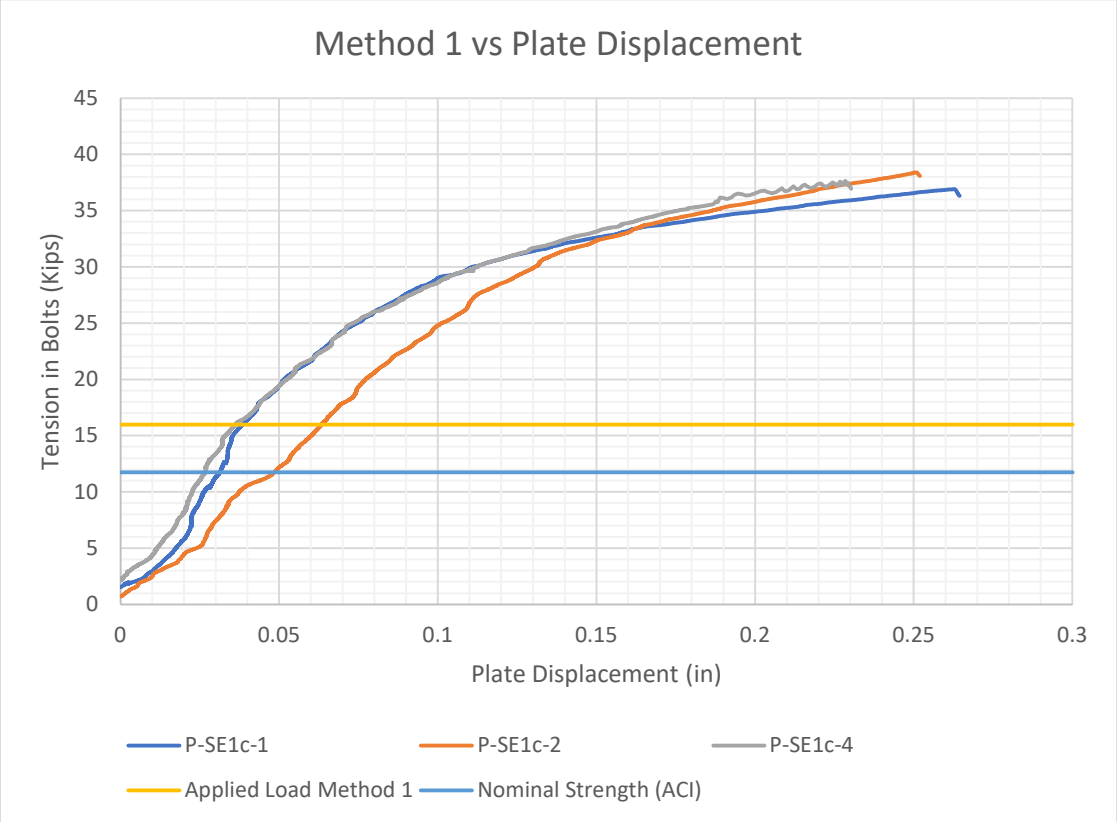

Figure A-17: Relation between tension in bolts using method 1 and displacement for P-SE1c

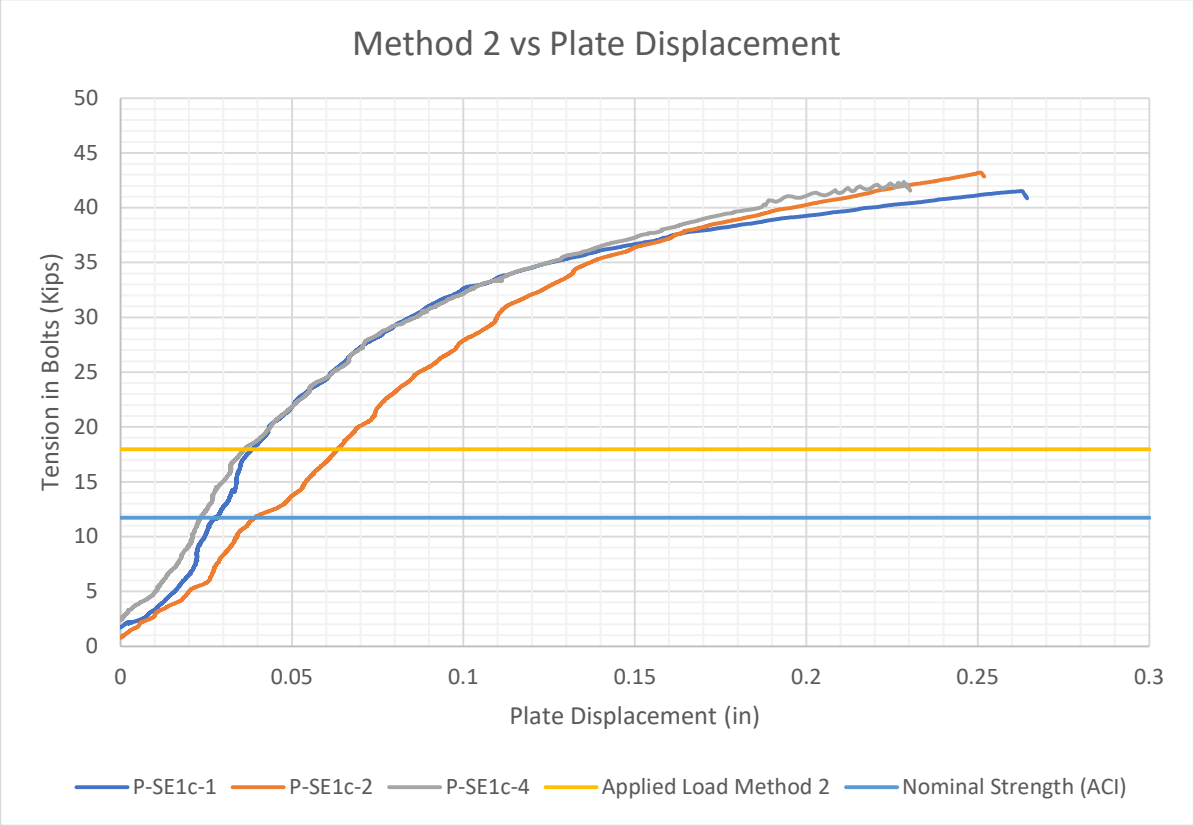

Figure A-18: Relation between tension in bolts using method 2 and displacement for P-SE1c

Figure A-19 - Figure A-24 illustrate photographic documentation of the failure of each specimen. Upon loading, all the bolts in the specimens exhibited bending, predominantly occurring at the neck region of the bolts. Notably, the bolt in specimen P-SE1c-2 displayed the maximum degree of bending compared to the other specimen bolts. The bolts in specimens P-SE1c-1 and P-SE1c-3 exhibited similar bending patterns. Prior to testing, all cracks present on the specimens were carefully marked for observation.

Among the specimens, P-SE1c-1 showed the most extensive damage, with a crack forming within the plate area. For specimen P-SE1c-2, a small crack was observed near the bolt hole. In contrast, no visible damage or cracks were detected on specimen P-SE1c-4.

Based on the results obtained from the monotonic and cyclic loading tests conducted on pedestrian railings attached to sidewalks, it can be concluded that the prevailing failure mode of the screw anchor is pullout failure. Notably, this failure mode exhibits a higher breakout capacity compared to the concrete breakout governed by the ACI equation.

Figure A-19: P-SE1c-1 specimen screw after cyclic loading

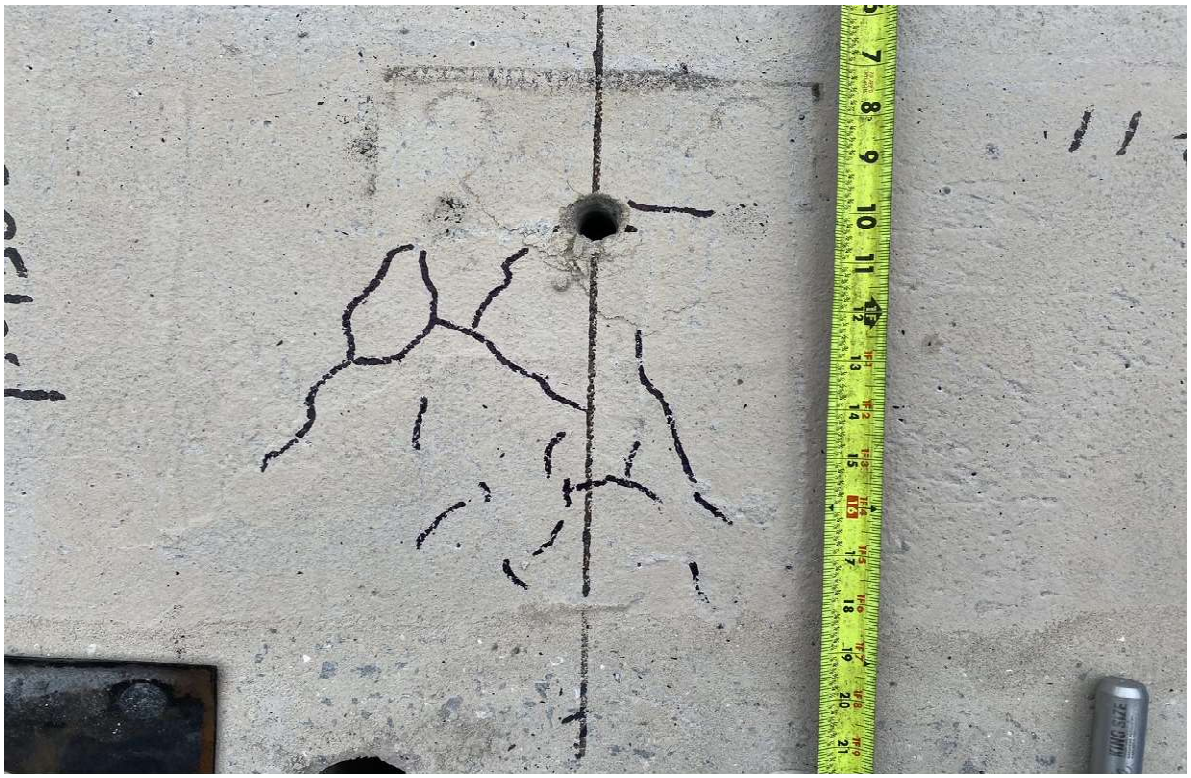
Figure A-20: P-SE1c-1 specimen concrete after cyclic loading

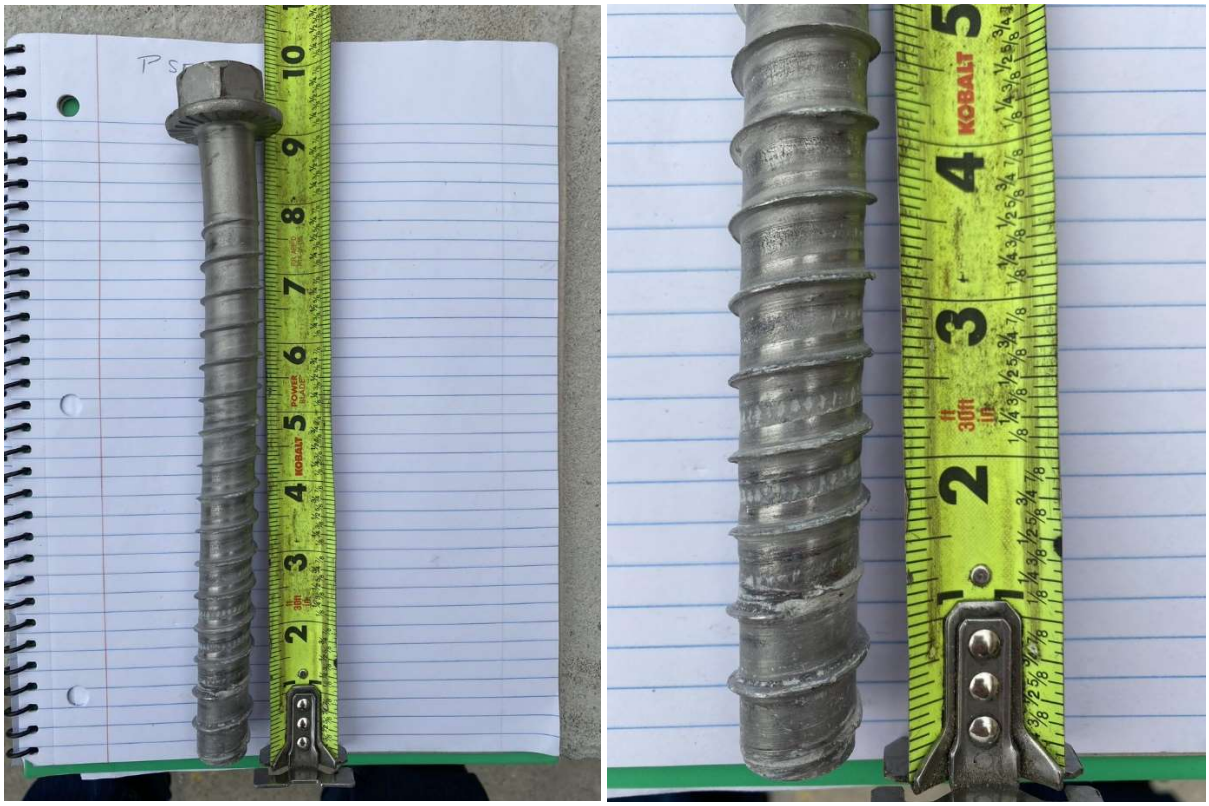

Figure A-21: P-SE1c-2 specimen screw after cyclic loading

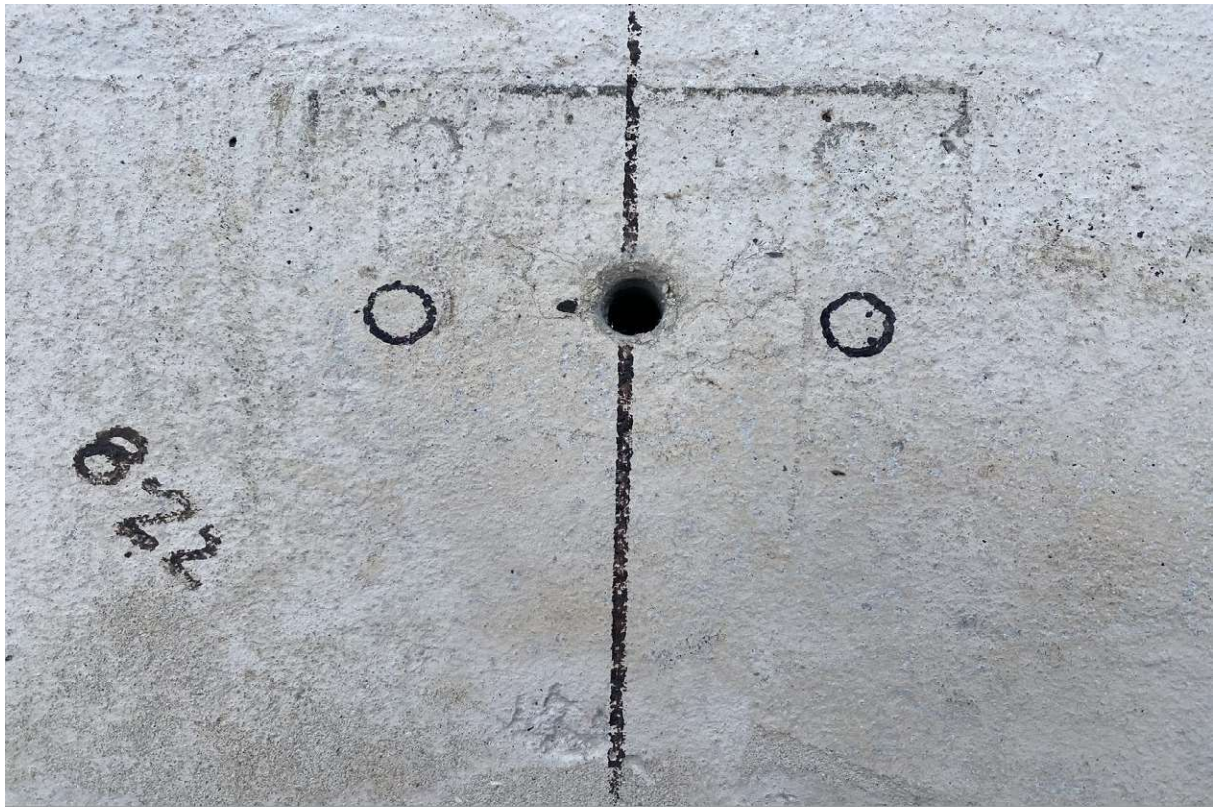
Figure A-22: P-SE1c-2 specimen concrete after cyclic loading

Figure A-23: P-SE1c-4 specimen screw after cyclic loading

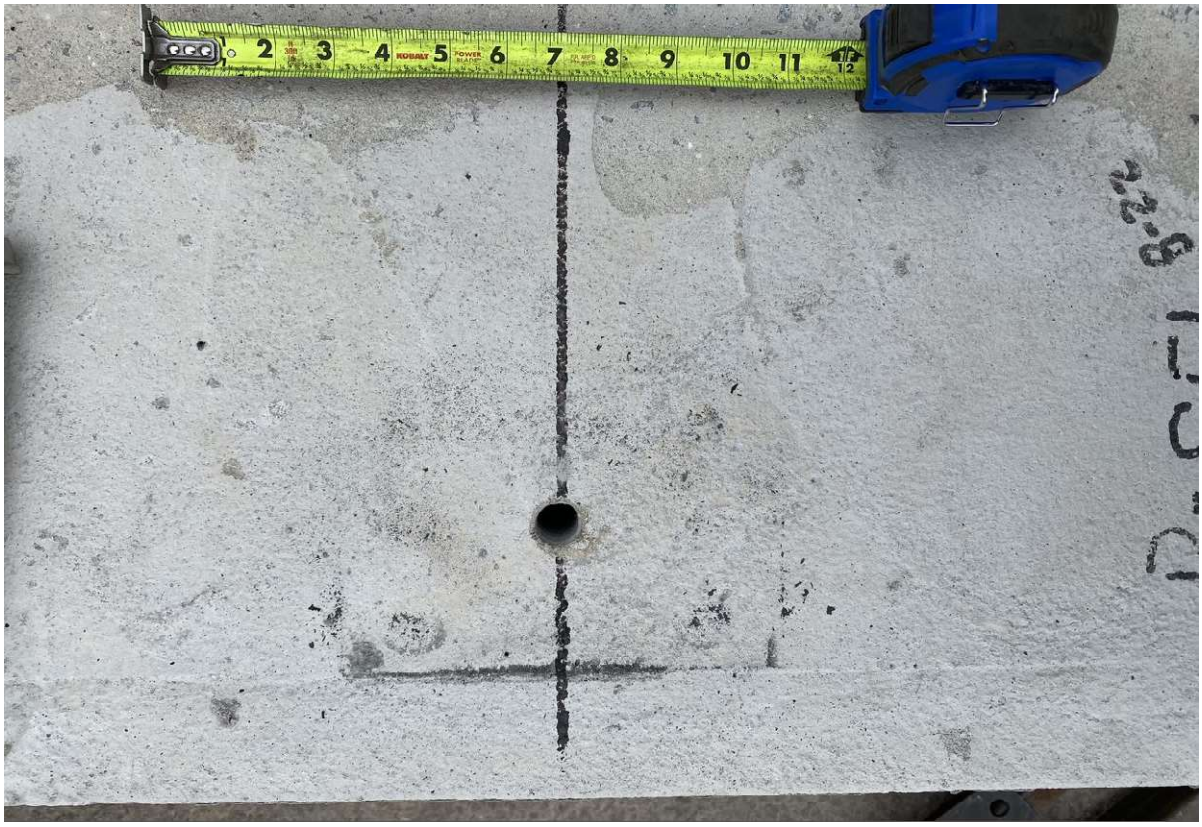
Figure A-24: P-SE1c-4 specimen concrete after cyclic loading

A1.3 – MONOTONIC LOADING OF PEDESTRIAN RAILING ON GRAVITY WALL SPECIMEN

Five pedestrian railings installed on gravity wall specimens were loaded monotonically to failure. Table A-3 provides the summary of the test results, and the lateral load versus plate displacement and tilt sensor are illustrated in Figure A-25 and Figure A-26. The conversion of the lateral load to anchor tensile capacity was also performed, and the results are plotted in Figure A-27 and Figure A-28 using methods 1 and 2, respectively.

All specimens in the test failed to reach the ultimate capacity of the railings before experiencing failure. Specifically, specimen P-G1-5 came closest to reaching the railing yield capacity before failing.

Remarkably, the average tension achieved in the bolts exceeded the nominal strength calculated using the ACI code by a factor of three. Similarly, the average tension achieved in the bolts surpassed the applied load calculated using method 1 and method 2 by a factor of 1.34.

When examining the individual specimens, it was observed that specimen P-G1-1 exhibited the lowest load capacity before failure, accompanied by the highest plate displacement. In contrast, specimen P-G1-3 demonstrated the shortest plate displacement among all the specimens.

Notably, specimen P-G1-5 achieved the highest load before failure and also exhibited the highest degree of tilt during testing.

Figure A-29 - Figure A-36 illustrate the failure modes of the gravity wall specimens. The screw anchors used in specimens P-G1-1, P-G1-2, P-G1-4, and P-G1-5 displayed noticeable bending when subjected to loading. Among these specimens, the screw anchor in P-G1-1 exhibited the most significant degree of bending, while the screw anchor in P-G1-4 had the least amount of bending. Interestingly, the screw anchor in P-G1-3 did not exhibit any noticeable bending.

It should be noted that specimen P-G1-1 had three drilled holes, but only the middle-drilled hole was utilized. After loading, cracks formed on specimen P-G1-1 were observed within the plate area, originating from the drilled hole.

For specimens P-G1-2 and P-G1-3, cracks formed beyond the plate area. Both specimens exhibited a similar crack pattern, with shear cracks at the back and compression cracks at the front.

In the case of specimen P-G1-4, a crack occurred on the right side of the hole within the plate area, while the crack on the left side extended beyond the plate area. The crack pattern on this specimen included both tension and shear cracks towards the front face.

Regarding specimen P-G1-5, most of the cracks occurred within the plate area, but two shear cracks were observed on either side of the bolt hole towards the front face.

Table A-3: Test results of pedestrian railing on gravity wall

Specimen's code	**P-G1-1**	**P-G1-2**	**P-G1-3**	**P-G1-4**	**P-G1-5**
Max Lateral Load (Kip)	1.105	1.268	1.387	1.268	1.604
Displacement (in)	0.174	0.192	0.101	0.145	0.158
Tilt (^{o}deg)	3.002	3.768	2.092	3.253	3.168
Tension in bolts (method 1) (Kip)	17.912	20.543	22.476	20.553	25.998

Table A-3, continued

Tension in bolts (method 2) (Kip)	20.151	23.118	25.286	23.122	29.248
Nominal Strength (ACI) (Kip)	7.38				
Applied load (Method 1) (Kip)	15.99				
Applied Load (Method 2) (Kip)	17.98				

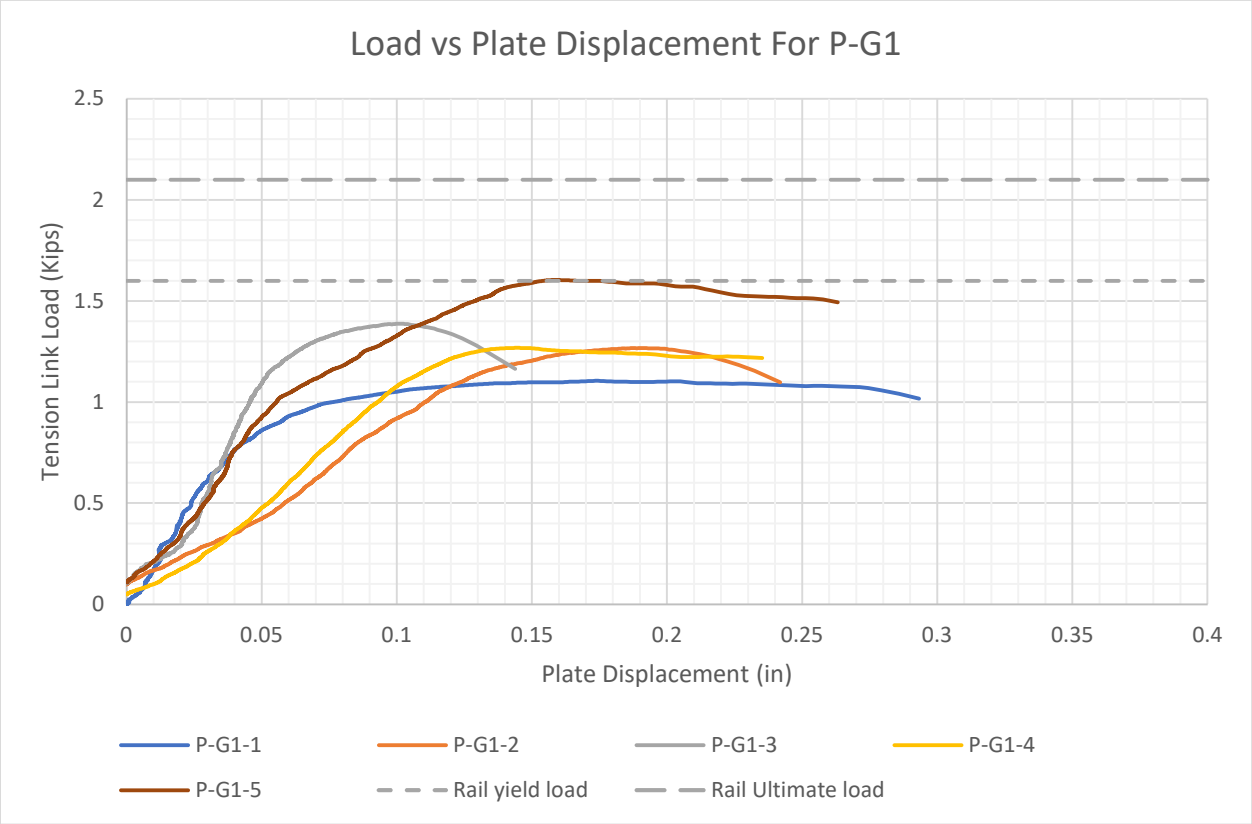

Figure A-25: Relation between load and displacement for P-G-1

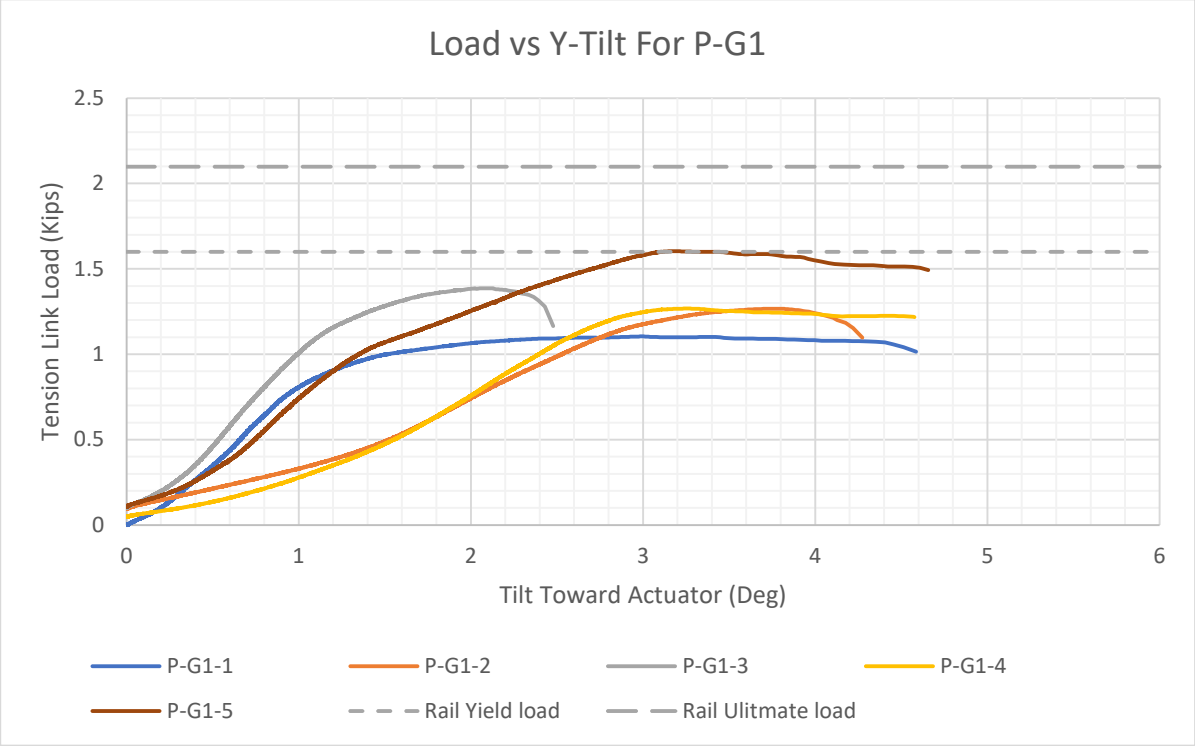

Figure A-26: Relation between load and y-axis tilt for P-G-1

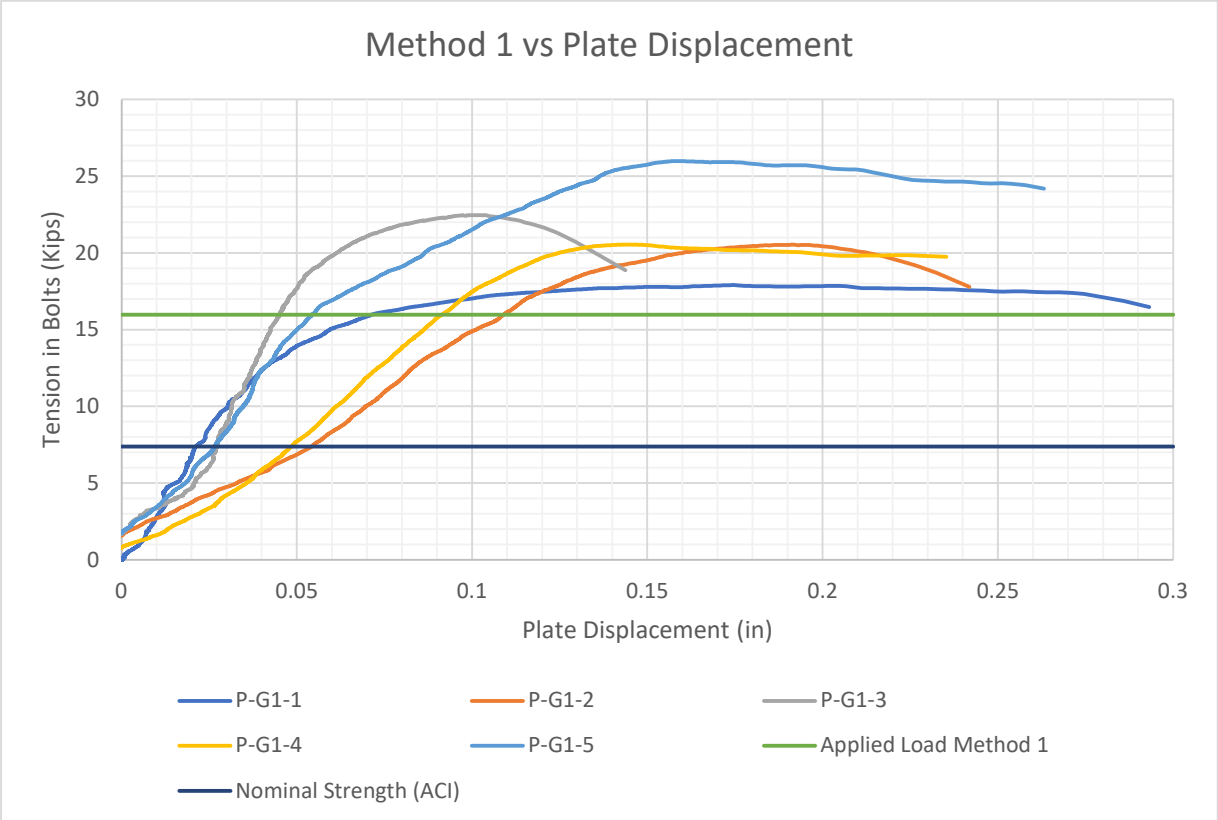

Figure A-27: Relation between tension in bolts using method 1 and displacement for P-G1

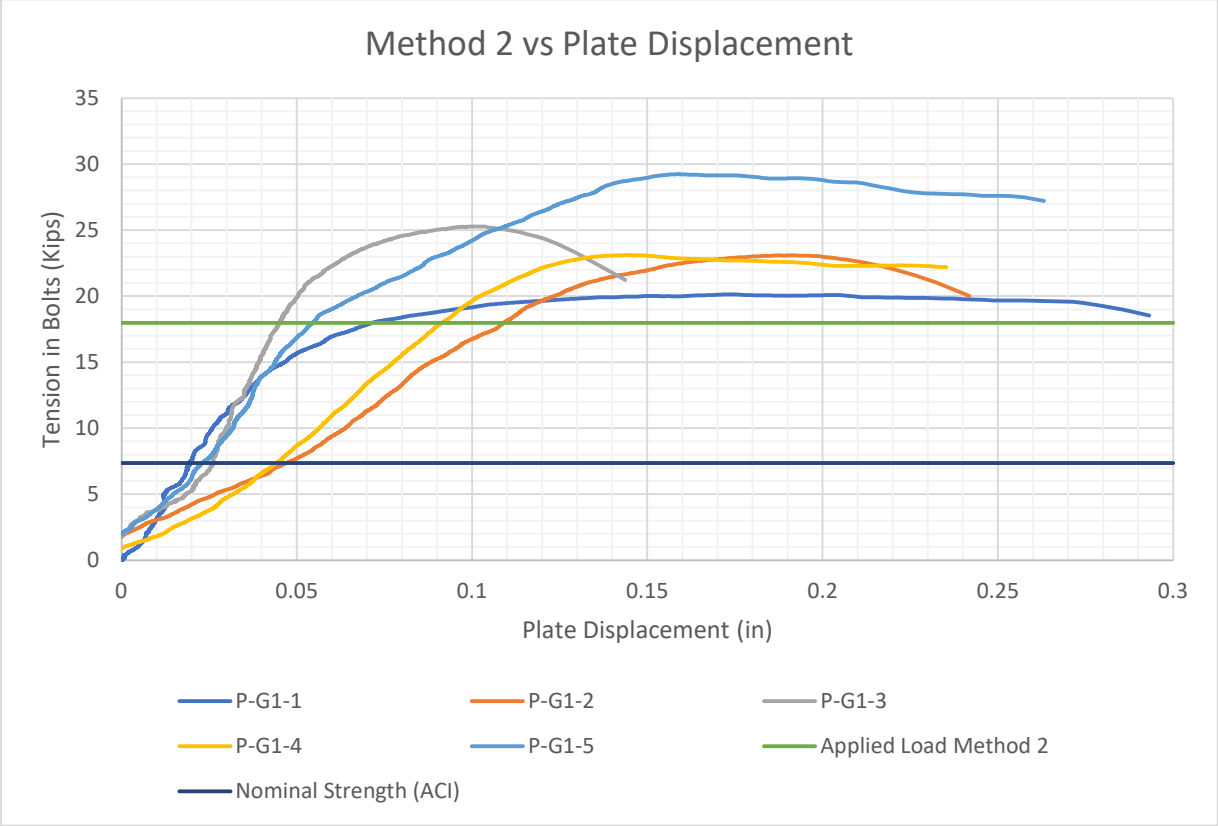

Figure A-28: Relation between tension in bolts using method 2 and displacement for P-G1

Figure A-29: P-G1-1 specimen screw after breakout

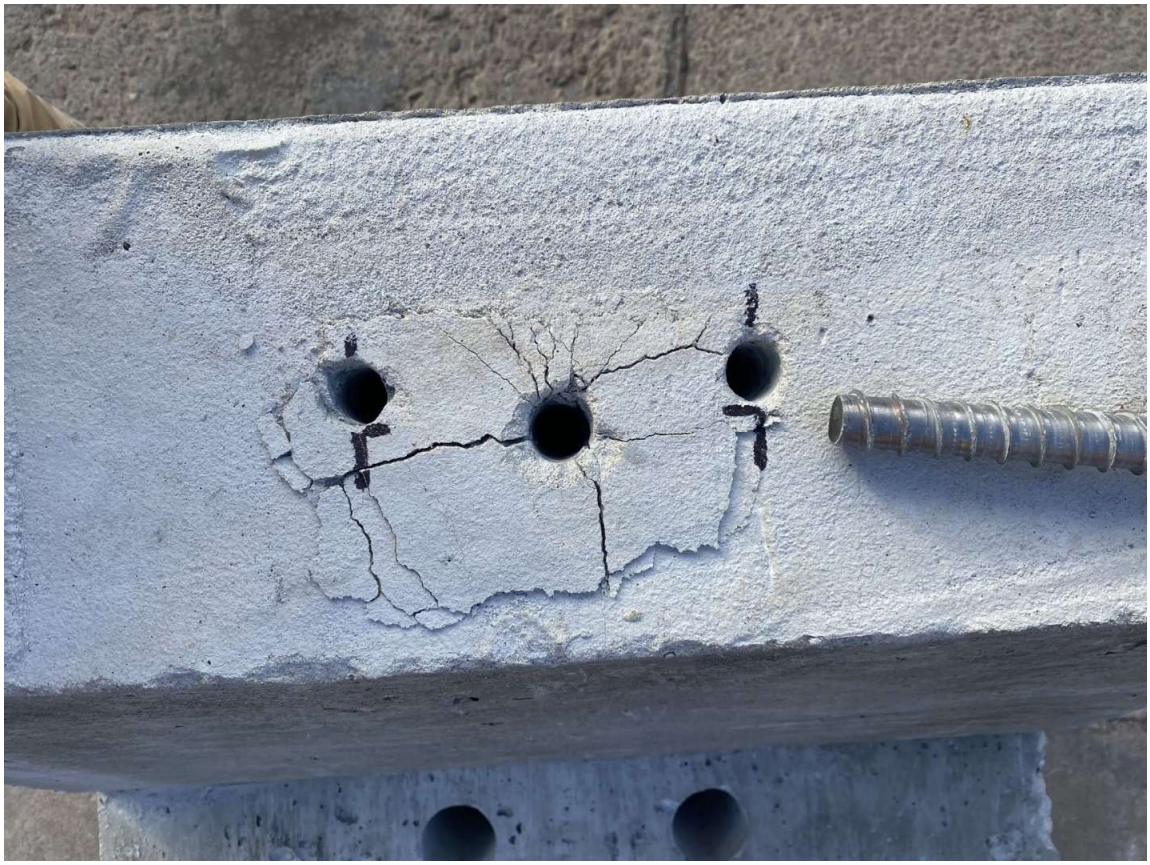

Figure A-30: P-G1-1 specimen concrete after anchor breakout

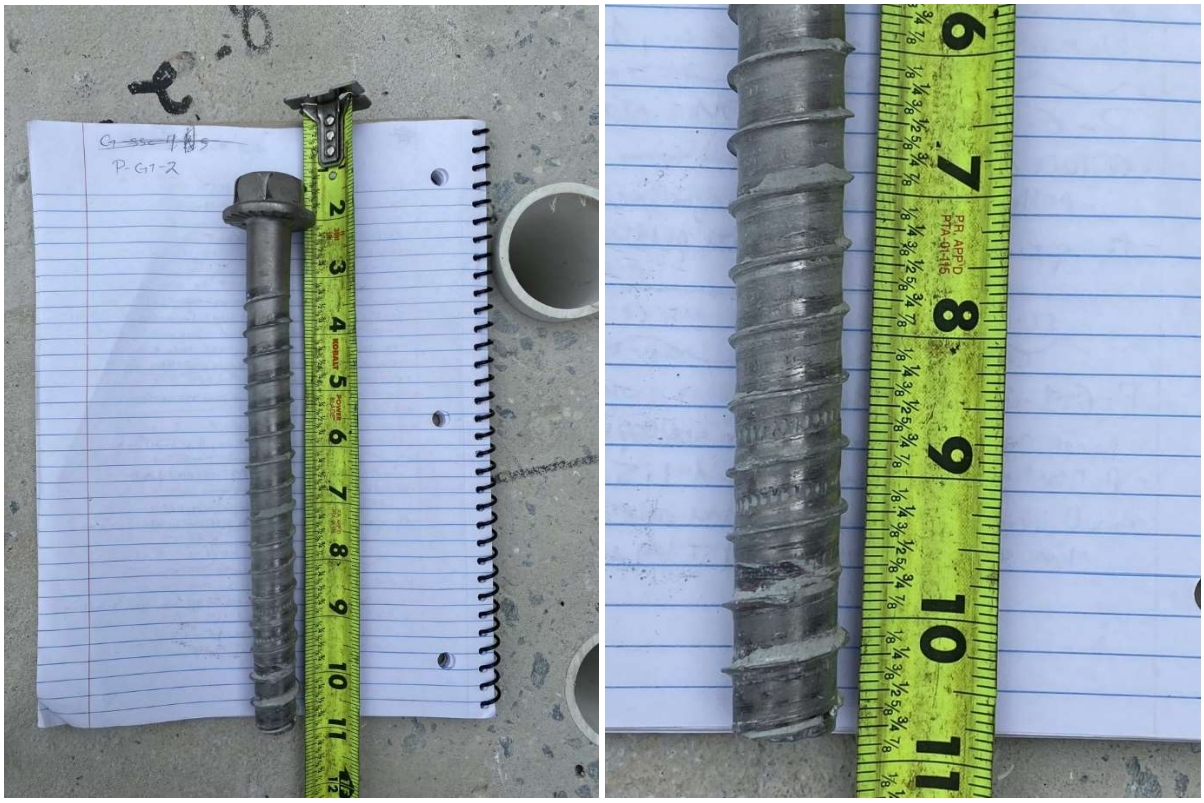

Figure A-31: P-G1-2 specimen screw after breakout

Figure A-32: P-G1-2 specimen concrete after anchor breakout

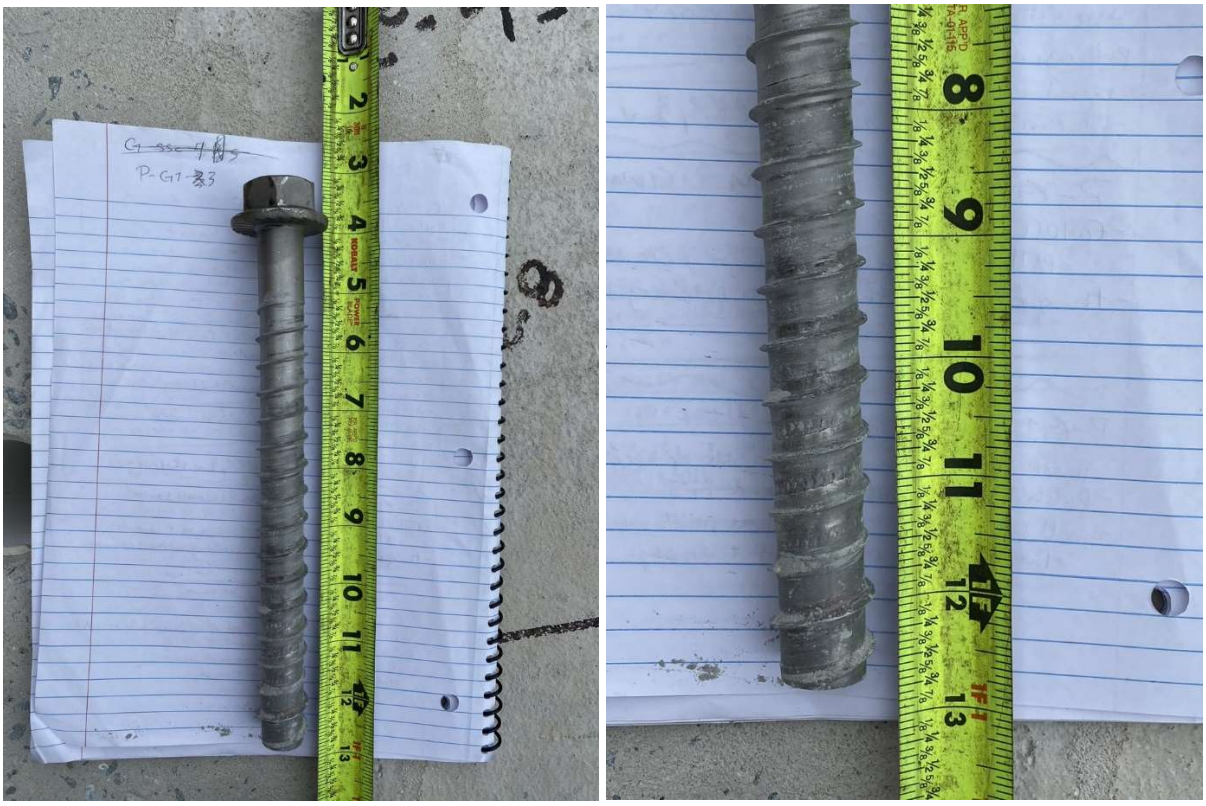

Figure A-33: P-G1-3 specimen screw after breakout

Figure A-34: P-G1-3 specimen concrete after anchor breakout

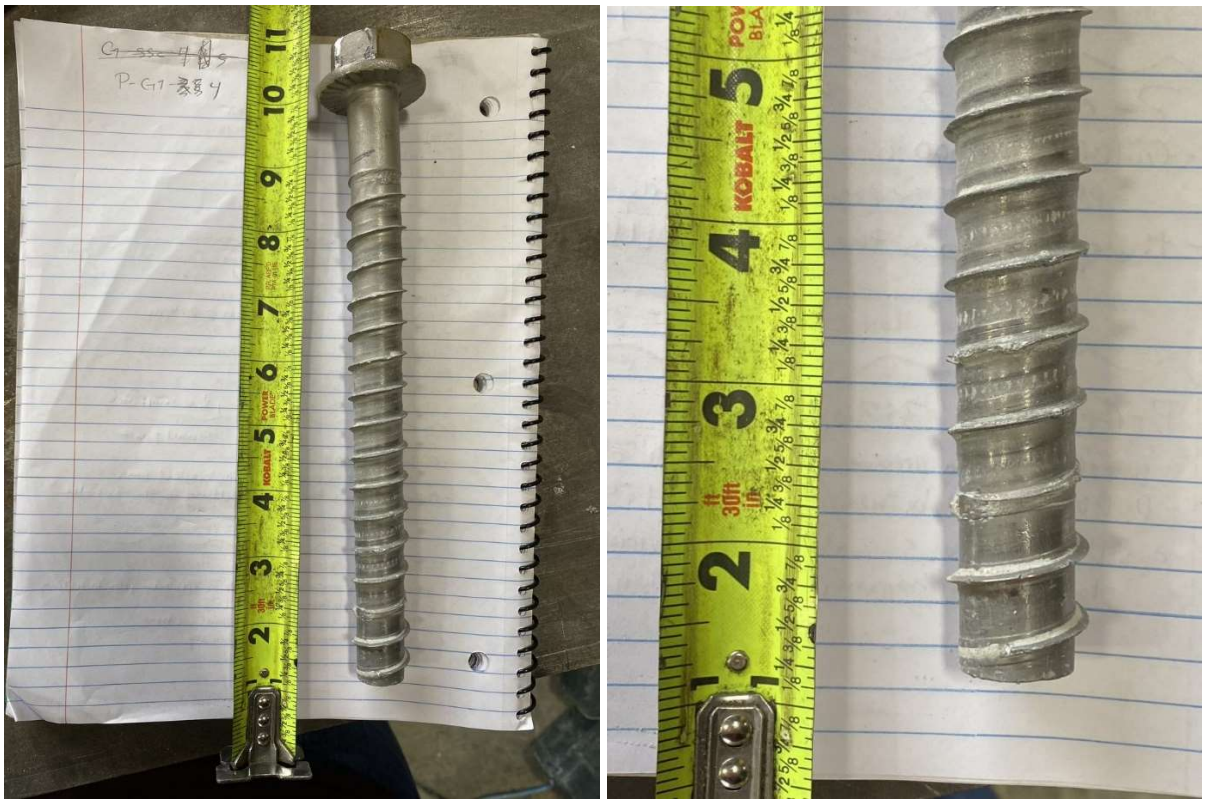

Figure A-35: P-G1-4 specimen screw after breakout

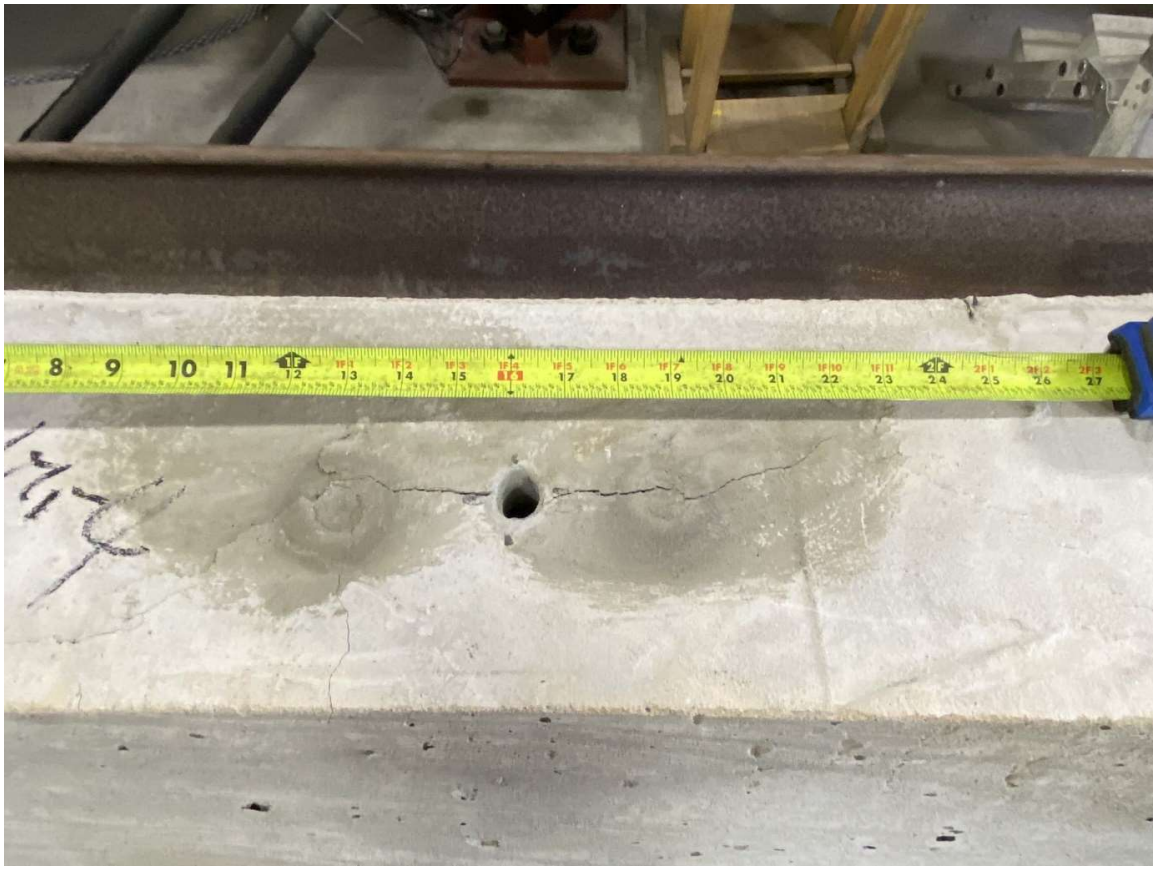

Figure A-36: P-G1-4 specimen concrete after anchor breakout

A1.4 –MONOTONIC LOADING OF PEDESTRIAN RAILING ON PARAPET WALL

Four specimens were used to evaluate the confinement effect of narrow baseplate or reaction area on anchor breakout of pedestrian railing with parapet wall under the monotonic load. Table A-4 provides a summary of the test results and the same plots are illustrated in Figure A-37 - Figure A-40.

In all tested specimens, failure occurred before reaching the ultimate capacity of the railings. Specifically, specimen P-P-4 came closest to achieving the maximum load, nearing the railing yield capacity before failure. Comparatively, specimens P-P-1 and P-P-2 exhibited the lowest load, displacement, and tilt among all the tested specimens.

Please note that due to technical issues, images for the P-P specimens were not available. Therefore, the following were based on lab notes. All the screw anchors in the tested specimens exhibited bending at the neck. Cracks observed in all specimens were located beyond the plate area. In the case of specimen P-P-1, the crack pattern formed was a shear crack towards the back.

For specimen P-P-2, the crack pattern consisted of a shear crack towards the back and a small tension crack towards the front, with the tension crack forming within the plate area.

Both specimen P-P-3 and P-P-4 exhibited a crack pattern featuring a shear crack towards the back and a tension crack towards the front. Importantly, all cracks formed in these specimens were located beyond the plate area.

Table A-4: Test results of scheme 1.3

Specimen's code	**P-P-1**	**P-P-2**	**P-P-3**	**P-P-4**
Max Lateral Load (Kip)	1.220	1.199	1.423	1.552
Displacement (in)	0.154	0.093	0.138	0.168
Tilt (^{o}deg)	3.238	2.015	2.625	3.393
Tension in bolts (method1) (Kip)	19.647	19.314	22.916	24.993
Tension in bolts (method 2) (Kip)	22.103	21.728	25.780	28.118
Nominal Strength (ACI) (Kip)	7.52			
Applied Load (Method 1) (Kip)	15.99			
Applied Load (Method 2) (Kip)	17.98			

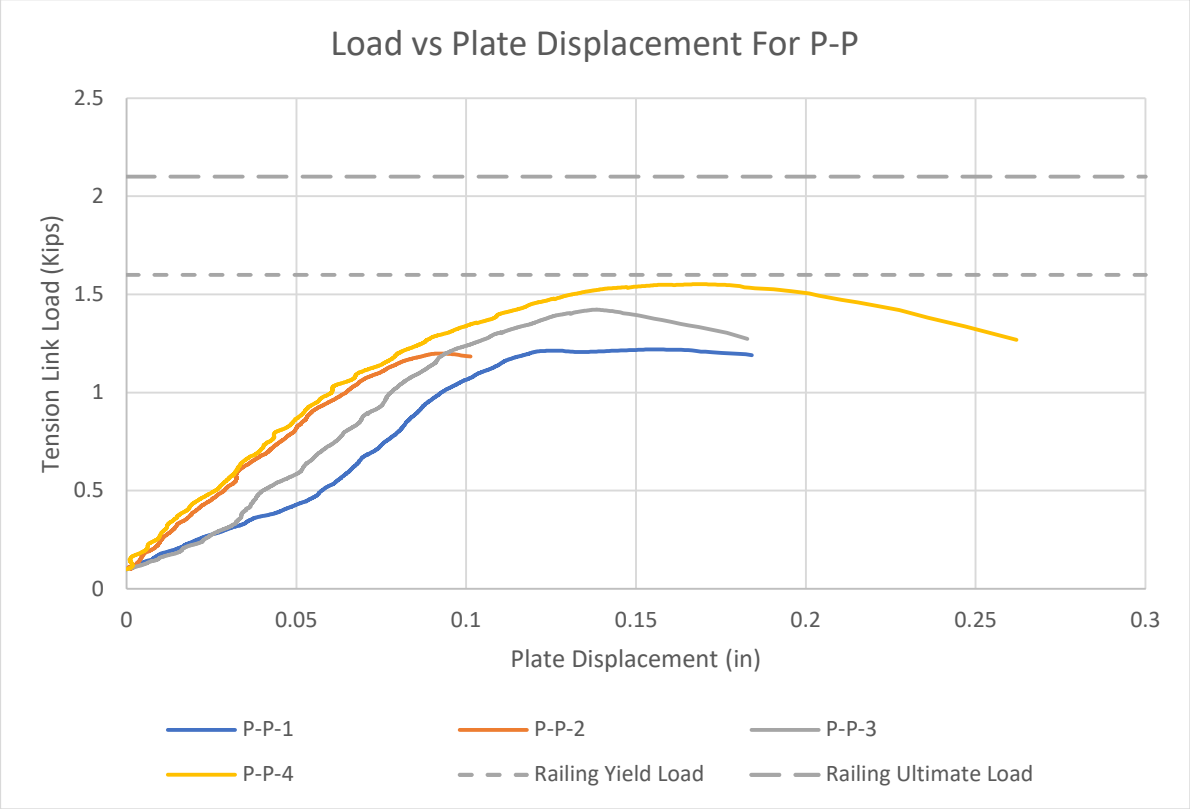

Figure A-37: Relation between load and displacement for P-P

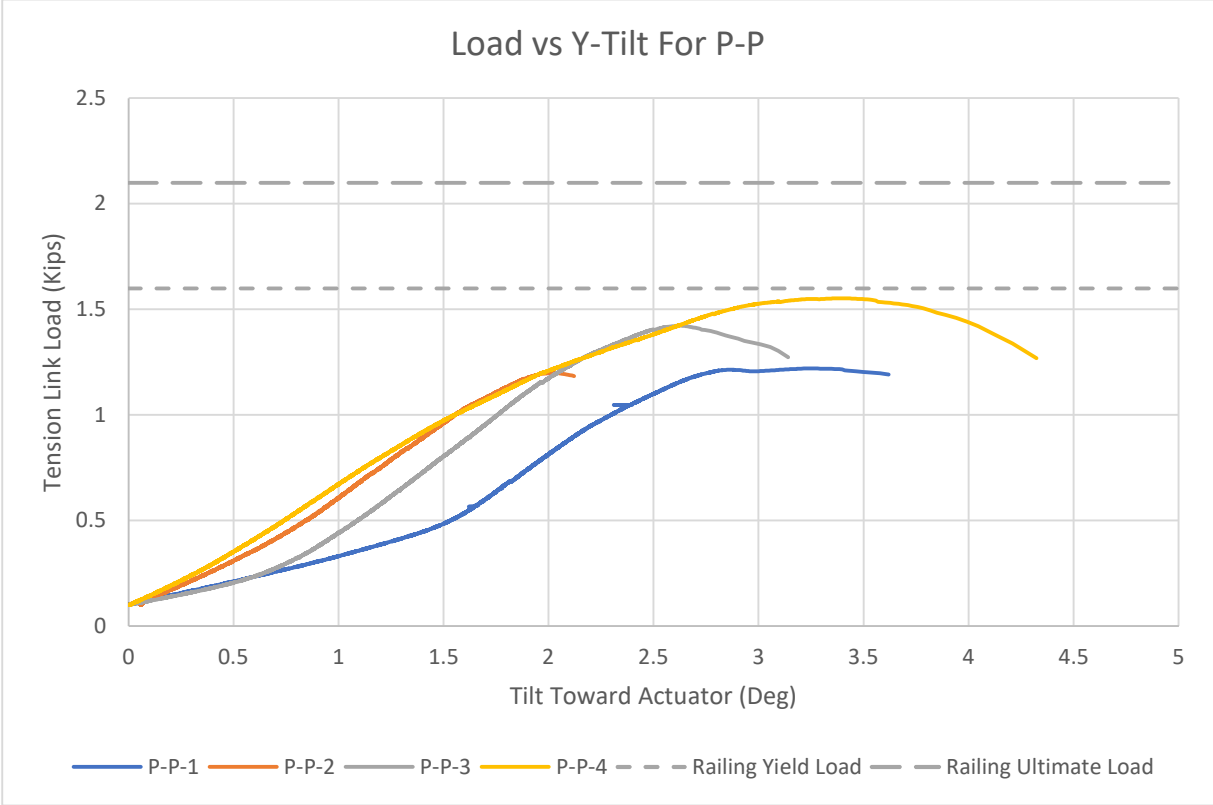

Figure A-38: Relation between load and y-axis tilt for P-P

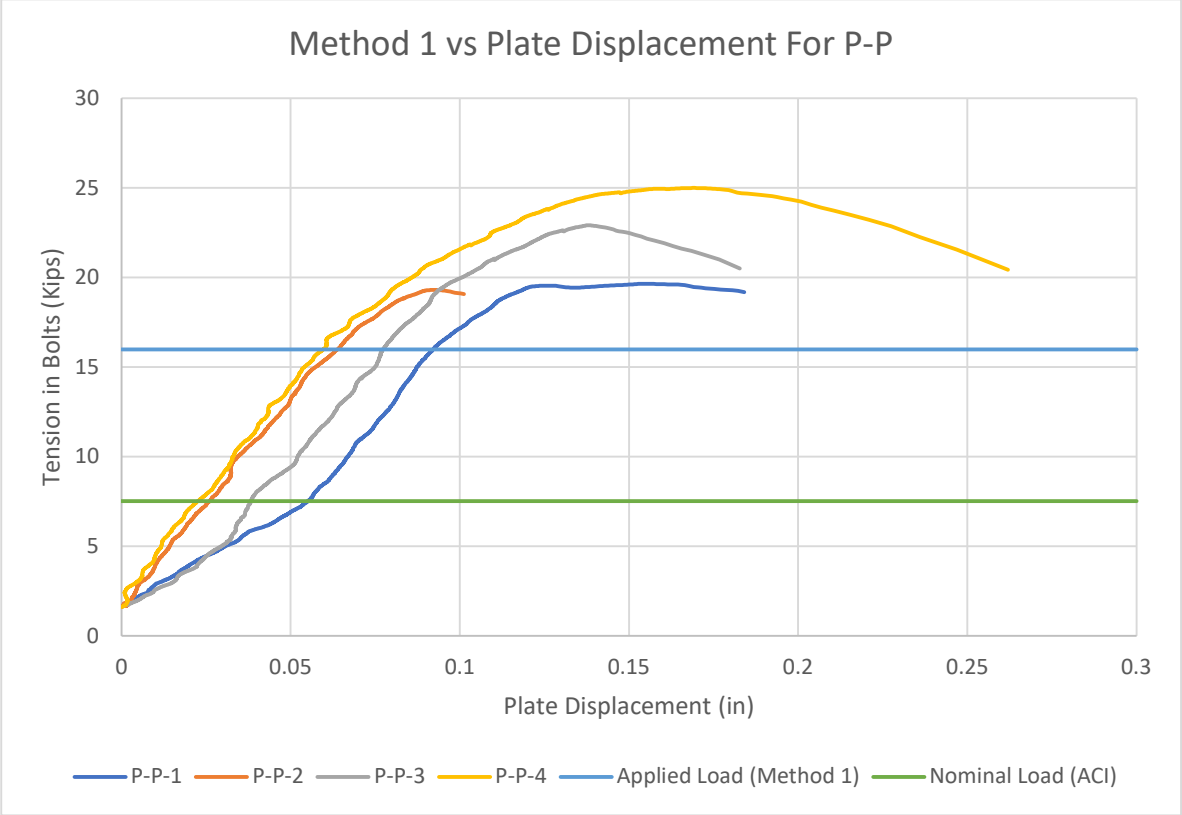

Figure A-39: Relation between tension between load using method 1 and displacement for P-P

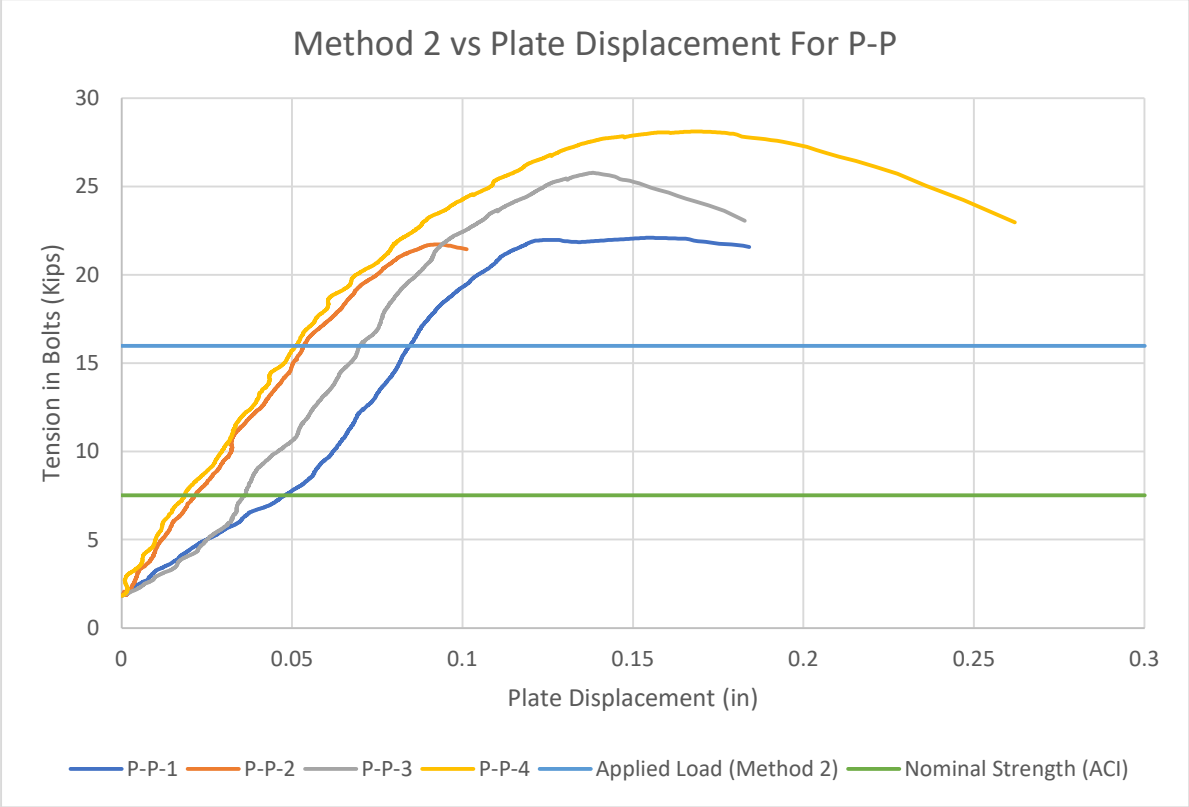

Figure A-40: Relation between load using method 2 and displacement for P-P

A2 – SCHEME 2 TEST RESULTS

A2.1 – MONOTONIC LOADING OF GUIDE RAIL ON SIDEWALK SPECIMEN

Five sidewalk specimens were used to evaluate the screw anchor breakout capacity under the monotonic load. Table A-5 provides a summary of the test results. Using methods 1 and 2, the average breakout resistance in the screw anchor is 15.368 kips and 17.289 kips, respectively. All the specimens were able to achieve much higher resistance than the required loads. With the exception of G-SS-2, all breakout resistances are higher than the nominal resistance using ACI. Figure A-41 - Figure A-44 illustrate the plots of the load versus displacement and tilt as well the tension forces using methods 1 and 2.

Table A-5: Test results of guiderail installed on sidewalk

Specimen's code	**G-SS-1**	**G-SS-2**	**G-SS-3**	**G-SS-4**	**G-SS-5**
Max Lateral Load (Kip)	1.277	1.007	1.050	1.360	1.089
Displacement (in)	0.266	0.185	0.123	0.220	0.099
Tilt (^{o}deg)	4.261	1.621	0.751	1.556	1.086
Tension in bolts (method1) (Kip)	20.429	16.314	17.013	22.037	17.649
Tension in bolts (method 2) (Kip)	22.982	18.353	19.139	24.792	19.856
Nominal Strength (ACI) (Kip)	16.95				
Applied Strength (Method 1) (Kip)	8.53				
Applied Strength (Method 2) (Kip)	9.59				

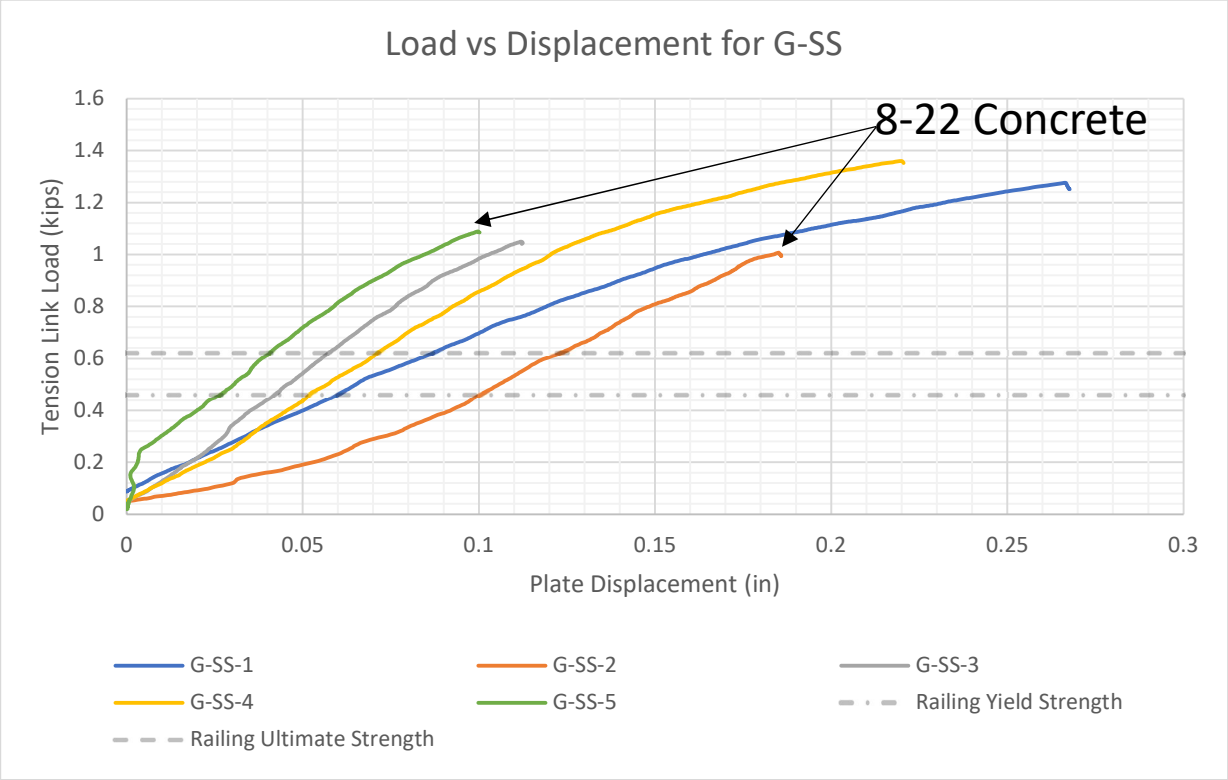

Figure A-41: Relation between load and displacement for G-SS

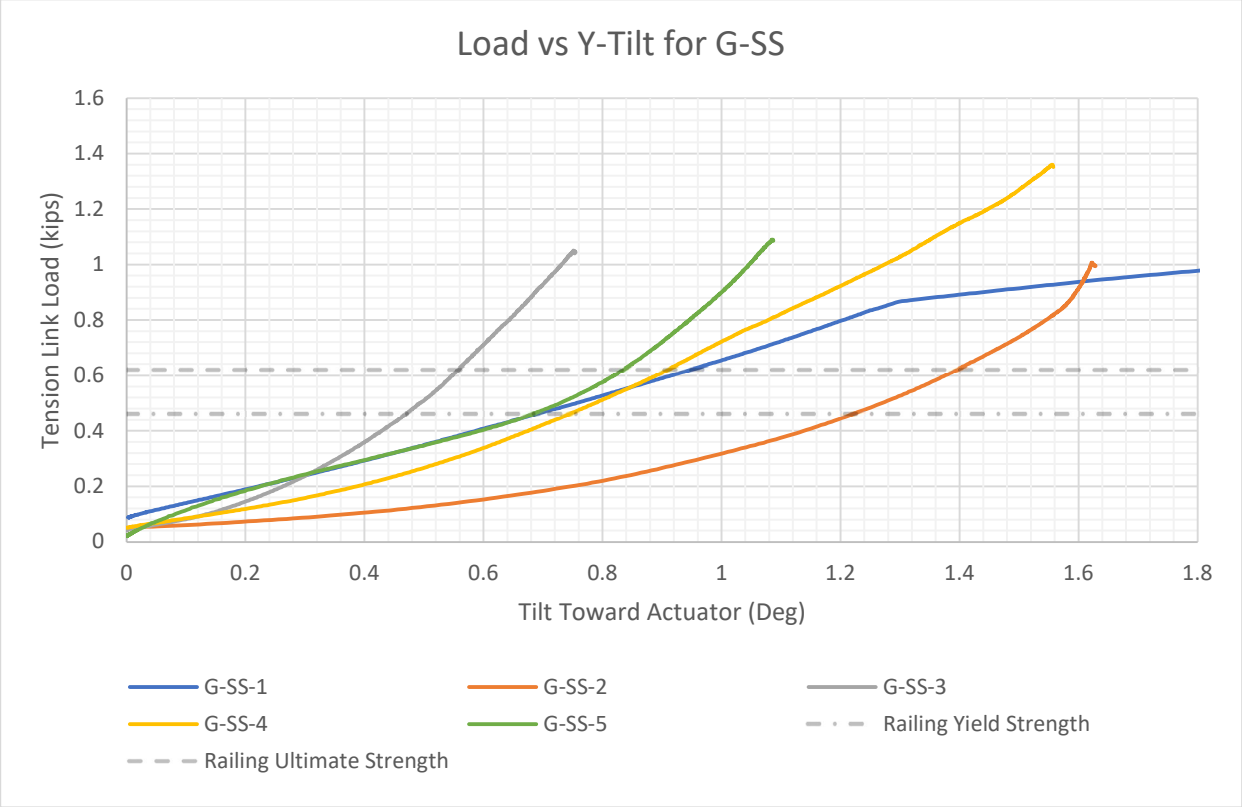

Figure A-42: Relation between load and y-axis tilt for G-SS

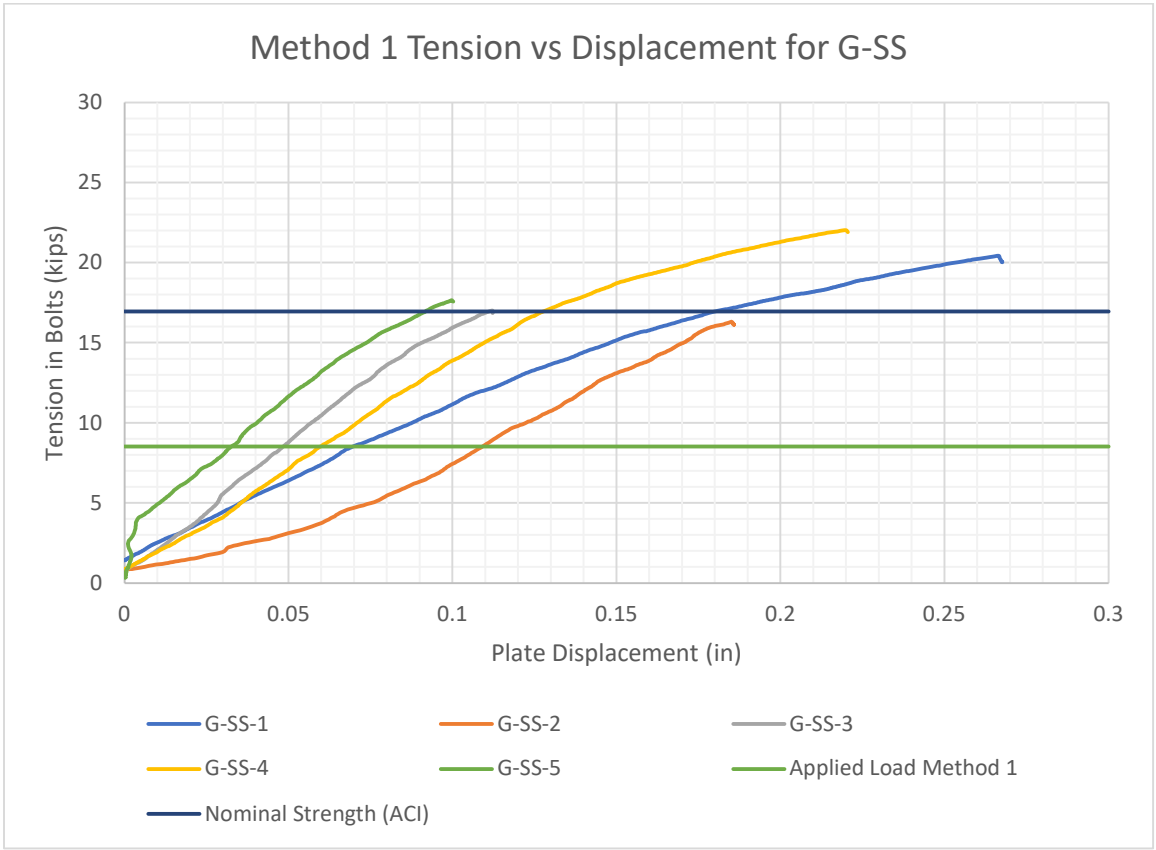

Figure A-43: Relation between tension in bolts using method 1 and displacement for G-SS

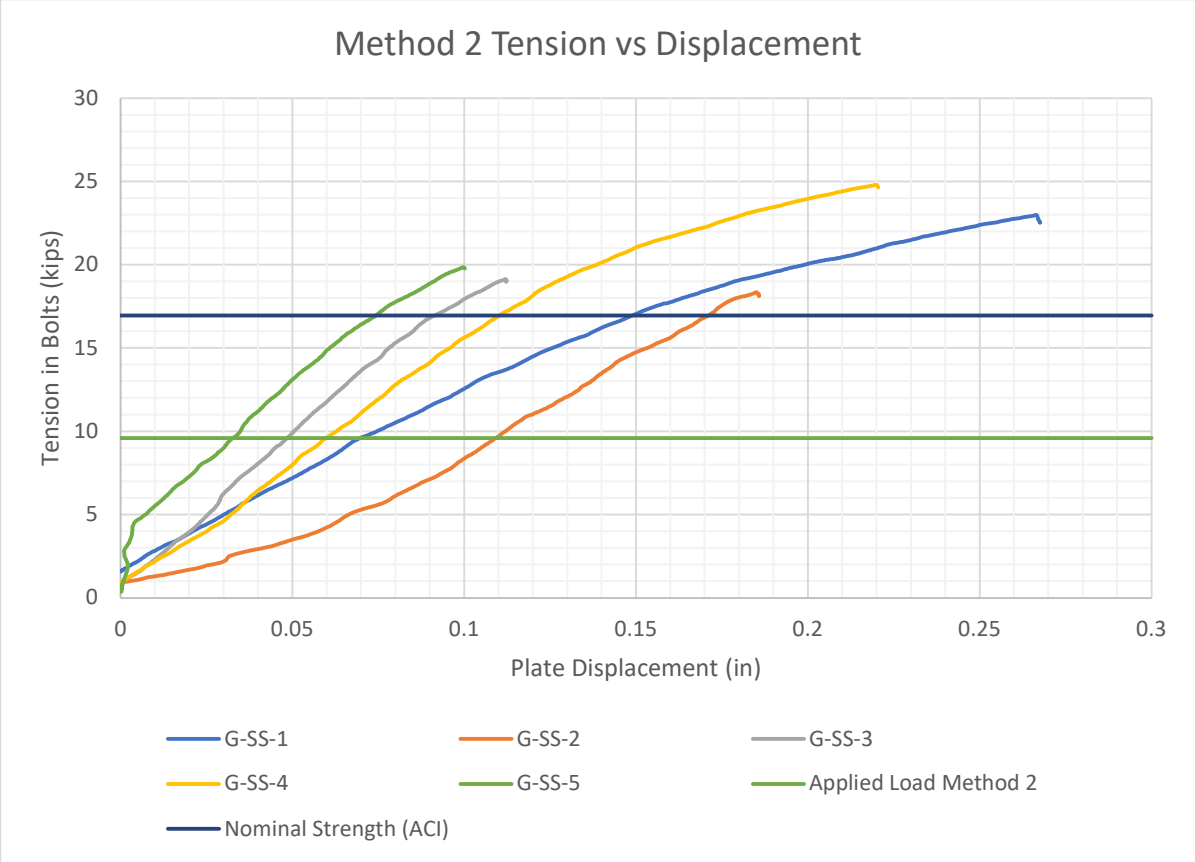

Figure A-44: Relation between tension in bolts using method 2 and displacement for G-SS

Figure A-45 - Figure A-51 depict the observation of the failure modes in the screw anchor and concrete sidewalk. There were no visible bending in any of the screw anchors. Damages were detected on the lower threads, which are normal and part of the installation process. In the case of specimens G-SS-1, G-SS-2, and G-SS-5, no visible cracks were found on the concrete surface. However, minor cracks were identified on the concrete surface within the plate area for specimens G-SS-3 and G-SS-4. All tested specimens exhibited damage around the bolt hole, indicating the stress concentration in that area. Interestingly, the base plate and railing utilized for specimen G-SS-2 were reused for specimen G-SS-4. During testing, the railing used for specimen G-SS-4 exhibited yielding, indicating that it had reached its limit and undergone permanent deformation.

Figure A-45: G-SS-1 specimen screw after loading

Figure A-46: G-SS-1 specimen concrete after loading

Figure A-47: G-SS-2 specimen south screw after loading

Figure A-48: G-SS-2 specimen north screw after loading

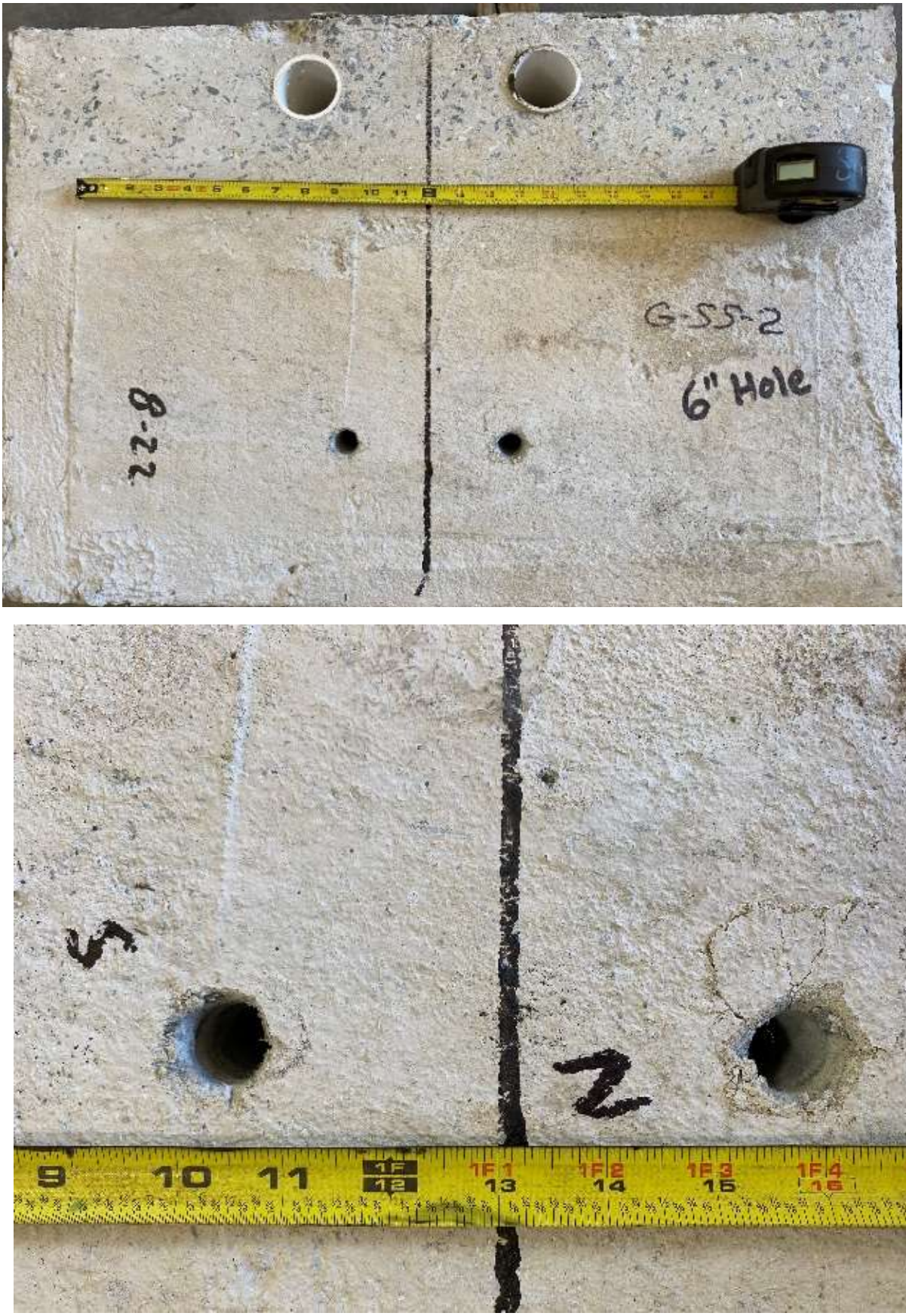

Figure A-49: G-SS-2 specimen concrete after loading

Figure A-50: G-SS-3 specimen north screw after loading

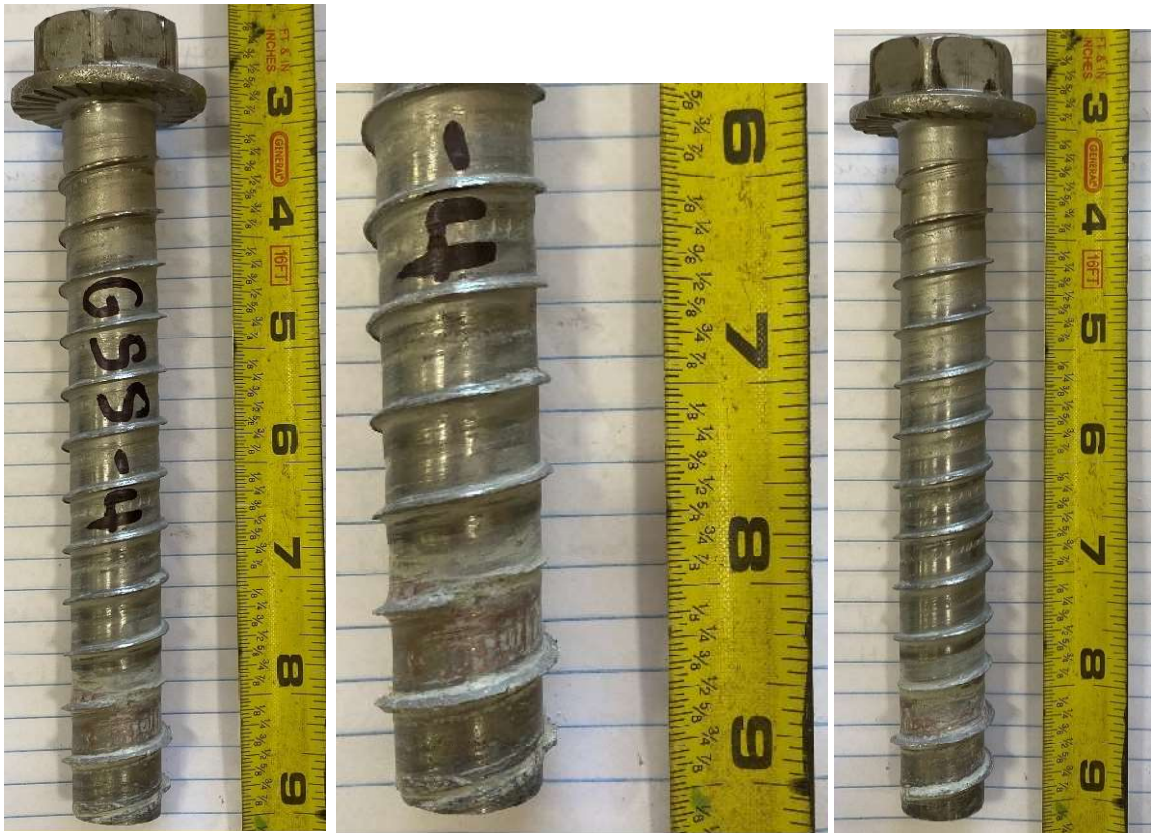

Figure A-51: G-SS-4 specimen south screw after loading

A2.2 – CYCLIC LOADING OF GUIDE RAIL ON SIDEWALK SPECIMEN

Four specimens were used to evaluate the impact of cyclic loading on screw anchor breakout resistance. The guiderail was loaded cyclically from 100 to 300 lbs for 1000 cycles prior to loading it to failure. Table A-6 provides the summary of the test results, which are also plotted in Figure A-52 - Figure A-55. Similar to the pedestrian railing, the cyclic load did not impact the screw anchor breakout resistance. Using methods 1 and 2, the average breakout resistance is 15.203 Kips and 17.103 Kips, respectively. All the specimens were able to resist more than their predicted yield load and their design anchor failure load.

Figure A-56 - Figure A-67 illustrate the failure modes in the screw anchor and sidewalk specimens. All screw anchors exhibited minor bending at the neck. Additionally, normal installation damage was also observed on the lower threads of all anchors. Notably, the north bolt of specimen G-SSc-2 showed the most significant damage to its threads. However, no major cracks were observed on any of the specimens. Only specimen G-SSc-1 displayed a minor crack within the plate area. It is important to note that the crack at the PVC location in specimen G-SSc-2 was already present before testing, indicating pre-existing damage.

Table A-6: Summary of results for cyclic loading of guiderail on sidewalk

Specimen's code	**G-SSc-1**	**G-SSc-2**	**G-SSc-3**	**G-SSc-4**
Max Lateral Load (Kip)	1.453	1.318	1.341	1.358
Displacement (in)	0.076	0.084	0.045	0.055
Tilt (^{o}deg)	0.792	1.457	0.968	0.614
Tension in bolts (method 1) (Kip)	23.258	21.088	21.464	21.729
Tension in bolts (method 2) (Kip)	26.166	23.724	24.147	24.225
Nominal Strength (ACI) (Kip)	16.95			
Applied Load (Method 1) (Kip)	8.53			
Applied Load (Method 2) (Kip)	9.59			

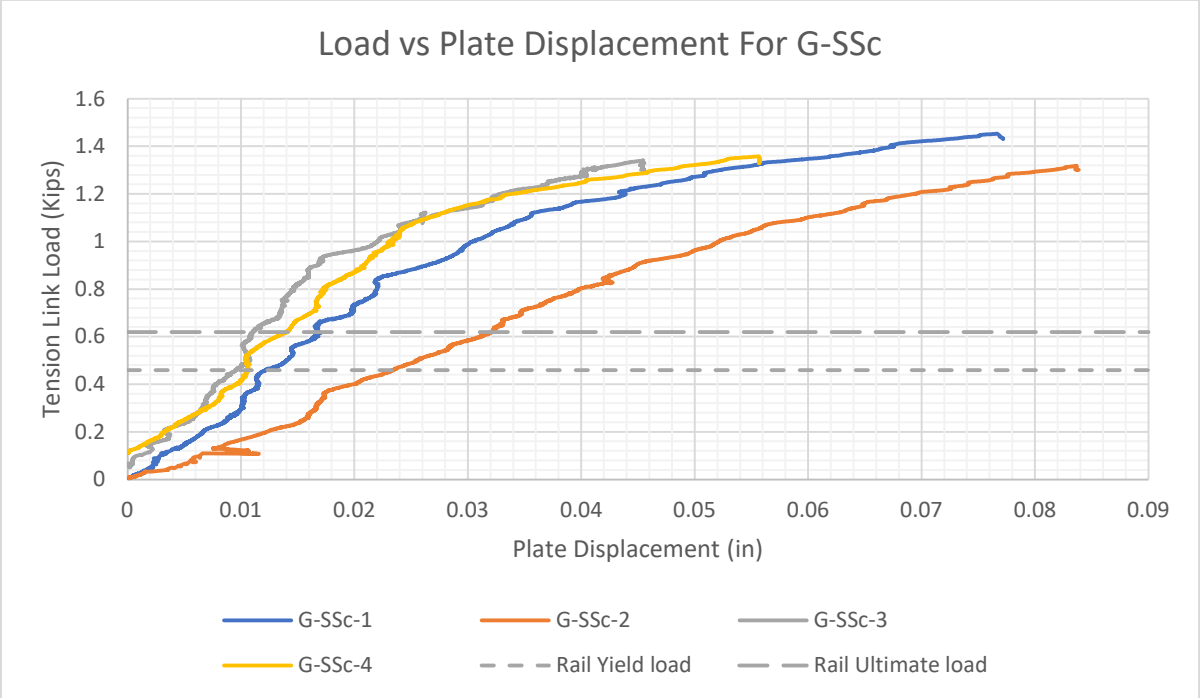

Figure A-52: Relation between load and displacement for G-SSc

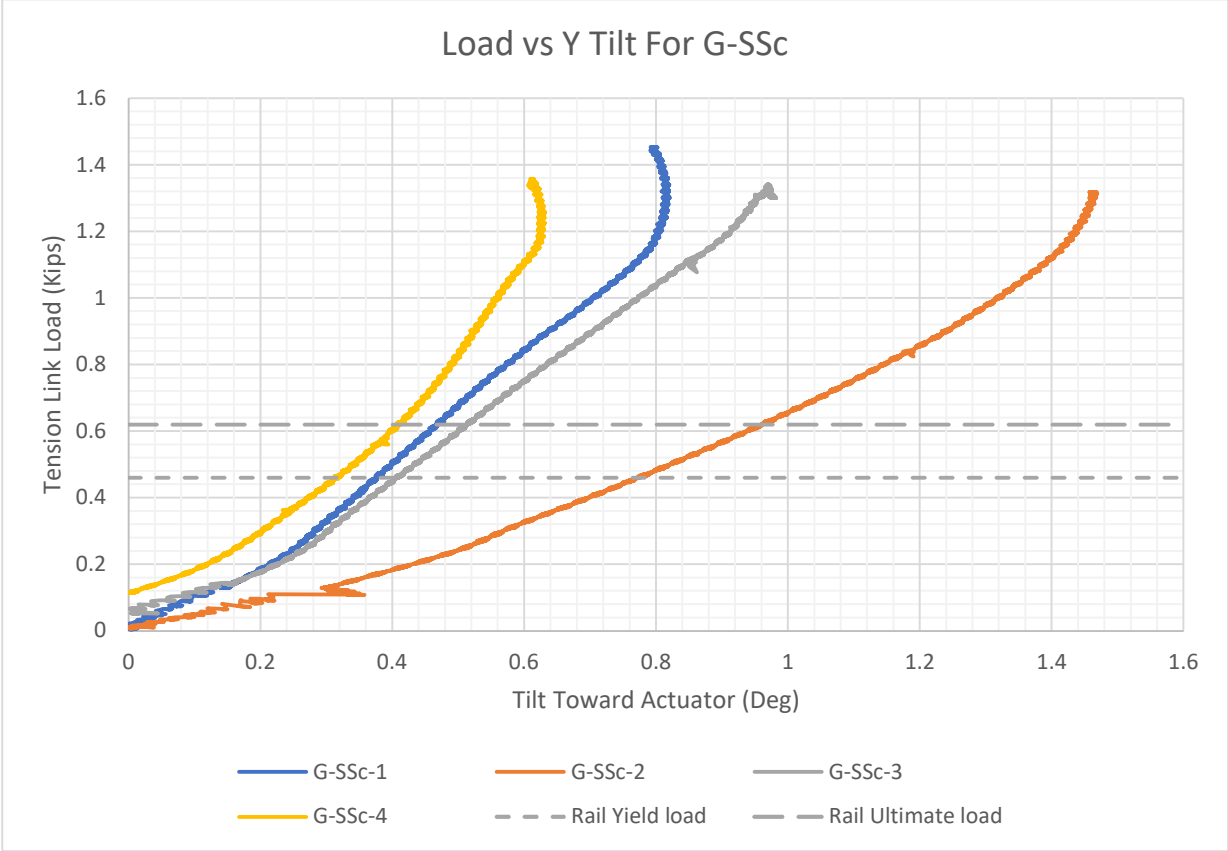

Figure A-53: Relation between load and y-axis tilt for G-SSc

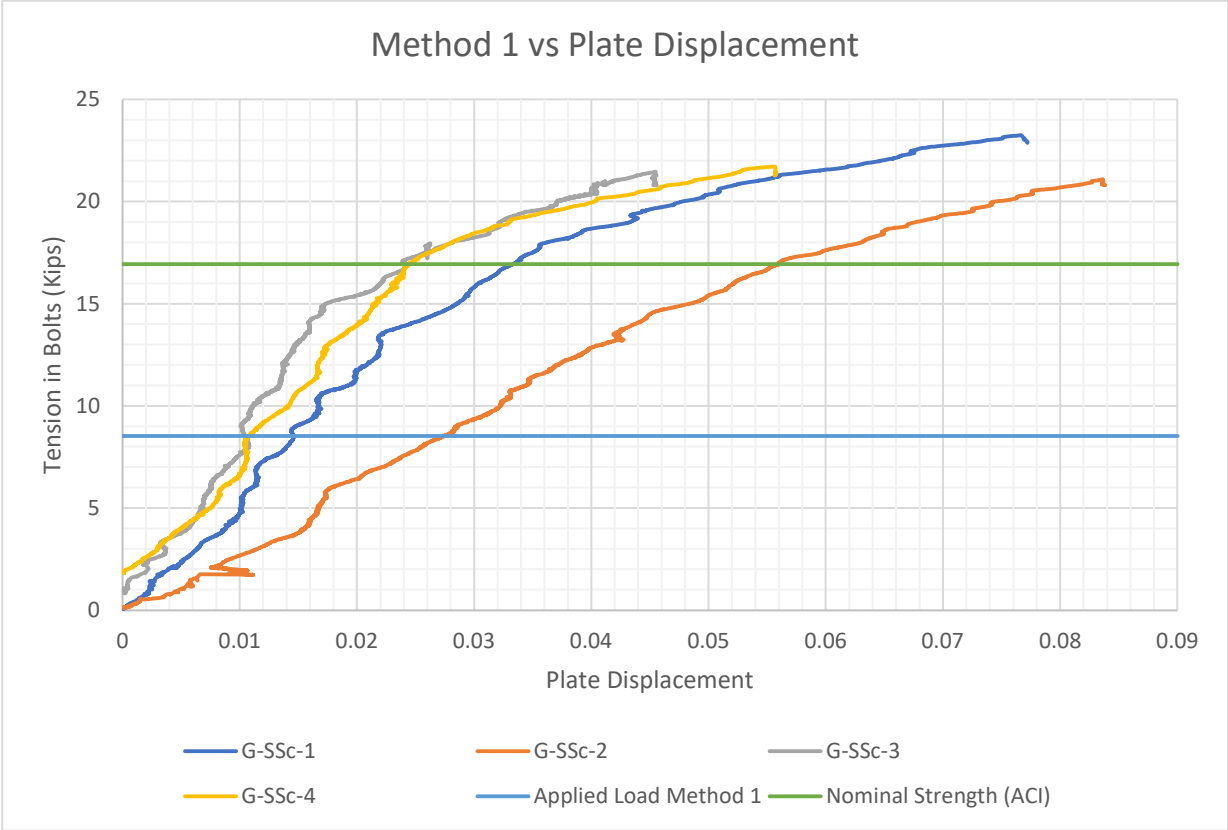

Figure A-54: Relation between tension in bolts using method 1 and MTS displacement for G-SSc

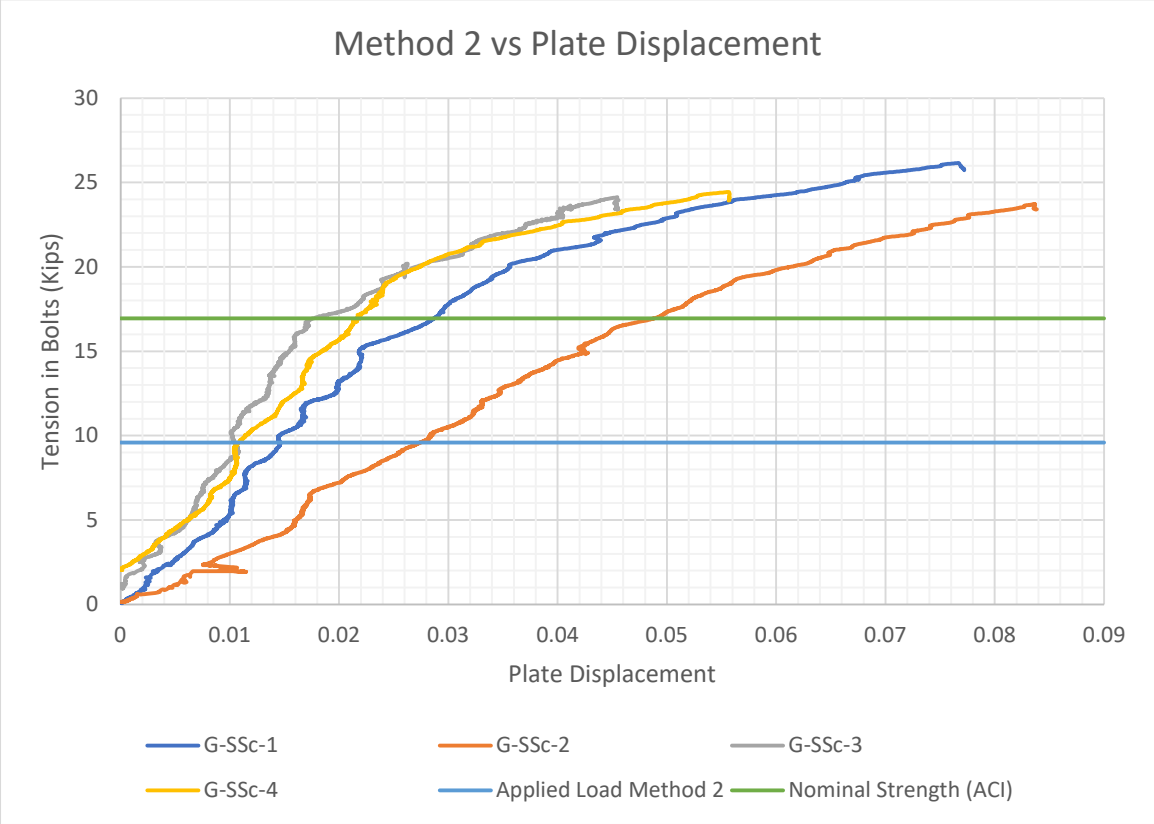

Figure A-55: Relation between tension in bolts using method 2 and MTS displacement for G-SSc

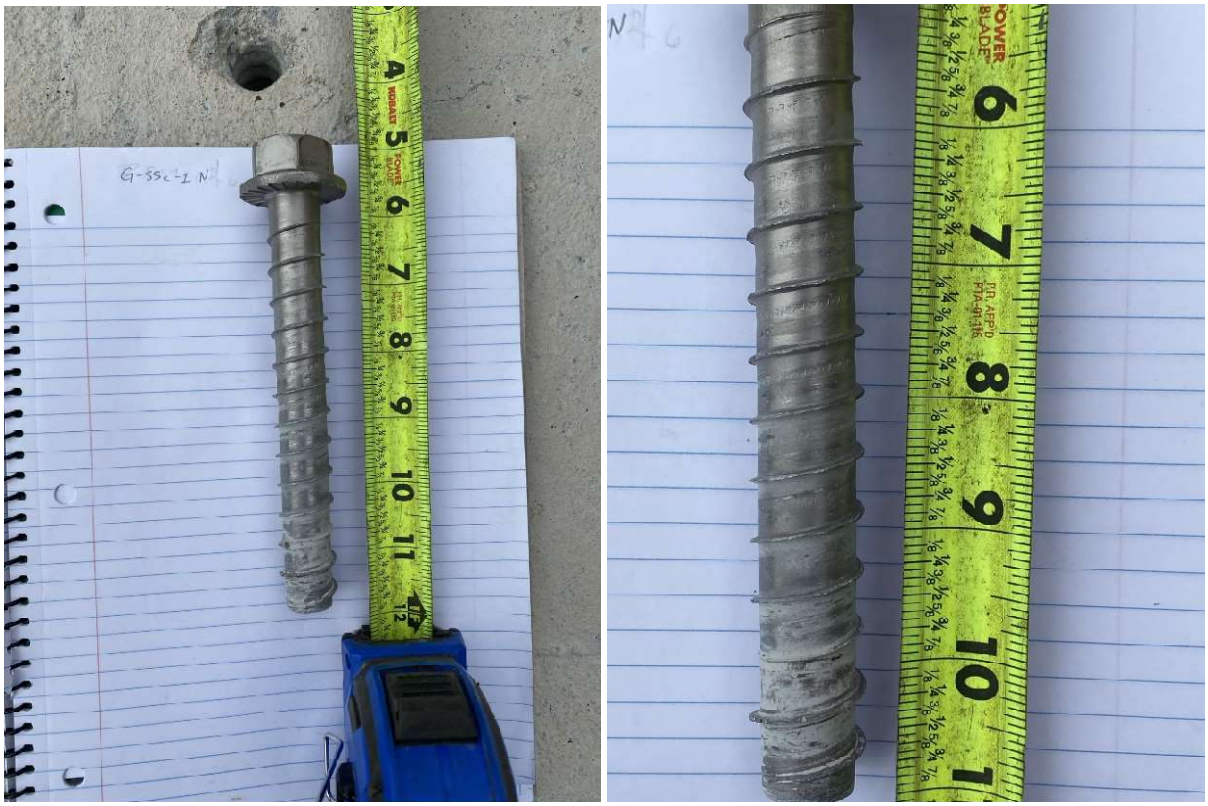

Figure A-56: G-SSc-1 specimen north screw after cyclic loading

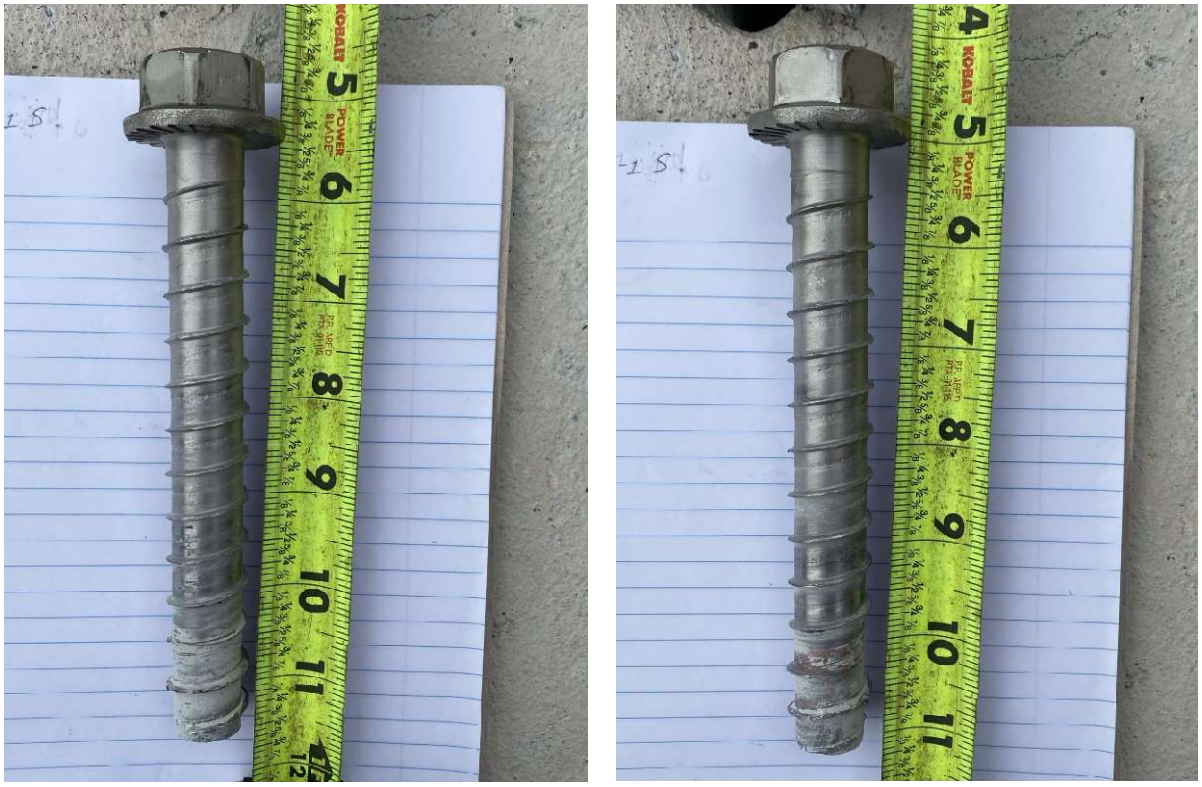

Figure A-57: G-SSc-1 specimen south screw after cyclic loading

Figure A-58: G-SSc-1 specimen concrete after cyclic loading

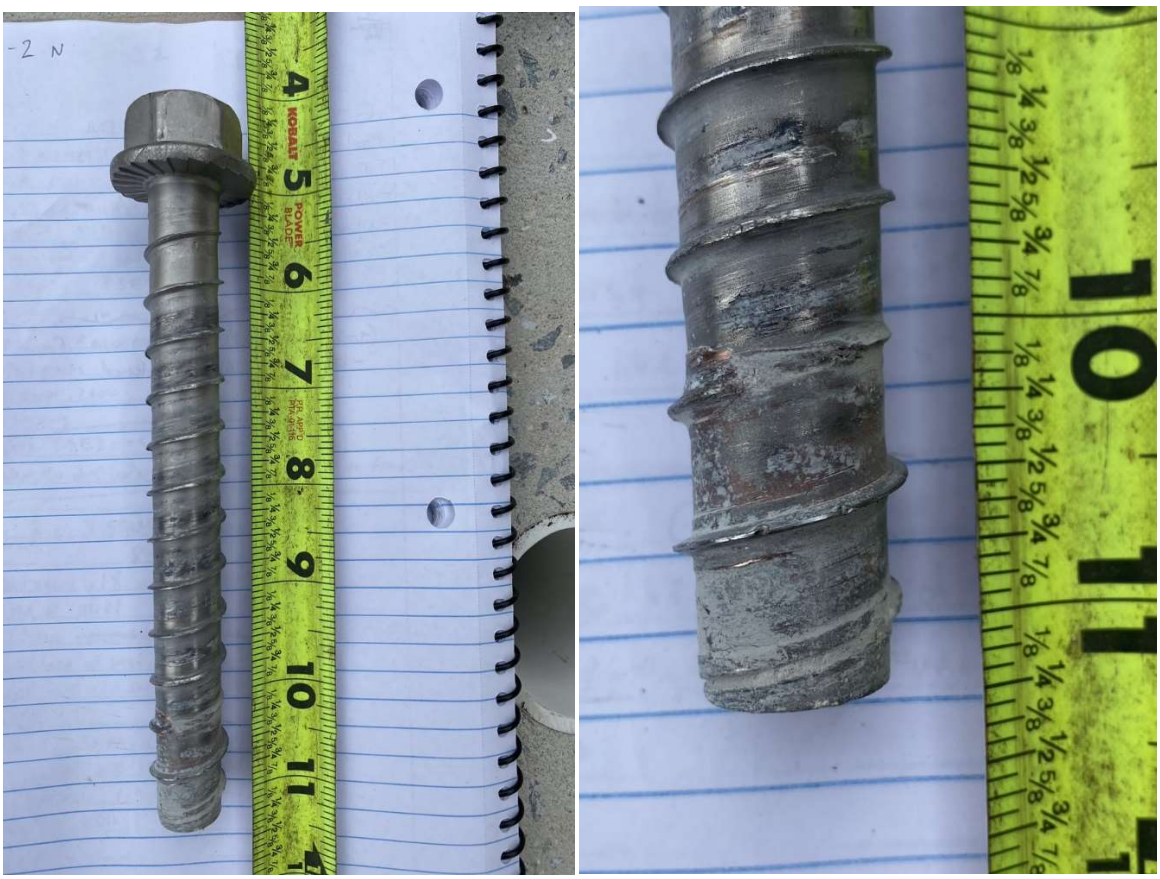

Figure A-59: G-SSc-2 specimen north screw after cyclic loading

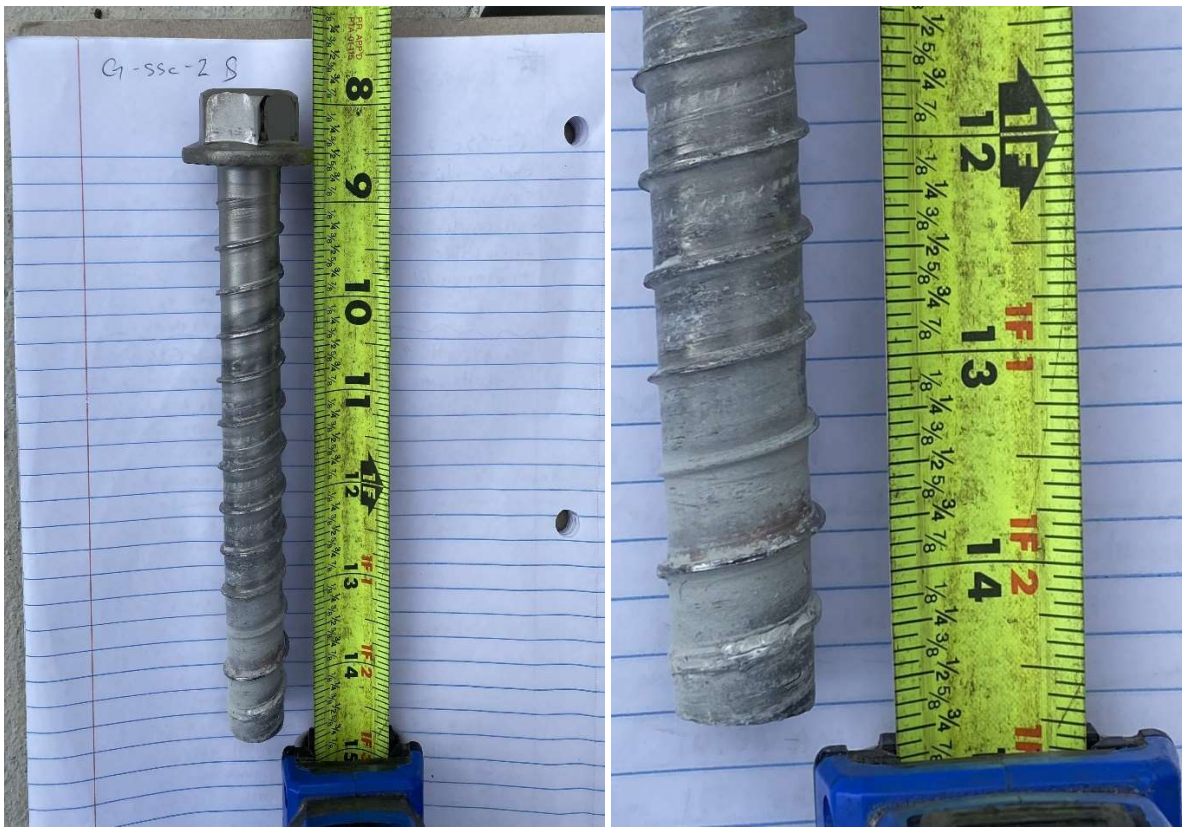

Figure A-60: G-SSc-2 specimen south screw after cyclic loading

Figure A-61: G-SSc-2 specimen concrete after cyclic loading

Figure A-62: G-SSc-3 specimen north screw after cyclic loading

Figure A-63: G-SSc-3 specimen south screw after cyclic loading

Figure A-64: G-SSc-3 specimen concrete after cyclic loading

Figure A-65: G-SSc-4 specimen north screw after cyclic loading

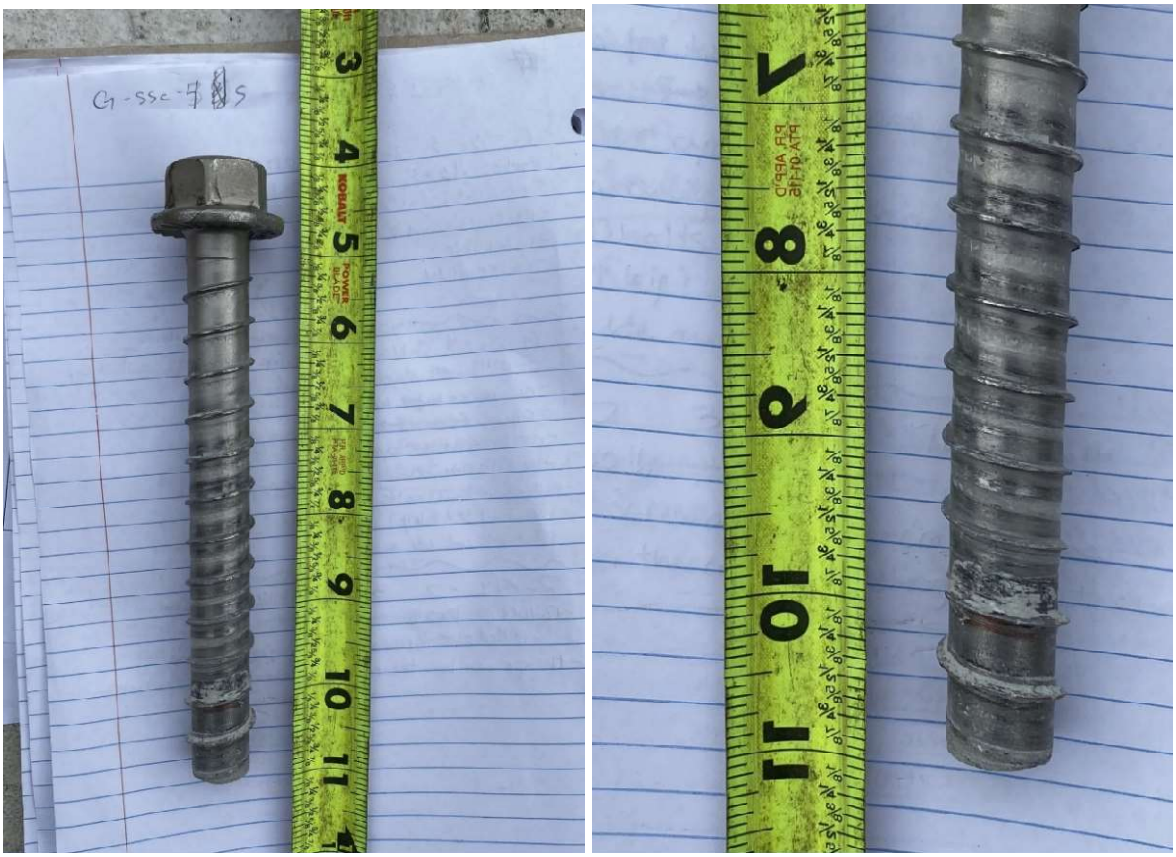

Figure A-66: G-SSc-4 specimen south screw after cyclic loading

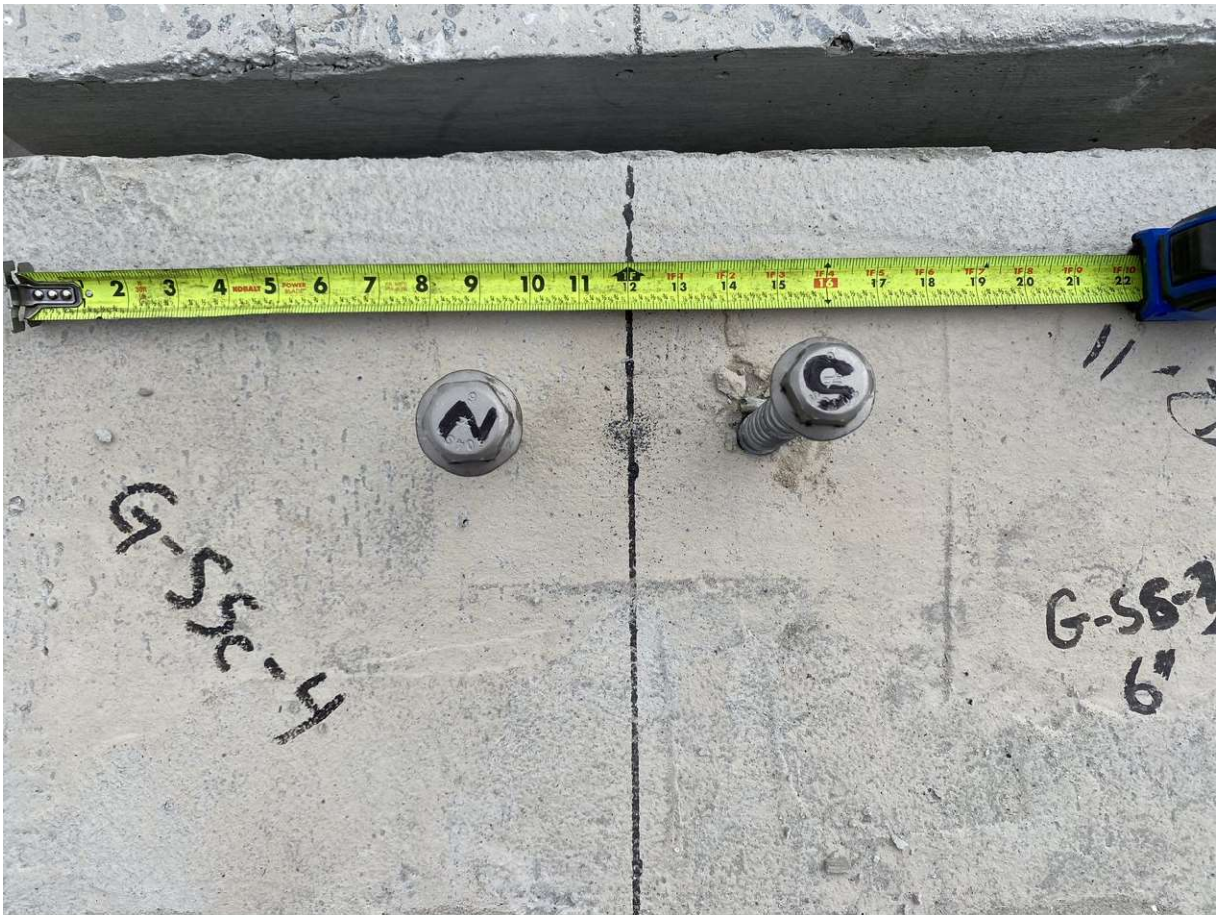

Figure A-67: G-SSc-4 specimen concrete after cyclic loading

A2.3 – MONOTONIC LOADING OF GUIDE RAIL ON GRAVITY WALL SPECIMEN

Six guiderail attached to gravity wall specimens were monotonic loaded to determine the anchor breakout resistance. Table A-7 provides a summary of the test results and the results are also plotted in Figure A-68 - Figure A-74. Additionally, the lateral load was also plotted against MTS displacement as the plate displacement provide odd trend to the data. Using methods 1 and 2, the average calculated tension in bolts is 10.884 Kips and 12.244 Kips, respectively. All the specimens were able to reach more than their predicted rail yield load and their design anchor failure load.

The failure modes that were observed are documented in Figure A-75 - Figure A-85. In the case of specimen G-G-1, both screw anchors displayed a minor bend and exhibited damage to the lower threads. The crack pattern on the gravity wall observed consisted of a shear crack on the north side and a tension crack on the south side, resulting in concrete crushing. The depth of the crack corresponded to the depth of the screw anchor.

For specimen G-G-2, the north screw anchor did not exhibit any bending and showed more damage to the lower threads. Conversely, the south screw anchor displayed a minor bend with less damage to the lower threads. The crack pattern in the gravity wall observed included shear cracks on both sides, leading to concrete crushing. The depth of the cracks matched the depth of the screw anchor.

In the case of specimen G-G-3, the north screw anchor displayed a minor bend with almost no damage to the lower threads, while the south screw anchor did not exhibit any bending but showed more damage to the lower threads. The crack pattern observed consisted of a shear crack at the back and a tension crack towards the front and on one side.

For specimen G-G-4, both screw anchors did not exhibit any bending but showed minor damage to the lower threads. The crack pattern observed included two shear cracks, one at the front and one at the back.

In the case of specimen G-G-5, both screw anchors did not exhibit any bending but displayed damage to the lower threads. No visible cracks formed on the concrete surface, but minor damage was observed around the bolt holes.

For specimen G-G-6, both screw anchors did not exhibit any bending, but the north bolt showed damage to the lower threads, while the south screw anchor did not exhibit any damage to the lower threads. No visible cracks formed on the concrete surface, but minor damage was seen around the bolt holes.

Table A-7: Test results of scheme 2.2

Specimen's code	**G-G-1**	**G-G-2**	**G-G-3**	**G-G-4**	**G-G-5**	**G-G-6**
Max Lateral Load (Kip)	1.036	1.309	1.136	1.038	1.383	1.396
Displacement (in)	0.126	0.063	-0.048	-0.062	0.047	0.070
MTS Displacement (in)	5.129	4.527	5.368	4.879	6.237	6.232
Tilt (^{o}deg)	3.917	3.337	2.592	2.513	1.158	1.644
Tension in bolts (method 1) (Kip)	16.576	20.956	18.189	16.620	22.131	22.348

Table A-7, continued

Tension in bolts (method 2) (Kip)	18.648	23.575	20.462	18.698	24.898	25.142
Nominal Strength (ACI) (Kip)	10.66					
Applied Load (Method 1) (Kip)	8.53					
Applied Load (Method 2) (Kip)	9.59					

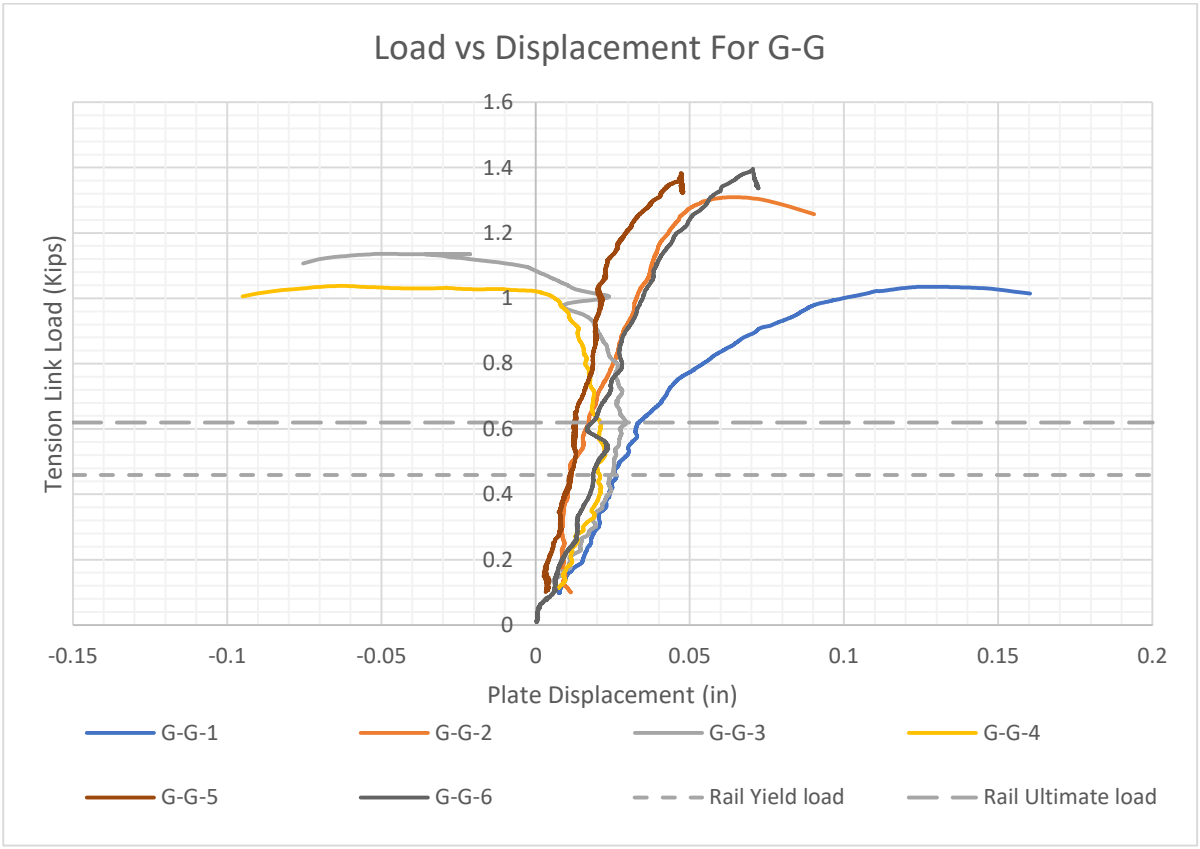

Figure A-68: Relation between load and displacement for G-G

"Note: - Specimens G-G-3and4 have faulty displacement data but still has a trend pattern."

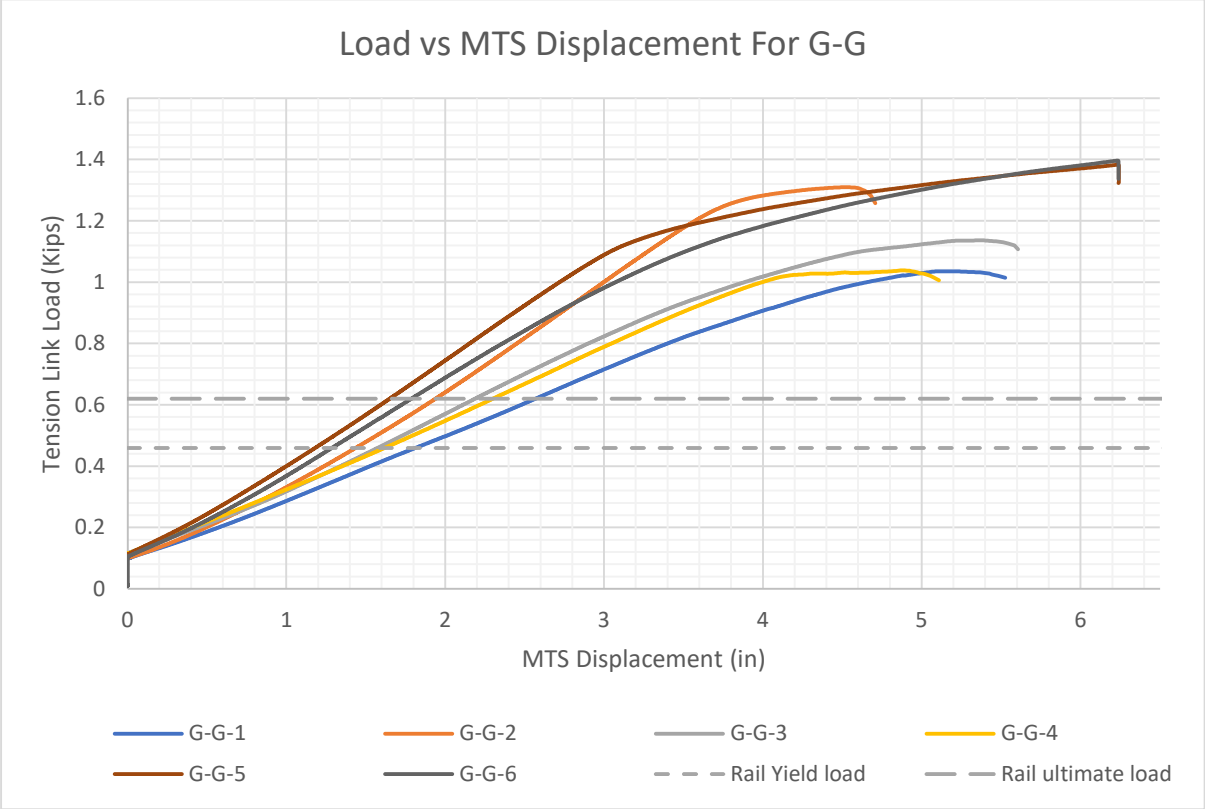

Figure A-69: Relation between load and MTS displacement for G-G

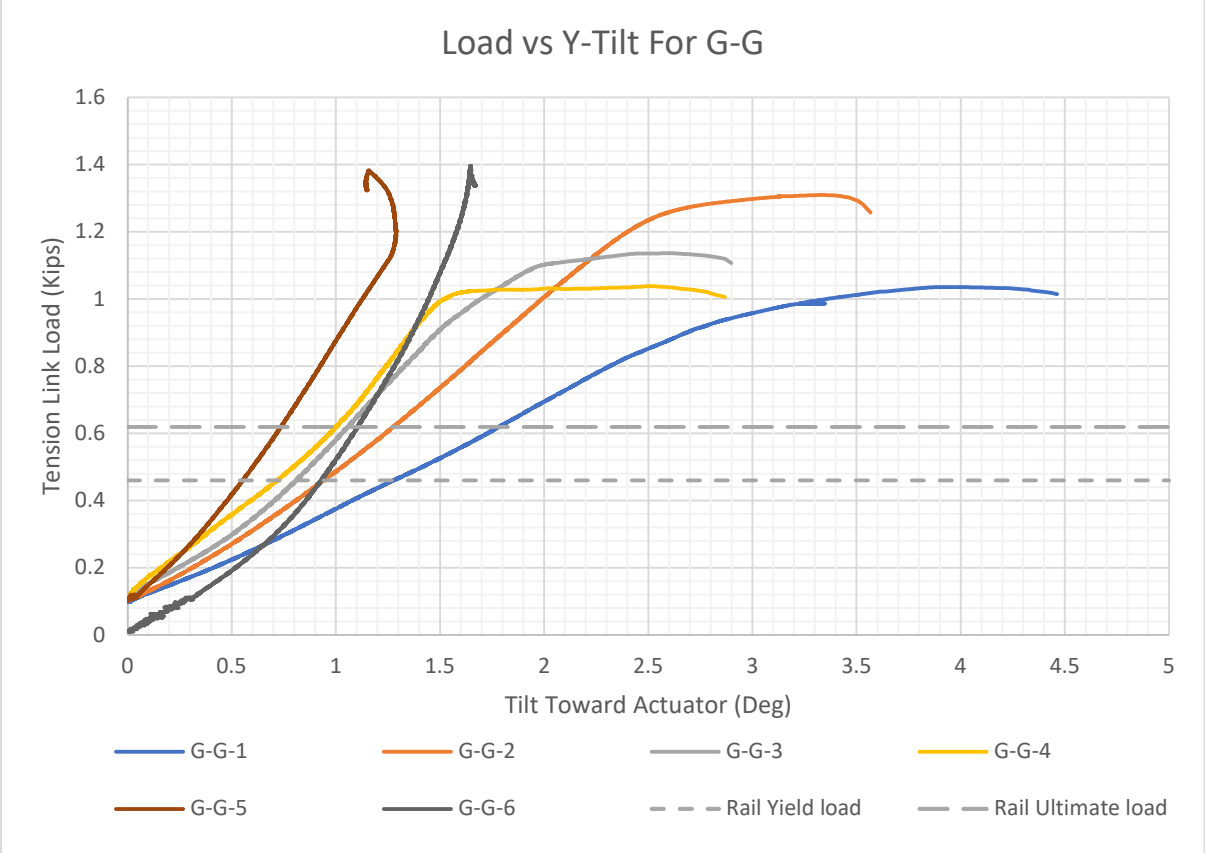

Figure A-70: Relation between load and y-axis tilt for G-G

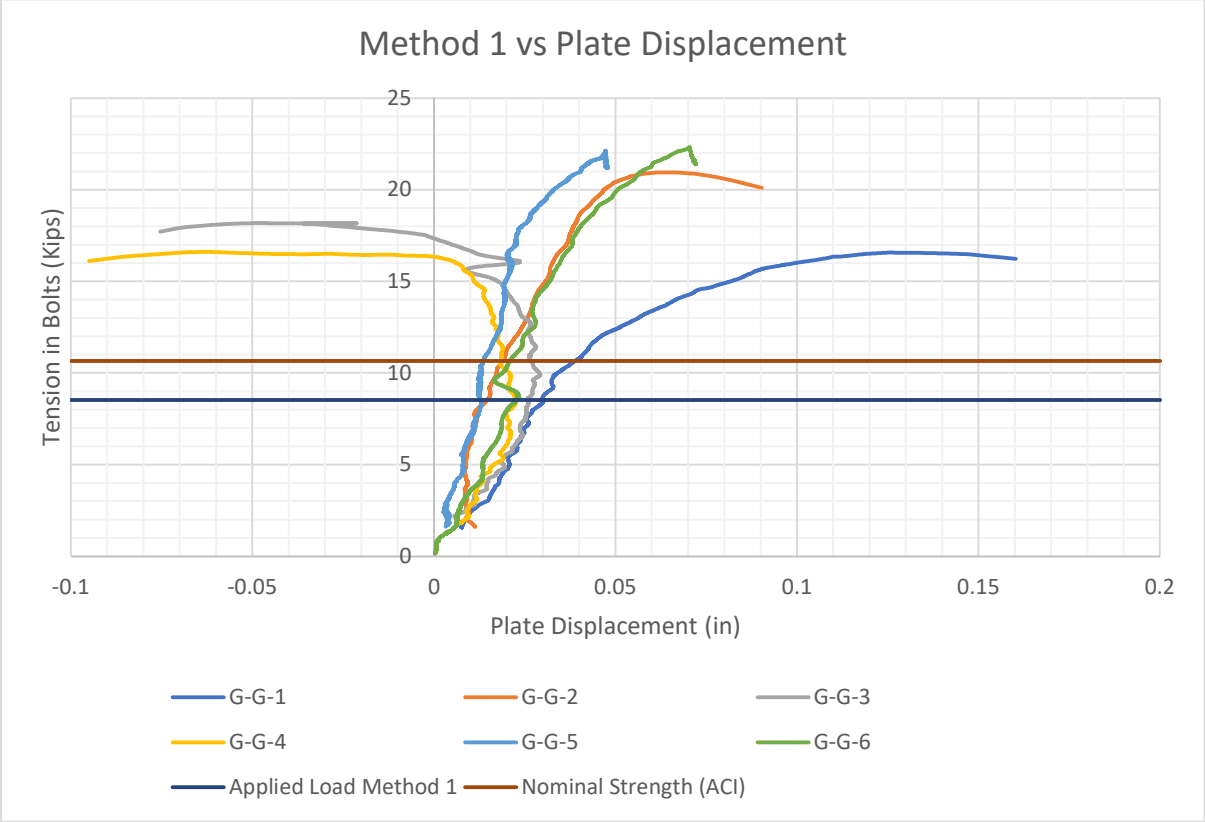

Figure A-71: Relation between tension in bolts using method 1 and displacement for G-G

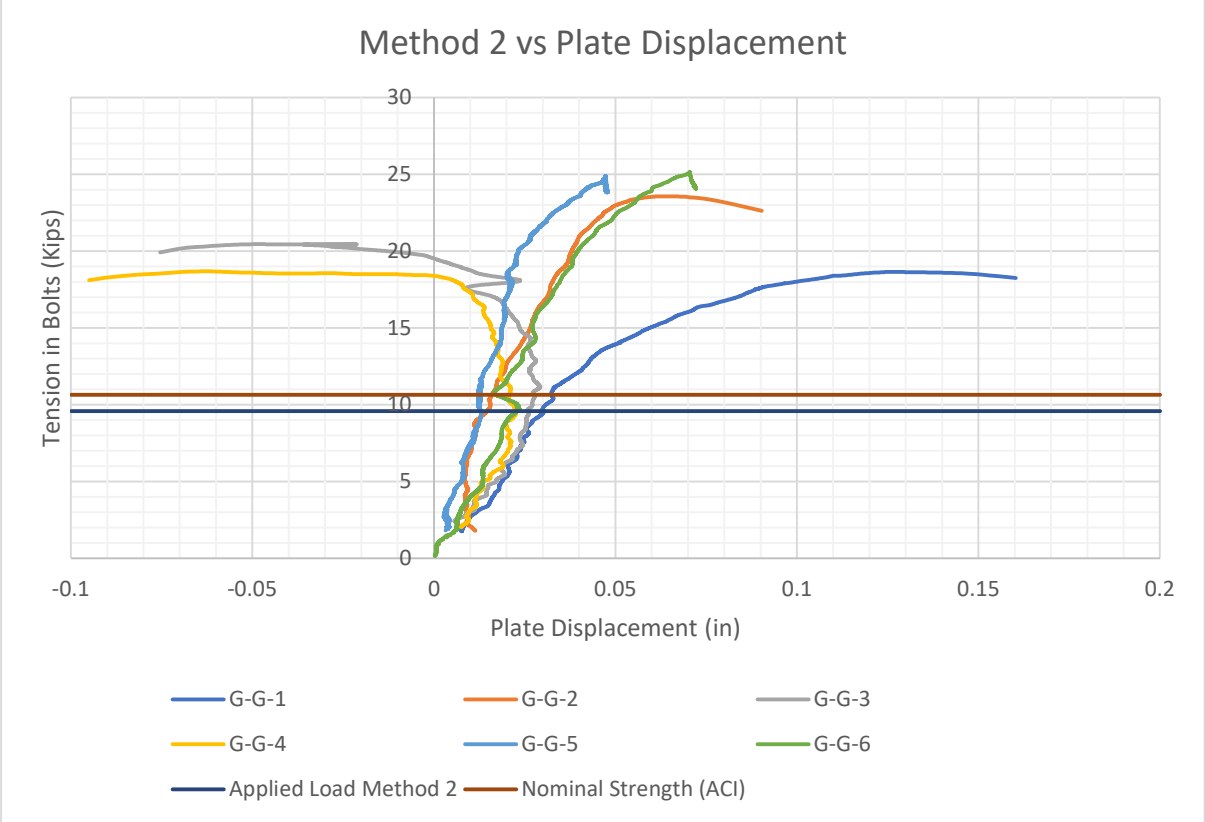

Figure A-72: Relation between tension in bolts using method 2 and displacement for G-G

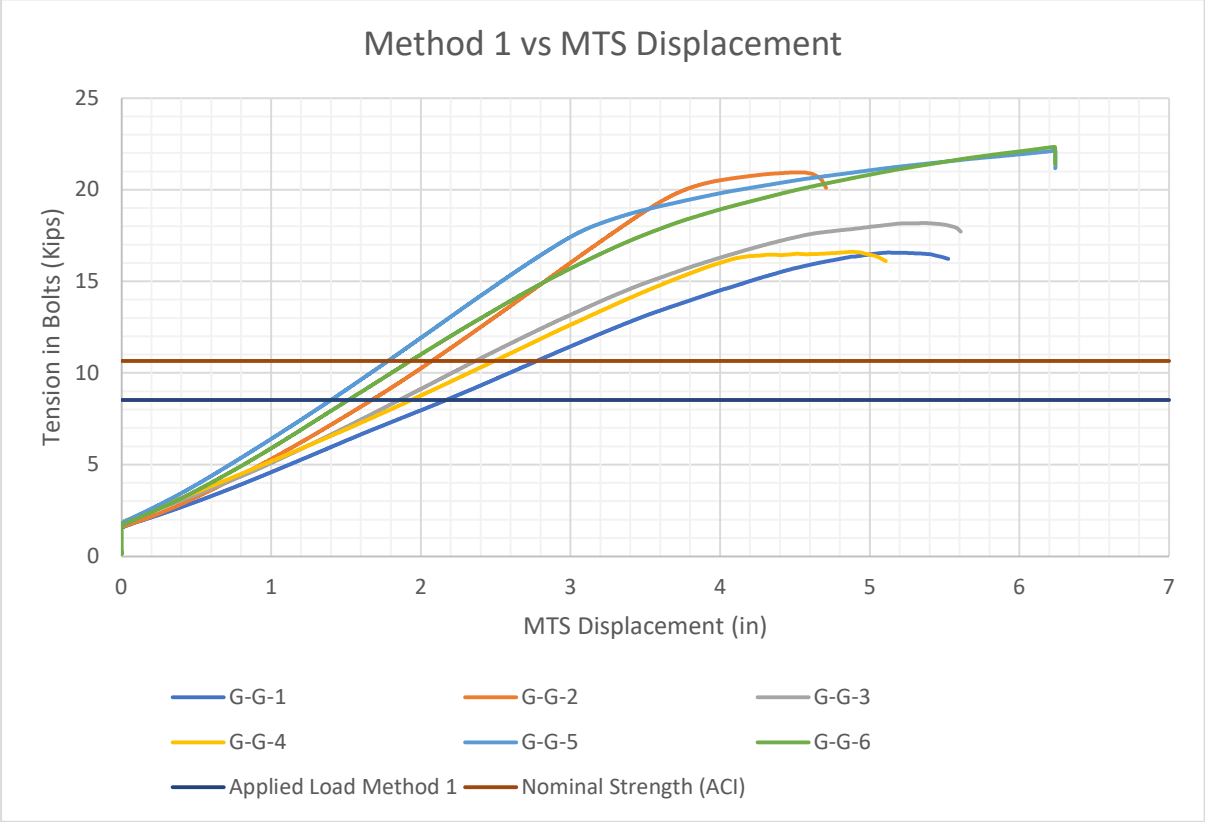

Figure A-73: Relation between tension in bolts using method 1 and MTS displacement for G-G

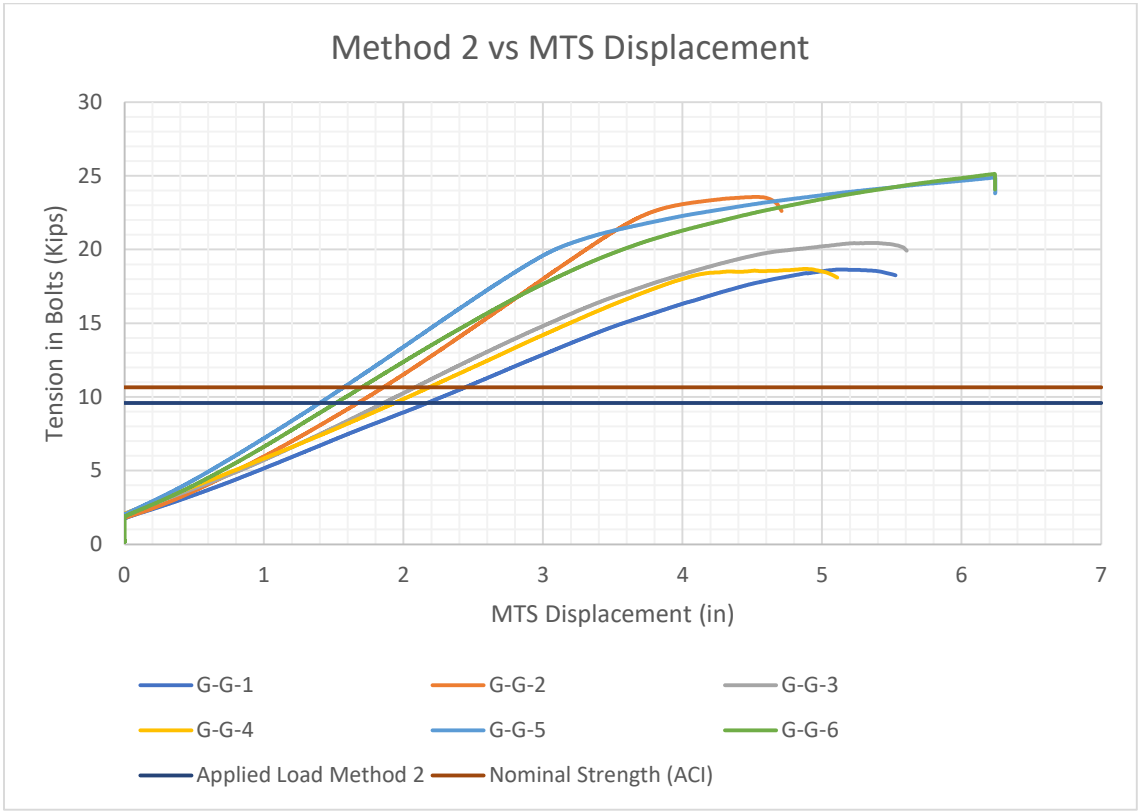

Figure A-74: Relation between tension in bolts using method 2 and MTS displacement for G-G

Figure A-75: G-G-1 specimen north screw after breakout

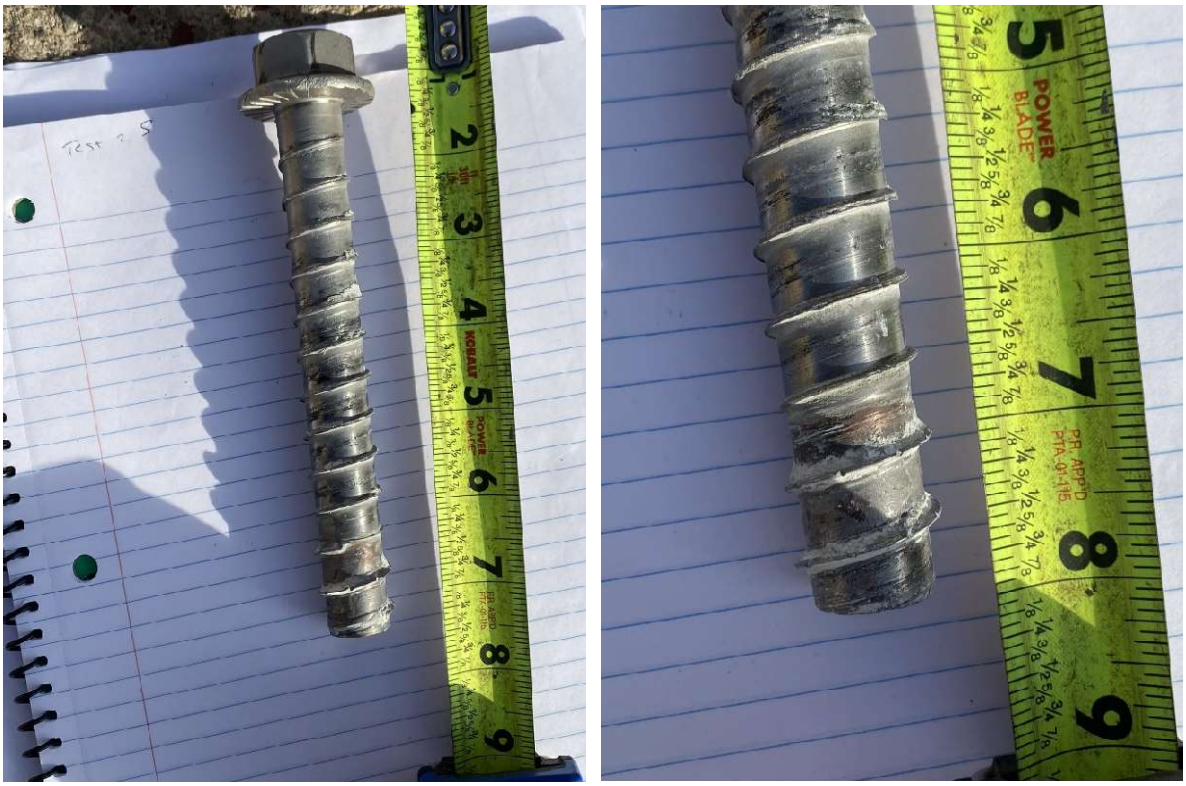

Figure A-76: G-G-1 specimen south screw after breakout

Figure A-77: G-G-1 specimen concrete after screw anchor breakout

Figure A-78: G-G-2 specimen north screw after breakout

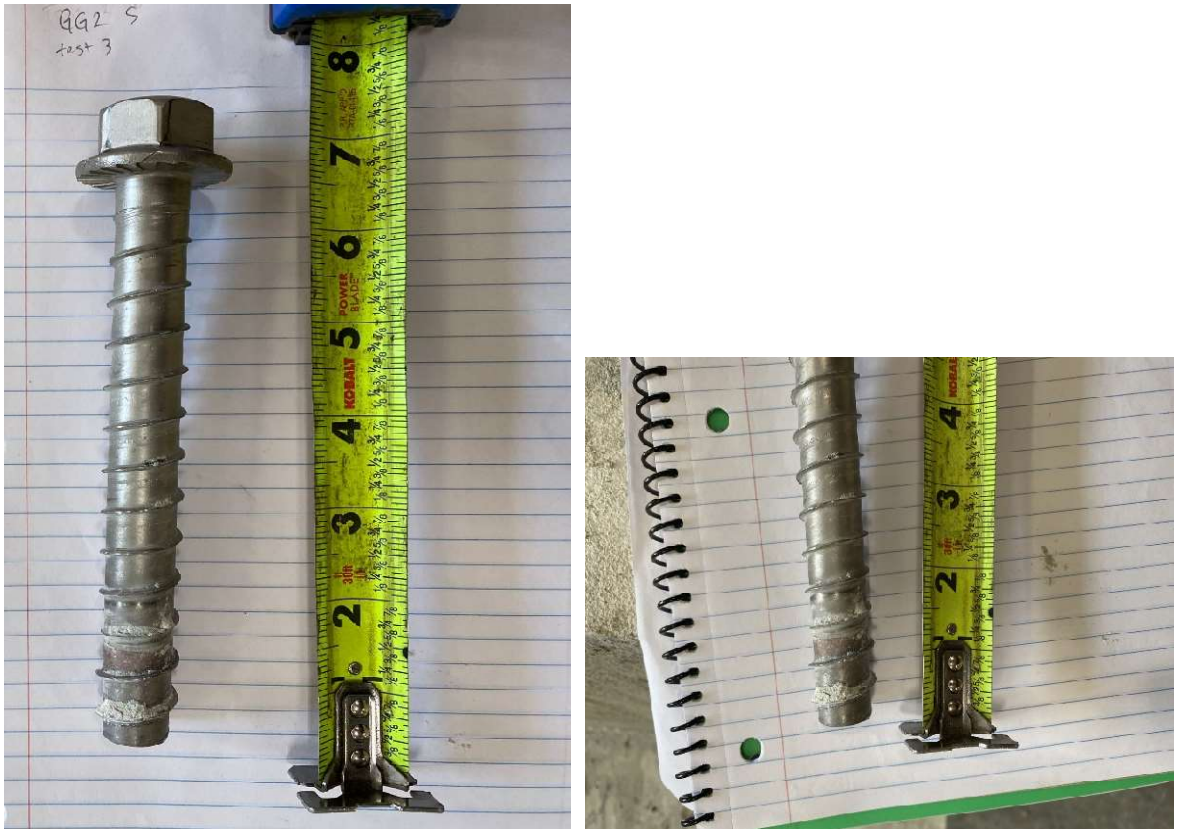

Figure A-79: G-G-2 specimen south screw after breakout


Figure A-80: G-G-2 specimen concrete after screw anchor breakout

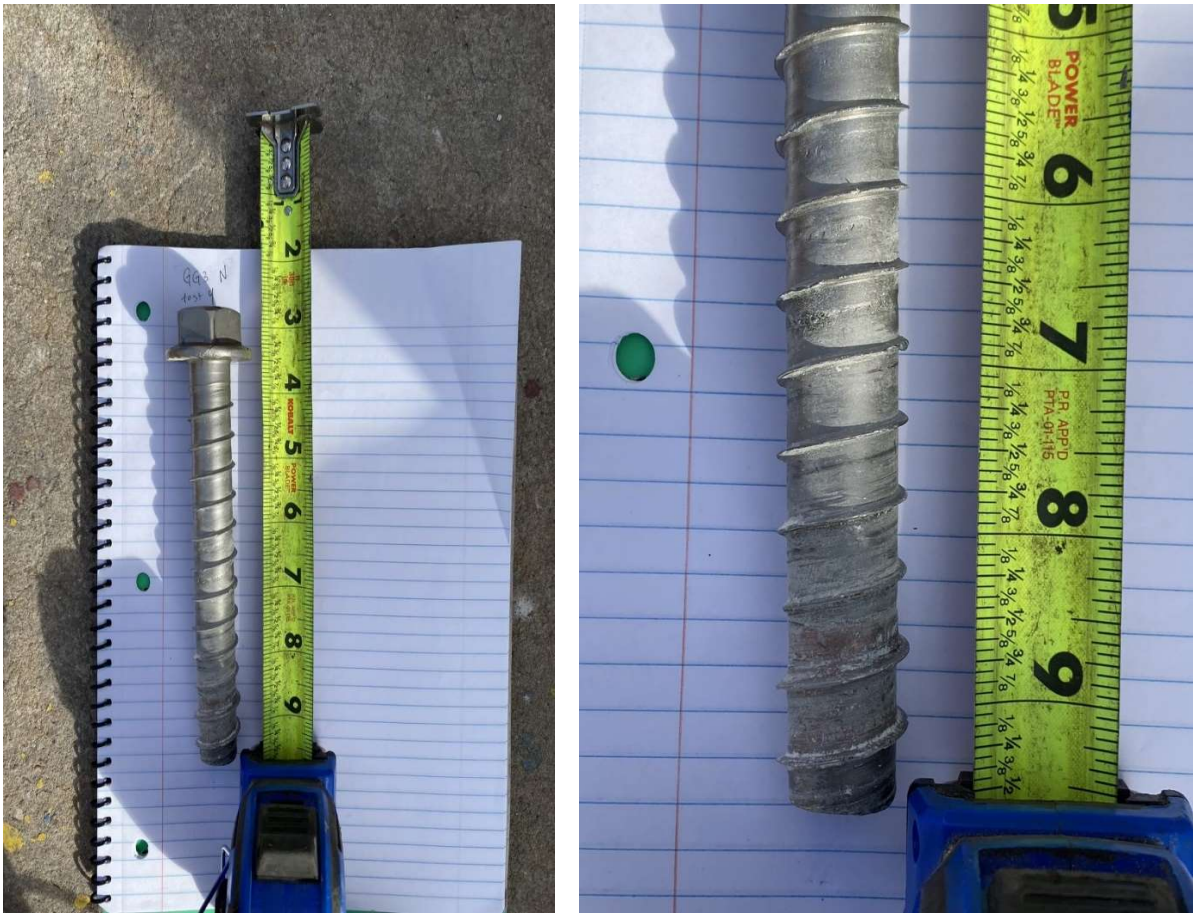

Figure A-81: G-G-3 specimen north screw after breakout

Figure A-82: G-G-3 specimen south screw after breakout

Figure A-83: G-G-3 specimen concrete after screw anchor breakout

Figure A-84: G-G-4 specimen south and north screw after breakout

Figure A-85: G-G-4 specimen concrete after screw anchor breakout

A2.4 – MONOTONIC LOADING OF GUIDE RAIL ON PARAPET WALL SPECIEMEN

Only three parapet wall specimens were used to evaluate the screw anchor breakout resistance on guiderail. Table A-8 provides the summary of the test results and plotted in Figure A-86 - Figure A-92. Using methods 1 and 2, the average calculated tension in bolts is 10.949 Kips and 12.318 Kips, respectively. All the specimens were able to reach more than their predicted rail yield load and their design anchor failure load. Due to technical issues images for G-P specimens were not found.

Table A-8: Test results of guiderail on parapet wall

Specimen's code	**G-P-1**	**G-P-2**	**G-P-3**
Max Lateral Load (Kip)	1.114	1.341	1.269
MTS Displacement (in)	3.817	6.145	6.156
Displacement (in)	-0.013	0.107	0.054
Tilt (^{o}deg)	0.569	0.820	2.065
Tension in bolts (method 1) (Kip)	17.946	21.600	20.436
Tension in bolts (method 2) (Kip)	20.190	24.300	22.991
Nominal Strength (ACI) (Kip)	10.18		
Applied Load (Method 1) (Kip)	8.53		
Applied Load (Method 2) (Kip)	9.59		

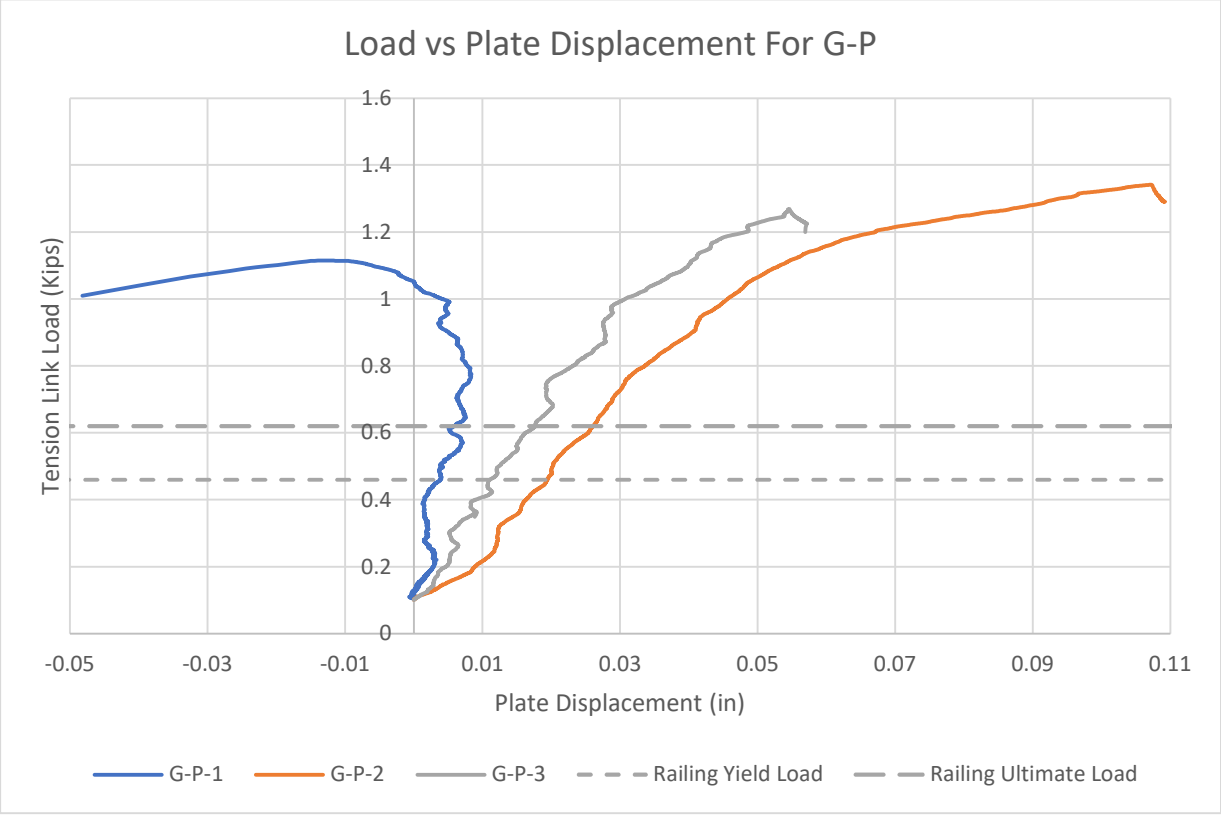

Figure A-86: Relation between load and displacement for G-P

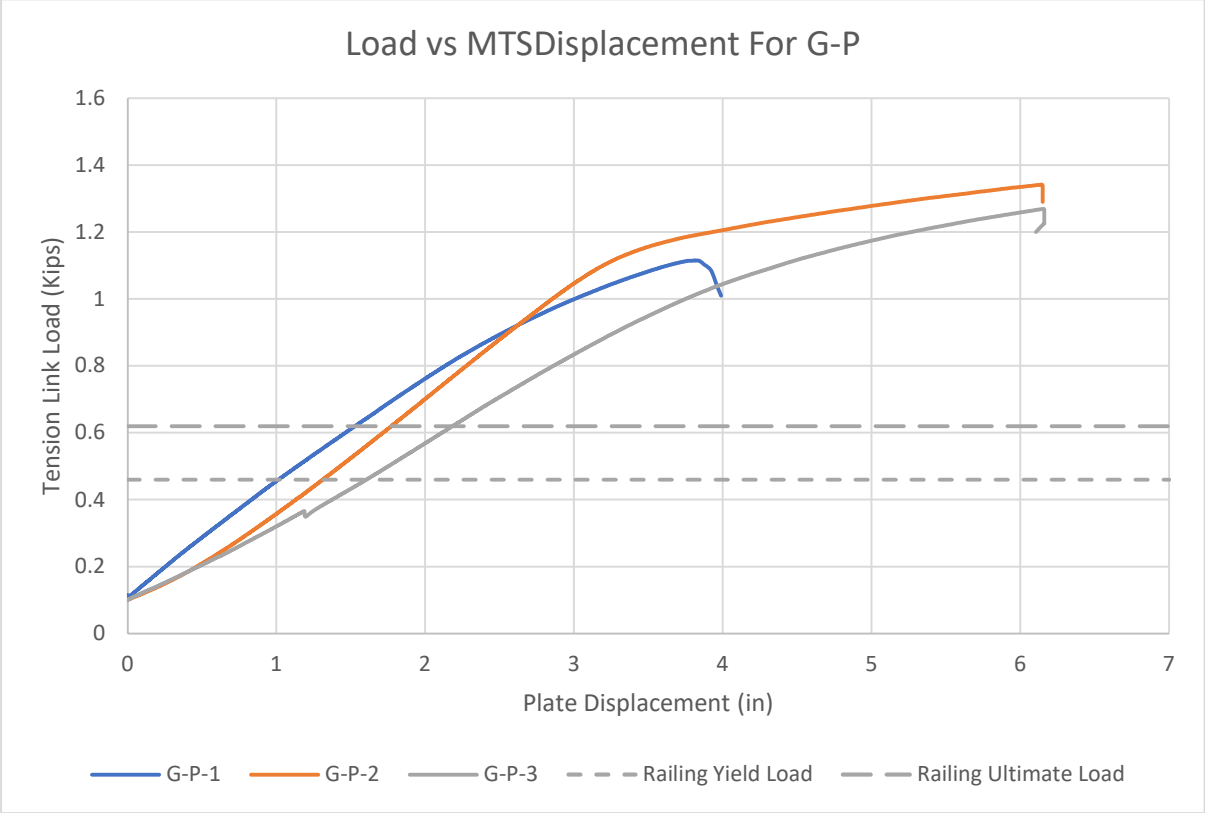

Figure A-87: Relation between load and MTS displacement for G-P

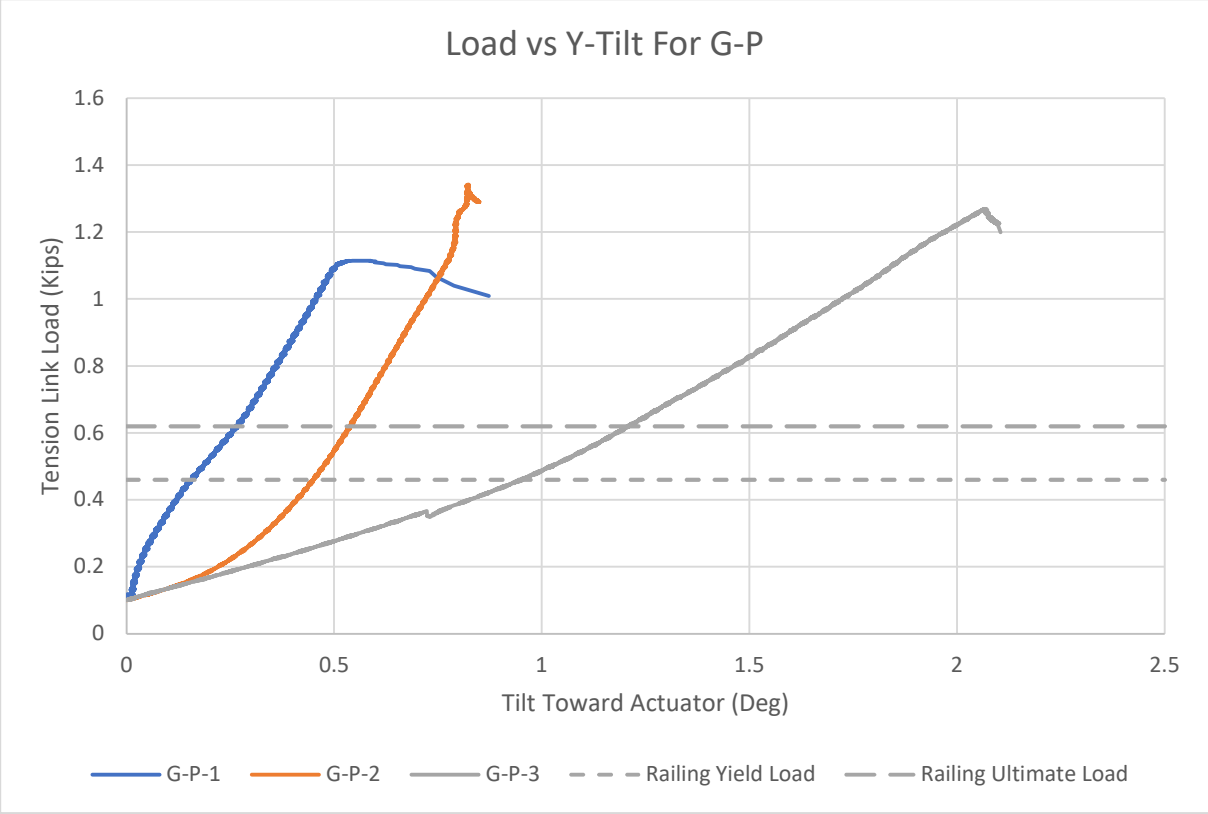

Figure A-88: Relation between load and y-axis tilt for G-P

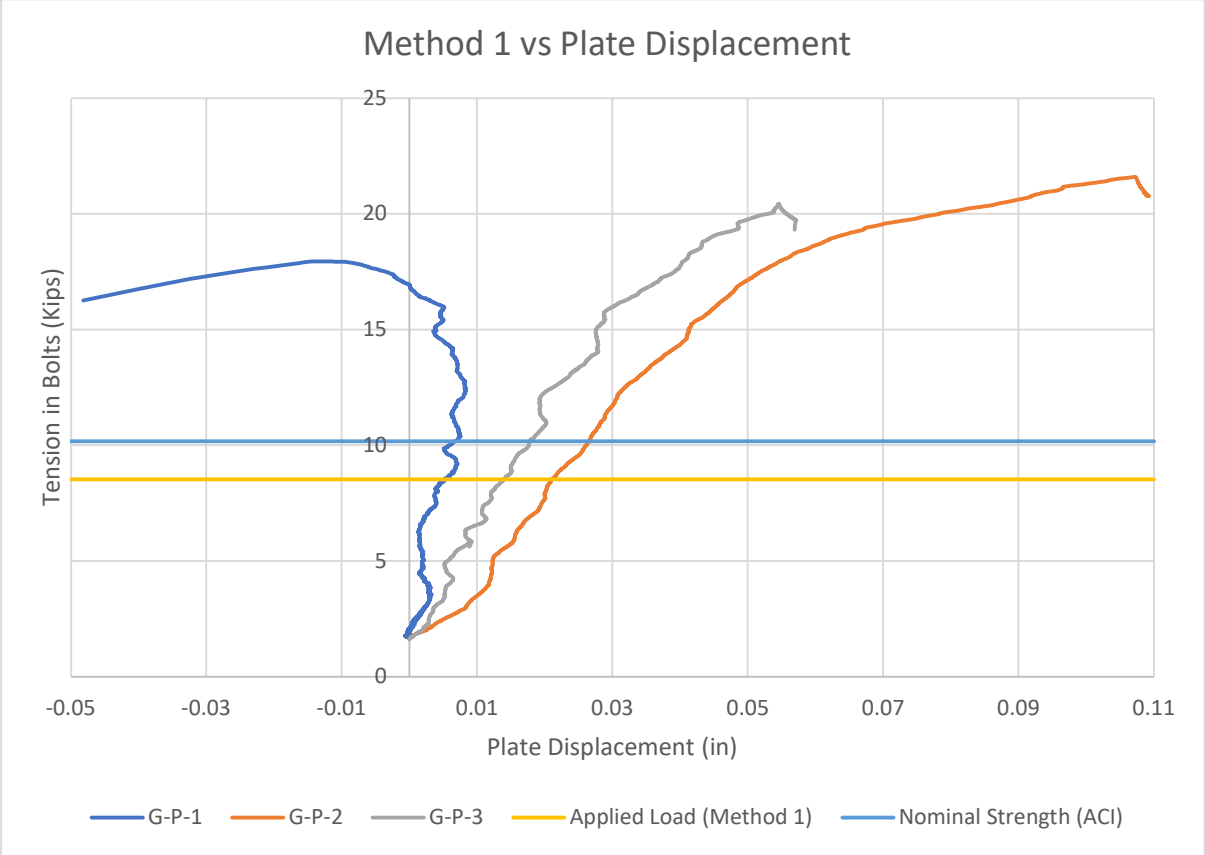

Figure A-89: Relation between tension in bolts using method 1 and displacement

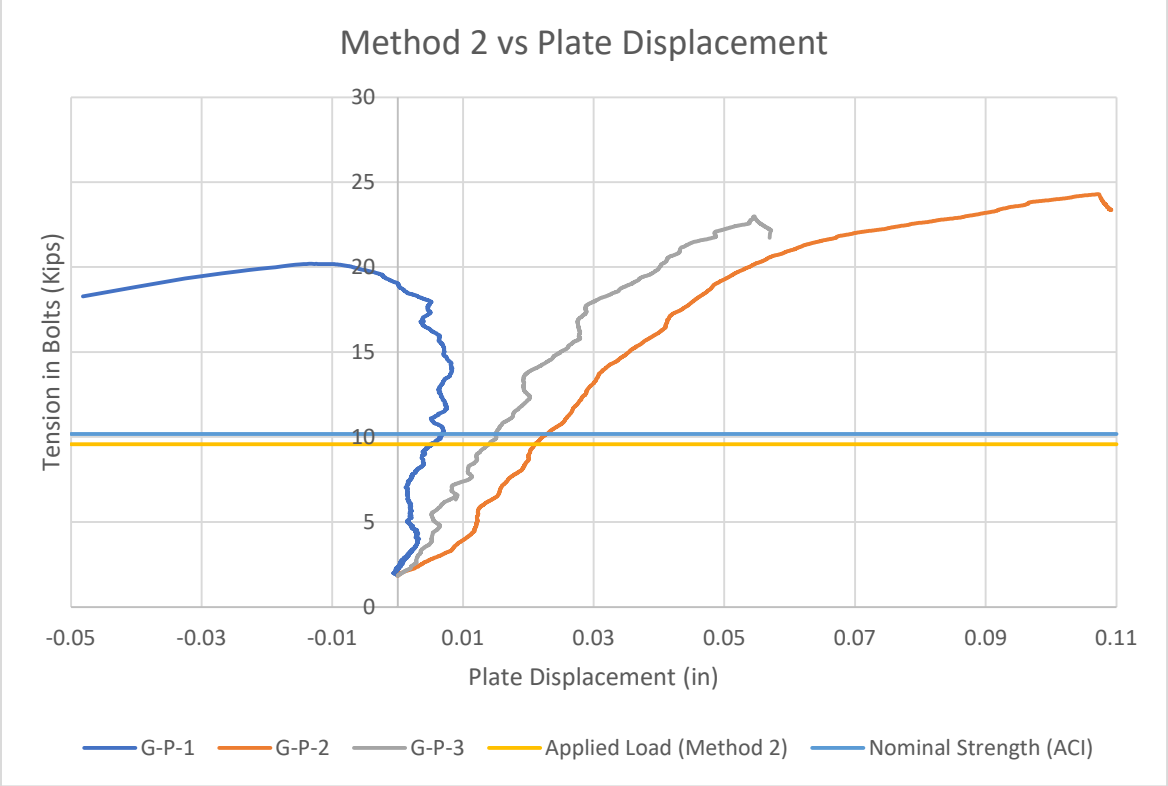

Figure A-90: Relation between tension in bolts using method 2 and displacement.

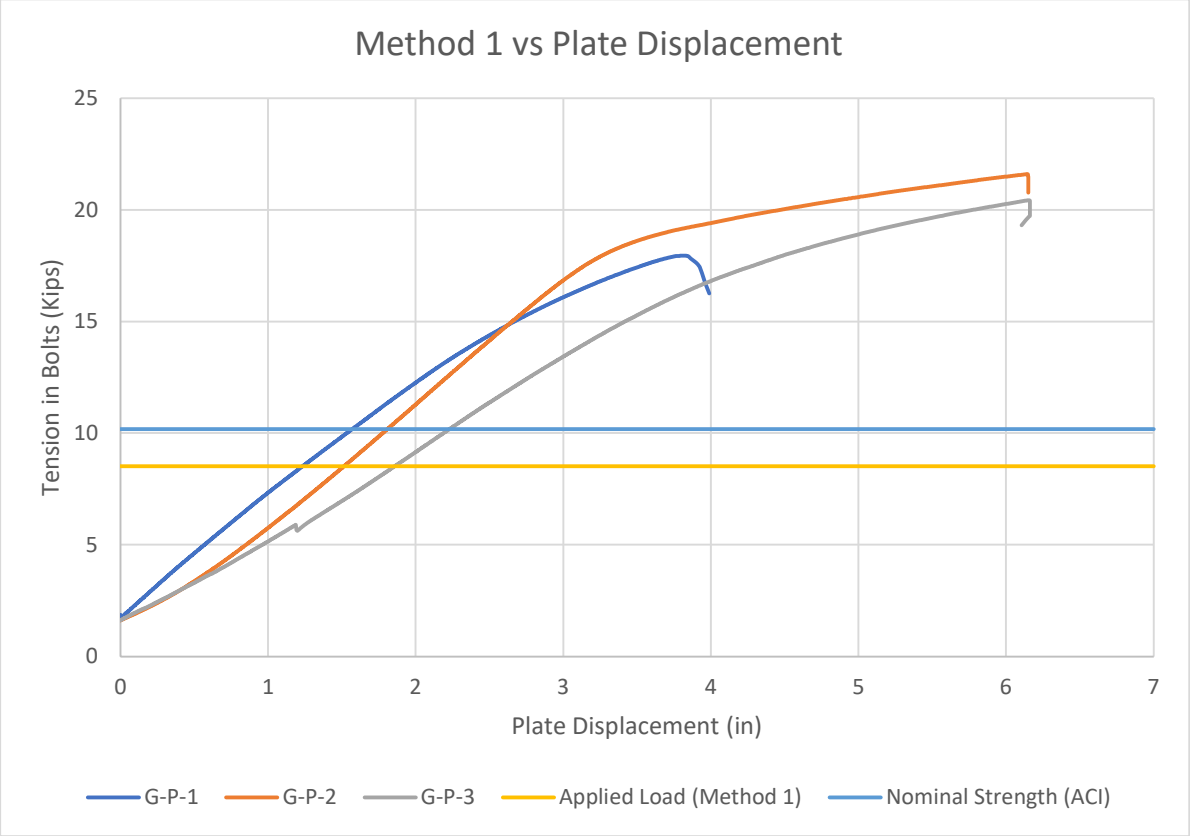

Figure A-91: Relation between tension in bolts using method 1 and MTS displacement

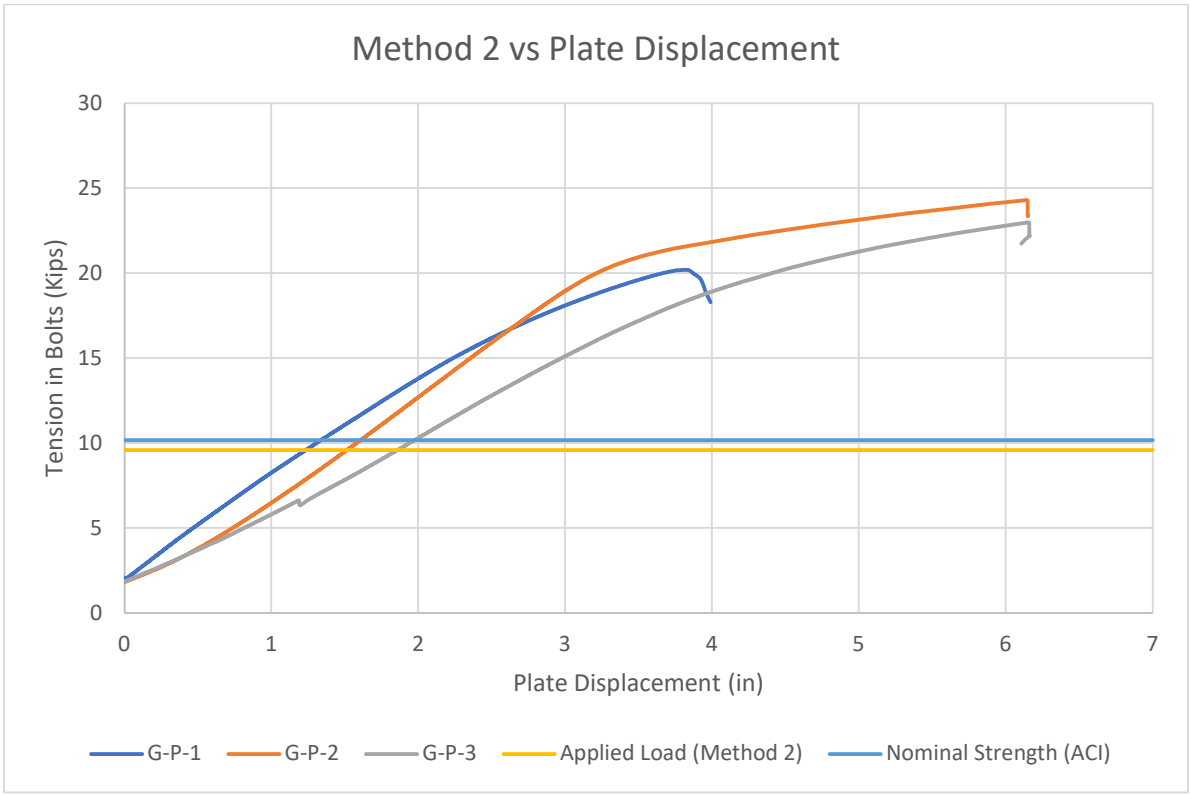

Figure A-92: Relation between tension in bolts using method 2 and MTS displacement

A3 – SCHEME 3 TEST RESULTS

A3.1 – MONOTONIC LOADING OF BULLET RAIL ON PARAPET WALL SPECIMEN

A total of six parapet wall specimens were used to evaluate the screw anchor breakout resistance for attaching bullet railing on parapet wall. The six parapet specimens were divided into two subgroup. Group 1 uses 8-in screw anchors, while group 2 uses 6-in. screw anchors. Table A-9 provides the summary of the test results and the corresponding graphs are plotted in Figure A-93 - Figure A-95. Using methods 1 and 2, the average calculated tension in bolts is 9.075 Kips and 10.210 Kips, respectively. All the specimens were able to reach more than their design anchor failure load. Figure A-96 - Figure A-105 illustrate the failure mode of the screw anchors and parapet wall. There were no sign of damaged on the screw anchors. All parapet wall specimens have the same failure mode regardless of the screw anchor length that is shear and concrete crushing, which resembled a prying action.

Table A-9: Test results bullet rail on parapet wall

Specimen's code	**B-P-1**	**B-P-2**	**B-P-3**	**B-P-4**	**B-P-5**	**B-P-6**
Max Lateral Load (Kip)	2.059	1.996	1.935	1.331	1.256	1.223
Displacement (in)	0.360	0.203	0.185	0.115	0.361	0.167
Tension in bolts (method 1) (Kip)	33.357	32.344	31.352	21.564	20.348	19.824
Tension in bolts (method 2) (Kip)	37.526	36.386	35.271	24.259	22.891	22.303
Nominal Strength (ACI) (Kip)	8" bolt – 8.84			6" bolt – 8.53		
Applied Load (Method 1) (Kip)	8.19					
Applied Load (Method 2) (Kip)	9.21					

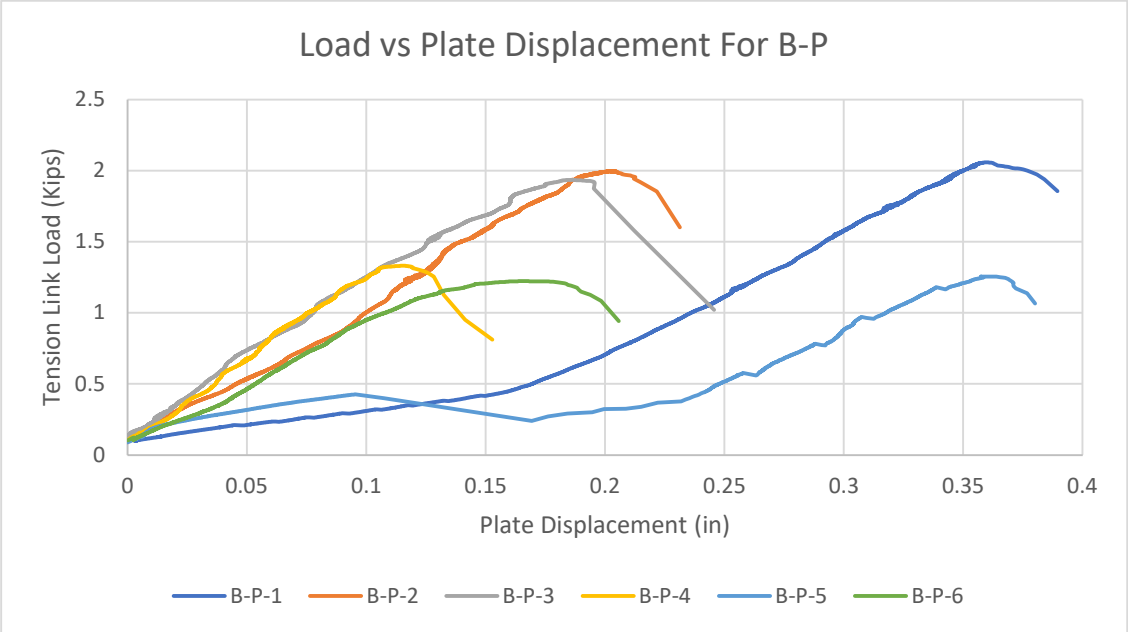

Figure A-93: Relation between load and displacement for B-P

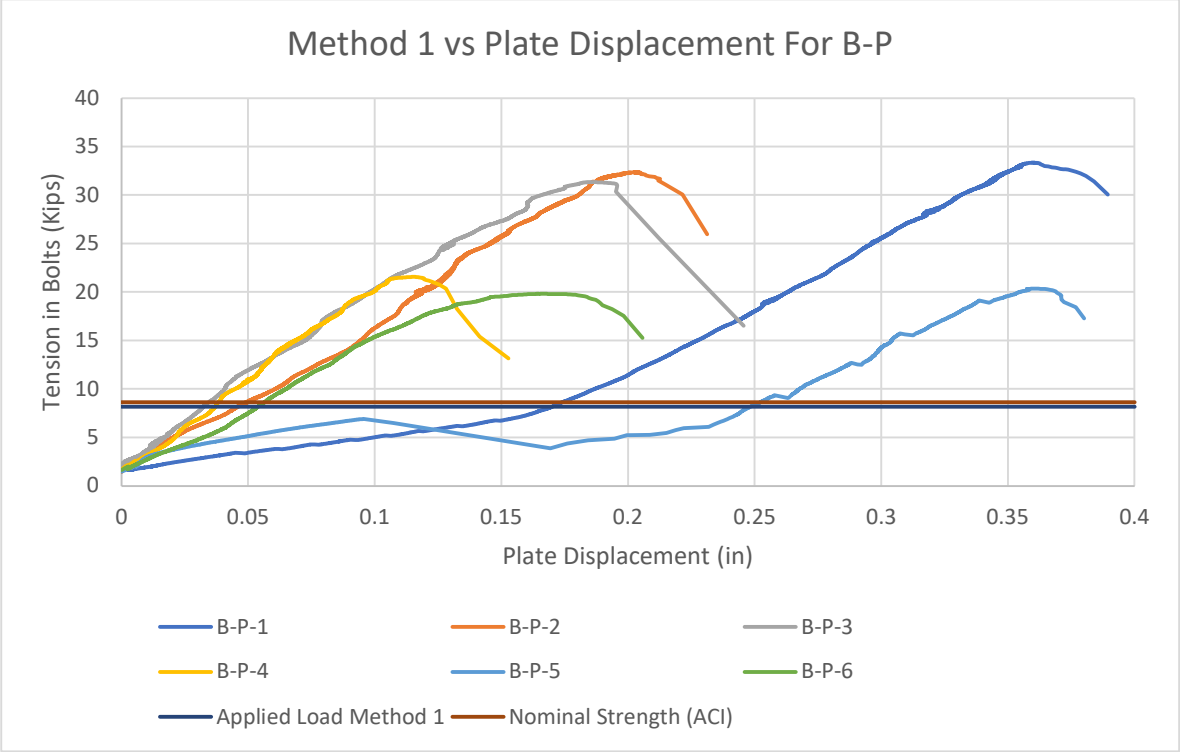

Figure A-94: Relation between tension in bolts using method 1 and displacement

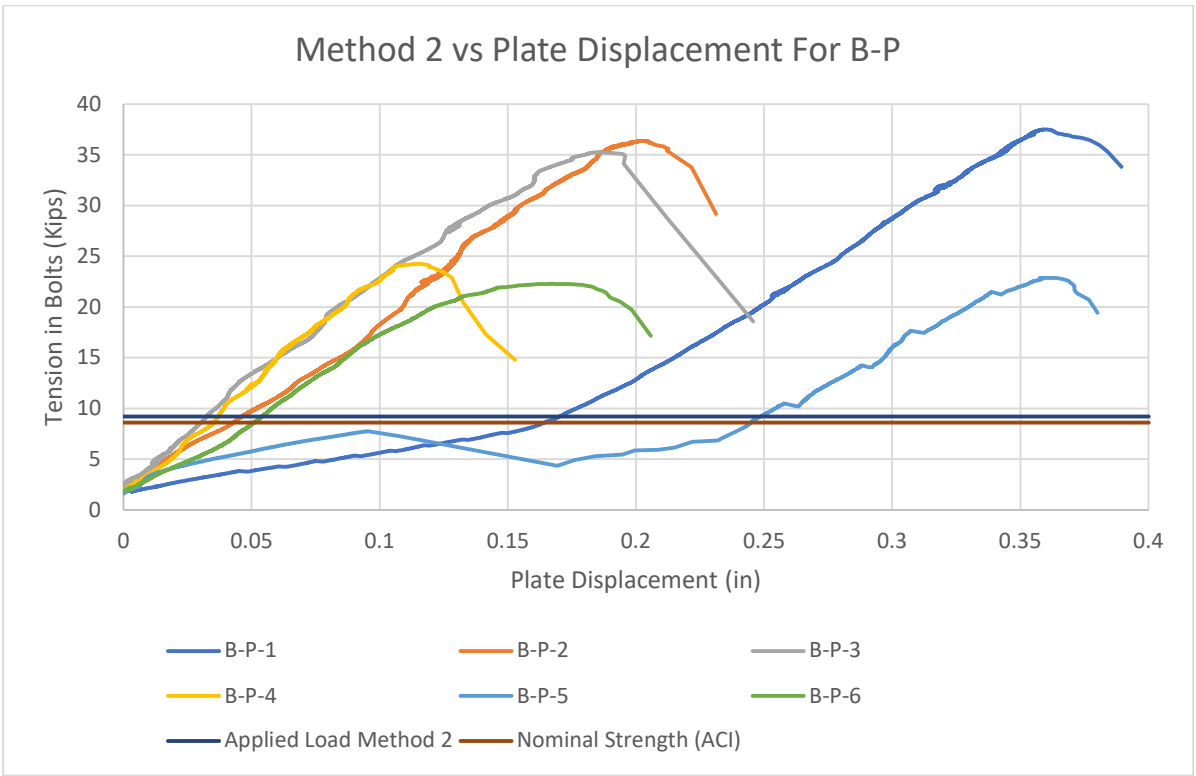

Figure A-95: Relation between tension in bolts using method 2 and displacement

Figure A-96: B-P-1 south and north screw after breakout

Figure A-97: B-P-1 specimen concrete after breakout

Figure A-98: B-P-2 specimens north and south screw anchors after breakout

Figure A-99: B-P-2 specimen concrete after breakout

Figure A-100: B-P-3 specimen south and north screw anchor after breakout

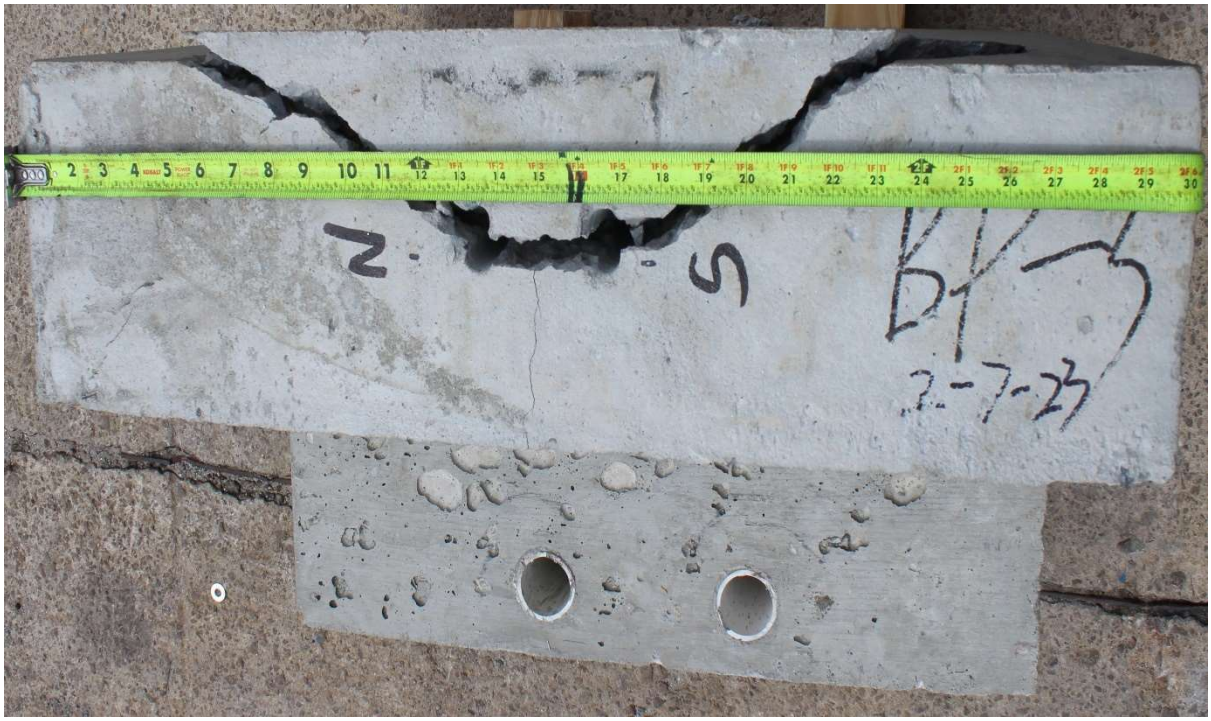

Figure A-101: B-P-3 specimen concrete after breakout

Figure A-102: B-P-4 specimen north and south screw anchor after breakout

Figure A-103: B-P-4 specimen concrete after breakout

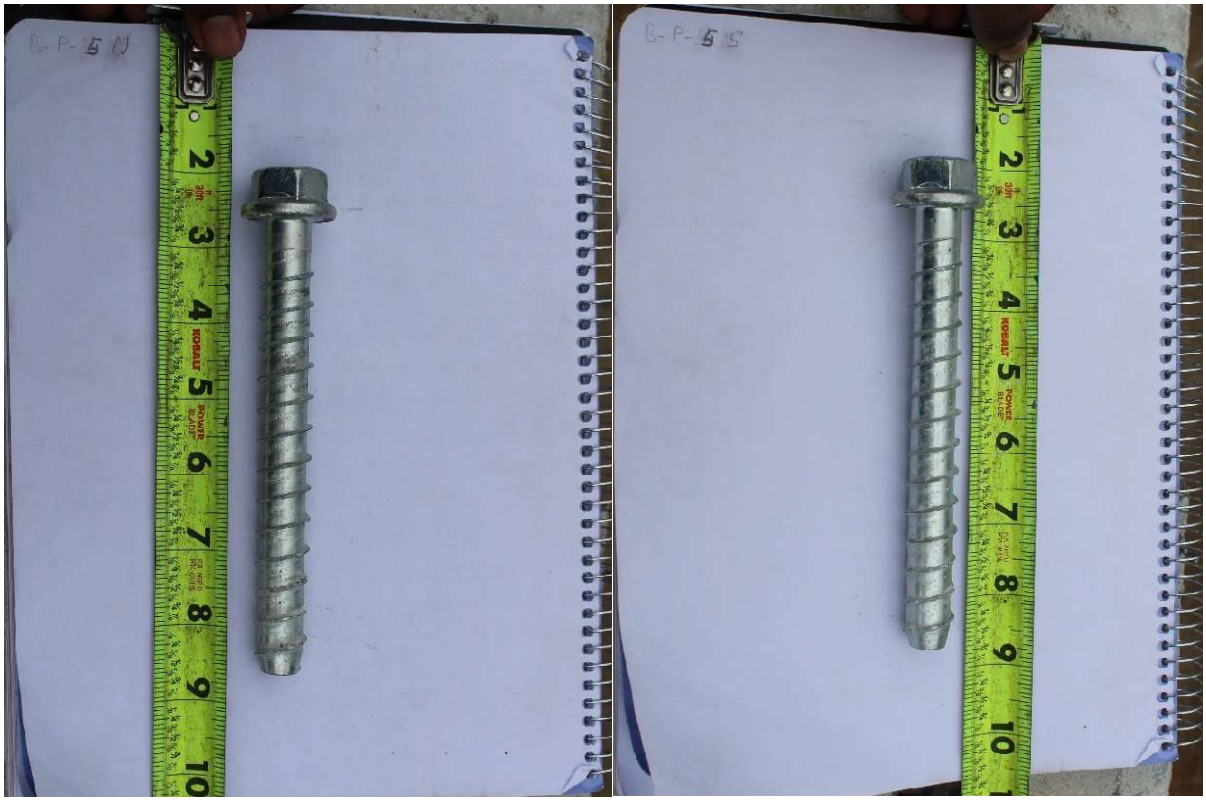

Figure A-104: B-P-5 specimen north and south screw anchor after breakout

Figure A-105: B-P-5 specimen concrete after breakout

A4 – SCHEME 4 TEST RESULTS

A4.1 – MONOTONIC LOADING OF MODIFIED PEDESTRIAN AND PICKET RAILING ON SIDEWALK SPECIMEN

Seven sidewalk specimens with minor damaged were used to evaluate the screw anchors breakout resistance to mount a modified parapet railing on sidewalk. Table A-10 provides the summary of the test results. Using methods 1 and 2, the average calculated tension in bolts is 9.633 Kips and 13.005 Kips, respectively. All specimens were able to reach more than the applied lateral loads. Figure A-106 - Figure A-112 illustrates the load vs displacement and tilt sensors.

Table A-10: Test results of modified parapet railing on sidewalk

Specimen's code	**G-S-32**	**G-S-33**	**G-S-34**	**G-S-35**	**G-S-36**	**G-S-37**	**G-S-38**
Max Lateral Load (Kip)	1.251	1.874	1.448	1.594	1.681	1.824	1.669
Displacement (in)	0.212	0.157	0.087	0.174	0.099	0.049	0.166
Tilt (^{o}deg)	4.235	2.597	0.208	4.201	2.438	0.312	0.693
Tension in bolts (method1) (Kip)	20.136	30.173	23.322	26.152	27.069	29.379	26.705
Tension in bolts (method 2) (Kip)	27.184	40.733	31.485	35.305	36.543	39.662	36.052
Nominal Strength (ACI) (Kip)	N/A						
Applied Load (Method 1) (Kip)	15.99						
Applied Load (Method 2) (Kip)	17.98						

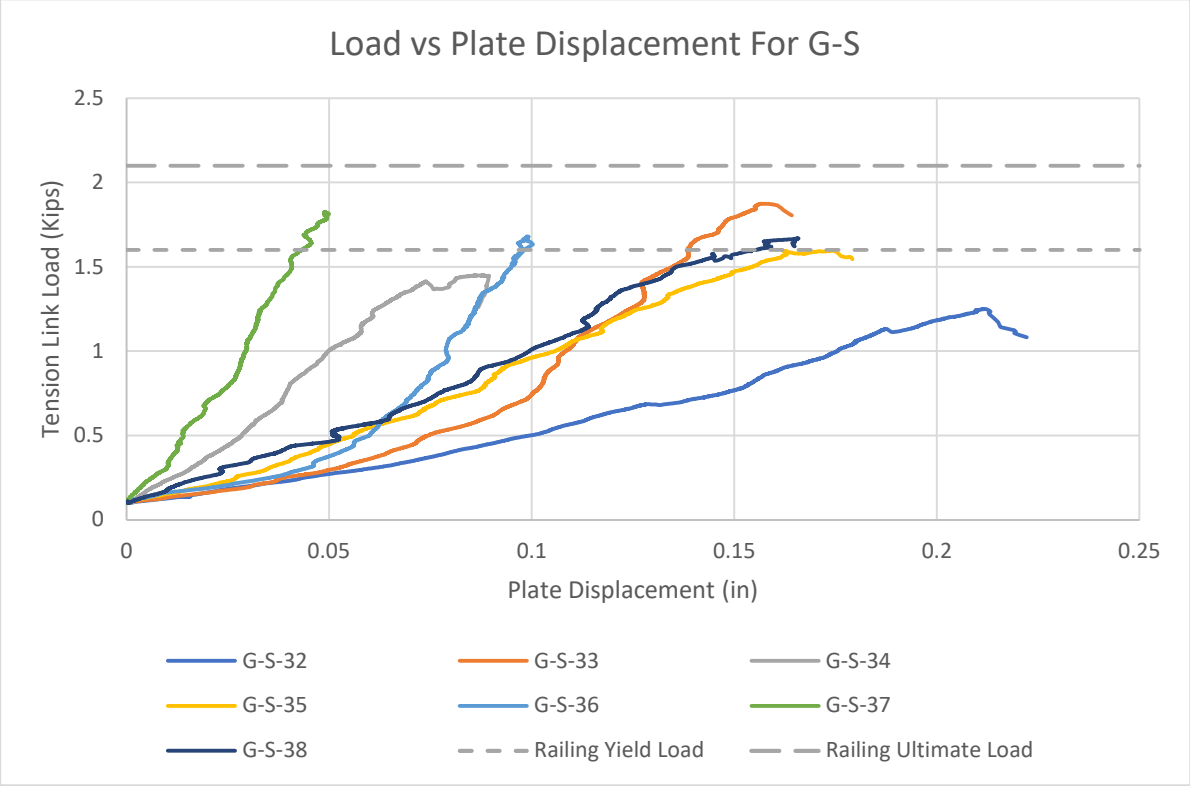

Figure A-106: Relation between load and displacement for G-S

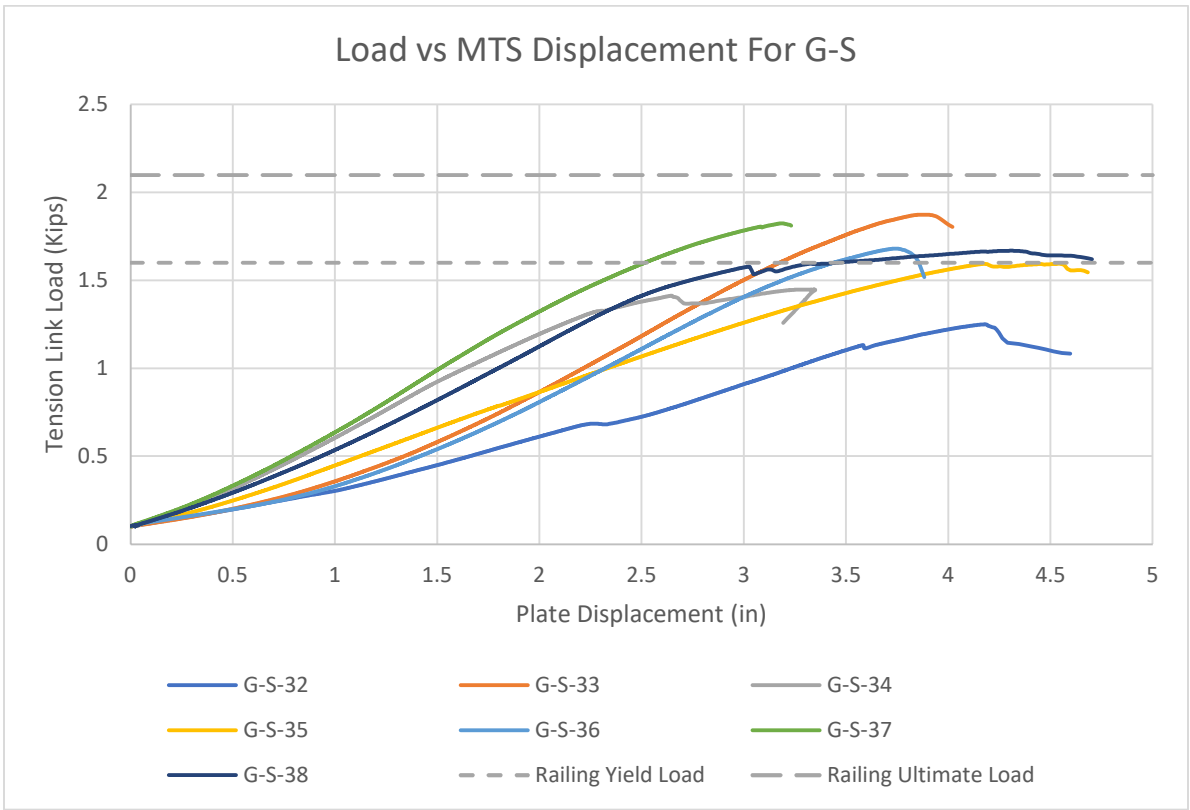

Figure A-107: Relation between load and MTS displacement for G-S

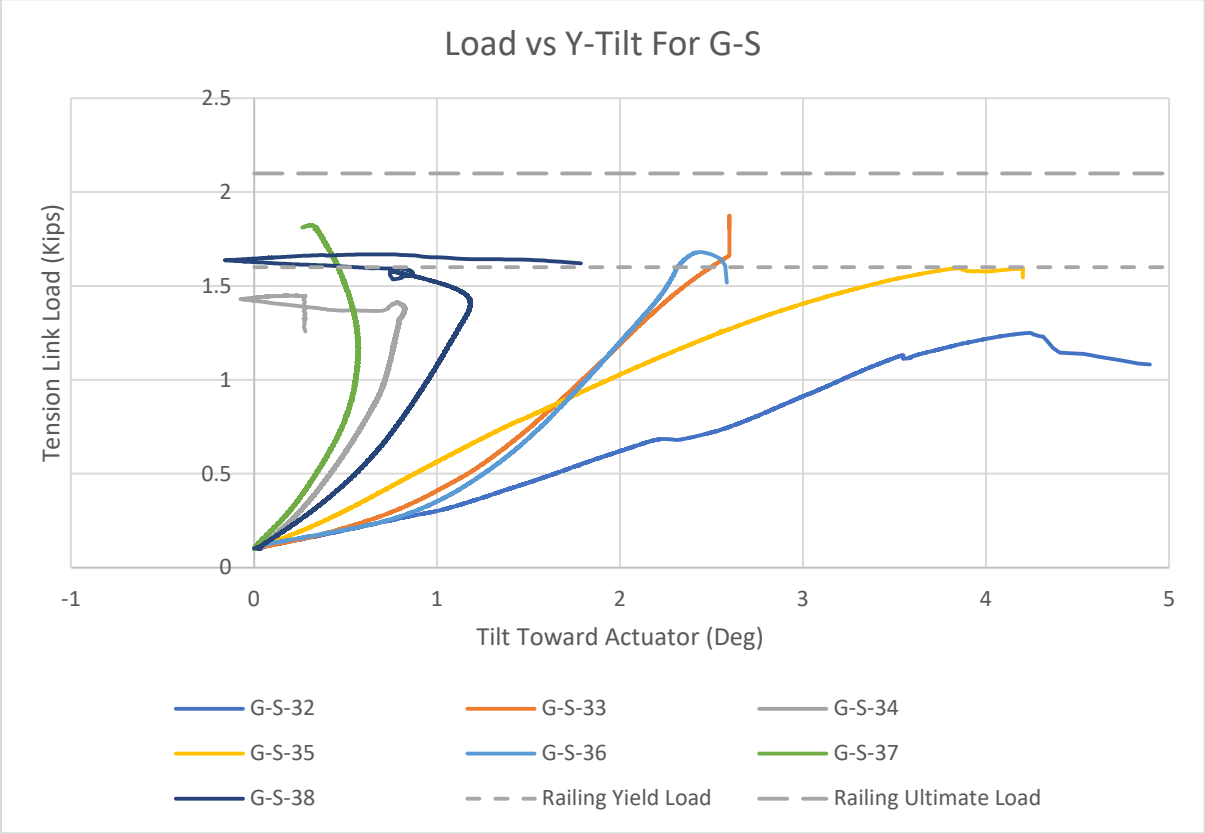

Figure A-108: Relation between load and y-axis tilt for G-S

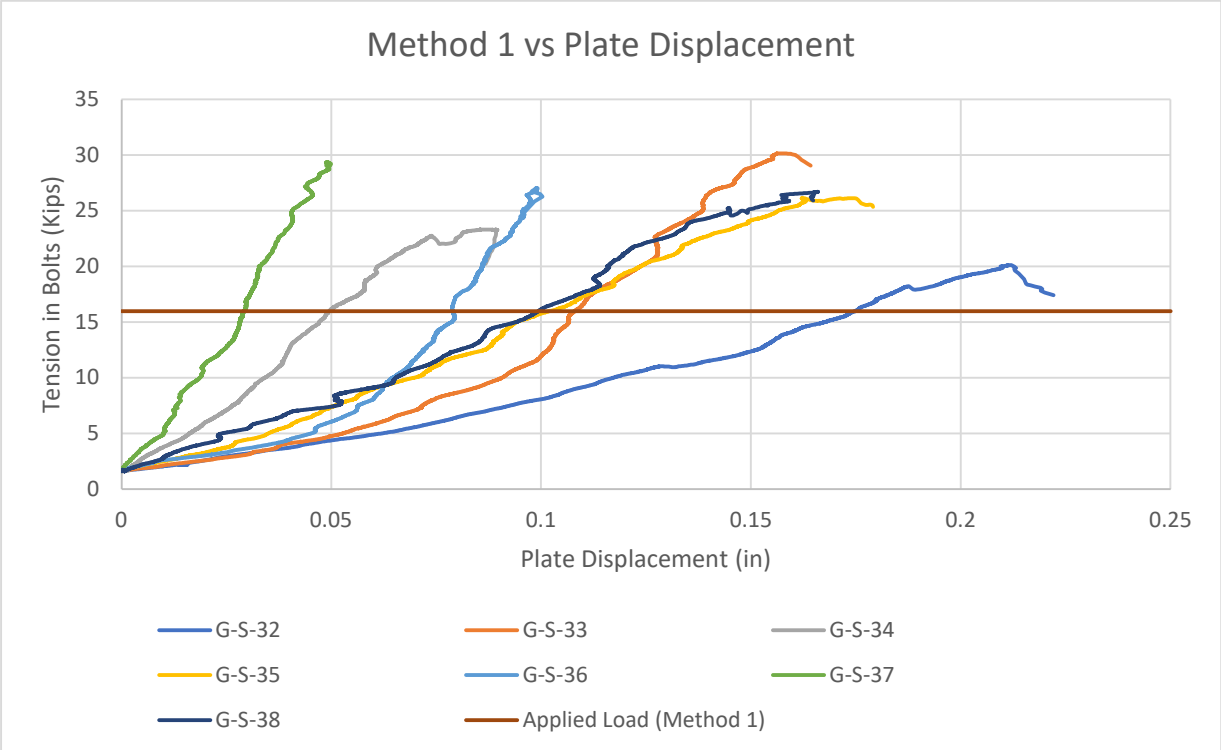

Figure A-109: Relation between tension in bolt using method 1 and displacement for G-S

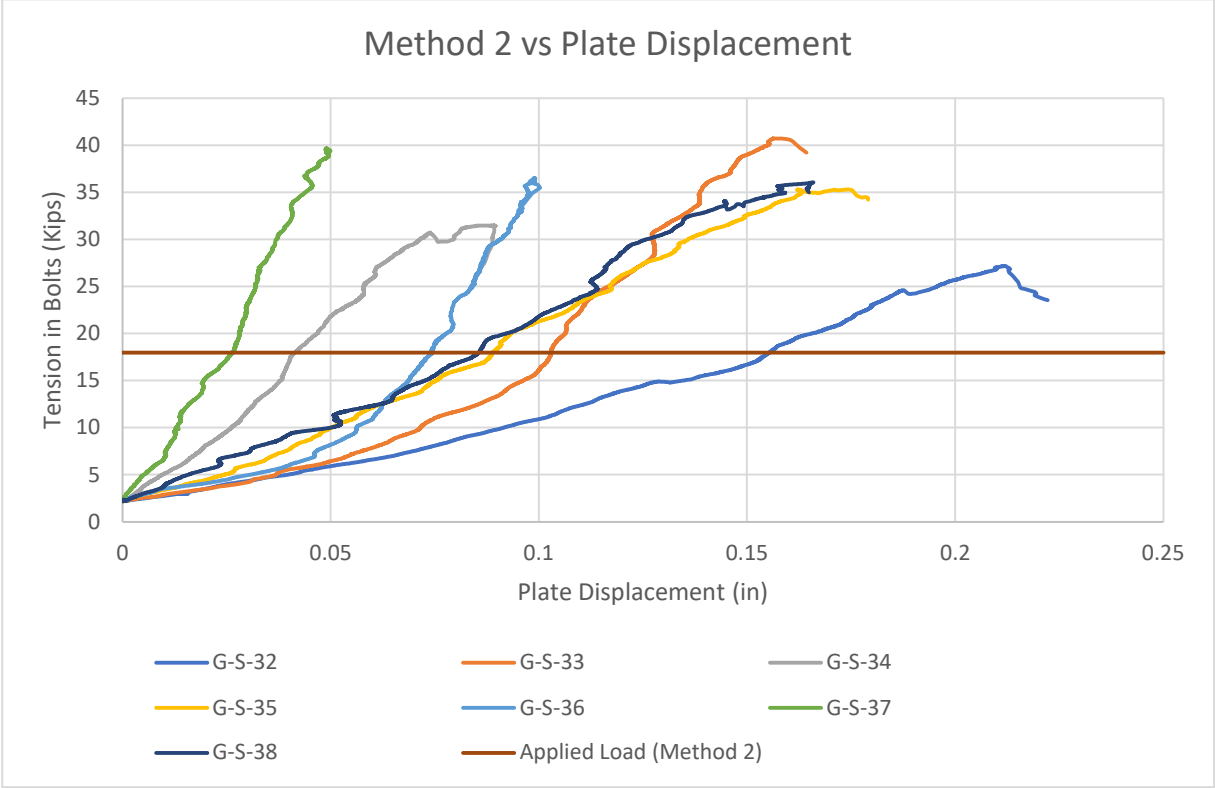

Figure A-110: Relation between tension in bolts using method 2 and displacement for G-S

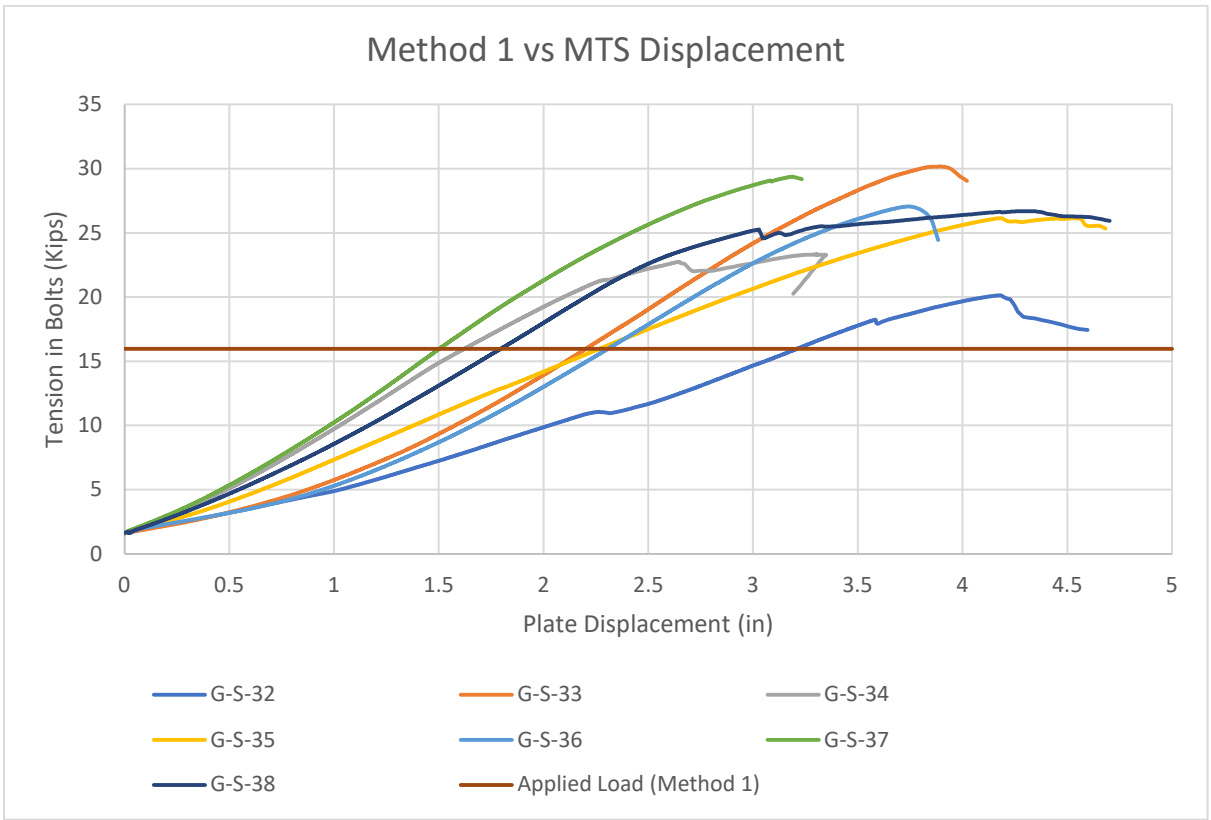

Figure A-111: Relation between tension in bolt using method 1 and MTS displacement for G-S

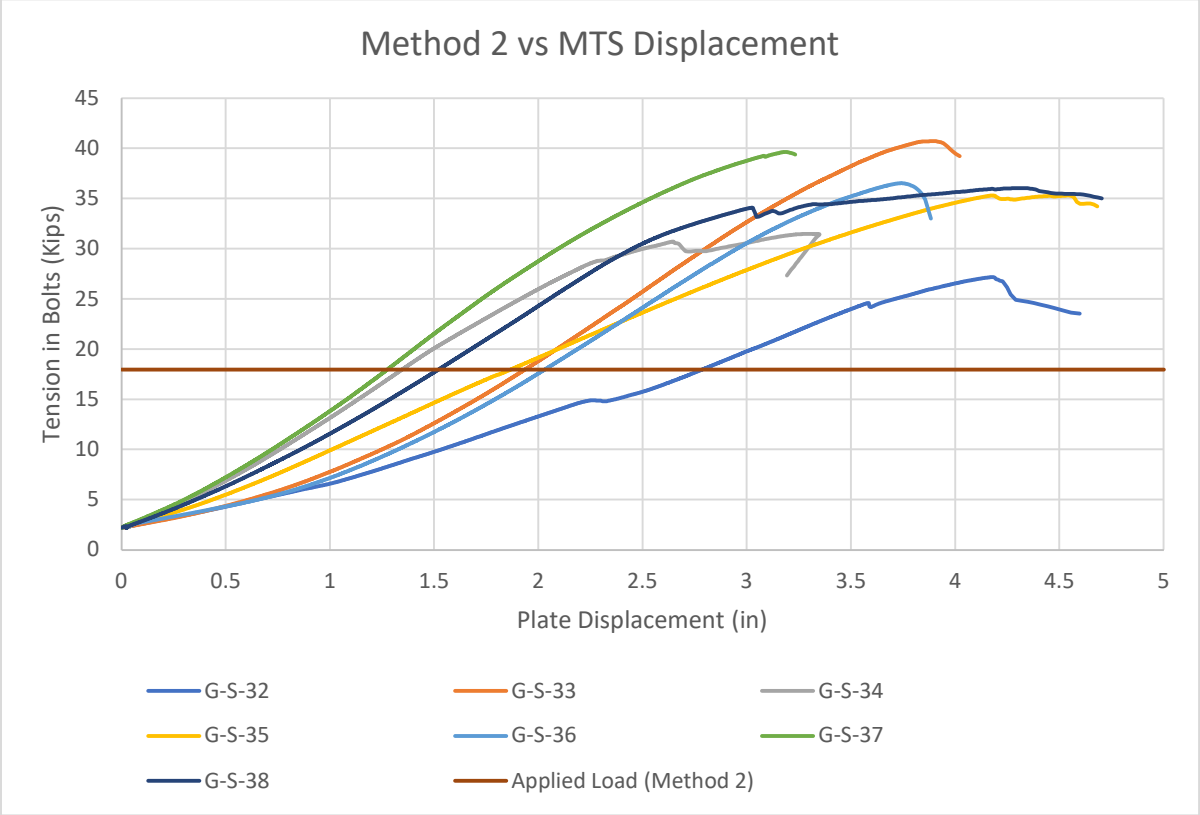

Figure A-112: Relation between tension in bolt using method 2 and MTS displacement for G-S

A4.2 – MONOTONIC LOADING OF MODIFIED PEDESTRIAN AND PICKET RAILING ON GRAVITY WALL AND PARAPET WALL

Two gravity walls and two parapet walls specimens were used to evaluate the screw anchor breakout resistance securing the modified pedestrian railing. The only reason for using only these four specimens is because these represent the least damaged specimens. Table A-11 provides the summary of the test results and the corresponding graphs are illustrated in Figure A-113 - Figure A-119. Using methods 1 and 2, the average calculated tension in bolts for G-G-38 and 310 is 6.905 Kips and 9.322 Kips, respectively. The average calculated tension in bolts for G-G-311 and 312 is 8.512 Kips and 11.492 Kips, respectively. All specimens were able to reach more than the applied lateral loads. Figure A-120 - Figure A-127 illustrate the failure modes of these specimens. All screw anchors showed sign of bending. All concrete specimens had the same failure mode, which is the prying action.

Table A-11: Test results of modified pedestrian railing on gravity and parapet walls

Specimen's code	**G-G-38**	**G-G-310**	**G-G-311**	**G-G-312**
Max Lateral Load (Kip)	1.354	1.351	1.399	1.429
Displacement (in)	0.027	0.058	0.076	0.114
Tilt (^{o}deg)	2.785	1.959	1.155	2.257
Tension in bolts (method1) (Kip)	21.659	21.749	22.386	23.002
Tension in bolts (method 2) (Kip)	29.239	29.362	30.222	31.052
Nominal Strength (ACI) (Kip)	N/A			
Applied Load (Method 1) (Kip)	15.99			
Applied Load (Method 2) (Kip)	17.98			

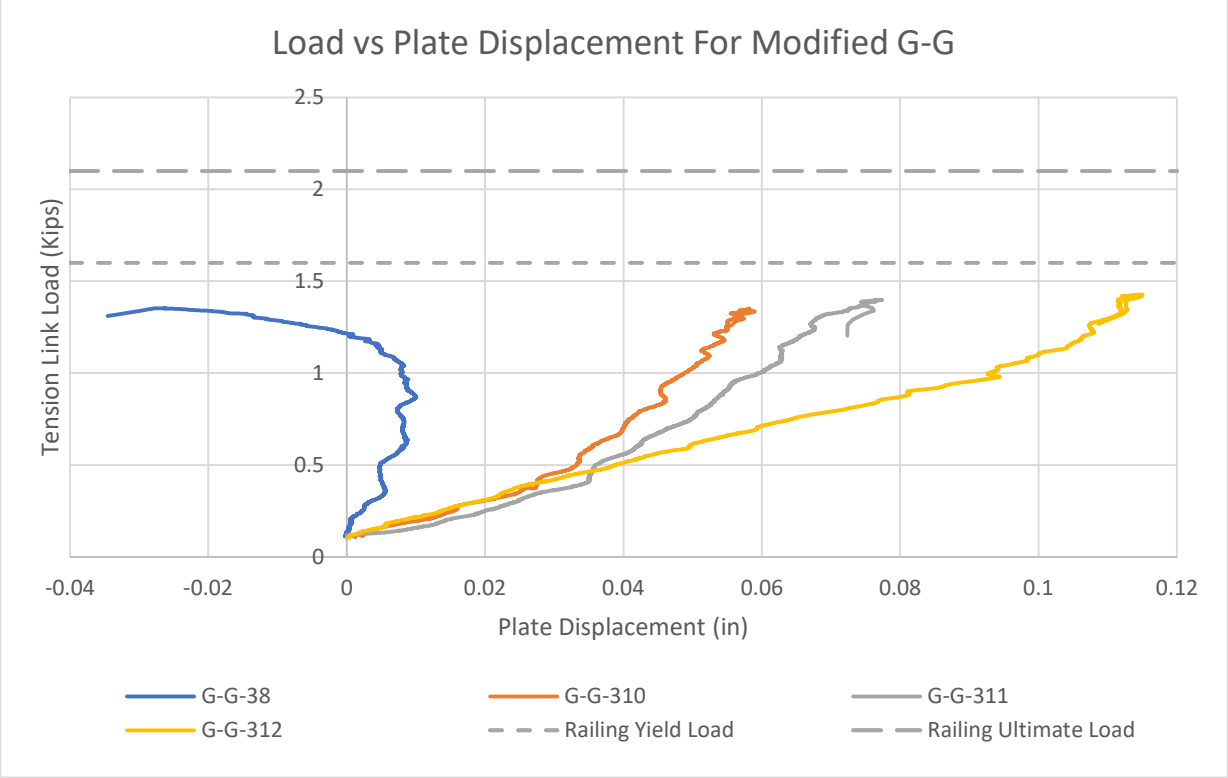

Figure A-113: Relation between load and displacement for modified G-G

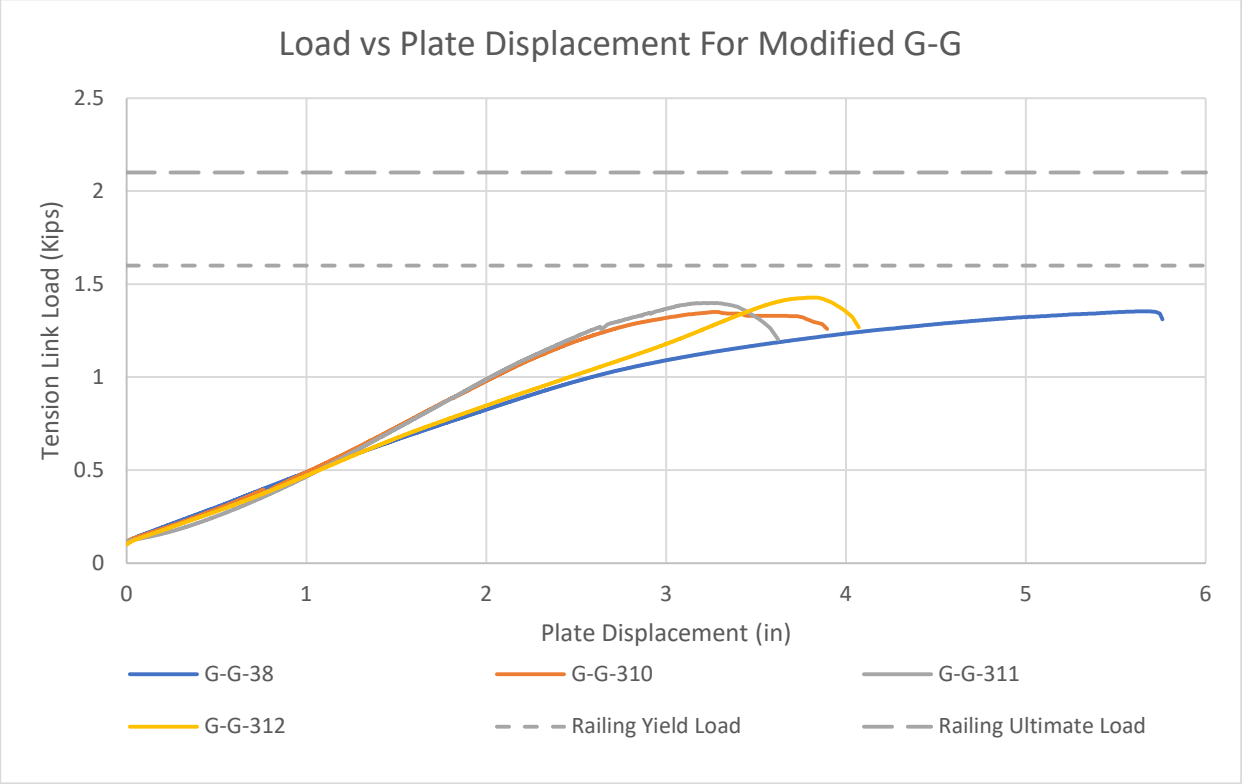

Figure A-114: Relation between load and MTS displacement for modified G-G

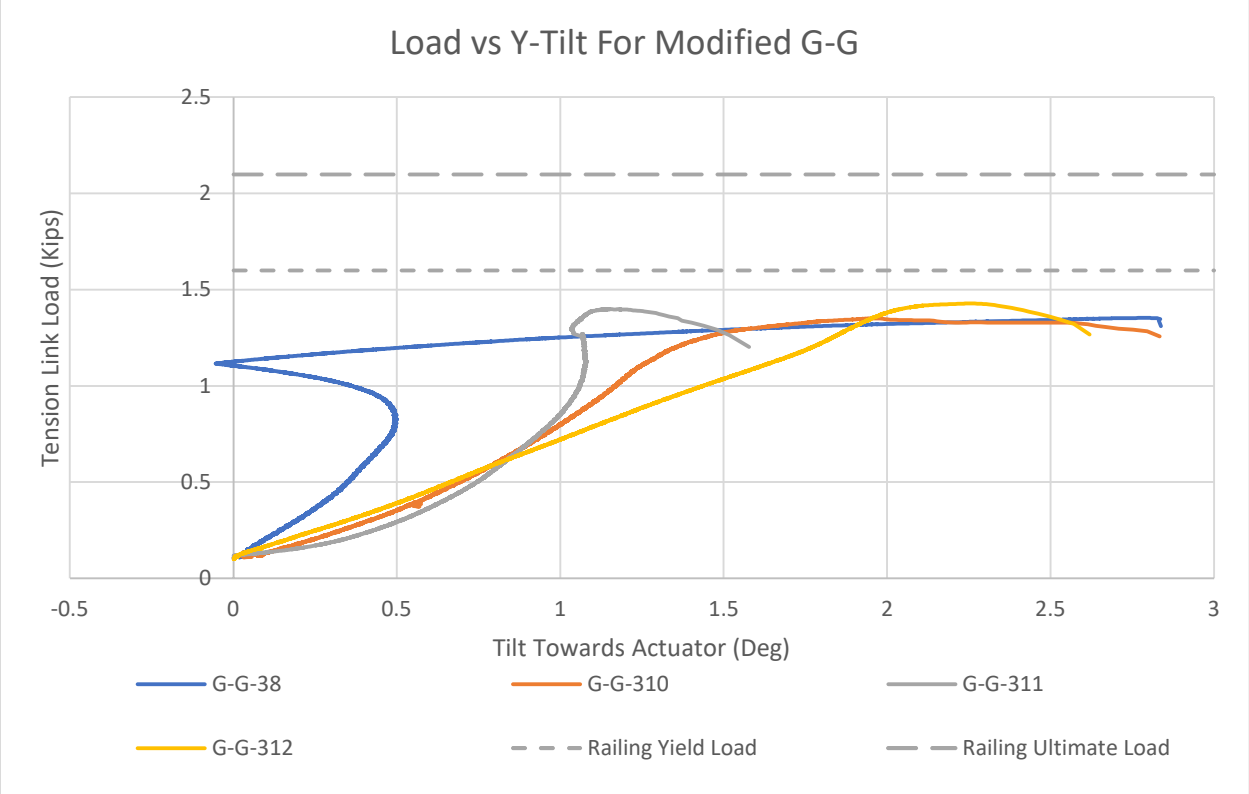

Figure A-115: Relation between load and y-axis tilt for modified G-G

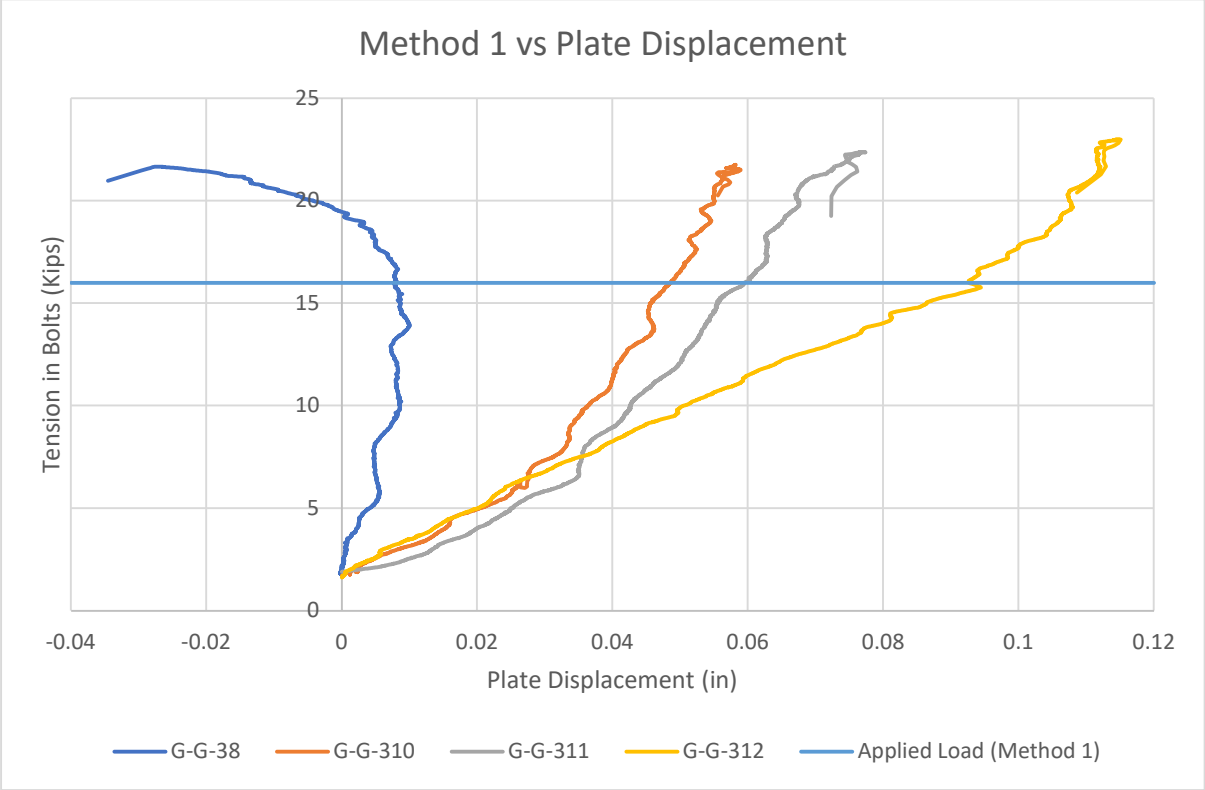

Figure A-116: Relation between tension in bolt using method 1 and displacement for modified G-G

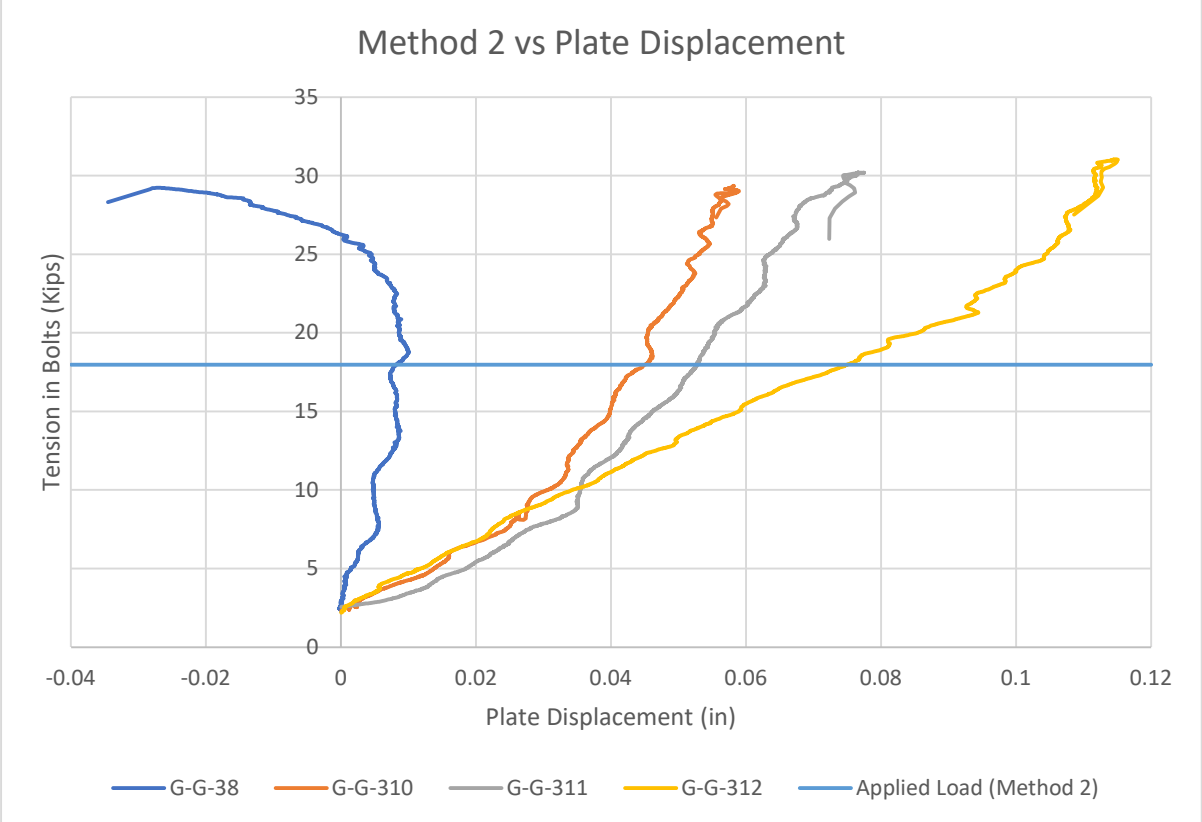

Figure A-117: Relation between tension in bolts using method 2 and displacement for modified G-G

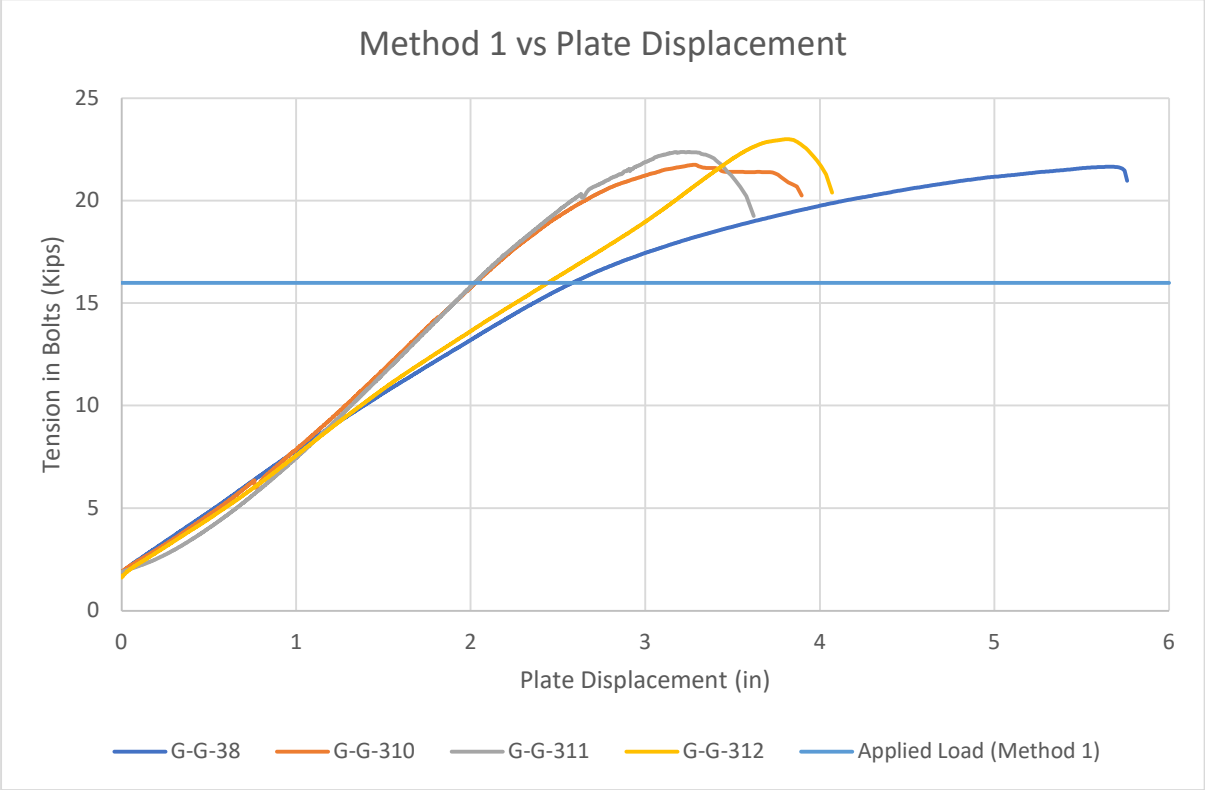

Figure A-118: Relation between tension in bolt using method 1 and MTS displacement for modified G-G

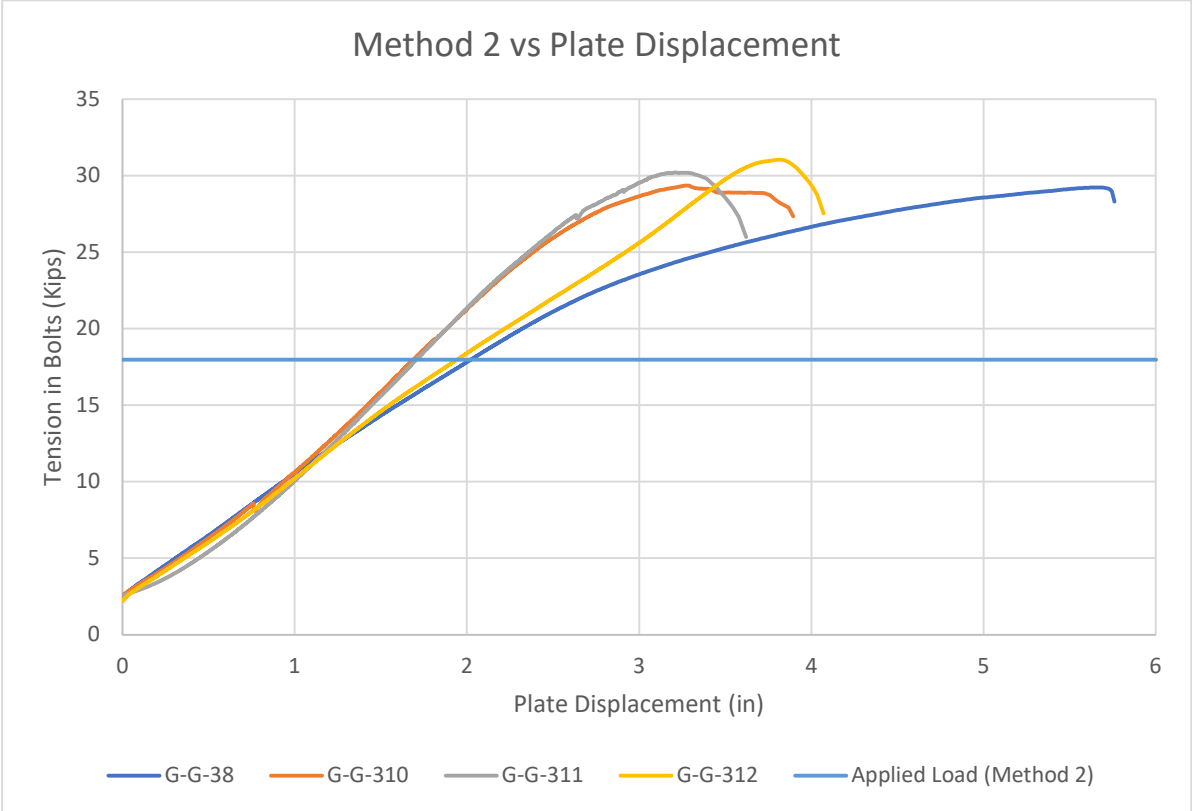

Figure A-119: Relation between tension in bolts using method 2 and MTS displacement for modified G-G

Figure A-120: G-G-38 specimen concrete after breakout

Figure A-121: G-G-38 specimen north and south screw anchor after breakout

Figure A-122: G-G-310 specimen concrete after breakout

Figure A-123: G-G-310 specimen screw anchors after breakout

Figure A-124: G-G-311 specimen concrete after breakout

Figure A-125: G-G-311 specimen screw anchors after breakout

Figure A-126: G-G-312 specimen concrete after breakout

Figure A-127: G-G-312 specimen screw anchor breakout

Appendix B: TEST SETUP

TEST SETUP NOTES

1. $1\frac{1}{2}$" ANCHOR HOLES DRILLED IN SPECIMEN MUST ALIGN WITH THREADED ANCHOR HOLE LOCATIONS ON THE STRONG FLOOR OF THE TESTING FACILITY.
2. THE FOLLOWING PROCEDURE SHOULD BE FOLLOWED:
   - 2.1. ALIGN SUPPORT BASE ON FLOOR.
   - 2.2. PLACE TEST SPECIMEN ATOP SUPPORT BASE, ALIGNING THE TWO $1\frac{1}{2}$" ANCHOR HOLES WITH THE STRONG FLOOR ANCHOR HOLES.
   - 2.3. INSERT TWO $1\frac{1}{2}$" THREADED RODS THROUGH HOLES IN SPECIMEN AND FIX THE RODS TO THE STRONG FLOOR.
   - 2.4. PLACE A 1"x5"X30" STEEL BEARING PLATE ATOP THE CONCRETE SPECIMEN, ALIGNING THE TWO HOLES IN THE PLATE WITH THE $1\frac{1}{2}$" RODS PROTRUDING FROM THE SPECIMEN.
   - 2.5. FIX THE BEARING PLATE TO THE SPECIMEN USING THE SPECIFIED HARDWARE.
   - 2.6. ATTACH THE STEEL CABLE EXTENDING FROM THE LOAD FRAME TO THE TOP OF THE SPECIMEN'S RAILING USING THE SPECIFIED HARDWARE.

SPECIMEN NOTES

1. SCREW ANCHORS ARE TO BE INSTALLED ACCORDING TO MANUFACTURER PROCEDURES.
2. CONCRETE REINFORCEMENT IS INTENDED TO PREVENT CONCRETE FAILURE OUTSIDE OF THE PREDICTED ZONE OF INFLUENCE.

TEST FRAME NOTES

SHAFT COLLAR
https://www.mcmaster.com/6432K21/

SPACER
https://www.mcmaster.com/92415A162/

PULLEY
INDUSTRIAL HARDWARE
SKU: 59A-7361222
https://www.industrialhardware.com/campbell-7361222-6-in-extra-heavy-iron-sheave-for-1-2-in-wire-rope-painted-blue.html

CABLE AND HOOK
https://www.mcmaster.com/3308T61-3308T602/

- $\frac{1}{2}$" DIAM. CABLE
- 10 FT. LENGTH, 5,300LB. CAPACITY

UBOLTS
https://www.mcmaster.com/8880T37/

TEST FRAME NOTES

1. THE FOUR $\frac{7}{8}$" THREADED RODS ASSOCIATED WITH THE ADAPTER PLATE USED TO MOUNT THE MTS 55 KIP ACTUATOR TO THE STRONG FLOOR ARE FIXED TO THE ADAPTER PLATE VIA TAPPED HOLES. THE CORRECT HOLE AND TAP SIZE FOR THE ACCEPTANCE OF A $\frac{7}{8}$" THREADED ROD SHOULD BE REFERENCED DURING THE MANUFACTURING PROCESS.

SCREW ANCHORS
TEST SETUP

FLORIDA TECH

TEST SETUP – SCREW ANCHOR APPLICATIONS

FLORIDA DEPARTMENT OF TRANSPORTATION

	FJR
4/27/22	NS
NOTED	JC

0-1

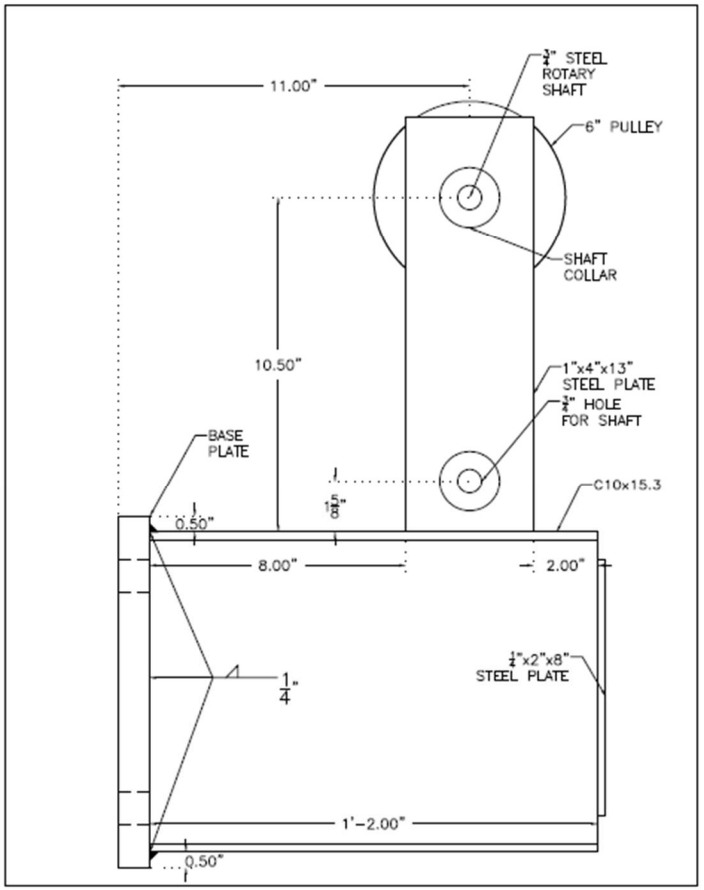

A1 PULLEY ASSEMBLY – SIDE VIEW

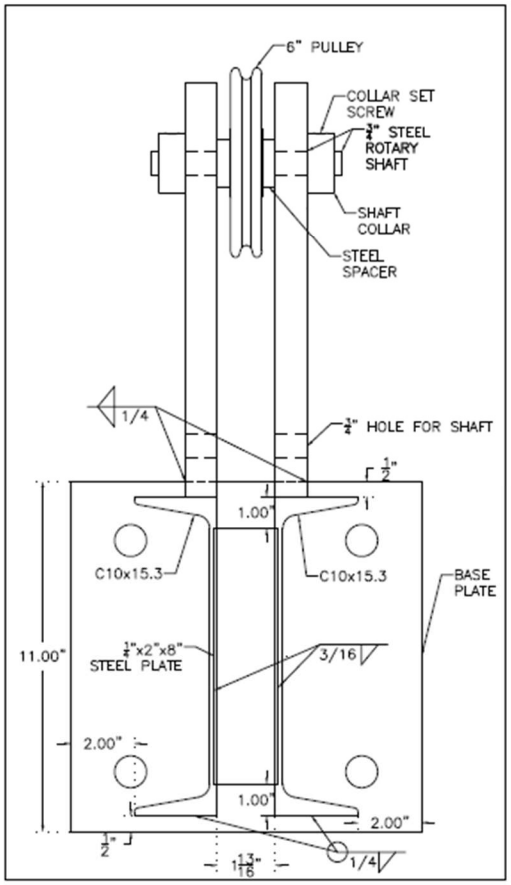

A2 PULLEY ASSEMBLY – FRONT VIEW

SCREW ANCHORS
TEST SETUP

FLORIDA TECH

TEST SETUP – SCREW ANCHOR APPLICATIONS

FLORIDA DEPARTMENT OF TRANSPORTATION

	FJR
4/27/22	NS
NOTED	JC

A–1

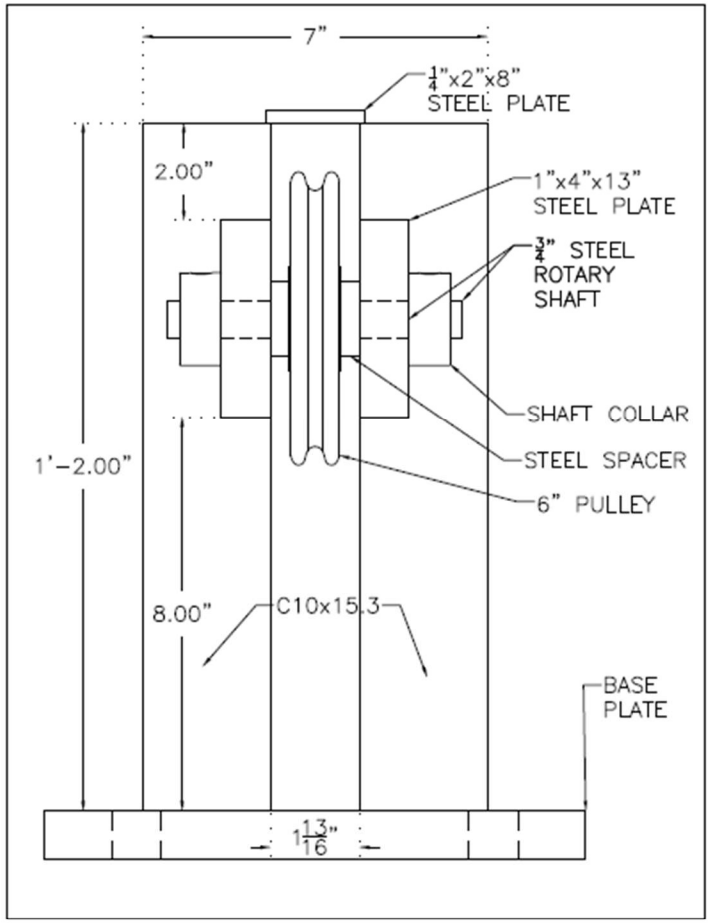

A3 PULLEY ASSEMBLY – TOP VIEW

SCREW ANCHORS
TEST SETUP

FLORIDA TECH

TEST SETUP – SCREW ANCHOR APPLICATIONS

FLORIDA DEPARTMENT OF TRANSPORTATION

	FJR
4/27/22	NS
NOTED	JC

A–2

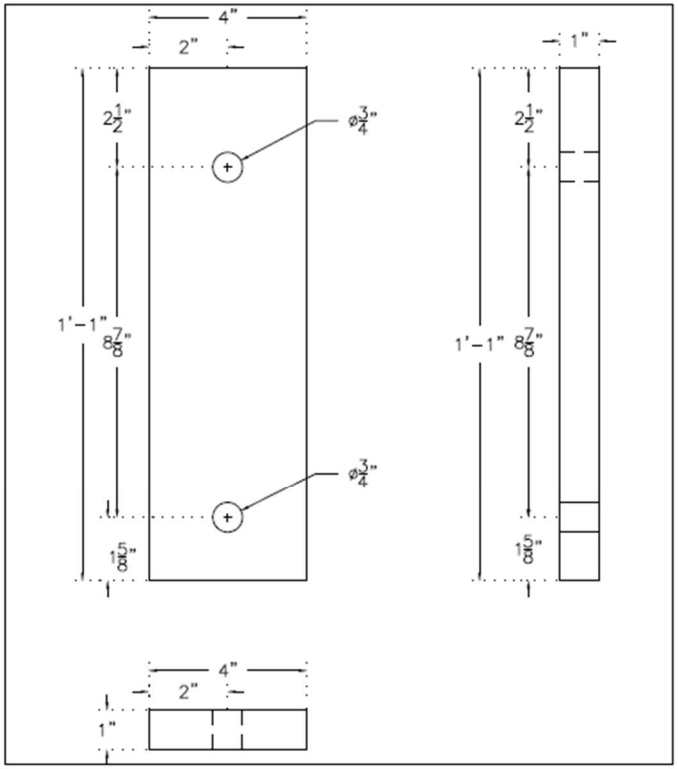

A4 PULLEY SUPPORT – VERTICAL PLATE

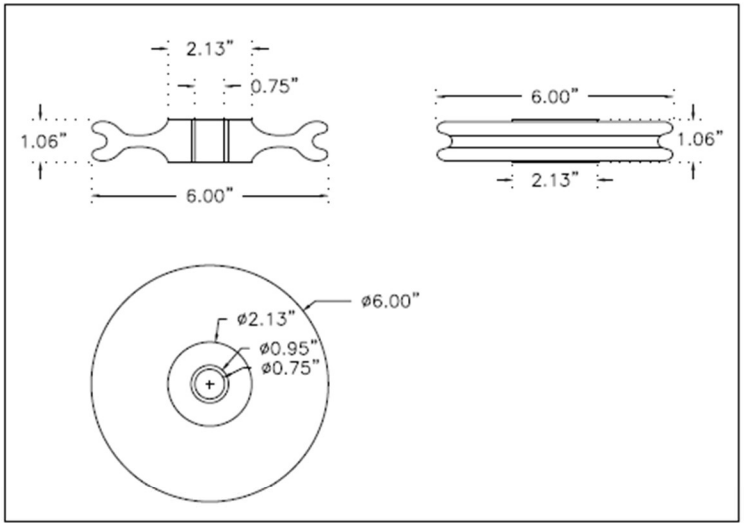

A5 PULLEY

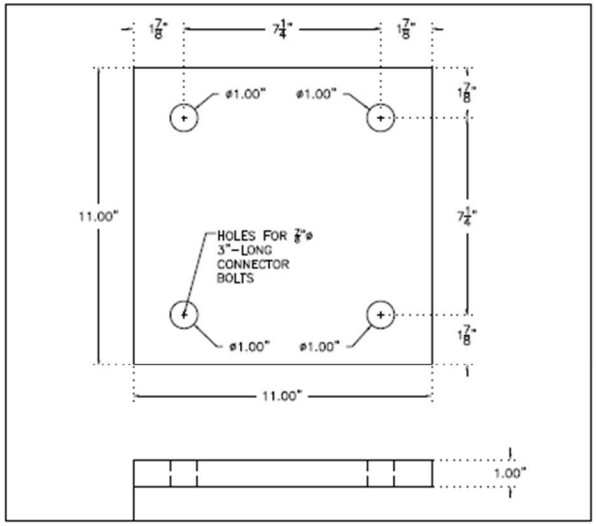

A6 BASE PLATE DETAILS

SCREW ANCHORS
TEST SETUP

FLORIDA TECH

TEST SETUP – SCREW ANCHOR APPLICATIONS

FLORIDA DEPARTMENT OF TRANSPORTATION

	FJR
4/27/22	NS
NOTED	JC

A–3

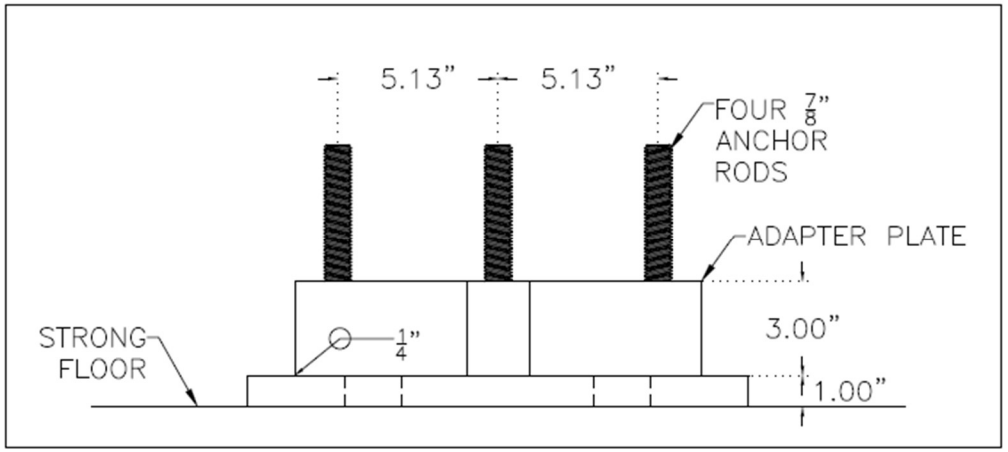

A7 FLOOR AND ADAPTER PLATE

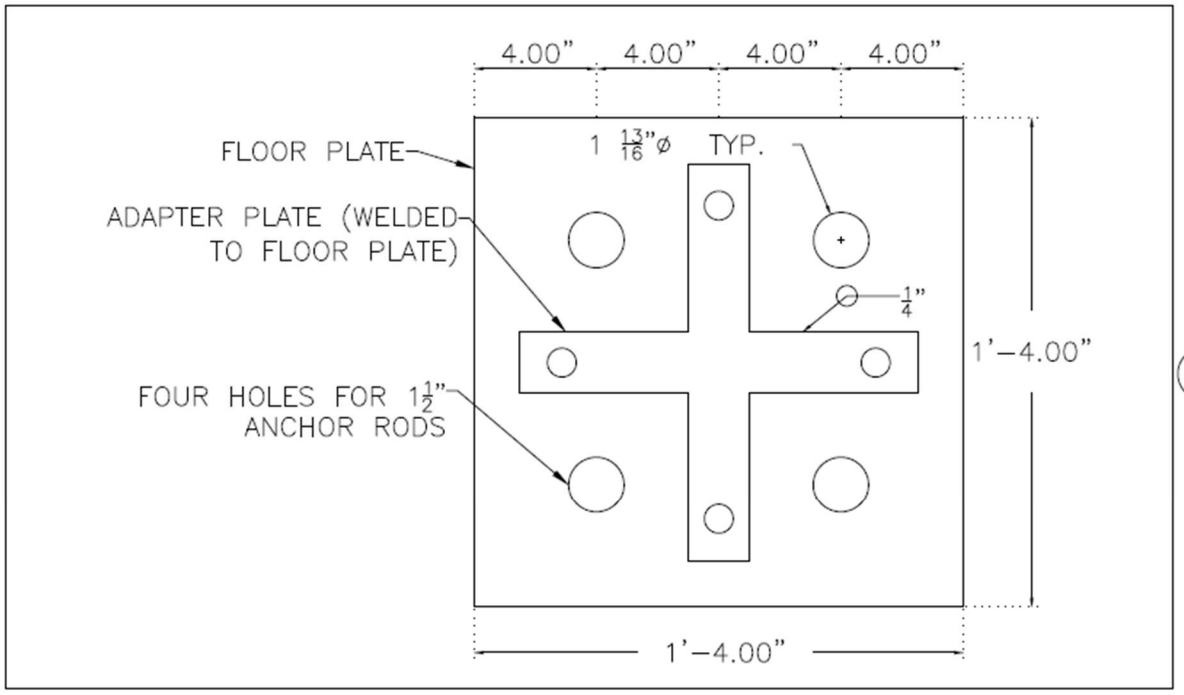

A8 FLOOR AND ADAPTER PLATE

SCREW ANCHORS TEST SETUP

FLORIDA TECH

TEST SETUP – SCREW ANCHOR APPLICATIONS

FLORIDA DEPARTMENT OF TRANSPORTATION

	RJR
4/27/22	NS
NOTED	JC

A-4

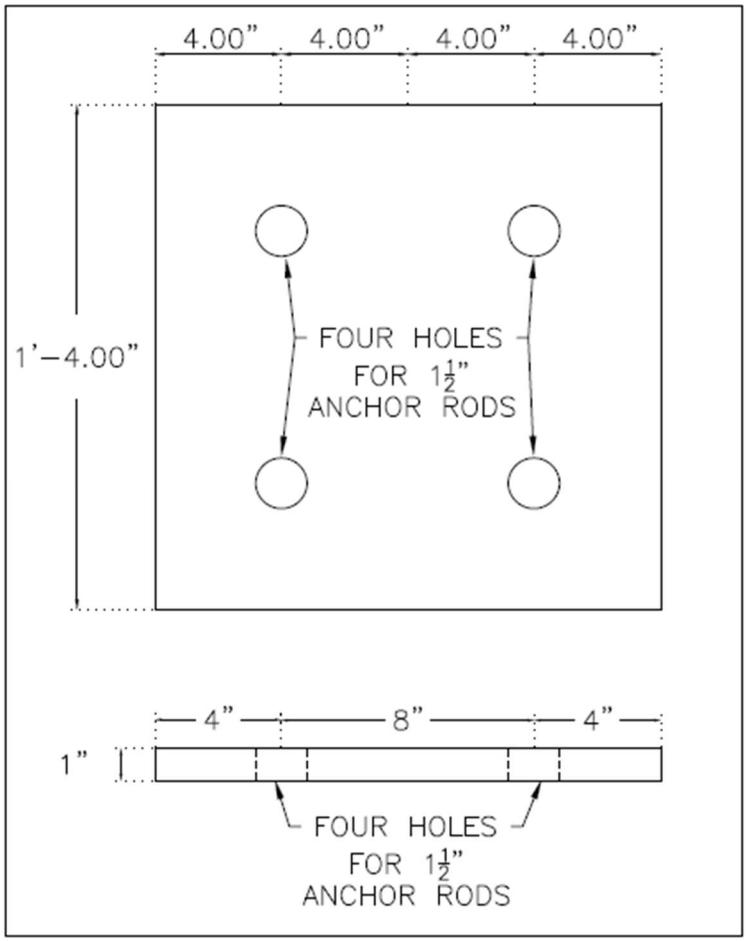

A9 FLOOR PLATE

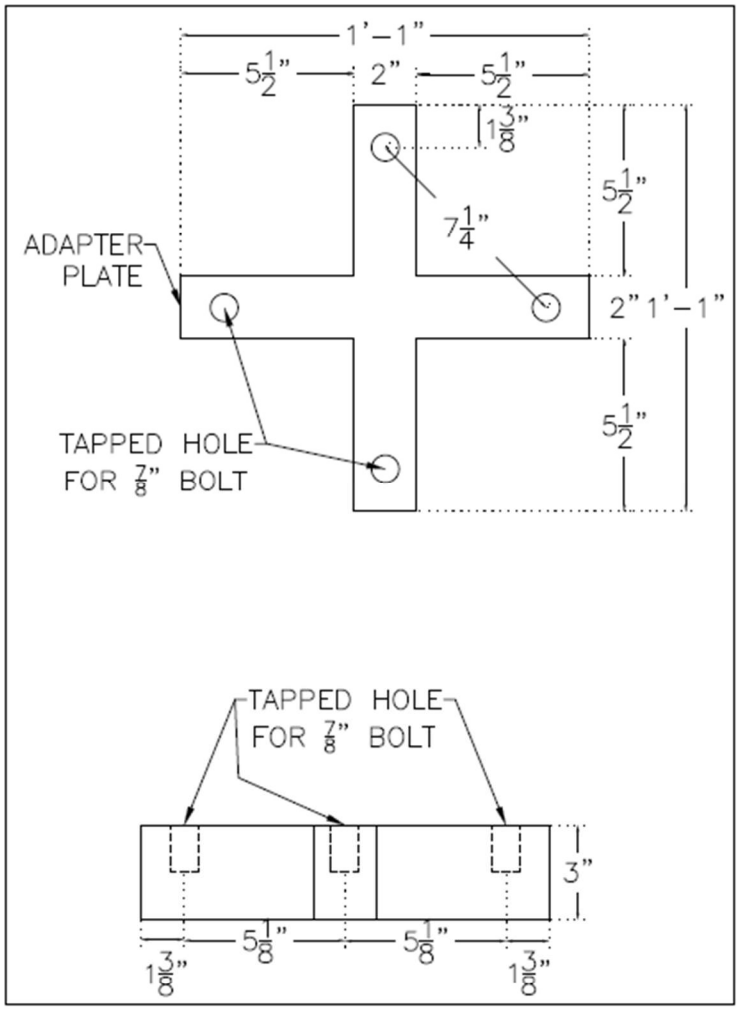

A10 ADAPTER PLATE

SCREW ANCHORS
TEST SETUP

FLORIDA TECH

TEST SETUP – SCREW ANCHOR APPLICATIONS

FLORIDA DEPARTMENT OF TRANSPORTATION

	FWR
4/27/22	NS
NOTED	JC

A–5

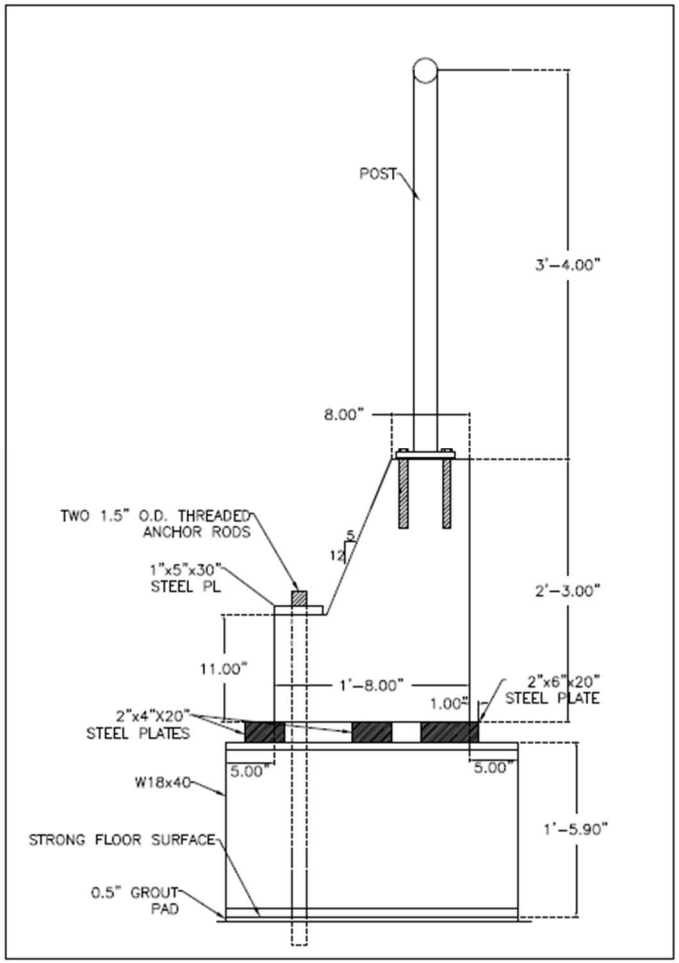

B5 GRAVITY WALL – SIDE VIEW

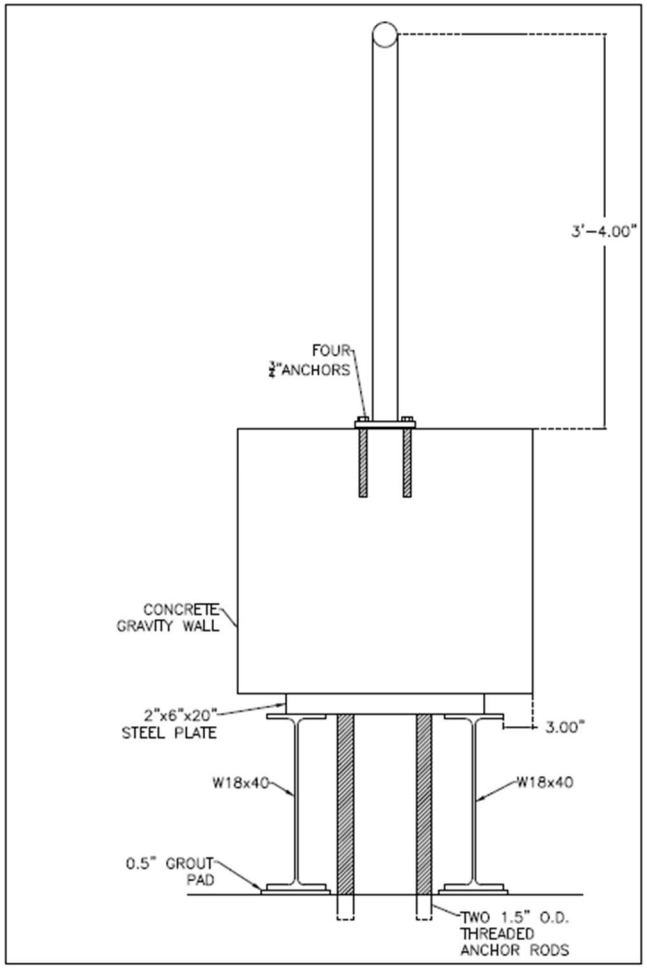

B6 GRAVITY WALL – FRONT VIEW

SCREW ANCHORS
TEST SETUP

FLORIDA TECH

TEST SETUP – SCREW ANCHOR APPLICATIONS

FLORIDA DEPARTMENT OF TRANSPORTATION

	RJR
4/27/22	NS
NOTED	JC

B–2

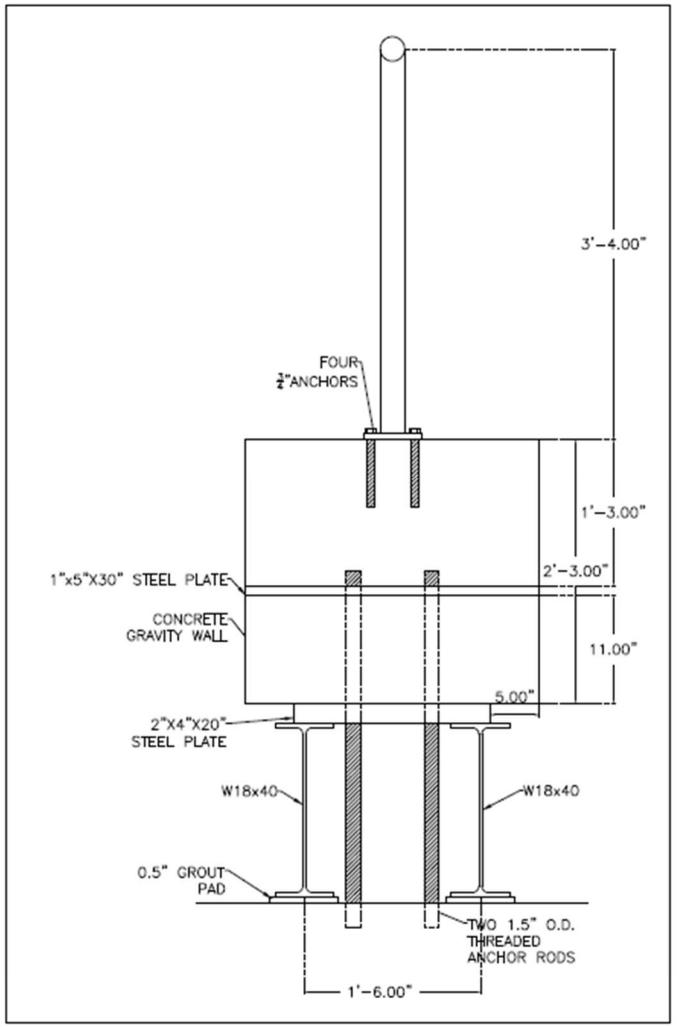

B7 GRAVITY WALL – REAR VIEW

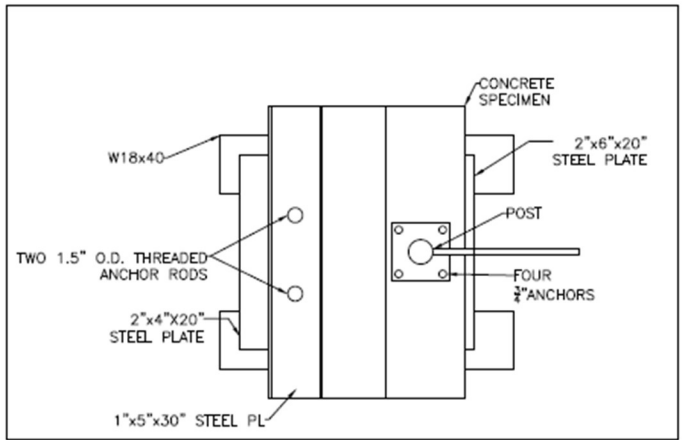

B8 GRAVITY WALL – TOP VIEW

SCREW ANCHORS
TEST SETUP

FLORIDA TECH

TEST SETUP – SCREW ANCHOR APPLICATIONS

FLORIDA DEPARTMENT OF TRANSPORTATION

	PJW
4/27/22	NS
NOTED	JC

B-3

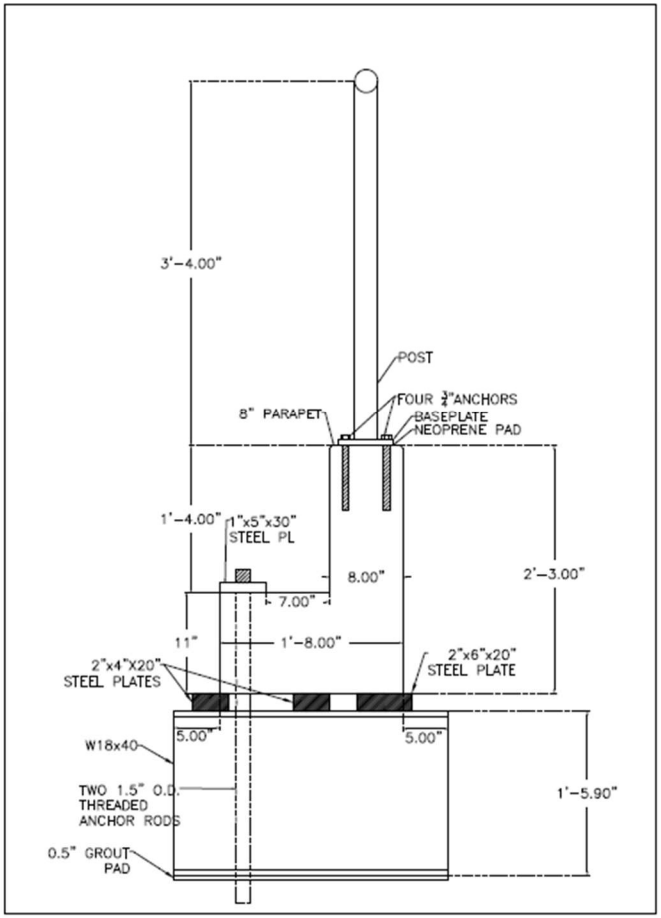

C5 PARAPET – SIDE VIEW

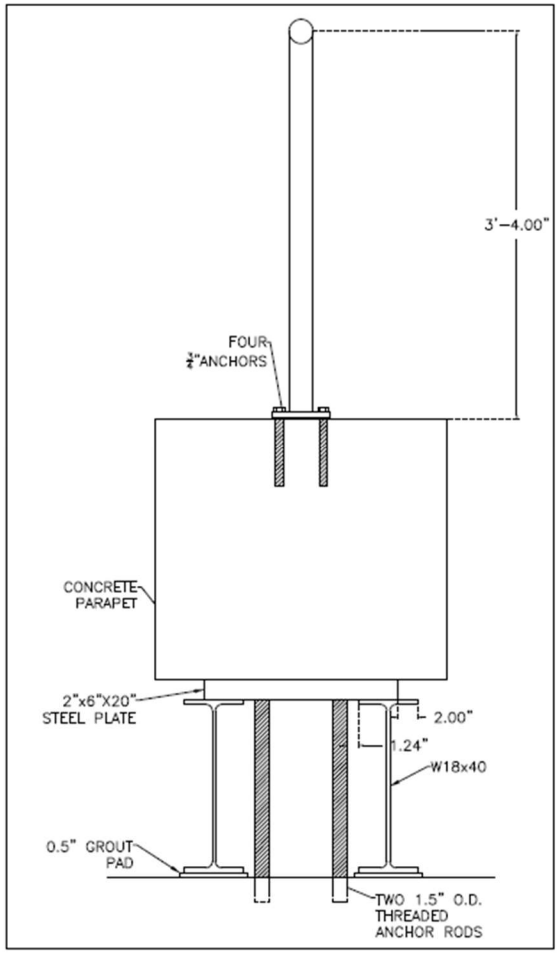

C6 PARAPET – FRONT VIEW

SCREW ANCHORS
TEST SETUP

FLORIDA TECH

TEST SETUP – SCREW ANCHOR APPLICATIONS

FLORIDA DEPARTMENT OF TRANSPORTATION

	PJR
4/27/22	NS
NOTED	JC

C-2

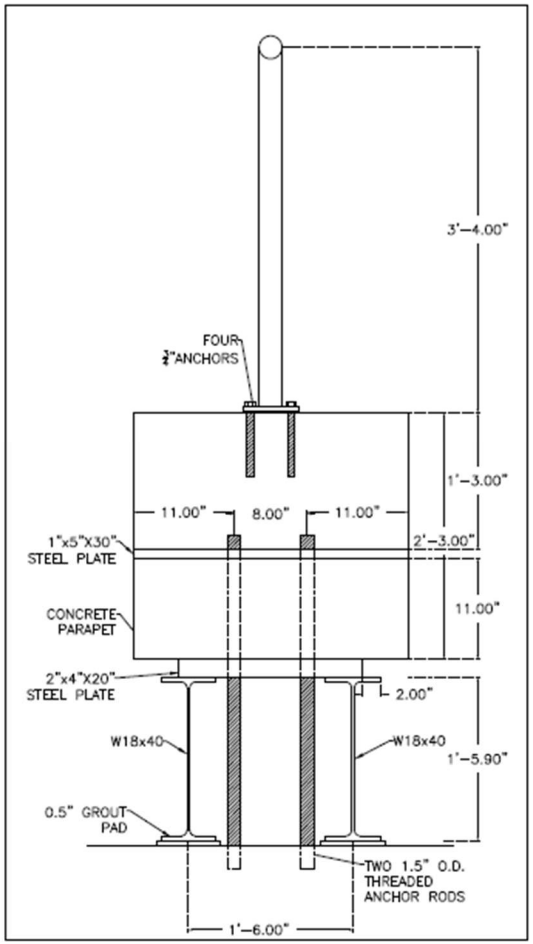

C7 PARAPET – REAR VIEW

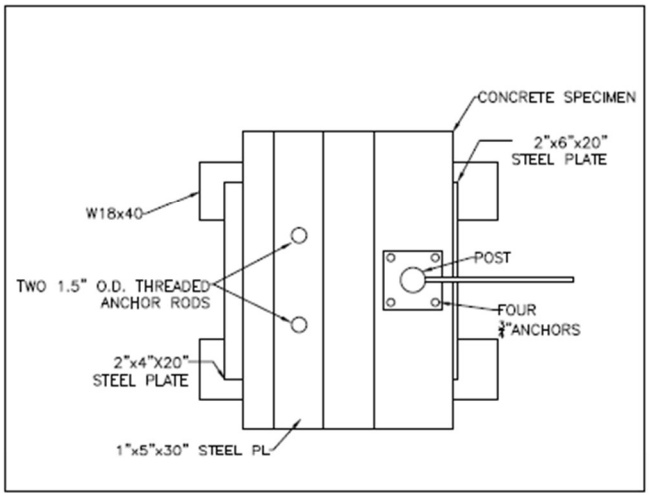

C8 PARAPET – TOP VIEW

SCREW ANCHORS
TEST SETUP

FLORIDA TECH

TEST SETUP – SCREW ANCHOR APPLICATIONS

FLORIDA DEPARTMENT OF TRANSPORTATION

	FUR
4/27/22	NS
NOTED	JC

C-3

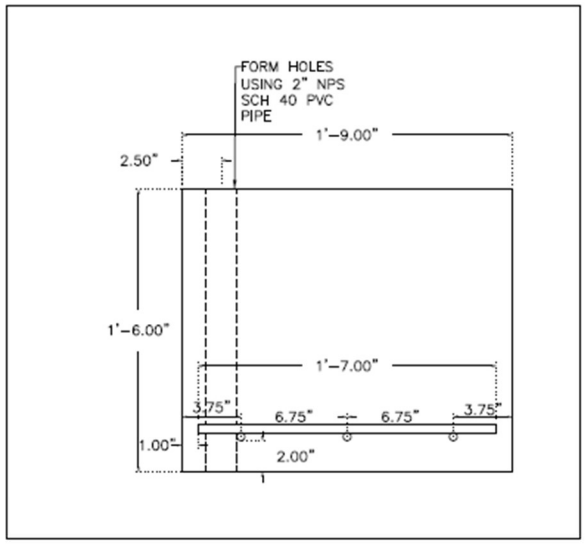

D1 SLAB REINFORCEMENT – SIDE VIEW

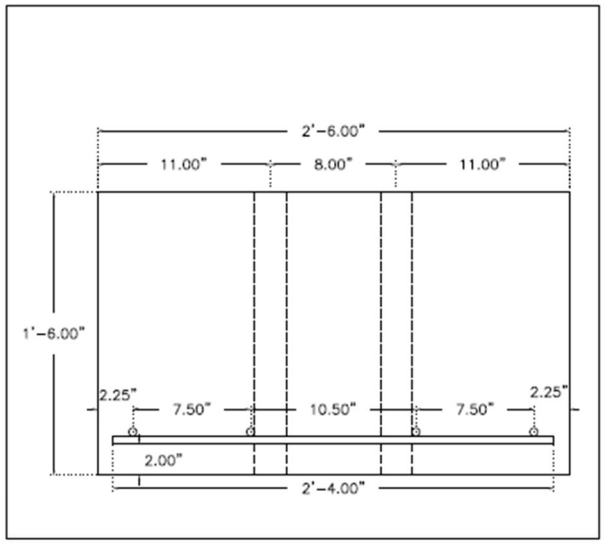

D2 SLAB REINFORCEMENT – FRONT VIEW

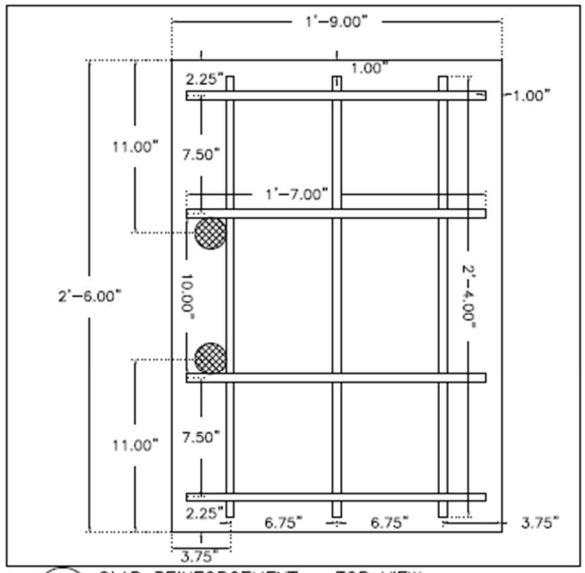

D3 SLAB REINFORCEMENT – TOP VIEW

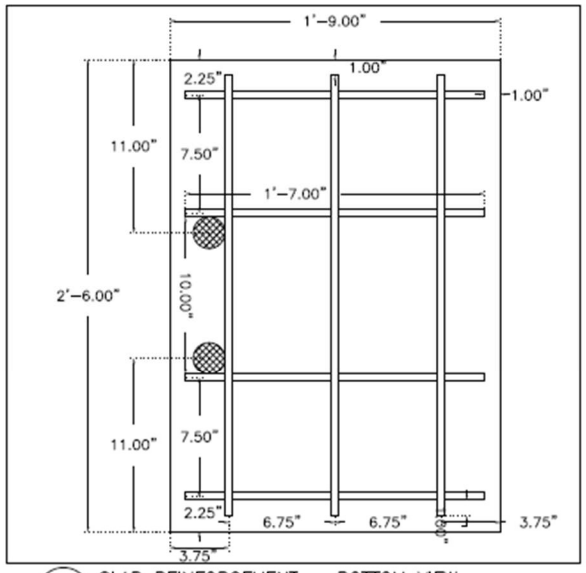

D4 SLAB REINFORCEMENT – BOTTOM VIEW

SCREW ANCHORS
TEST SETUP

FLORIDA TECH

TEST SETUP – SCREW ANCHOR APPLICATIONS

FLORIDA DEPARTMENT OF TRANSPORTATION

	PJW
4/27/22	NS
NOTED	JC

D–1

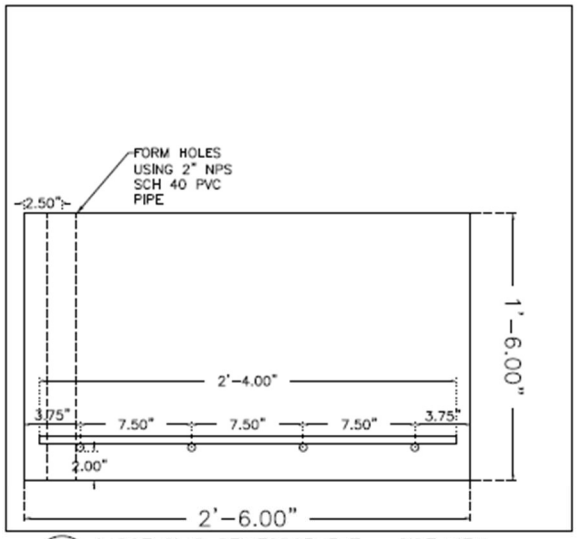

D9 LARGE SLAB REINFORCEMENT – SIDE VIEW

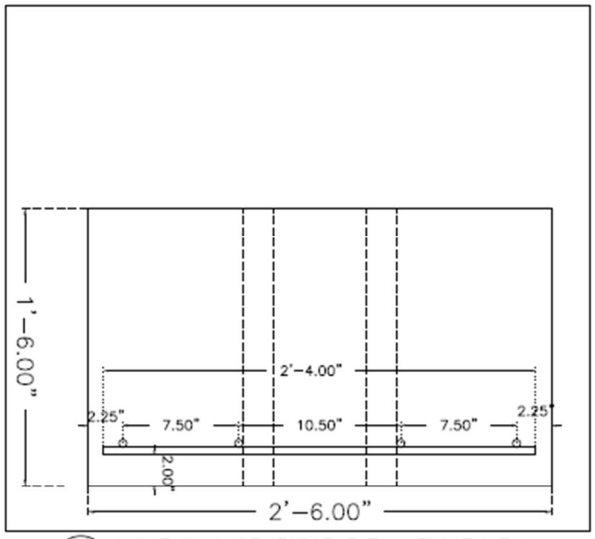

D10 LARGE SLAB REINFORCEMENT – FRONT VIEW

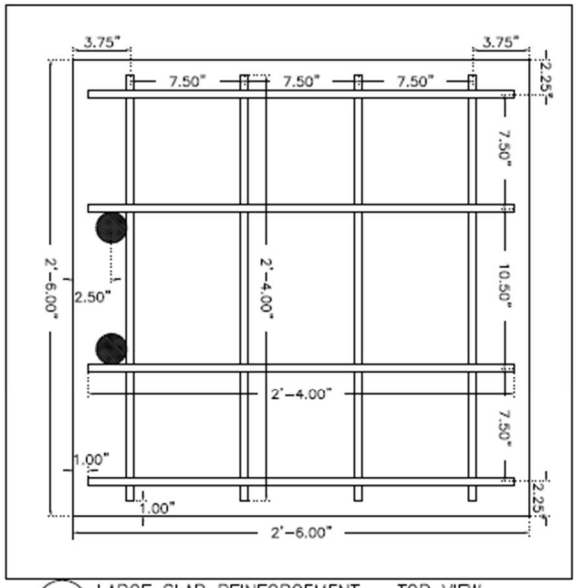

D11 LARGE SLAB REINFORCEMENT – TOP VIEW

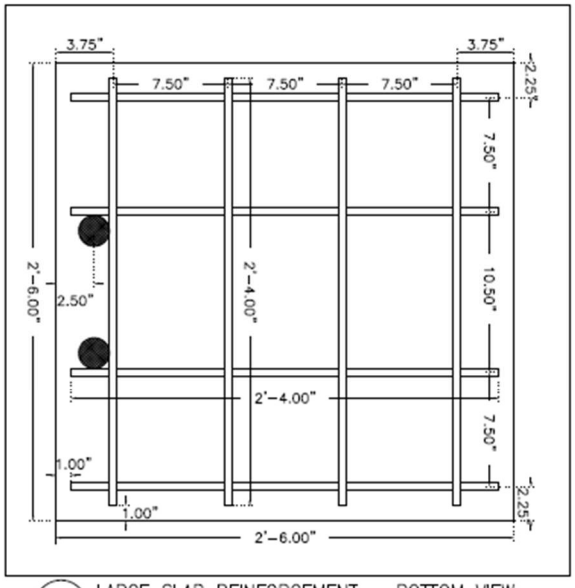

D12 LARGE SLAB REINFORCEMENT – BOTTOM VIEW

SCREW ANCHORS
TEST SETUP

FLORIDA TECH

TEST SETUP – SCREW ANCHOR APPLICATIONS

FLORIDA DEPARTMENT OF TRANSPORTATION

	PJR
4/27/22	NS
NOTED	JC

D-1

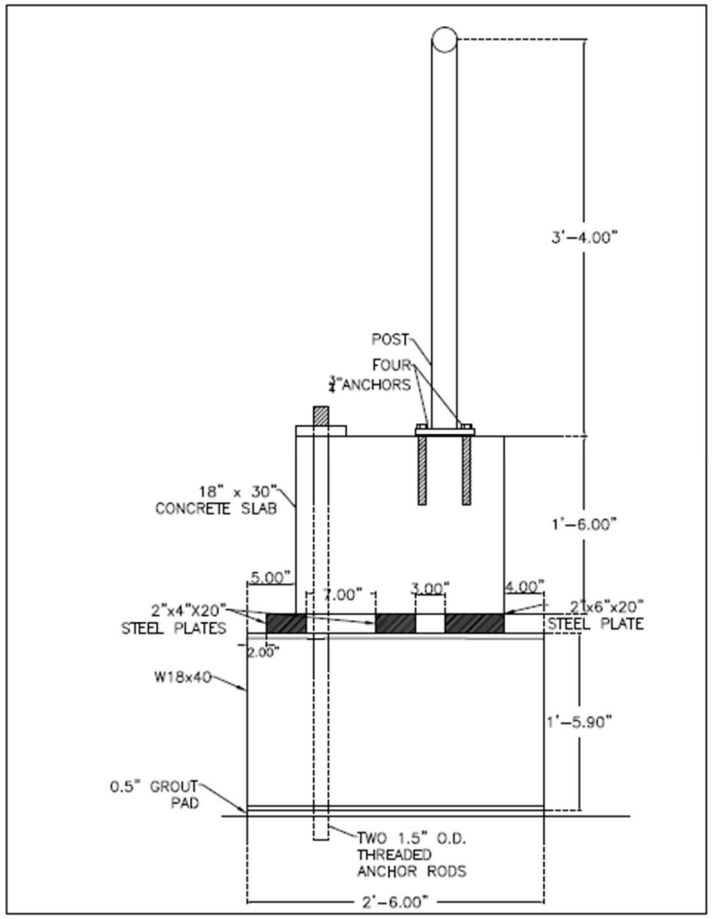

D5 SLAB – SIDE VIEW

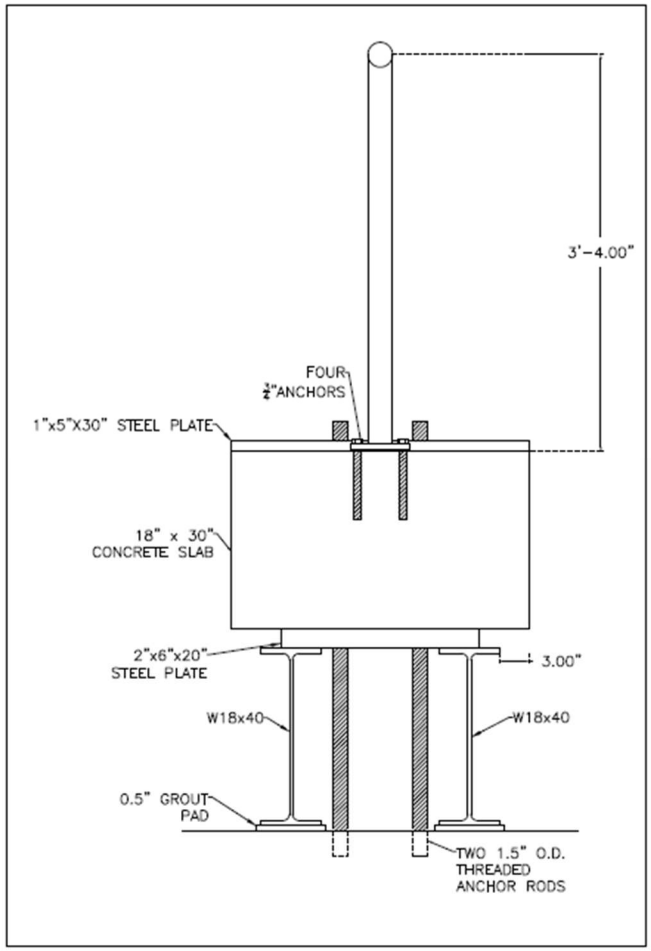

D6 SLAB – FRONT VIEW

SCREW ANCHORS
TEST SETUP

FLORIDA TECH

TEST SETUP – SCREW ANCHOR APPLICATIONS

FLORIDA DEPARTMENT OF TRANSPORTATION

	PJR
4/27/22	NS
NOTED	JC

D–2

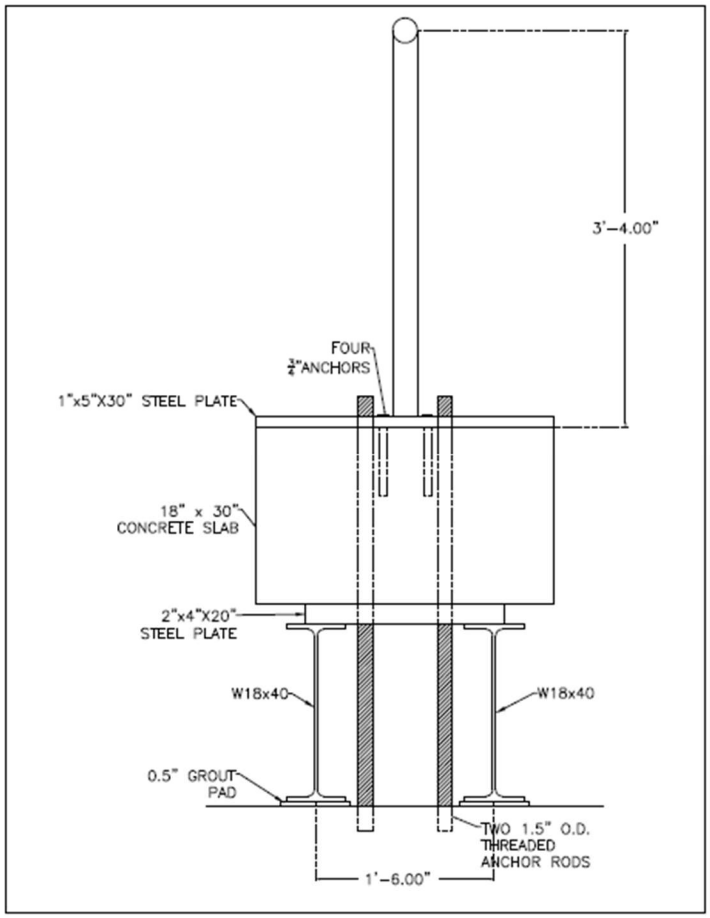

D7 SLAB – REAR VIEW

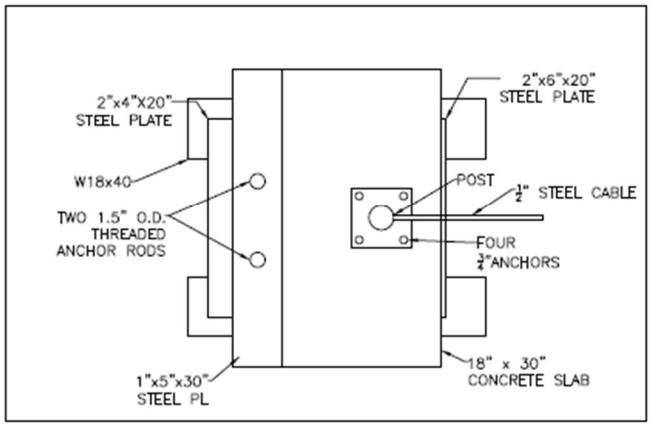

D8 SLAB – TOP VIEW

SCREW ANCHORS
TEST SETUP

FLORIDA TECH

TEST SETUP – SCREW ANCHOR APPLICATIONS

FLORIDA DEPARTMENT OF TRANSPORTATION

	PJR
4/27/22	NS
NOTED	JC

D-3

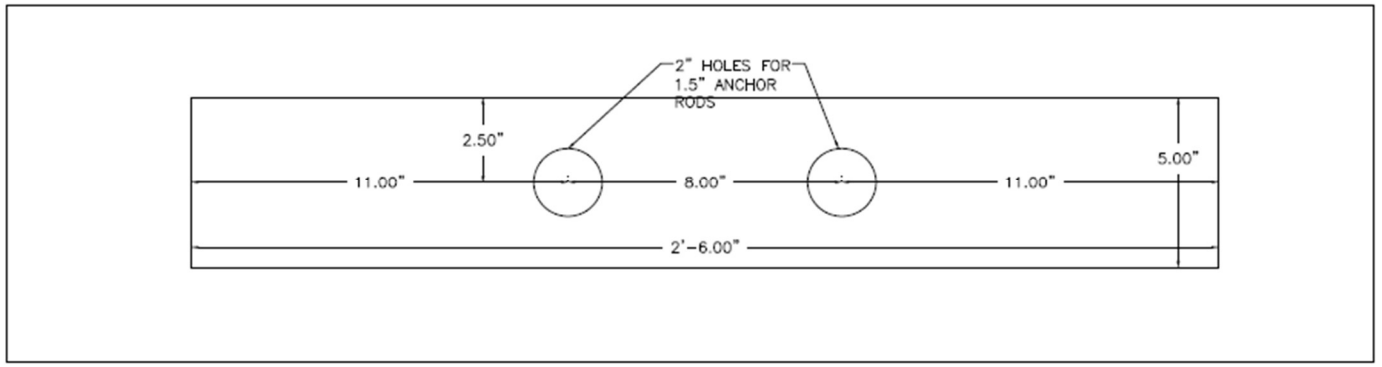

X4 1"x5"x30" STEEL PLATE – TOP VIEW

SCREW ANCHORS
TEST SETUP

FLORIDA TECH

TEST SETUP – SCREW ANCHOR APPLICATIONS

FLORIDA DEPARTMENT OF TRANSPORTATION

	PJR
4/27/22	NS
NOTED	JC

X-3

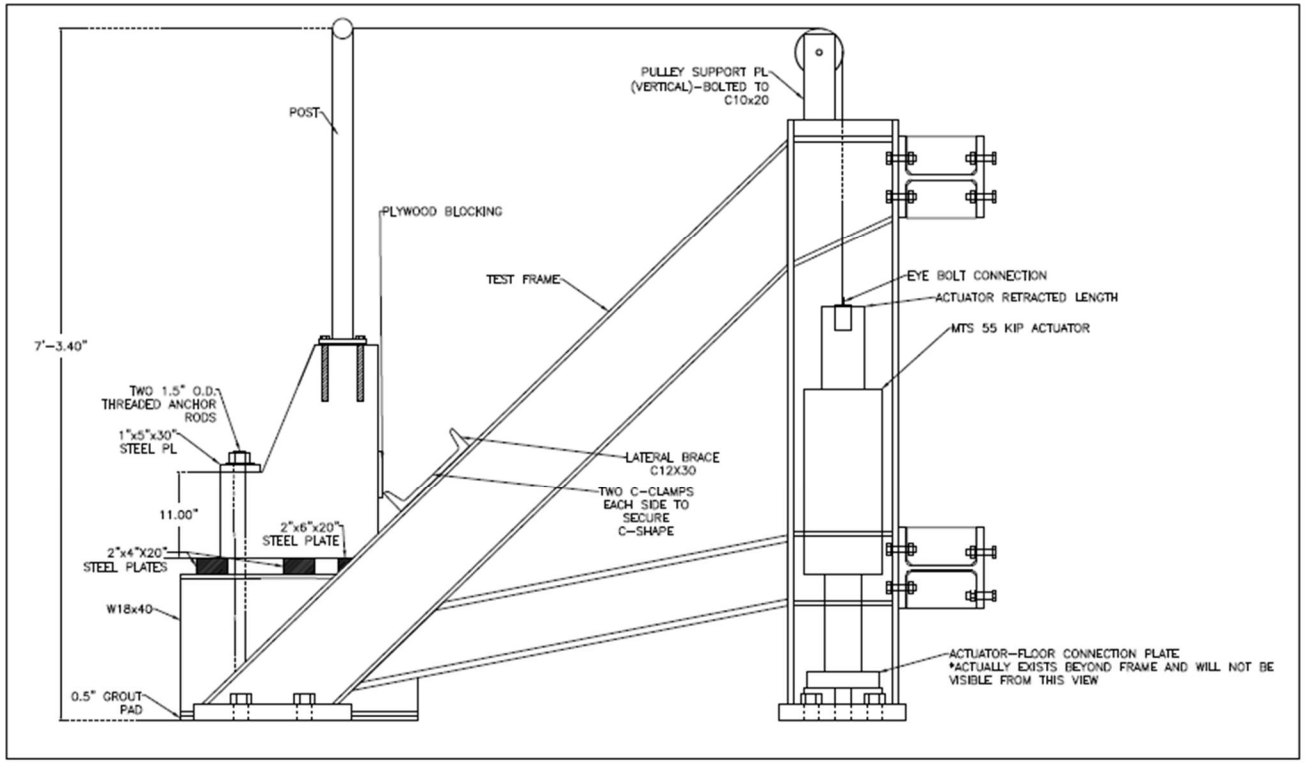

E1 GRAVITY WALL – SIDE VIEW

SCREW ANCHORS
TEST SETUP

FLORIDA TECH

TEST SETUP – SCREW ANCHOR APPLICATIONS

FLORIDA DEPARTMENT OF TRANSPORTATION

	FJR
4/27/22	HS
NOTED	JC

E–1

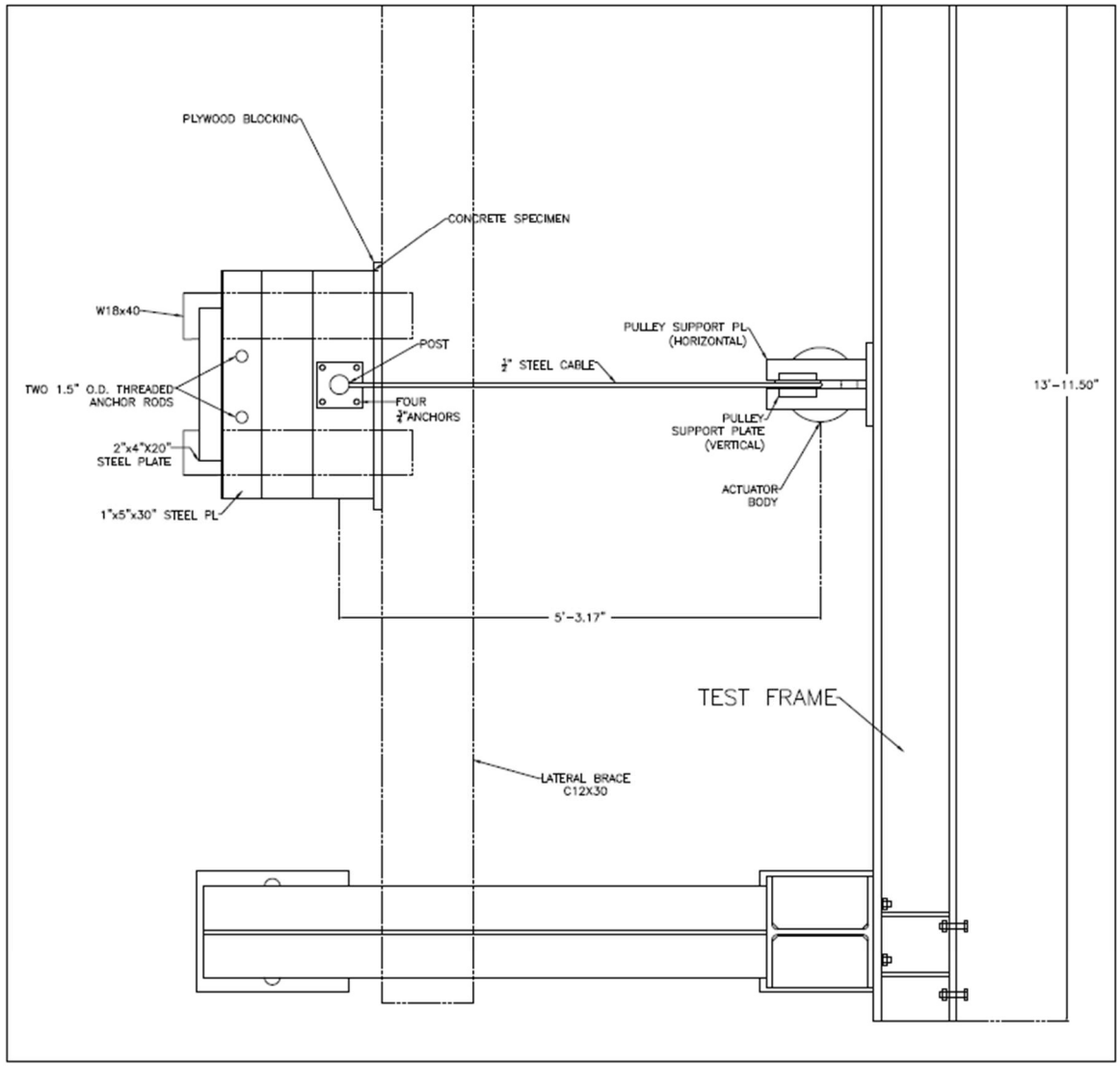

E2 GRAVITY WALL – TOP VIEW

SCREW ANCHORS TEST SETUP

FLORIDA TECH

TEST SETUP – SCREW ANCHOR APPLICATIONS

FLORIDA DEPARTMENT OF TRANSPORTATION

	PJR
4/27/22	NS
NOTED	JC

E-2

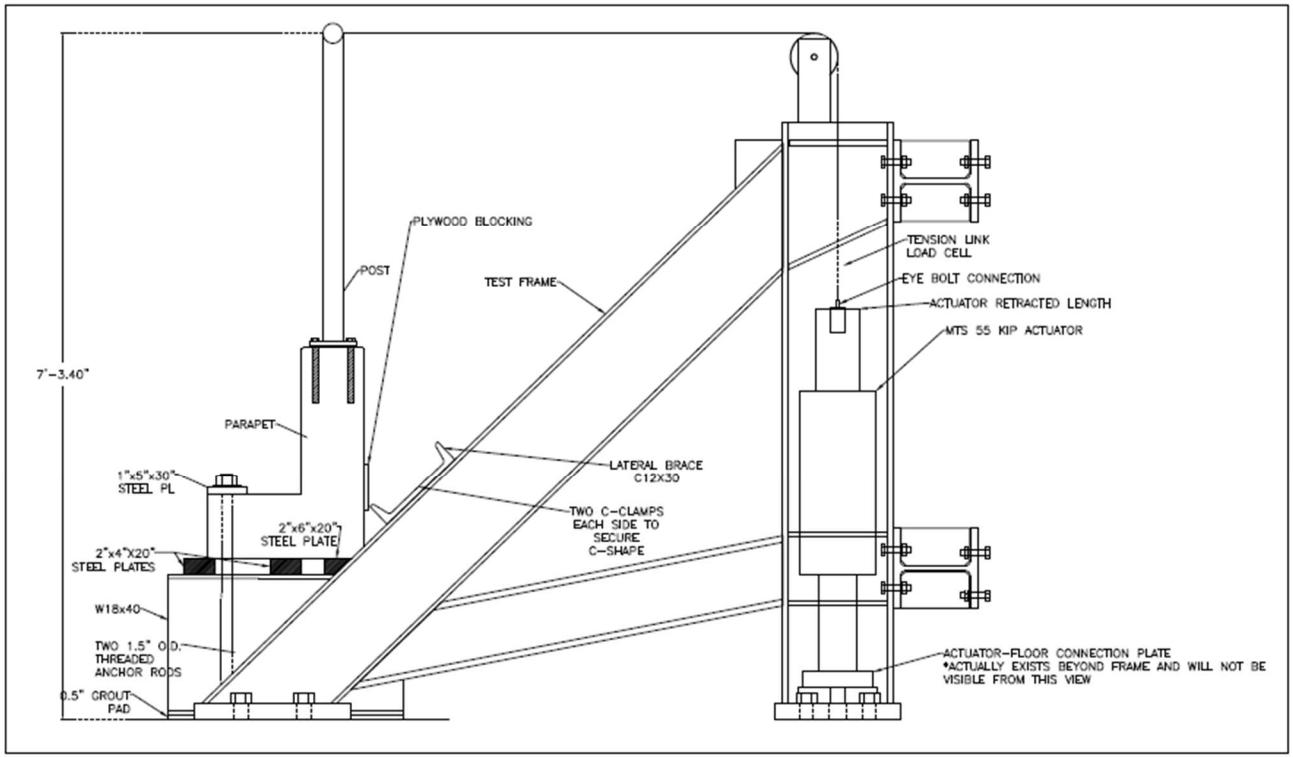

E3 PARAPET – SIDE VIEW

SCREW ANCHORS
TEST SETUP

FLORIDA TECH

TEST SETUP – SCREW ANCHOR APPLICATIONS

FLORIDA DEPARTMENT OF TRANSPORTATION

	RJR
4/27/22	NS
NOTED	JC

E-3

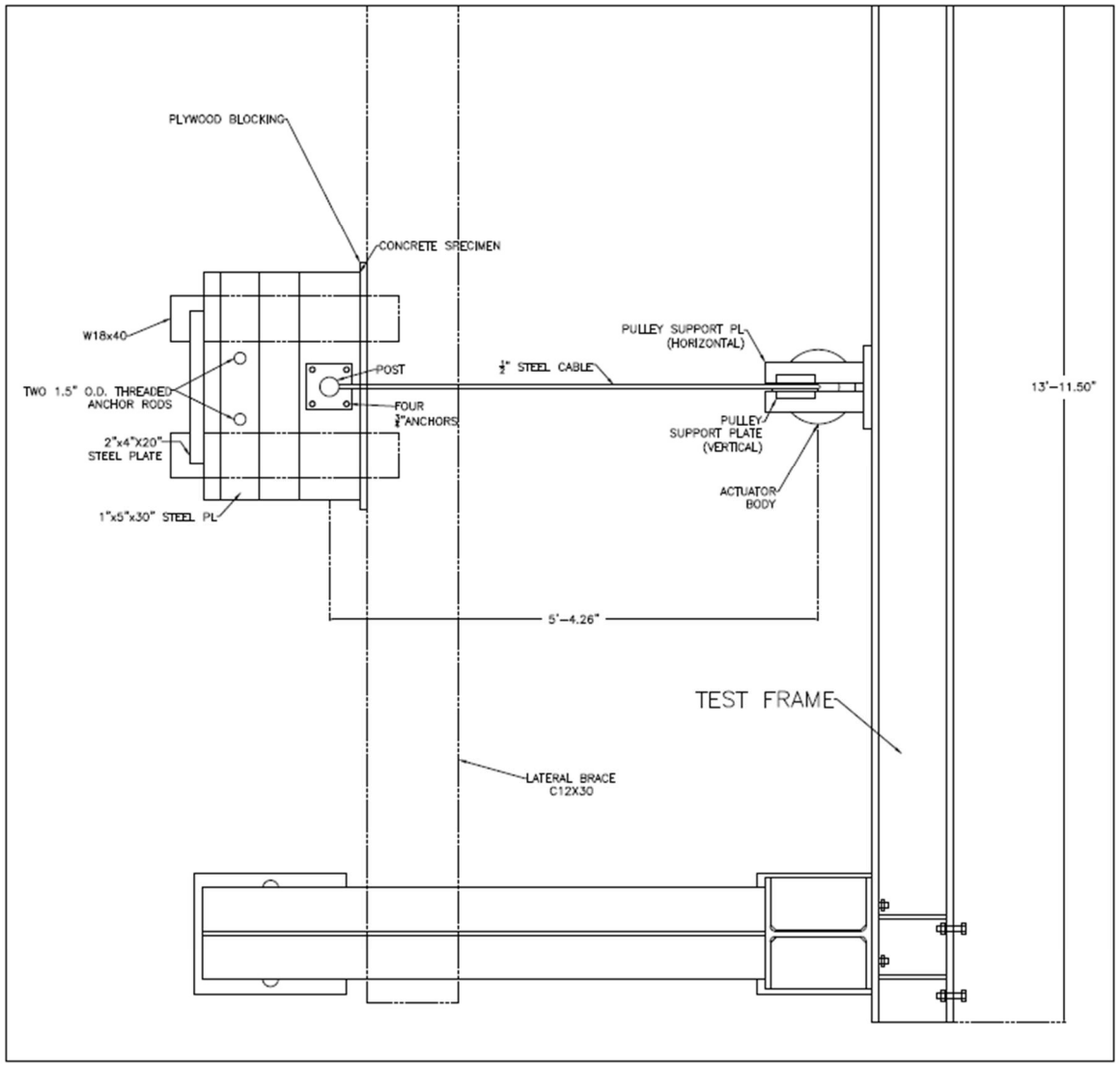

E4 PARAPET – TOP VIEW

SCREW ANCHORS TEST SETUP

FLORIDA TECH

TEST SETUP – SCREW ANCHOR APPLICATIONS

FLORIDA DEPARTMENT OF TRANSPORTATION

	PJR
4/27/22	NS
NOTED	JG

E-4

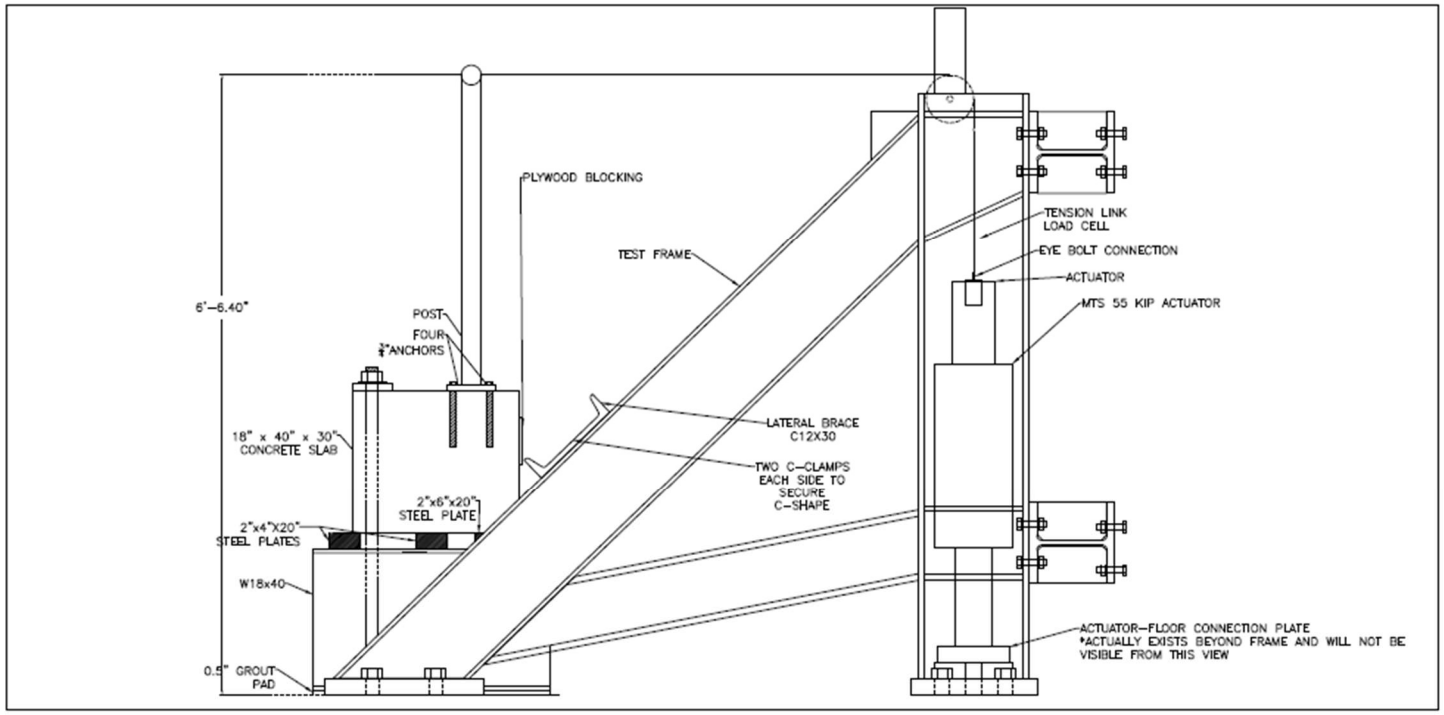

E5 SLAB – SIDE VIEW

SCREW ANCHORS
TEST SETUP

FLORIDA TECH

TEST SETUP – SCREW ANCHOR APPLICATIONS

FLORIDA DEPARTMENT OF TRANSPORTATION

	FJR
4/27/22	NS
NOTED	JC

E–5

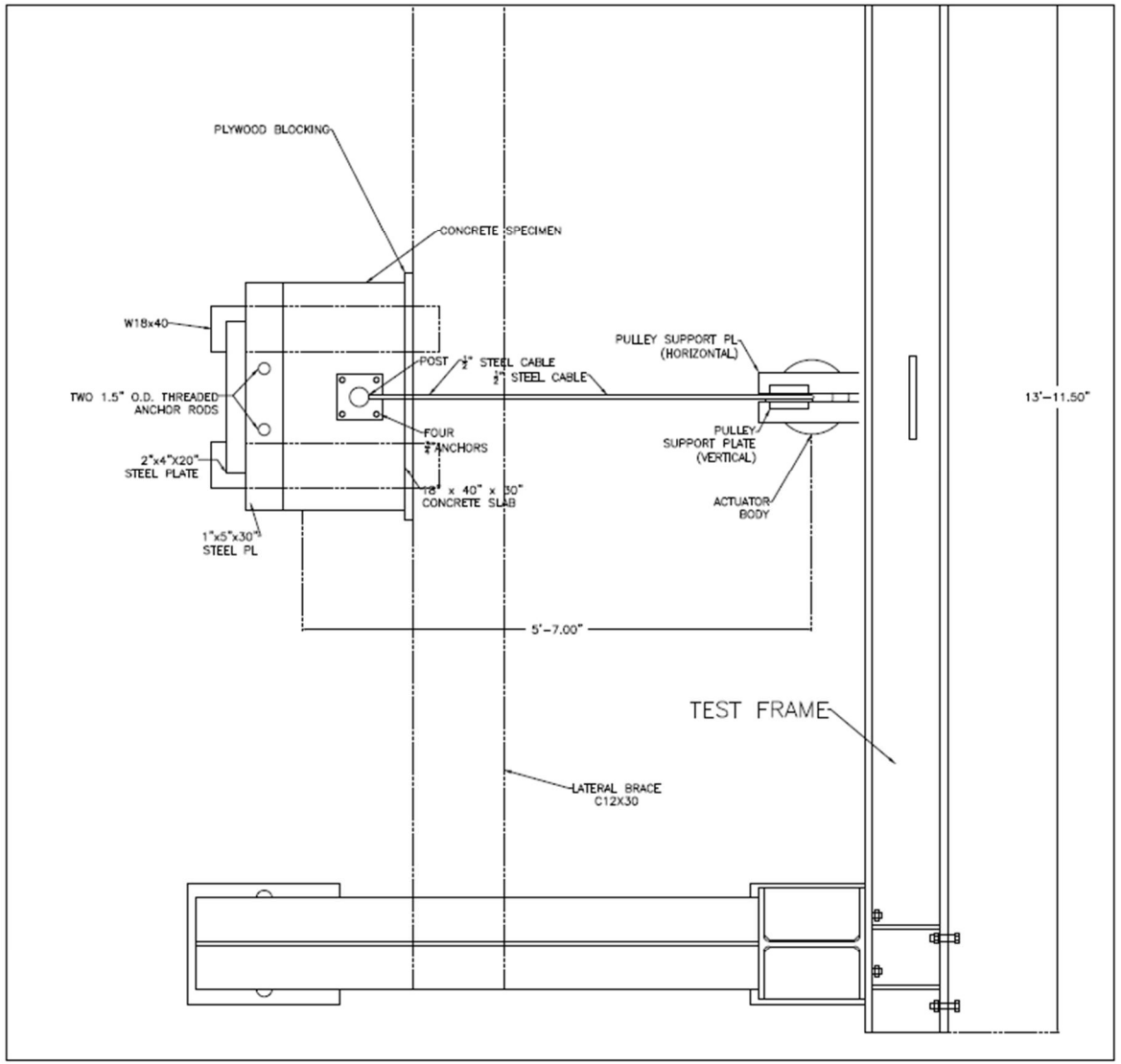

E6 SLAB – TOP VIEW

SCREW ANCHORS TEST SETUP

FLORIDA TECH

TEST SETUP – SCREW ANCHOR APPLICATIONS

FLORIDA DEPARTMENT OF TRANSPORTATION

	PJR
4/27/22	NS
NOTED	JC

E-6

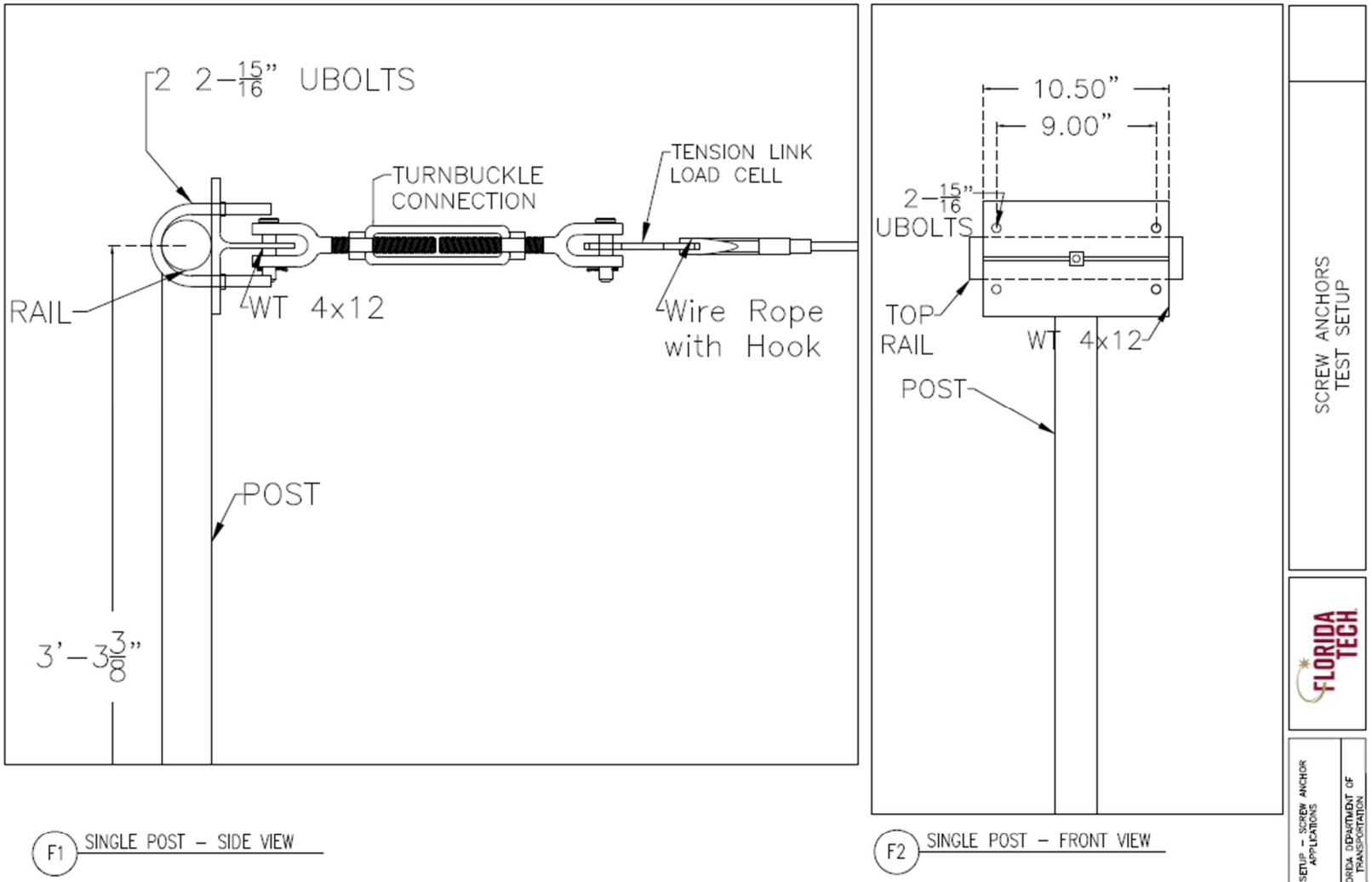
2 2–15/16" UBOLTS
TURNBUCKLE CONNECTION
TENSION LINK LOAD CELL
RAIL
WT 4x12
Wire Rope with Hook
POST
3'–3 3/8"
10.50"
9.00"
2–15/16" UBOLTS
TOP RAIL
WT 4x12
POST
F1 SINGLE POST – SIDE VIEW
F2 SINGLE POST – FRONT VIEW
SCREW ANCHORS TEST SETUP
FLORIDA TECH
TEST SETUP – SCREW ANCHOR APPLICATIONS
FLORIDA DEPARTMENT OF TRANSPORTATION
PJR
4/27/22 NS
NOTED JC
F–1

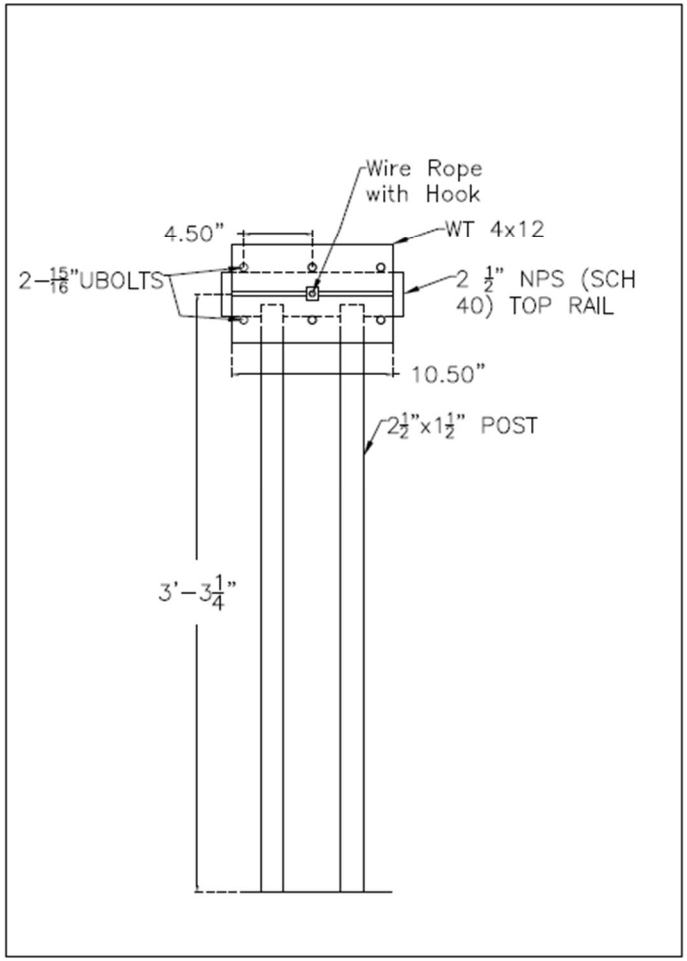

F3 DOUBLE POST – SIDE VIEW

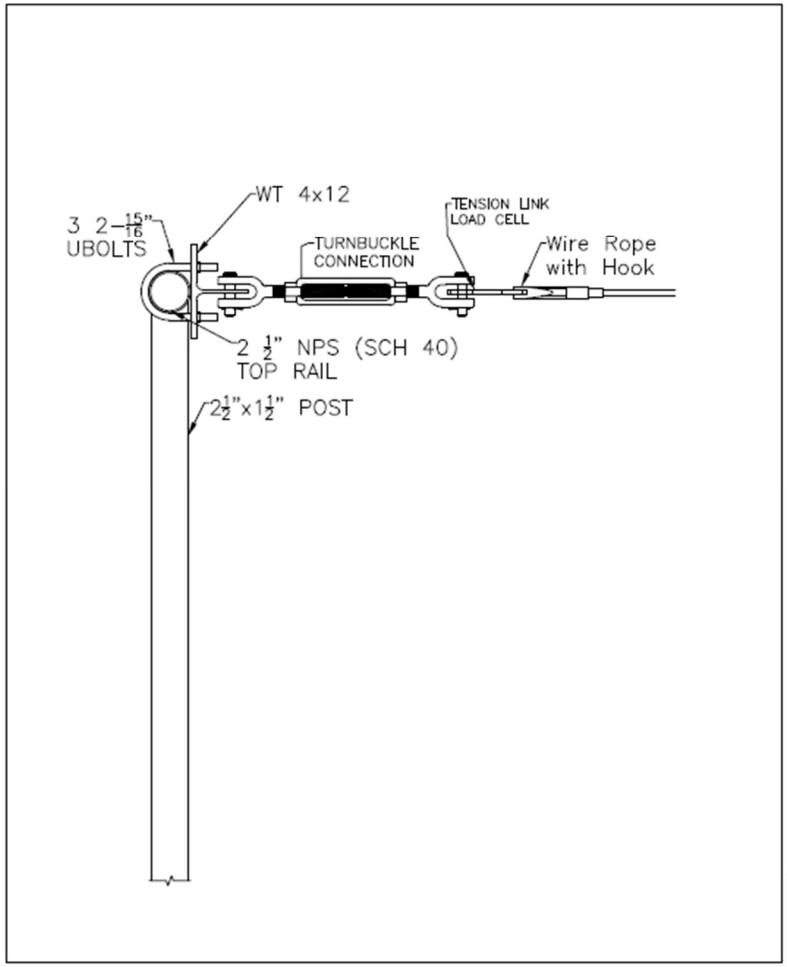

F4 DOUBLE POST – FRONT VIEW

SCREW ANCHORS
TEST SETUP

FLORIDA TECH

TEST SETUP – SCREW ANCHOR APPLICATIONS

FLORIDA DEPARTMENT OF TRANSPORTATION

	PJR
4/27/22	NS
NOTED	JC

F–2

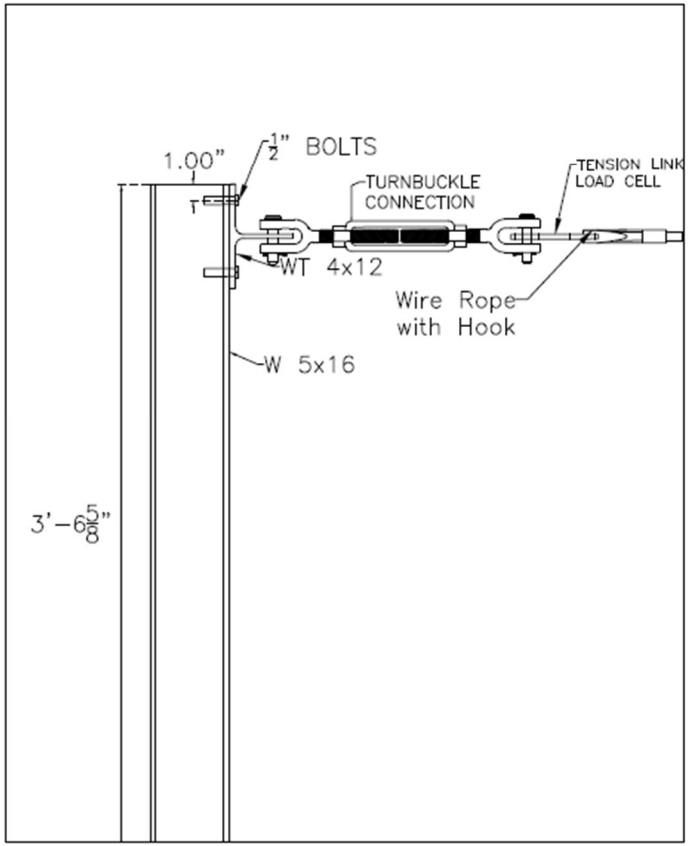

G4 BULLET RAILING ATTACHMENT – SIDE VIEW

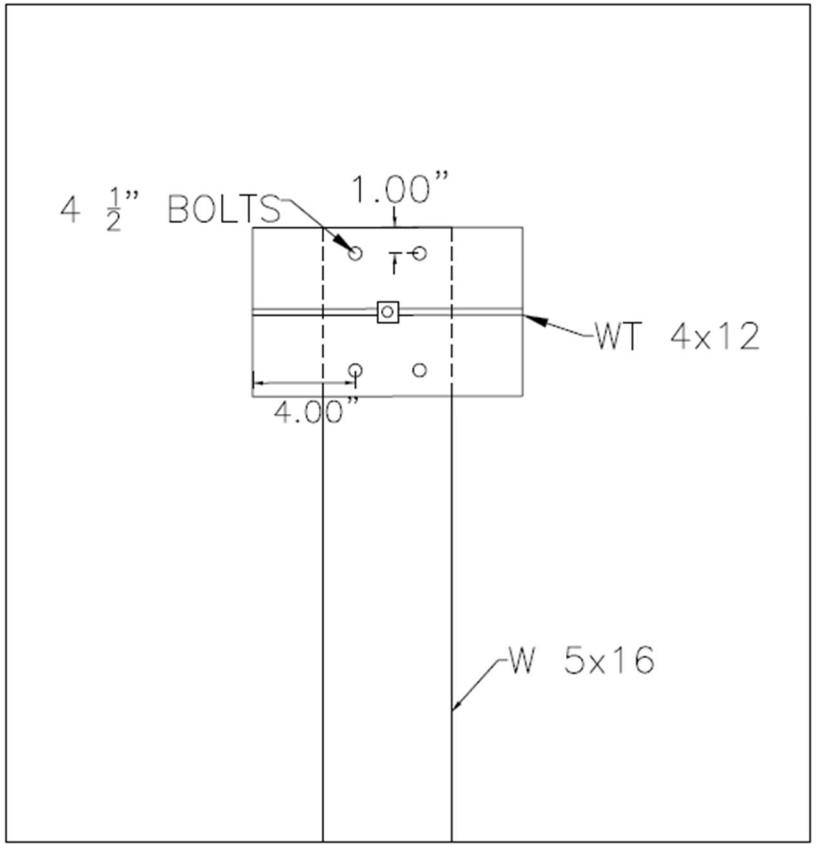

G5 BULLET RAILING ATTACHMENT – FRONT VIEW

SCREW ANCHORS
TEST SETUP

FLORIDA TECH

TEST SETUP – SCREW ANCHOR APPLICATIONS

FLORIDA DEPARTMENT OF TRANSPORTATION

	FJR
4/27/22	NS
NOTED	JC

G–3

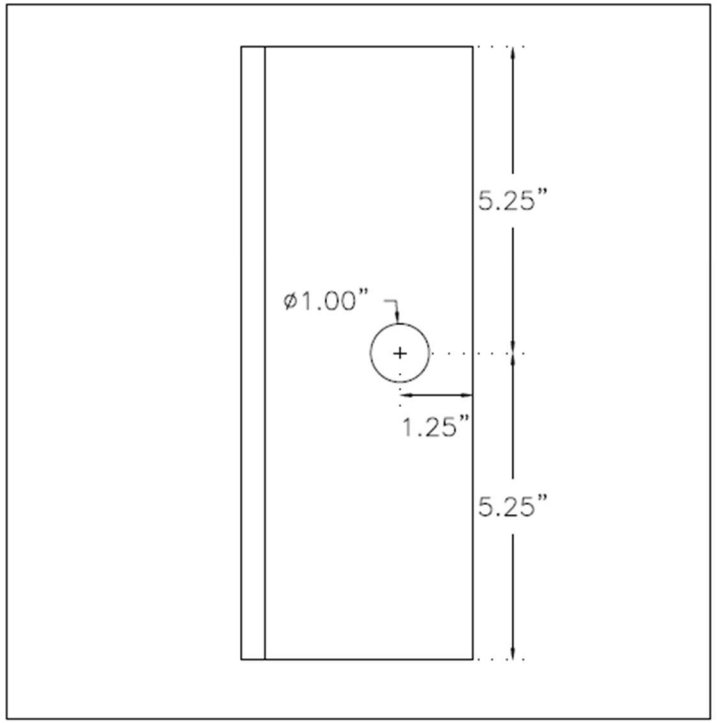

X1 WT 4X12 – TOP VIEW

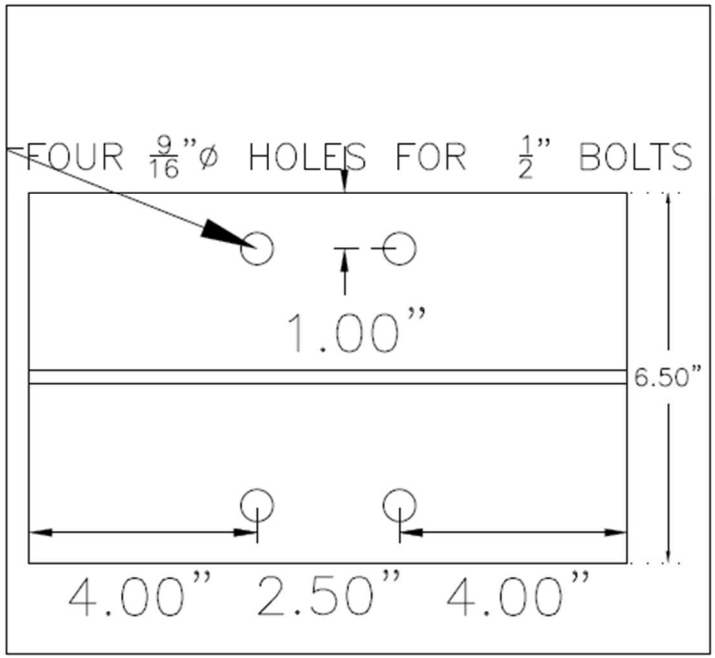

X2 BULLET WT 4X12 – FRONT VIEW

SCREW ANCHORS
TEST SETUP

FLORIDA TECH

TEST SETUP – SCREW ANCHOR APPLICATIONS

FLORIDA DEPARTMENT OF TRANSPORTATION

	PJR
4/27/22	MS
NOTED	JC

X–1

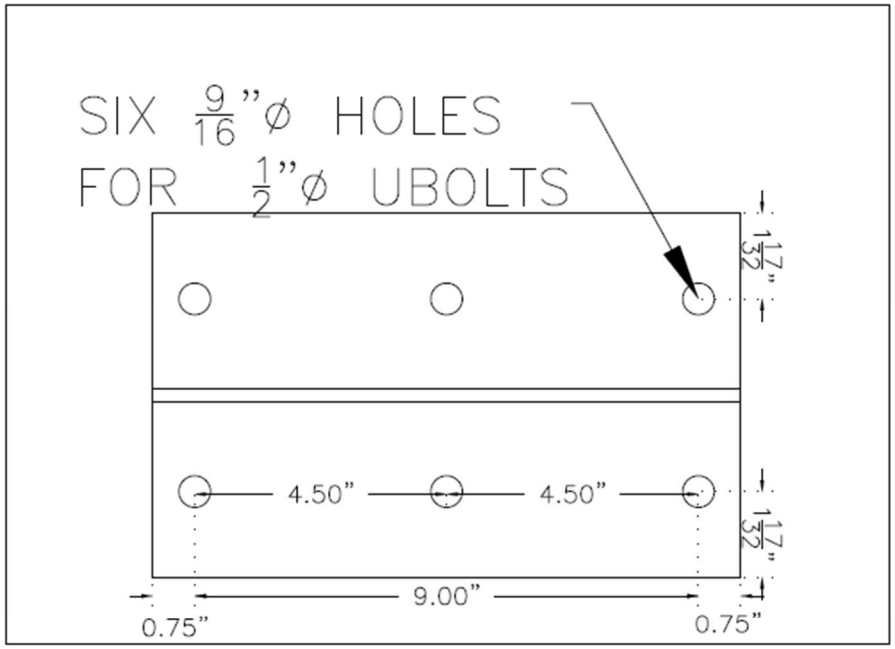

X3 SINGLE & DOUBLE POST WT 4X12 – FRONT VIEW

SCREW ANCHORS
TEST SETUP

FLORIDA TECH

TEST SETUP – SCREW ANCHOR APPLICATIONS

FLORIDA DEPARTMENT OF TRANSPORTATION

	PJR
4/27/22	HS
NOTED	JC

X–2

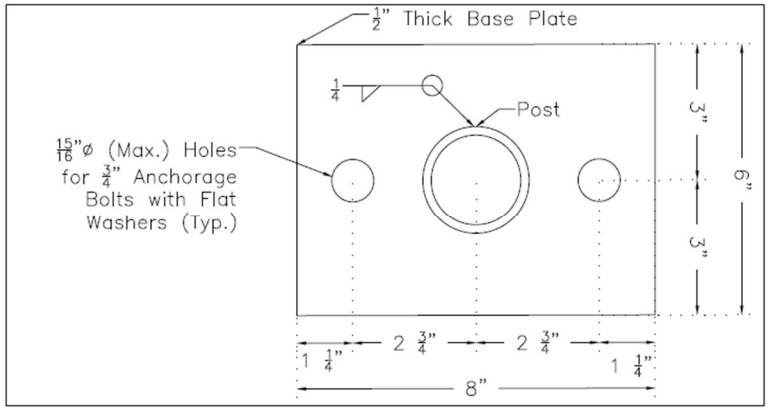

H6 SINGLE POST – BASE PLATE TOP VIEW (2 BOLT)

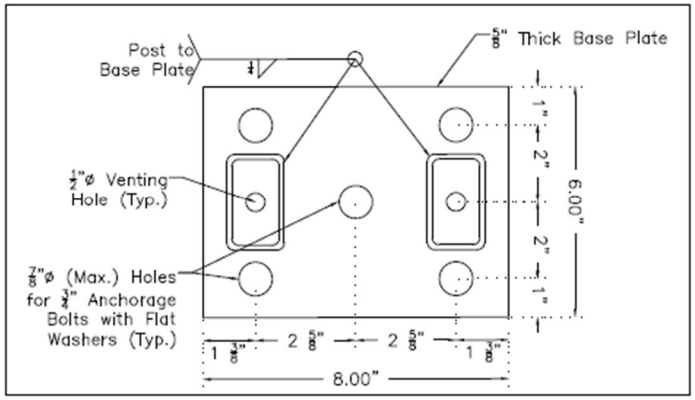

H9 DOUBLE POST – BASE PLATE TOP VIEW

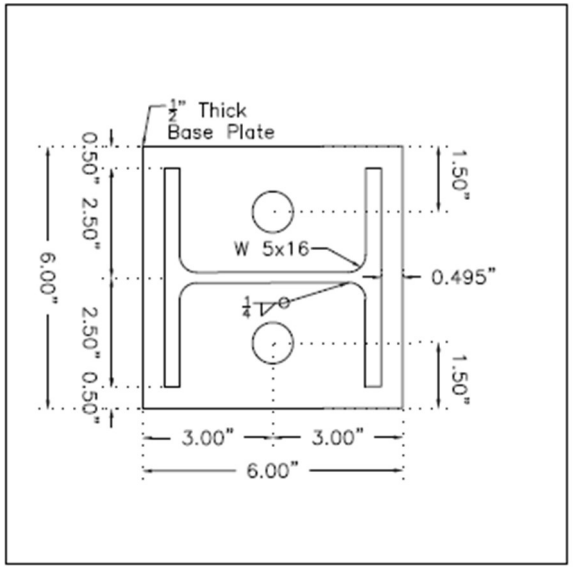

H3 BULLET RAILING – BASEPLATE TOP VIEW